# Chemistry of the Upper and Lower Atmosphere

## *Theory, Experiments, and Applications*

Barbara J. Finlayson-Pitts
*Department of Chemistry*
*School of Physical Sciences*
*University of California, Irvine*
*Irvine, California*

James N. Pitts, Jr.
*Department of Chemistry*
*School of Physical Sciences*
*University of California, Irvine*
*Irvine, California*

2000
ISBN: 0-12-257060-X

**ACADEMIC PRESS**
A Harcourt Science and Technology Company

*San Diego San Francisco New York Boston London Sydney Tokyo*

CHAPTER

# 11

# Analytical Methods and Typical Atmospheric Concentrations for Gases and Particles

As seen throughout this book, the chemistry of the troposphere and stratosphere is sufficiently complex that an interplay between laboratory, field, and modeling studies is critical to elucidate fundamental processes and their relationships to each other. Accurate data on the geographical and temporal distribution of pollutants and trace species are essential for testing of models that incorporate the results of laboratory studies. Clearly, the predictions of such models can only be as good as the data against which they are tested. Hence, methods of measurement that are sensitive, specific, and accurate and that have good time resolution (generally of the order of seconds or better) are an essential element of understanding atmospheric chemistry.

Historically, atmospheric compounds were measured using wet chemical techniques. For example, ozone was measured by bubbling air through a solution containing iodide, and the $I_2$ formed was measured using wet chemical techniques. Such methods were used as early as the mid-1800s to measure ozone in a number of locations worldwide, providing data on the increase in its concentrations since then, discussed in Chapter 14.B.2d.

However, not surprisingly, wet chemical methods are frequently subject to a number of potential interferences, both positive and negative. In the case of ozone measured using iodide oxidation, for example, $SO_2$ gives a 1:1 negative interference, whereas $NO_2$ gives a positive interference with a response that is equivalent to about 5–10% that of ozone on a molecular basis. In addition, calibrations can be sensitive to the exact procedure used. For a discussion of many of the factors affecting $O_3$ measurements made using this technique, and the air quality implications, see Finlayson-Pitts and Pitts (1986) and references therein. Because this technique is not specific for $O_3$, the measured values are often reported as "oxidant," rather than $O_3$, although the latter is, under most circumstances, the major contributor.

As a result, while such methods have been very useful in the past and continue to be applied for initial surveys of air quality in areas in which measurements have not been made in the past, they have generally been abandoned in favor of instrumental methods of analysis. As a result, this chapter focuses on the most commonly used instrumental, often spectroscopic, methods for measuring air pollutants, trace gases, and particles in air (e.g., see Roscoe and Clemitshaw, 1997). The focus is on tropospheric measurements, although, in most cases, the same techniques are used in the stratosphere.

In many countries around the world, air quality standards for specific gases are set to protect public health (see Chapter 2.D). Standards are often set for particles in terms of mass $m^{-3}$ less than a certain size, e.g., 10 $\mu$m. With the increasing focus on the health effects of fine particles, there is also great interest in composition as a function of size. The gases for which air quality standards are set are generally referred to as "criteria pollutants" and include $NO_2$, $O_3$, CO, and $SO_2$ in the United States. Reference and equivalent methods, summarized in Table 11.1, have been established by the U.S. Environmental Protection Agency for the measurement of these compounds. Since nonmethane hydrocarbons and organics (for which a number of different names and acronyms are used; see later) are precursors to $O_3$ and a number of other species of atmospheric interest, a variety of methods for measuring the total organics or individual compounds have been developed for these as well.

TABLE 11.1 Reference and Equivalent Methods Designated by the U.S. Environmental Protection Agency for Monitoring Criteria Gaseous Air Pollutants

| Gas | Reference or equivalent method |
|---|---|
| $NO_2$ | Ozone chemiluminescence<br>Differential optical absorption spectrometry<br>Sodium arsenite |
| $O_3$ | UV absorption<br>Chemiluminescence<br>Differential optical absorption spectrometry |
| CO | Nondispersive infrared |
| $SO_2$ | UV fluorescence<br>Differential optical absorption spectrometry<br>Pararosaniline |

The principles behind these and other techniques used to measure a variety of trace gases in the atmosphere, including the criteria pollutants and free radicals such as $NO_3$, OH, $HO_2$, and $RO_2$, are described in the following sections. In addition, typical tropospheric concentrations in regions from remote to urban areas are given.

In the second section of this chapter, techniques for measuring and characterizing particles are described.

## A. GASES

### 1. Optical Spectroscopic Techniques

#### *a. Chemiluminescence*

As described in Chapter 3, the products of some chemical reactions are initially produced in electronically excited states. If the excited state has a sufficiently short radiative lifetime, it will emit light faster than collisional quenching by air molecules can occur (see Problem 1). The effective concentration of the emitting species (and hence emitted light intensity) is proportional to the concentrations of the reactants. As a result, the chemiluminescence intensity can be used to monitor one of the reactants if the second reactant is kept at a constant (excess) concentration.

For example, ozone reacts with nitric oxide to form electronically excited $NO_2$:

$$O_3 + NO \rightarrow NO_2^* + O_2, \quad (1)$$

$$NO_2^* \rightarrow NO_2 + h\nu. \quad (2)$$

The light emission from electronically excited $NO_2$ extends from 590 nm out to 2800 nm, a region that is relatively easily and sensitively monitored using conventional photomultipliers. This reaction is a standard technique for monitoring NO.

To measure NO using chemiluminescence, the air is mixed with a stream containing excess $O_3$ and the chemiluminescence intensity monitored. In principle, the reverse procedure can be used; i.e., excess NO can be added and the chemiluminescence intensity used to measure $O_3$. However, this requires a source of NO such as a gas cylinder, which is often not convenient for field studies.

Another chemiluminescence method for monitoring ozone involves the production of electronically excited formaldehyde in the $O_3$ reaction with ethene:

$$O_3 + C_2H_4 \rightarrow HCHO^* + \text{Other products}, \quad (3)$$

$$HCHO^* \rightarrow HCHO + h\nu. \quad (4)$$

The light emission is again in a region that can be followed quite sensitively, from ~300 to 550 nm. A disadvantage of this method is again the need to have a gas cylinder of ethene available.

A chemiluminescence method used for atmospheric measurements of $NO_2$ involves its reaction with luminol (5-amino-2,3-dihydro-1,4-phthalazinedione) in alkaline solution or on a wick wetted with such a solution (Maeda *et al.*, 1980; Wendel *et al.*, 1983; Schiff *et al.*, 1986). Although this technique can be quite sensitive, down to ~5 ppt, there can be interferences from species such as PAN and $O_3$. Ozone can be selectively removed from the airstream prior to measurement, although simultaneous removal of some of the $NO_2$ by the scrubber has been problematic in some studies (Fehsenfeld *et al.*, 1990). Alternatively, the contributions of interfering gases to the measured signal can be taken into account (assuming they are measured separately), which has been shown to be effective at $NO_2$ concentrations greater than 0.3 ppb (e.g., see Fehsenfeld *et al.*, 1990). Nonlinearity at low concentrations has also been reported for this method (Kelly *et al.*, 1990), requiring careful correction. In addition, NO and $CO_2$ suppress the $NO_2$ signal if they are present at high concentrations relative to $NO_2$ (Spicer *et al.*, 1994a).

The application of chemiluminescence to atmospheric measurements is reviewed by Navas *et al.* (1997).

#### *b. Fluorescence*

Fluorescence is the basis of a number of measurement methods for atmospheric gases. In the case of $SO_2$, for example, a Zn (213.8 nm) or Cd (228.8 nm) lamp is used to excite the $SO_2$ and the fluorescence in the 200- to 400-nm region is monitored (Okabe *et al.*, 1973; Schwarz *et al.*, 1974). Again, this technique works for those species whose excited states are sufficiently

short-lived that quenching does not totally dominate (see Problem 2). As discussed in more detail later, this technique is also used to measure NO as well as the OH free radical in air.

### c. *Infrared Spectroscopy (IR)*

Infrared spectroscopy has been applied to ambient air measurements since the mid-1950s (Stephens, 1958). Indeed, PAN was first identified in laboratory systems by its infrared absorptions and dubbed "compound X" because its identity was not known (Stephens *et al.*, 1956a, 1956b). It was subsequently measured in ambient air (Scott *et al.*, 1957). Since then, IR has been applied in many areas and has provided unequivocal and artifact-free measurements of a number of compounds. Because of its specificity, it has often been used as a "standard" for intercomparison studies (e.g., for $HNO_3$; see later).

Other infrared absorption techniques are also used in ambient air measurements, including tunable diode laser spectroscopy (TDLS), nondispersive infrared (NDIR) spectroscopy, and matrix isolation spectroscopy. These are discussed in more detail later.

A major advantage of infrared absorption spectroscopy derives from the characteristic "fingerprints" associated with infrared-active molecules. On the other hand, interferences from common atmospheric components such as $CO_2$ and $H_2O$ are significant, so that the sensitivity and detection limits that can be obtained are useful primarily for polluted urban air situations. For atmospheric work, long optical path lengths are needed. To obtain these, multiple-pass cells are commonly used. Such cells are also often used in UV–visible spectroscopic measurements in air, discussed in Section A.1.d.

***(1) Multipass cells*** There are several different configurations of multipass cells in use. The most common approach is a three-mirror multiple-pass cell (Fig. 11.1a) known as a *White cell* after the individual who first put forth the basic design (White, 1942). The light is first focused on the entrance to the cell. The beam diverges and falls on spherical mirror M1, which reflects the image and refocuses it onto mirror M2, known as the field mirror. The diverging beam from M2 is reflected to spherical mirror M3, which, like M1, reflects and refocuses the image at the opposite end of the cell. If the mirrors are adjusted so that this image is at the exit aperture of the cell, the light beam leaves and strikes a detector. A total of four passes of the cell has therefore been made and the effective path length for absorption is $L = 4a$, where $a$ is the length of the cell. However, the mirrors may be adjusted so that the reflected image from M3 falls on mirror M2 and is again reflected to M1 at a small angle to the original input light beam, leading to another set of four passes along the length of the cell.

For example, in the spot pattern shown in Fig. 11.1b, the beam enters the cell at the gap marked "0" in the field mirror and, after multiple reflections, exits at the gap in the field mirror on the opposite side, marked "28." A total of 28 passes (or $2n + 2$, where $n$ is the

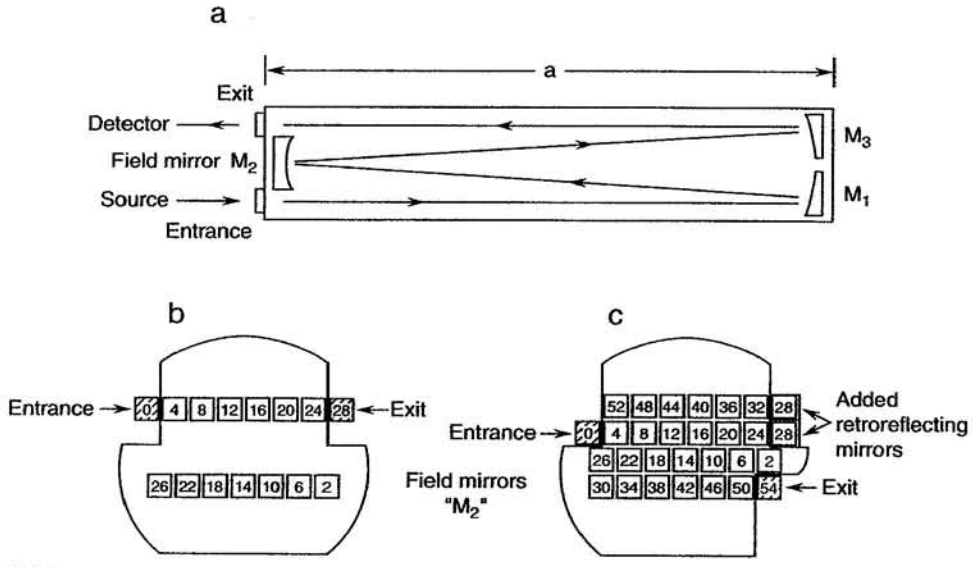


FIGURE 11.1 (a) Schematic diagram of a multipass White cell, (b) sequence of images on filled mirror for White cell design, and (c) sequence of images on field mirror for Horn and Pimentel design (1971). (Adapted from Finlayson-Pitts and Pitts, 1986; and Hanst and Hanst, 1994.)

number of spots on the field mirror) has been made in this case.

The advantage of such a White cell is that the source is reimaged on the field mirror M2 after each double traversal of the cell. This keeps the energy that enters the cell within the mirror system so that energy losses occur mainly through light absorption by the mirrors and, of course, by the gases in the cell. In practice, the loss of light energy through absorption by the mirrors imposes a major limitation on the number of passes that can be used. The fraction of the energy lost after $n$ reflections from a mirror whose reflectivity is $R$ is given by $(1 - R^n)$. Thus, if a mirror reflects 98% of the incident light and absorbs 2%, only 36% of the incident intensity will remain after 50 reflections from the mirror. After 100 reflections, only 13% of the incident intensity is left. While the path length and hence absorbance have increased, the energy loss may be so severe that such a large number of reflections becomes impractical.

The number of reflections is also limited by the size of the image striking the entrance and the size of the mirror M2. As seen in Fig. 11.1b, the images that are refocused from M1 and M3 onto the field mirror M2 are "stacked" beside each other. The width of M2 therefore determines how many of these images can be accommodated (i.e., how many reflections are possible). A practical problem arising when the images are too closely spaced (i.e., at long path length) is one of adjustment; temperature changes, for example, can cause very small changes in the mirror adjustments which result in moving the exit beam away from the exit aperture.

*Variations of the White cell are also in use.* For example, Horn and Pimentel (1971) added a corner mirror assembly to redirect the beam that would normally exit the cell back into it. This doubles the number of passes, giving four rows of spots on the field mirror. The image pattern for such a design is shown in Fig. 11.1c (Hanst and Hanst, 1994).

More complex multiple-reflection systems that give a much greater number of traversals have also been developed. For example, Tuazon *et al.* (1980) describe a system using four collecting mirrors that focus the light onto four field mirrors. The advantages and disadvantages of such multiple-mirror cells are discussed by Hanst (1971) and Hanst and Hanst (1994).

*An alternate design for folded optics was described* by White in 1976. In this design, the light beam is folded back on itself, giving larger path lengths and greater optical stability. The effects of vibration, thermal expansion, and astigmatism are reduced and alignment errors are minimized with this design.

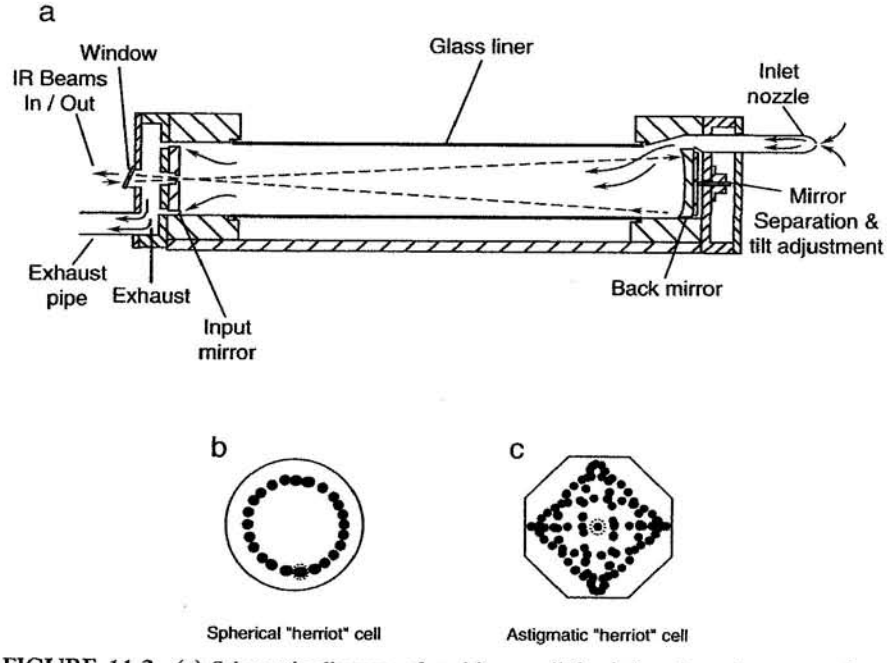


FIGURE 11.2 (a) Schematic diagram of multipass cell for infrared spectroscopy using astigmatic Herriott configuration (adapted from McManus *et al.*, 1995), (b) spot configurations for normal Herriott multipass cell, and (c) spot configurations for astigmatic configuration (adapted from Zahniser *et al.*, 1997).

A second multipass cell configuration is the Herriott cell (Herriott *et al.*, 1964; Herriott and Schulte, 1965). This is particularly useful for coherent light sources such as lasers used in tunable diode laser spectroscopy but has also been used with incoherent light sources using optical fibers cemented to a ball lens at the entrance to the cell (Zahniser, personal communication). Two spherical mirrors are separated by a distance close to their radius of curvature, and the light beam enters through a hole in one of them, directed in an off-axis direction. After multiple reflections between the two mirrors, the light beam exits through the same hole as it entered, but at a different angle (Fig. 11.2a). The beam remains collimated throughout, in contrast to the White cell system, and gives the spot pattern shown in Fig. 11.2b. The path length is changed by changing the distance between the mirrors; in practice this means that this design is most useful for fixed path length systems.

An astigmatic variant of the Herriott cell designed for use in ambient air studies is shown in Fig. 11.2a and described by McManus *et al.* (1995) and Zahniser *et al.* (1997). In this design, the two mirrors have different radii of curvature, giving the spot patterns shown in Fig. 11.2c. The spots more evenly fill the mirror, so that for a given number of passes, the spots are more widely spaced, or conversely, more passes can be obtained without problems of beam overlap (McManus *et al.*, 1995).

Major advantages of such cells are that they are relatively easy to align and folded optical paths can be obtained in small volumes. This is important when small amounts of sample are available, for example, in laboratory studies or when a fast response is needed; cells of smaller volume can be pumped out faster, giving shorter residence times in the cell.

*(2) **FTIR*** Fourier transform infrared spectroscopy has been used for many years to measure atmospheric gases. Because FTIR has become such a common analytical method, we do not describe the technique itself here but rather refer the reader to several excellent books and articles on the subject (e.g., see Griffiths and de Haseth, 1986; Wayne, 1987). For reviews of some atmospheric applications, see Tuazon *et al.* (1978, 1980), Marshall *et al.* (1994), and Hanst and Hanst (1994).

A problem in the application of FTIR to ambient air is that water vapor, $CO_2$, and $CH_4$ are all present in significant concentrations and absorb strongly in certain regions of the spectrum. As a result, the spectral regions that are useful for ambient air measurements are 760- to 1300-$cm^{-1}$, 2000- to 2230-$cm^{-1}$, and 2390- to 3000-$cm^{-1}$.

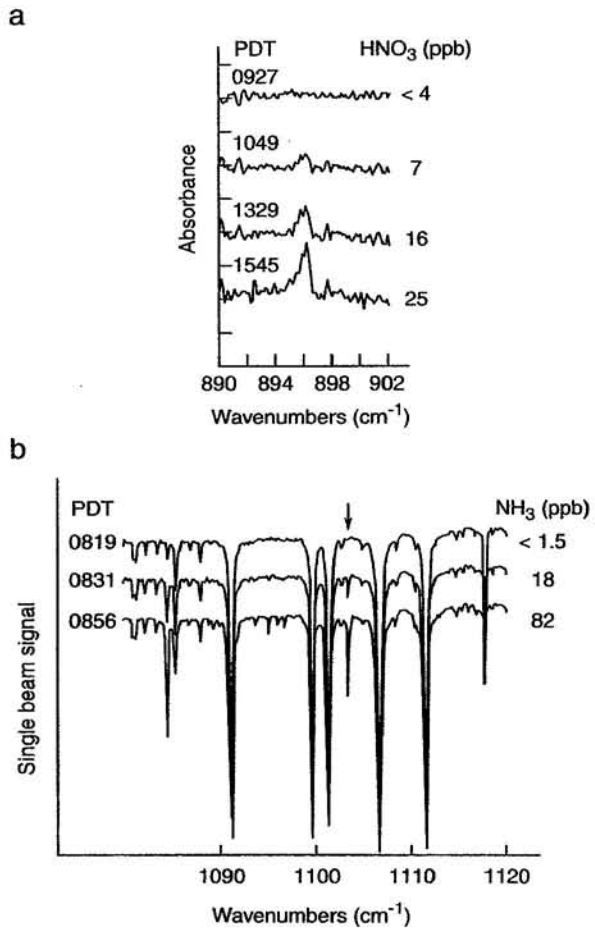


**FIGURE 11.3** Typical FT-IR spectra in ambient air as a function of time in (a) the $HNO_3$ region and (b) the $NH_3$ region on September 14 and 16, 1985, respectively, in Claremont, California. $NH_3$ peak is marked by the arrow. Concentrations of each are shown on the right-hand side (adapted from Biermann *et al.*, 1988).

Figure 11.3 shows typical ambient air spectra in two regions in which $HNO_3$ (Fig. 11.3a) and $NH_3$ (Fig. 11.3b), respectively, have characteristic absorption bands (Biermann *et al.*, 1988). Figure 11.4 shows, for comparison, some typical reference spectra for $HNO_3$ and $NH_3$ taken at much higher concentrations in a 25-cm-long cell (see Problem 6). It can be seen that the absorption bands in air even in a polluted urban area are relatively weak. However, FTIR has also proven particularly useful as a standard for intercomparison studies in polluted urban atmospheres (e.g., see Hering *et al.*, 1988).

Table 11.2 summarizes the detection limits for FTIR measurements in the atmosphere for some gases of interest. Typical concentrations of each in remote to polluted atmospheres are discussed below with respect to the individual species; however, in general, it can be stated that FTIR is most suitable for measuring

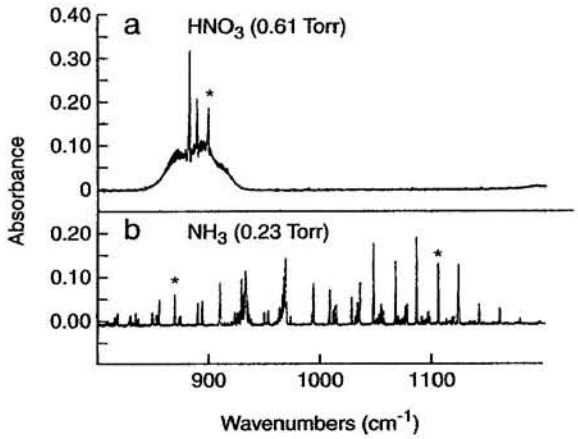


FIGURE 11.4 Reference spectra of gaseous $HNO_3$ and $NH_3$, respectively, at $L = 25$ cm and $P_{TOT} = 740$ Torr in $N_2$. Asterisks denote peaks used in analysis of ambient air (adapted from Biermann *et al.*, 1988).

atmospheric trace gases in polluted urban areas or close to sources where they are found at the highest concentrations.

For example, Yokelson *et al.* (1996, 1997a, 1997b) have used FTIR to measure species emitted from combustion processes; this has permitted the simultaneous measurement of such species as HCHO, $CH_3OH$, $CH_3OOH$, $C_2H_4$, $C_2H_2$, $C_3H_6$, $C_6H_5OH$, $CS_2$, HCN, and $NH_3$ produced in fires, in addition to CO, $CO_2$, and $CH_4$. Indeed, such FTIR studies permitted the first identification of 2-hydroxyethanal ($HOCH_2CHO$) in smoke from fires (Yokelson *et al.*, 1997a). Although such compounds could be detected and measured using chromatographic methods (see later), losses during sampling would likely be problematical, unlike open-pass FTIR, where the measurement can be made without direct sampling.

***(3) Tunable diode laser spectroscopy (TDLS)*** A second technique based on infrared absorption spectrometry is tunable diode laser spectrometry, TDLS. The practice and application of TDLS in atmospheric measurements have been reviewed by Schiff *et al.* (1994a, 1994b) and Brassington (1995) and in the symposium proceedings edited by Grisar *et al.* (1992). As in the case of FTIR, this technique relies on measuring the absorbance at specific wavelengths due to the absorption of IR radiation by various pollutants. However, rather than using a continuous-wavelength light source and scanning the entire infrared spectrum, tunable diode laser spectroscopy employs a laser light source of very narrow linewidth that is tunable over a smaller (e.g., 100–200 $cm^{-1}$) wavelength range.

TABLE 11.2 Detection Limits for Some Trace Gases in Air by FTIR,[a] TDLS[b], and Matrix Isolation IR[c]

| Gas | FTIR detection wavenumber ($cm^{-1}$) | FTIR detection limit[c] (ppb at $L = 1$ km) | TDLS detection wavenumber ($cm^{-1}$) | TDLS detection limit[d] (ppb at $L = 150$ m) | Matrix isolation detection limit[e] (ppb) |
|---|---|---|---|---|---|
| $SO_2$ | 1133 | 25[g] | 1360.7 | 0.5 | 0.01 |
| $NH_3$ | 931 | 4 | 1065 | 0.025 | |
| | 967.5 | 3 | | | |
| | 993 | 4 | | | |
| HCHO | 2779, 2781.5 | 6 | 2781 | 0.05 | 0.03 |
| HCOOH | 1105 | 2 | 1107 | 1.0 | 0.02 |
| $HNO_3$ | 896 | 6 | 1720 | 0.1 | 0.01 |
| $N_2O_5$ | 740, 1248 | 4 | | | 0.02[f] |
| HONO | 791 (*trans*) | 10 | | | 0.01 |
| | 853 (*cis*) | | | | |
| PAN | 1162 | 3 | | | 0.05 |
| $H_2O_2$ | 1251 | 40 | 1285.7 | 0.1 | |

[a] From Tuazon *et al.* (1980).
[b] From Schiff *et al.* (1994b).
[c] Resolution 0.5 $cm^{-1}$.
[d] 150 m, integration time 3–5 min.
[e] From Griffith and Schuster (1987); for a 15-L air sample.
[f] Based on laboratory spectra only.
[g] From E. Tuazon, personal communication, 1998.

The advantages of TDLS over FTIR are increased resolution and sensitivity. The widths of the laser lines are less than $10^{-4}$ $cm^{-1}$. This can be compared to typical pressure-broadened half-widths of infrared absorption bands of species of atmospheric interest, which are of the order of 0.05 $cm^{-1}$ at atmospheric pressure; at low pressures (e.g., <1 Torr), where the linewidth is limited by Doppler broadening, typical half-widths are 0.0005–0.005 $cm^{-1}$. Thus the TDL output is usually sufficiently narrow to scan rotational absorption lines even at low pressures where Doppler broadening is the limiting factor on lineshape. This narrow laser linewidth allows one to measure weak absorptions between the ambient $H_2O$ and $CO_2$ lines. Thus one can measure accurately small absorbances due to specific rotational lines in a vibration–rotation spectrum with high selectivity. However, for many molecules of interest, the presence of such rotational fine structure requires lowering the total pressure of the sample to ~10–30 Torr to minimize pressure broadening of the absorption lines. (For larger molecules, the absorption spectrum appears as a continuum even at these lowered pressures.)

A disadvantage of TDLS is that scanning the entire IR spectrum quickly is not possible since each diode normally covers a limited wavelength range and even the use of several diodes in one instrument does not provide the wide range of FTIR. Thus TDLS is more useful for following specific pollutants known to be present than for searching for previously unidentified species. In addition, the high-resolution capability is not of use for very large molecules with many overlapping bands. While reducing the pressure of the sample helps in reducing the absorbing linewidth, it also results in a loss of sensitivity through reductions in concentration and the possibility of interactions with the walls of the cell.

Commonly used tunable diode lasers are made of lead salt compounds such as $PbS_{1-x}Se_x$, $Pb_{1-x}Sn_xTe$, $Pb_{1-x}Ge_xTe$, $Pb_{1-x}Sn_xSe$, and $Pb_{1-x}Cd_xS$. Diodes made from Group III (Ga, Al, and In) and Group V (P, As, and Sb) elements are not in widespread use for atmospheric applications because they emit at wavelengths beyond 2 $\mu$m (5000 $cm^{-1}$) where the molecular absorptions are much weaker overtone and combinaton bands, limiting the detection sensitivity (Schiff *et al.*, 1994a, 1994b; Brassington, 1995). A p–n junction is formed in the crystal and the diode is mounted onto a support such as copper that serves as a temperature controller during operation. When an electrical current is applied, the diode emits light spontaneously at a wavelength corresponding to the energy band gap in the semiconductor. Laser action results from reflections from the end faces of the crystal. This gap depends on the chemical composition of the laser and hence different wavelengths from 3 to 30 $\mu$m (3300–330 $cm^{-1}$) can be produced by altering the diode composition. The actual structure of these devices is more complex than a simple p–n junction, typically involving double heterostructures (e.g., see Brassington, 1995).

Tuning of the emitted wavelength can be accomplished, in principle, through variation of one of three possible parameters: applied magnetic field strength, diode temperature, and hydrostatic pressure. In practice, temperature, which can be controlled by changing the current through the diode, is used. Typical variations of output with temperature are about 3 $cm^{-1}$ per K (Brassington, 1995). Figure 11.5, for example, shows the output of laser frequency as a function of temperature from a lead salt diode laser (Werle *et al.*, 1992). The output at a given current is a series of longitudinal modes whose separation, typically about 2 $cm^{-1}$, is determined by $(2\eta L)^{-1}$, where $\eta$ is the index of refraction of the salt (usually 4.5–7) and $L$ is the length of the laser cavity, i.e., separation of the end faces of the crystal (typically 300–400 $\mu$m). Tuning of such semiconductor lasers over ~100–200 $cm^{-1}$ can typically be carried out, which is sometimes sufficient to measure more than one pollutant with a single laser. Alternatively, several different diode lasers are included in the same apparatus.

A number of different modulation techniques can be used to increase the signal-to-noise ratio (e.g., see Schiff *et al.*, 1994a, 1994b; and Brassington, 1995). For example, the laser beam can be mechanically chopped and detected using phase-sensitive detection with a lock-in amplifier. A more commonly used method for accurately measuring small absorbances is to modulate

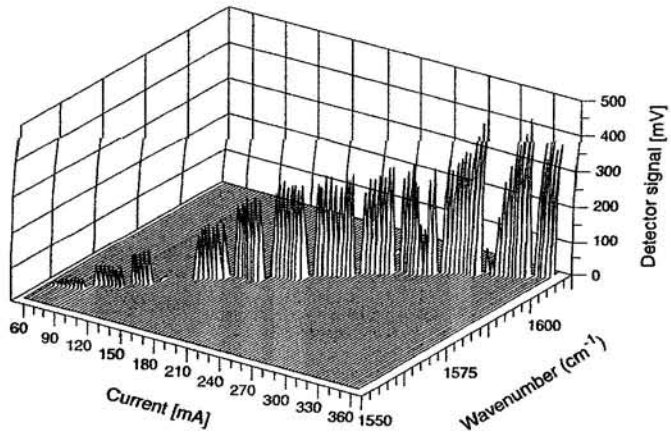


**FIGURE 11.5** Variation of laser frequency and signal with current for a typical lead salt diode laser (adapted from Werle *et al.*, 1992).

the frequency output of the laser by modulating the current and thus the temperature of the diode (Reid *et al.*, 1978). Absorbances down to $\sim 10^{-5}$ to $3 - 10^{-6}$ can be measured using multipass cells, corresponding to ppb to sub-ppb concentrations for many pollutants of atmospheric interest; the limits for open-reflection systems are not as good ($10^{-3}$–$10^{-4}$) due to interference from atmospheric turbulence (Schiff *et al.*, 1994a, 1994b).

Figure 11.6 shows the major elements of a typical TDLS apparatus used for aircraft measurements (Hastie *et al*, 1983). Two diode lasers can be mounted on the dewar cold finger used for temperature/wavelength tuning; one is chosen for use by moving it into the appropriate position. A series of flat and off-axis parabolic mirrors are used to direct the laser beam into a White cell through which the air is pumped and back out to the sample detector. The He–Ne laser is used for alignment. A reference cell containing a high concentration of the species of interest can be inserted into the light path for calibration.

Figure 11.7 shows a typical $2f$ spectrum for the 1597-$cm^{-1}$ line of $NO_2$ obtained using this apparatus, compared to a calibration obtained using 1.4 ppb $NO_2$. Fitting the ambient air spectrum to the reference gives an ambient air concentration of 72 ppt (Schiff *et al.*, 1990).

TDLS is particularly useful for species such as $H_2O_2$ that are present at small concentrations and while very important in atmospheric chemistry, are difficult to measure. Figure 11.8 compares ambient $H_2O_2$ concentrations measured using TDLS and a wet scrubbing with enzyme fluorescence technique (Kleindienst *et al.*, 1988a; Schiff *et al.*, 1994a, 1994b). The two are generally in agreement to within about 30%.

Table 11.2 gives reported detection limits for some gases that have also been measured in the atmosphere by FTIR. As expected, the sensitivity of TDLS is significantly better than that of FTIR. For most species of atmospheric interest, detection limits are $\sim 0.1$ ppb for measurement times of 1 min in a 200-m White cell (G. Mackay, personal communication, 1998).

***(4) Nondispersive infrared spectroscopy (NDIR)*** Figure 11.9 is a schematic diagram of the major components of an NDIR device (Skoog *et al.*, 1998). As the name implies, it measures infrared-absorbing gases without dispersing the radiation or using FT techniques to derive wavelength-dependent signals. This method is also referred to as gas filter correlation. Infrared radiation is directed into two cells, one of which (the reference cell) is filled with a non-infrared-absorbing gas and the second of which (the sample cell) holds the sample (in a flow mode). The IR beams passing through the two cells then individually strike the compartments of the sensor cell, which are filled with the gas of interest and are separated by a thin, flexible metal diaphragm. When IR reaches this sensor cell, it is absorbed, causing heating and hence changes in pressure.

If the concentration of the absorbing gas is zero in the sample cell, the radiation striking both compartments is the same, and hence the heating is the same and there is no movement of the diaphragm separating

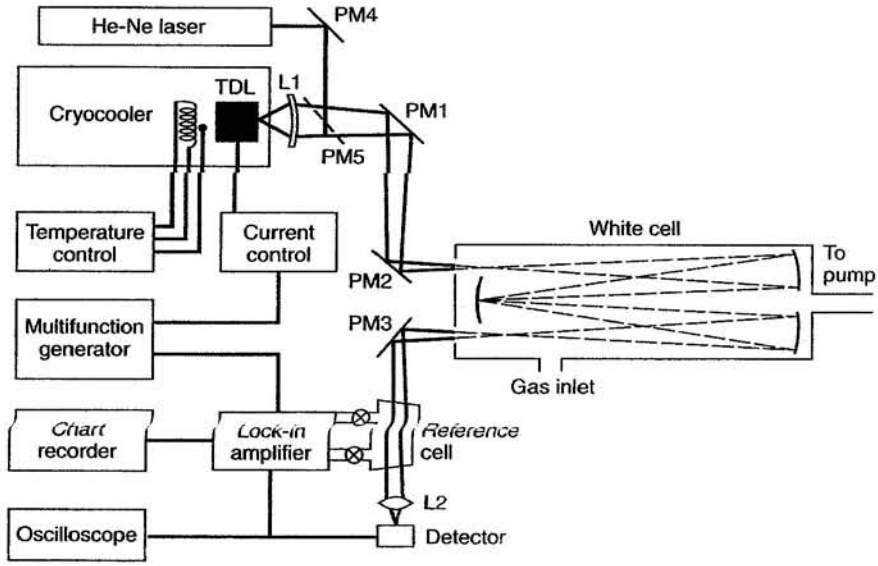


FIGURE 11.6 Schematic diagram of a TDLS apparatus (adapted from Hastie *et al.*, 1983).

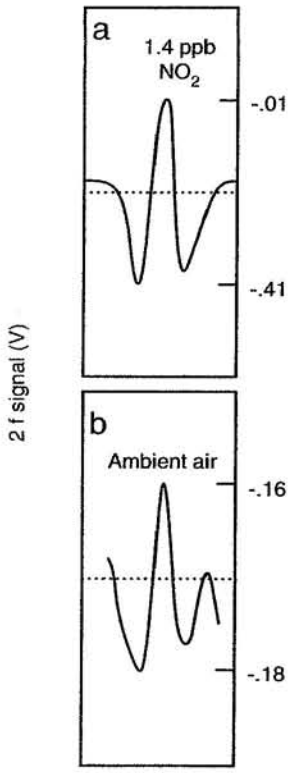


FIGURE 11.7 Typical TDLS spectra of $NO_2$ in the 1597-$cm^{-1}$ region: (a) calibration spectra of 1.4 ppb $NO_2$; (b) ambient air, corresponding to 72 ppt $NO_2$ (adapted from Schiff *et al.*, 1990).

the two compartments of the sensor cell. However, if the gas of interest is present in the sample cell, it absorbs some of the IR, and less reaches that compartment of the sensor cell. This results in uneven heating of the two compartments of the sensor and higher pressures on the reference side. This moves the flexible metal diaphragm to the right, and the movement is measured by a change in capacitance between the diaphragm and a fixed capacitance plate. This method is used for CO, for example (Table 11.1). Atmospheric systems and applications of NDIR are described by Hanst and Hanst (1994).

*(5) **Matrix isolation spectroscopy (MI)*** Matrix isolation was first used in laboratory studies about four decades ago by Pimentel and co-workers (Whittle *et al.*, 1954). The method involves condensing the sample along with an inert "matrix" substance onto a cold infrared-transmitting or infrared-reflecting surface. At low temperatures in a matrix, rotation is essentially stopped for all but a very few small species. As a result, the infrared absorption is due solely to the vibrational transition, giving a single strong band instead of a series of rotational lines around the (0,0) vibrational

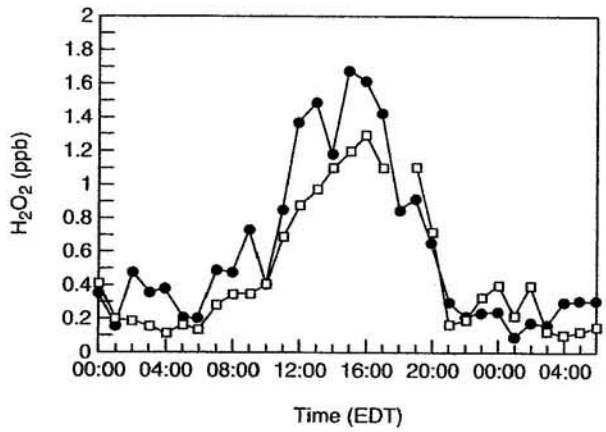


FIGURE 11.8 Ambient $H_2O_2$ concentrations measured by TDLS (●) and the continuous scrubbing enzyme fluorometric technique (□) during the period June 24–26 at Research Triangle Park, North Carolina (adapted from Schiff *et al.*, 1994a, 1994b).

transition. The low temperature of the matrix, lack of diffusion in the matrix, and the isolation of trapped molecules also help to minimize decomposition and other reactions of labile species.

This approach has also been used in the analysis of air by infrared spectroscopy (e.g., see Griffith, 1994). As discussed later, matrix isolation has also been used in conjunction with electron spin resonance (ESR) to measure free radical species, including $NO_2$, $NO_3$, $HO_2$, and $RO_2$.

In the matrix-FTIR studies, about 10–80 L of air is typically trapped using either a liquid nitrogen or liquid argon trap. At these temperatures, $N_2$, $O_2$, $H_2$, $CH_4$, and CO are not trapped, but $CO_2$ and trace gases are. The $CO_2$ in air acts as the inert matrix material when the sample is condensed on the infrared sample stage

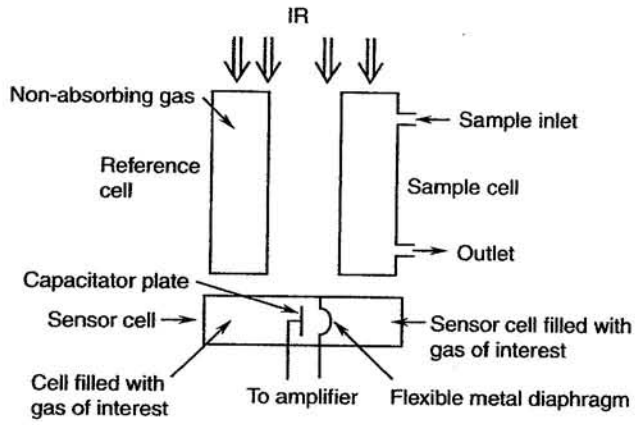


FIGURE 11.9 Schematic diagram of nondispersive infrared device (adapted from Skoog *et al.*, 1998).

in the second step. Water must be removed either before or after collection of the sample to minimize its contribution to absorption and scattering of IR. The cryogenically trapped air sample is then transferred to a low-temperature window for infrared analysis, usually by reflection–absorption spectroscopy. The $CO_2$ matrix is used as an internal standard, and because its concentration in air is well known (see Chapter 14), the concentrations of the trapped gases can be obtained from the strength of their infrared absorptions compared to those of $CO_2$.

Table 11.2 also shows the detection limits for some atmospheric gases using MI infrared spectoscopy and a 15-L air sample (Griffith and Schuster, 1987). Clearly, this technique can measure quite small concentrations, typically in the ppt range. The disadvantage is that in the configuration used to date, samples must be collected and brought back to the laboratory for analysis. As a result, it is not a "real-time" measurement, as is the case for FTIR and TDLS. In addition, the possibility of reactions during sampling and transfer onto the analysis window must be considered.

### *d. DOAS (UV–Visible Absorption Spectroscopy)*

***(1) Basis of technique*** Because of the relatively large absorption cross sections in the UV and visible for many gases of atmospheric interest, use of absorption spectroscopy in this region presents an obvious analytical approach. In the case of laboratory studies, measurement of the light intensity in the absence ($I_0$) and presence ($I$) of the species of interest is readily applied to obtain concentrations using the Beer–Lambert law (see Chapter 3.B):

$$A = \ln(I_0/I) = \sigma NL, \qquad \text{(A)}$$

where $\sigma$ is the absorption cross section ($cm^2$ $molecule^{-1}$), $N$ is the concentration (molecules $cm^{-3}$), and $L$ is the path length.

However, the fact that so many species in air absorb in this region presents a limitation in that one must be able to distinguish various species from each other as well as from background broad absorption and Rayleigh and Mie scattering of light by gases and particles. Because of these factors, UV–visible spectroscopy is, in practice, applied in air only to those species with banded structures, i.e., "fingerprints," of width ~5 nm or less. The technique used to do this is differential optical absorption spectrometry (DOAS). For reviews of DOAS, see Platt (1994) and Plane and Smith (1995).

Figure 11.10 illustrates the basis of this technique for a species that has narrow absorption bands at wavelengths $\lambda_A$ and $\lambda_B$, superimposed on a slowly varying background. Because of Rayleigh and Mie scattering, the "true" $I_0$ shown by the upper dashed line, i.e., the intensity in the absence of air, cannot be measured. Scans of this spectral region do allow the broad background $I_0'$, however, to be interpolated from the measurements of $I(\lambda)$. Thus, rather than measuring $(I_0/I)$, the ratios $(I_0^{A'}/I_A)$ and $(I_0^{B'}/I_B)$ are measured and used to obtain the concentration of the absorbing species. That is, one is measuring the *differential* optical absorption ($D$) rather than the true optical absorption ($A$). However, this can be used for measuring concentrations as well since the differential optical absorption also follows a Beer–Lambert relationship:

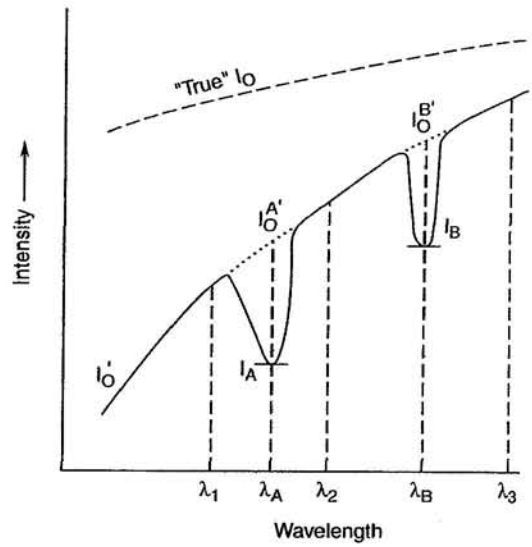


FIGURE 11.10 Light intensities relevant to DOAS spectrometry.

$$D = \ln(I_0^{A'}/I_A) = \sigma' NL. \qquad \text{(B)}$$

In this case, $\sigma'$ is the differential optical absorption cross section for the absorption band. In practice, of course, there are many different absorbers, $i$, present at different concentrations $N_i$ and absorbing at different wavelengths over the path length $L$.

Returning to Fig. 11.10, the relationship between $I$ and the "true" $I_0$ can be expressed as

$$I(\lambda) = I_0(\lambda)A(\lambda)e^{\{-L[\Sigma\sigma_i(\lambda)N_i + \varepsilon_R(\lambda) + \varepsilon_M(\lambda)]\}}. \qquad \text{(C)}$$

In Eq. (C), $A(\lambda)$ is an attenuation factor characteristic of the measurement system, $\varepsilon_R$ and $\varepsilon_M$ are the equivalent extinction coefficients due to Rayleigh and Mie scattering of gases and particles, and $\sigma_i$ are the total absorption cross sections of the absorbing gases, all of which are wavelength dependent. Although the Rayleigh and Mie scattering contributions are not absorption processes, their contributions to the reduction

in light intensity can be treated for DOAS measurements as if they were. The value of $\varepsilon_R(\lambda)$ is $1.3 \times 10^{-6}$ $cm^{-1}$ at 300 nm for STP conditions, reducing the light intensity by about 12% in each kilometer. The value of $\varepsilon_M(\lambda)$ strongly varies with aerosol loading. Typical values at 300 nm range from $1 \times 10^{-6}$ $cm^{-1}$ for clean maritime air (without sea spray) to $\sim 10^{-5}$ $cm^{-1}$ for rural continental air. However, fog or heavy pollution can limit the application of DOAS because of the associated high values of the extinction.

The total absorption cross sections ($\sigma_i$) of a single trace gas $i$ can be broken down into a contribution from the structured portion, $\sigma_i'$, and one from the broadband portion that varies only slowly with wavelength, $\sigma_i^B$:

$$\sigma_i = \sigma_i' + \sigma_i^B. \qquad \text{(D)}$$

Substituting into Eq. (C), one obtains

$$I(\lambda) = \left\{I_0(\lambda) A(\lambda) e^{-L[\Sigma \sigma_i^B(\lambda) N_i + \varepsilon_R(\lambda) + \varepsilon_M(\lambda)]}\right\} e^{-L[\Sigma \sigma_i'(\lambda) N_i]}$$
$$= I_0'(\lambda) e^{-L[\Sigma \sigma_i' N_i]}. \qquad \text{(E)}$$

Taking natural logarithms, the differential optical absorbance ($D'$) is given by

$$D'(\lambda) = \ln[I_0'(\lambda)/I(\lambda)] = L[\Sigma \sigma_i'(\lambda) N_i]. \qquad \text{(F)}$$

A major advantage of DOAS is its high sensitivity for species that meet the requirement of having narrow absorption bands in the UV–visible. Furthermore, because the differential optical absorption coefficients are fundamental spectroscopic properties of the molecule, the measurements need not be calibrated in the field.

***(2) Analysis of spectra*** Different approaches to spectral analysis are described by Platt (1994) and Plane and Smith (1995). Calibration spectra of the absorbing species must be available for fitting the DOAS spectra. These spectra are usually obtained using the same instrument and settings. However, literature spectra of the same or higher resolution can be used if they are converted to the same resolution as used in the measurements.

To quantify the measured spectra, a combination of linear and nonlinear least-squares fitting routines are used, in which the measured intensities are fit to those of scaled reference spectra while minimizing the residual absorbance. Taking the natural logarithm of Eq. (E), one obtains

$$\ln I(\lambda) = \ln I_0'(\lambda) - L[\Sigma \sigma_i'(\lambda) N_i]. \qquad \text{(G)}$$

This is of the form

$$F(\lambda) = P(\lambda) + \Sigma a_j S_j(\lambda), \qquad \text{(H)}$$

where $a_j$ are scaling factors for each species $j$ chosen to give the best fit to the total spectrum and $S_j$ are the known reference absorption spectra of each of the species. It has been observed that the term $P(\lambda)$ in Eq. (H), which contains the components that vary slowly with wavelength, i.e., $I_0(\lambda)$, $A(\lambda)$, $\varepsilon_R(\lambda)$, $\varepsilon_M(\lambda)$, and $\sigma_i^B(\lambda)$, can be approximated by a polynomial function of the form $P(\lambda) = \Sigma a_n \lambda^n$, where $n$ is typically $\sim 5$. Thus, $\ln I(\lambda)$ is fit using least-squares analysis with combination of a polynomial and the second term to obtain the scaling factors $a_j$. From these scaling factors and the known path length, $L$, the concentration of the absorber $j$ can be calculated. Care must be taken to ensure that the wavelengths are properly calibrated (e.g., using a low-pressure Hg lamp) and that small drifts in the spectra due to thermal drift (typically $\sim 0.1$ pixel $K^{-1}$) are taken into account. In addition, changes in air pressure can cause shifts, $\sim 0.2$ pixels in going from 1000 to 750 mbar. Such problems and the details of analysis of DOAS spectra, including methods of error estimation, are discussed by Stutz and Platt (1996).

***(3) Typical apparatus*** Figure 11.11 is a schematic diagram of the components of a typical DOAS system. A broadband light source is needed, which, for example, can be a high-pressure Xe or incandescent quartz–iodine lamp, a broadband laser, or the sun or moon. The light traverses the air sample, either in a single-pass system or in a multipass system using an open White cell. The light strikes the entrance slit of a spectrograph which disperses the radiation. Detection as a function of wavelength of the dispersed light is carried out using a slotted-disk mechanism or, more commonly, a photodiode array (PDA) or charge-coupled device (CCD).

The use of the sun or moon as the light source allows one to measure the total column abundance, i.e., the concentration integrated through a column in the atmosphere. This approach has been used for a number of years (e.g., see Noxon (1975) for $NO_2$ measurements) and provided the first measurements of the nitrate radical in the atmosphere (Noxon *et al.*, 1978). As discussed later in this chapter, such measurements made as a function of solar zenith angle also provide information on the vertical distributions of absorbing species. Cloud-free conditions are usually used for such measurements; as discussed by Erle *et al.* (1995), the presence of tropospheric clouds can dramatically increase the effective path length (by an order of

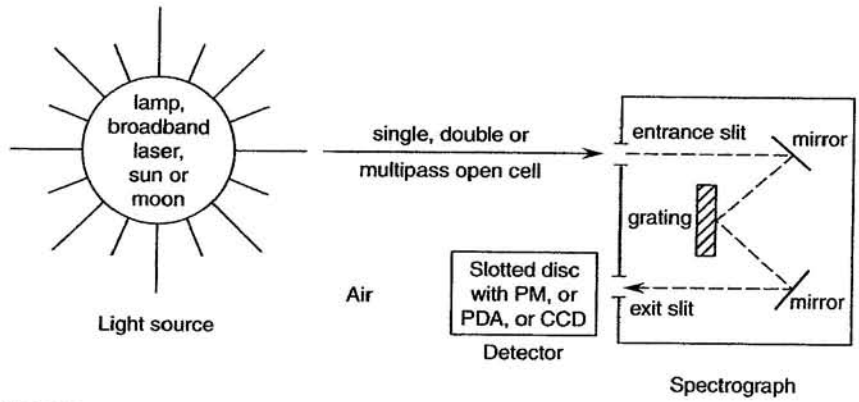


FIGURE 11.11 Schematic diagram of components of a DOAS system.

magnitude) through the atmosphere because of Mie scattering by the cloud droplets.

Surface-based instruments have also been developed for the application of DOAS to measure the integrated absorptions either over long direct path lengths or over folded light paths that give large total path lengths and hence high sensitivity but more closely approximate point measurements. There are two common approaches that have been used. In the earlier systems, a slotted-disk arrangement with a photomultiplier was used. These have been largely supplanted by the use of photodiode arrays.

In conventional spectroscopy, the grating of the spectrograph disperses the light so that the spectrum spreads out across the exit plane. The exit slit is stationary and wavelength scanning is achieved by slowly rotating the grating so that a series of wavelengths strike the exit sequentially and are detected by the photomultiplier. However, this is not suitable for ambient air studies where atmospheric turbulences with frequencies of $<10$ Hz make it desirable that spectra be scanned at rates $>100$ Hz. The use of the slotted disk, developed by Platt, Perner, and co-workers, allows one to attain the high scan rates needed. In this technique, the conventional exit slit is replaced by a mask that allows a 6- to 40-nm segment of the dispersed spectrum to fall on a rotating wheel, with the central wavelength set by the spectrograph wavelength setting. The rotating wheel contains a number of narrow slits (typically 50) around its perimeter. As seen in Fig. 11.12, as the wheel rotates, the slits "scan" the portion of the spectum dispersed across the monochromator exit slit. The slits in the rotating wheel are sufficiently well spaced that only one rotating slit is in the aperture at one time and also sufficiently narrow that only the light from a small portion of the dispersed spectrum passes through the rotating slit to the detector.

The signal, detected using a photomultiplier, is measured at several hundred different locations of the rotating slit across the exit aperture (i.e., at several hundred different wavelength intervals), and these signals are stored in different channels of a computer for subsequent data analysis. The light barrier on the edge of the mask shown in Fig. 11.12 triggers the computer so that as a rotating slit enters the mask aperture, data accumulation is started. As each rotating slit crosses the exit plane of the monochromator and performs one scan, the signals are added to the appropriate channels in the computer, resulting in many scans being superimposed; this signal averaging increases the signal-to-noise ratio.

As described in standard analytical chemistry books (e.g., Skoog *et al.*, 1998), photodiode arrays consist of a series (typically 1024) of side-by-side semiconductor rectangular detectors, or pixels. In this second type of DOAS instrument, the exit slit of the spectrograph is replaced by the photodiode array detector (PDA). Light striking the spectrograph grating is dispersed onto the PDA. The particular range of wavelengths striking the PDA is determined by the rotation of the grating, and

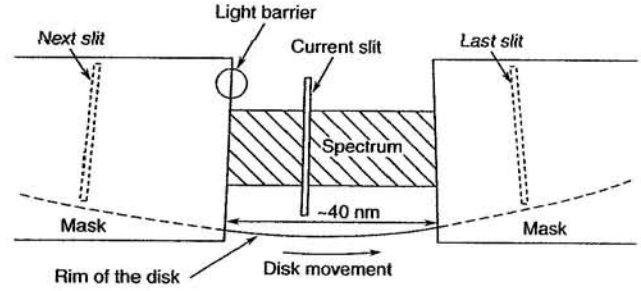


FIGURE 11.12 Schematic diagram of slotted-disk rapid-scanning mechanism used in DOAS studies (adapted from Platt, 1994).

the resolution, i.e., nanometers per pixel, by the entrance slit width. For example, a typical spectral range covered in one scan or set of scans is 40 nm, and with a 1024-element PDA, the resolution is then 40 nm/1024 pixels = 0.04 nm per pixel.

The advantage of using a PDA is that it records all wavelengths simultaneously, the so-called "multiplex" advantage. As a result, total photons detected are about 100–500 times greater in a given time period than for the slotted-disk arrangement, resulting in at least an order of magnitude increase in signal-to-noise (Stutz and Platt, 1997). However, there are some complications with using PDA that must be taken into account. First, the response of each of the pixels is not identical, which must be taken into account, for example, using multichannel scanning techniques described by Brauers *et al.* (1995). Second, under atmospheric conditions, different angles of incidence of the light on the PDA can give rise to "residual structures" in the spectrum that remain after all of the true absorptions have been removed; these can be quite large, of the order of $10^{-2}$ absorbance units, thus limiting the sensitivity to an order of magnitude less than the slotted-disk instruments. The use of a quartz fiber mode mixer overcomes this problem by acting as a diffuser, providing even illumination of the PDA with relatively small losses (~20%) in the intensity (Stutz and Platt, 1997).

***(4) Typical DOAS spectra and detection limits*** Table 11.3 shows detection limits for some gases of atmospheric interest at a path length of 5 km for the slotted-disk and PDA techniques, respectively, and for the PDA at a path length of 15 km (Stutz and Platt, 1997). Also shown are detection limits for a 5-km path length estimated by Plane and Smith (1995). With the improvements in the PDA method described by Stutz and Platt (1997), the sensitivity is as good as, or better than, that using the slotted-disk approach. Detection limits for 15 km using the PDA vary from sub-ppt levels for $NO_3$ to about 100 ppt for HCHO.

Figure 11.13 shows a typical DOAS spectrum measured in air after correcting for atmospheric background light and an electronic offset (Stutz and Platt, 1997). Below the spectrum are shown reference spectra for the gases that contribute to the atmospheric spectrum, scaled by the $a_j$ factors determined using Eq. (H). In this case, $O_3$, $NO_2$, $SO_2$, and HCHO all contribute, leaving a residual spectrum with a peak-to-peak absorbance of $6 \times 10^{-4}$.

DOAS has proven particularly useful for $NO_3$, for which other widely used methods are not available, and for HONO. In the latter case, denuder techniques have been applied, but a great deal of care must be exercised to recognize and, if possible, avoid artifacts (see later). Figure 11.14 shows the application of DOAS to the measurement of the nitrate radical during the night in Riverside, California. Since $NO_3$ photolyzes rapidly, it is only detectable at night. Bands at 623 and 662 nm can be seen growing in, peaking in this case at ~290 ppt around 8 p.m. local time (Platt *et al.*, 1980b). As discussed in Chapter 7.D, the diurnal profile and time of the peak are quite variable, depending not only on its rate of formation but also on the scavenging processes.

DOAS has also been used for the measurement of the OH (see later) as well as BrO, ClO, and IO free radicals in the atmosphere (Platt and Hausmann, 1994; Platt and Janssen, 1995; Tuckermann *et al.*, 1997; Hebestreit *et al.*, 1999; Alicke *et al.*, 1999), all of which have absorption bands in the UV (see Chapter 4 and DeMore *et al.* (1997)). For example, Fig. 11.15 shows OH concentrations measured as a function of time using DOAS (Dorn *et al.*, 1996). The OH bands clearly

TABLE 11.3 Detection Limits for DOAS Measurements of Some Gases of Atmospheric Interest Using the Slotted-Disk or Photodiode Array (PDA) Techniques[a,b]

| Gas | Technique | Path length | Detection limit | |
|---|---|---|---|---|
| | | | Platt *et al.*[a] | Plane *et al.*[b] |
| $O_3$ | Slotted disk | 5 | 2 ppb | 2 ppb |
| | PDA | 5 | 0.17–1.4 ppb | |
| | PDA | 15 | 0.2–0.45 ppb | |
| $SO_2$ | Slotted disk | 5 | 100 ppt | 10 ppt |
| | PDA | 5 | 50–100 ppt | |
| | PDA | 15 | 16–33 ppt | |
| $NO_2$ | Slotted disk | 5 | 200 ppt | 50 ppt |
| | PDA | 5 | 100–200 ppt | |
| | PDA | 15 | 33–66 ppt | |
| HCHO | Slotted disk | 5 | 500 ppt | 50 ppt |
| | PDA | 5 | 200–500 ppt | |
| | PDA | 15 | 66–166 ppt | |
| HONO | Slotted disk | 5 | 60 ppt | 30 ppt |
| | PDA | 5 | 30–60 ppt | |
| | PDA | 15 | 10–20 ppt | |
| $NO_3$ | Slotted disk | 5 | 2 ppt | 0.4 ppt |
| | PDA | 5 | 1–3 ppt | |
| | PDA | 15 | 0.33–1 ppt | |
| OH | PDA | 5 | $1.5 \times 10^6$ cm$^{-3}$ (0.06 ppt) | $3 \times 10^6$ cm$^{-3}$ (0.12 ppt) |
| ClO | PDA | 5 | 1 ppt | 20 ppt |
| BrO | PDA | 5 | 0.5 ppt | 30 ppt |
| IO | PDA | 5 | 0.4 ppt | 10 ppt |

[a] Adapted from Stutz and Platt (1997) and Platt and Hausmann (1994).

[b] From Plane and Smith (1995) for $L = 5$ km and a minimum optical density of $10^{-4}$.

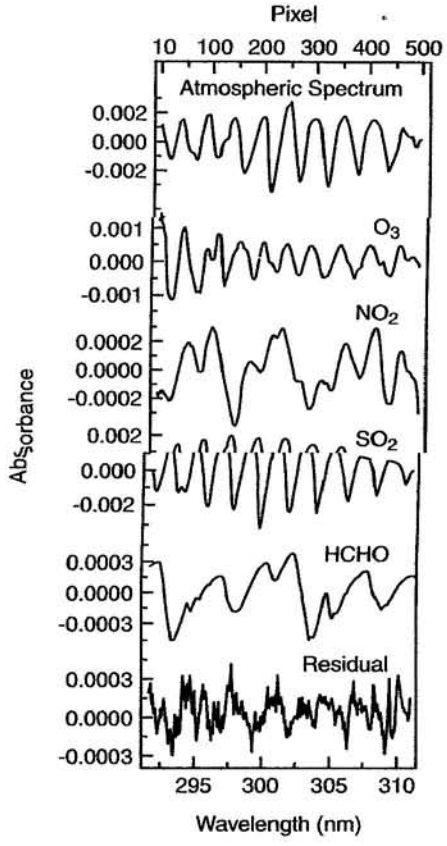


FIGURE 11.13 Typical spectrum measured using DOAS and its component contributions (see text) (adapted from Stutz and Platt, 1997).

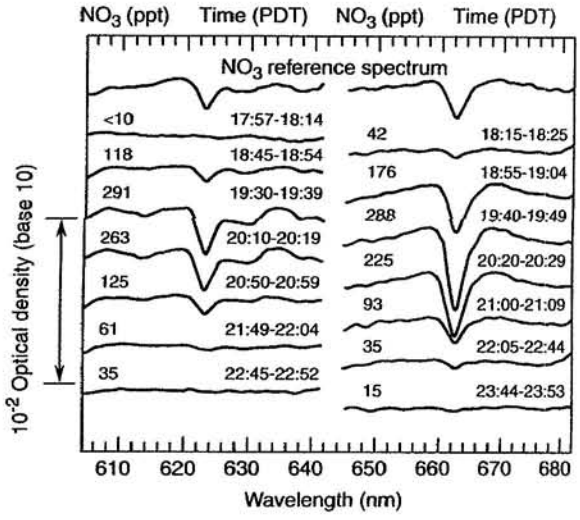


FIGURE 11.14 Measurement of $NO_3$ using DOAS in Riverside, California, on the evening of September 12, 1979 (adapted from Platt *et al.*, 1980b).

grow in as the sun comes up, initiating photolysis which forms OH (see Chapter 1.B).

As discussed in Chapter 6.J.4, there is a halogen-catalyzed destruction of surface-level $O_3$ at polar sunrise in the Arctic and bromine atoms are believed to be the major reactant destroying $O_3$:

$$Br + O_3 \rightarrow BrO + O_2. \qquad (5)$$

In this case, BrO should be generated, and indeed, it has been observed by DOAS under these conditions at concentrations up to ~30 ppt (Tuckermann *et al.*, 1997). Figure 11.16 shows a DOAS spectrum taken at polar sunrise at Alert in April 1992 and a reference spectrum of BrO (instrument features are included in this); clearly, BrO is present, in this case at a concentration of 17 ppt (Platt and Hausmann, 1994). BrO has also been detected at the Dead Sea, Israel, and attributed to heterogeneous reactions of the sea salt. ClO has also been detected at concentrations up to ~40 ppt under these conditions using DOAS (Tuckermann *et al.*, 1997), and IO in a midlatitude coastal marine environment in Ireland at concentrations up to 6 ppt (Alicke *et al.*, 1999).

Table 11.3 gives detection limits reported for DOAS measurements of OH and the halogen oxide radicals at a path length of 5 km and assuming a detectable absorbance of $10^{-4}$. This method provides ppt to sub-ppt sensitivities for these radicals.

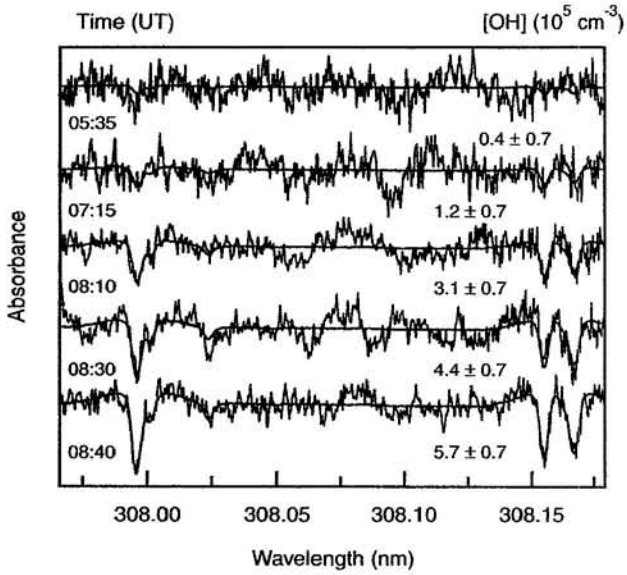


FIGURE 11.15 Measurement of OH using DOAS as a function of time (UT) after subtraction of the contributions of other known absorbers. The solid lines through the data are OH reference spectra (adapted from Dorn *et al.*, 1996).

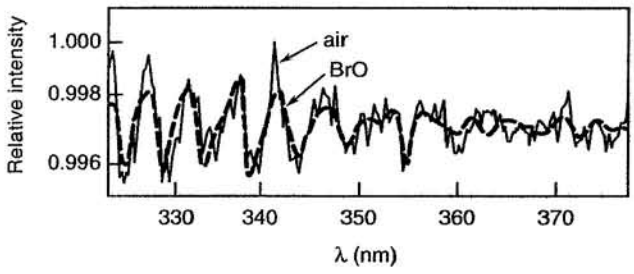


FIGURE 11.16 DOAS spectrum taken at Alert, N.W.T., on April 20, 1992, overlaid by fitted BrO reference spectrum (---) (adapted from Platt and Hausmann, 1994).

## 2. Mass Spectrometry

Mass spectrometry has the potential for being a very powerful analytical technique for atmospheric measurements, and indeed, it has been used for a number of decades in upper atmosphere measurements of ions and neutrals. Viggiano (1993) has reviewed ion chemistry and the application of mass spectrometry to tropospheric and stratospheric measurements through 1993. The first mass spectrometric measurements were made in the upper atmosphere from 64 to 112 km in 1963 (Narcisi and Bailey, 1965), followed by stratospheric measurements in 1977 (Arnold *et al.*, 1977) and, finally, tropospheric measurements in 1983 (Eisele, 1983; Heitmann and Arnold, 1983). They have also been extended to measurements in jet aircraft exhaust (e.g., Arnold *et al.*, 1998).

Table 11.4 summarizes measurements of various species in the stratosphere and troposphere by mass spectrometry through the early 1990s (Viggiano, 1993, and references therein). The altitude at which they were measured and the concentration ranges are shown, as well as whether they were detected using positive or negative ions (see later discussion).

Mass spectrometric measurements require four components: (1) an inlet to introduce the sample; (2) a means of ionizing the species of interest; (3) mass filtering/separation; (4) detection of the ions. Accomplishing this under atmospheric conditions is difficult due to the high sample pressure, which is incompatible with the high voltages used in the ion acceleration region and mass analyzers, and to the complexity of the mixtures found in air. Special considerations imposed by atmospheric conditions are discussed briefly next.

### *a. Sample Introduction*

Because mass separation techniques use high voltages and hence require high vacuum, a means of transmitting the sample from the relatively high pressures found in the atmosphere into the low pressures in the analyzer is required. This typically involves differential pumping stages or the use of pulsed nozzles, which results in lowering of the sample pressure but also a proportionate loss of sensitivity.

TABLE 11.4 Some Species Measured by Mass Spectrometry in the Atmosphere up to about 1990[a]

| Species | Altitude (km) | Detect by +/− Ion | Concentration range |
|---|---|---|---|
| $C_5H_5N$, pyridine | 0–4 | + | 1–10 pptv |
| $CH_3COCH_3$, acetone | 6–14 | + | 1–100 pptv |
| $CH_3CN$, acetonitrile | 10–45 | + | 0.1–10 pptv |
| $NH_3$, ammonia | 0–10 | + | $0.1–10^3$ pptv |
| HOCl, hypochlorous acid | 35–39 | − | 0.1–1 ppbv |
| $SO_2$, sulfur dioxide | 0–11 | − | 1 ppbv |
| $HNO_3$, nitric acid | 4–50 | − | $1–10^4$ pptv |
| $H_2SO_4$, sulfuric acid | 0–45 | − | 0.01–10 pptv |
| $H_2O$ | 38–40 | + | 1–10 ppmv |
| NO, nitric oxide | 10 | − | 1 ppmv |
| $NO_2$, nitrogen dioxide | 10 | − | 0.1 ppmv |
| HONO, nitrous acid | 10 | − | 1 ppbv |
| $CH_3SO_3H$, methanesulfonic acid | 0 | − | $\ll$ 1 pptv |
| $C_6H_7N$, picoline | 0 | + | 1 pptv |
| $C_7H_9N$, lutidine | 0 | + | 1 pptv |
| $C_3H_4O_4$, malonic acid | 0 | − | 0.1–10 pptv |
| $CH_3SCH_3$, dimethyl sulfide | 0 | + | 1–100 pptv |
| $C_{15}H_{24}$, $\beta$-caryophyllene | 0 | + | 1–10 pptv |
| $CH_3SOCH_3$, dimethyl sulfoxide | 0 | + | 1 pptv |

[a] Adapted from Viggiano (1993); see references therein for original literature.

*b. Ionization*

Electron impact ionization is often used in conventional mass spectrometry. However, because of the often complex fragmentation patterns that result, it is not ideal for the direct analysis of complex mixtures such as air. In addition, the hot filaments used to generate the electron beam burn out at high pressures in air. If, in order to avoid this, the sample pressure is reduced prior to the ionization region, there is a loss of sensitivity that is sufficiently severe as to preclude the measurement of trace gases. As a result, alternate ionization processes must be used that either have higher sensitivity (and more selectivity) than electron impact so that the reduction of sample pressure in the ionization region does not present a sensitivity problem or that can ionize the trace species under conditions of atmospheric pressure. Chemical ionization using ion–molecule reactions and laser photoionization have both been used.

*(1) Chemical ionization* Ion chemistry in air is reasonably well understood (see Viggiano, 1993, and references therein). Ion–molecule reactions in the troposphere and stratosphere quickly ($\sim 10^{-3}$ s) give positively charged protonated water clusters, $H_3O^+(H_2O)_n$, where $n$ is typically 3–5, and negatively charged $O_2^-$ and its clusters with water. In the presence of $CO_2$, $O_2^-$ and its clusters are rapidly ($\sim 10^{-3}$ s) converted into $CO_3^-(H_2O)_n$ ions. Subsequent ion–molecule reactions with trace gases (T) generate ionized products of T that are then detected.

For example, if a compound (T) has proton affinity $> 170$ kcal mol$^{-1}$, transfer of a proton from $H_3O^+(H_2O)_n$ occurs:

$$H_3O^+(H_2O)_n + T \rightarrow HT^+(H_2O)_n, \qquad (6)$$

and if the water is stripped from the cluster, the ion $HT^+$ remains and can be separated and detected by MS. That is, an $(M + 1)$ peak results, where $M$ is the molecular weight of the trace gas. Carbonyl compounds such as acetone have been detected with high sensitivity using this approach. For example, Fig. 11.17 is a schematic diagram of a mass spectrometer flown in an aircraft that was used to detect acetone in the lower stratosphere (Arnold and Hauck, 1985). The air is drawn in and the acetone reacts with $H_3O^+(H_2O)_n$ formed using a high-frequency glow discharge ion source. The $(M + 1)$ peak corresponding to $[H \cdot CH_3C(O)CH_3]^+$ is sampled downstream through an inlet orifice into the quadrupole mass spectrometer.

Near the earth's surface, there is sufficient ammonia in air that it undergoes a reaction with $H_3O^+(H_2O)_n$ to form $NH_4^+(H_2O)_n$, and this can also act as an ionizing agent. However, the proton affinity of the trace gas must be $>204$ kcal mol$^{-1}$ for proton transfer to occur from $NH_4^+(H_2O)_n$ to the trace gas.

In the negative ion mode, species with electron affinities greater than 44 kcal mol$^{-1}$ can accept an electron from $O_2^-(H_2O)_n$ ions, forming a $T^-$ ion with mass equal to the molecular weight, $M$:

$$O_2^-(H_2O)_n + T \rightarrow T^- + O_2 + nH_2O. \qquad (7)$$

For example, tropospheric $Cl_2$ has been uniquely identified for the first time using its ionization in air to $Cl_2^-$ followed by tandem MS detection (Spicer *et al.*, 1998).

If a molecule has a high gas-phase acidity, it can react with $CO_3^-$ clusters as is the case for nitric acid, for example (e.g., Knop and Arnold, 1987a):

$$CO_3^-(H_2O)_n + HNO_3 \rightarrow NO_3^-(H_2O)_n + HCO_3,$$
$$\rightarrow NO_3^-(HCO_3)(H_2O)_{n-1} + H_2O.$$

Nitrate clusters with $H_2O$ and/or $HNO_3$ such as $NO_3^-(HNO_3)_n$ are common in the atmosphere (Perkins and Eisele, 1984). Proton transfer to such clusters can occur, but clearly, the trace gas must be more acidic than $HNO_3$. This limits the number of trace gases that can be ionized through this mechanism but includes the important atmospheric species $H_2SO_4$ and methanesulfonic acid, $CH_3SO_3H$ (Tanner and Eisele, 1991; Viggiano, 1993).

In short, positive and negative ions in air containing the trace gases of interest can be formed through discharge techniques and ions of the trace gases of interest generated via ion–molecule reactions. As discussed in more detail later, this approach has been used quite successfully to measure a number of species *in air, including formic acid, acetic acid,* dimethyl sulfide, and $Cl_2$ (Spicer *et al.*, 1994a, 1998). An alternate method is to add another compound to the mass spectrometer inlet, ionize this added species, and use its ion–molecule reactions to form ions and/or ion adducts of the species of interest. This has been used to measure HONO, for example, in air where a chloride ion adduct of HONO is formed when $CHCl_3$ is added in the corona discharge region (Spicer *et al.*, 1993a). Other examples include the measurement of $HNO_3$. For example, as described in Section A.4a(5), radioactive ionization of added $SF_6$ generates daughter ions that react with $SiF_4$ to give $SiF_5^-$. The $SiF_5^-$ forms an adduct with $HNO_3$ and this adduct can be used to measure $HNO_3$ in air (Huey *et al.*, 1998).

*(2) Laser photoionization* Another ionization method with great potential for ambient air applications is

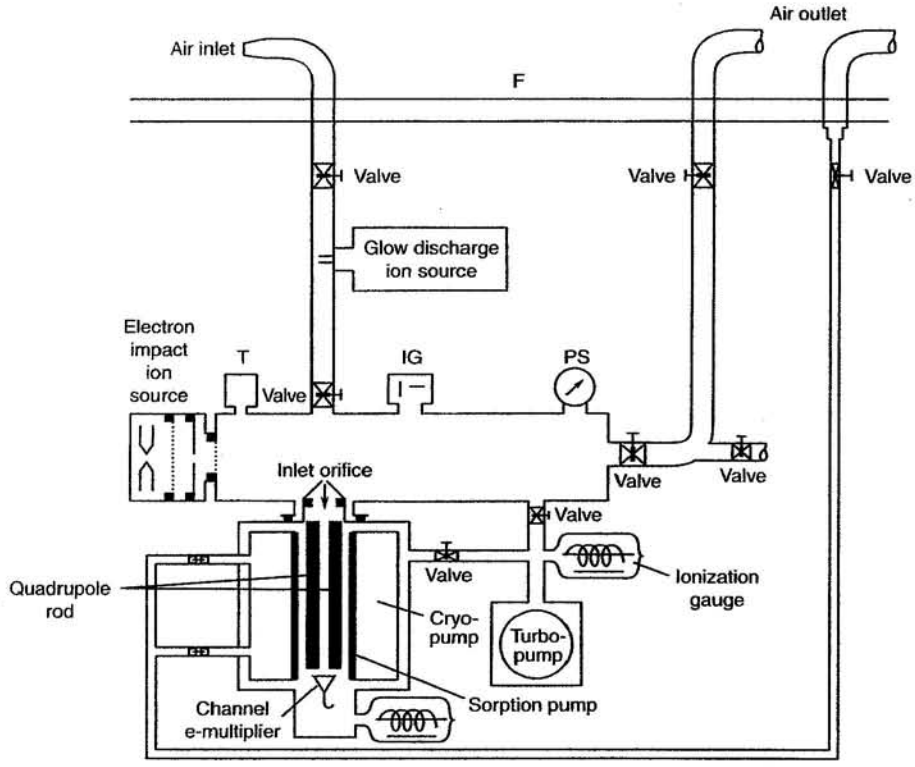


FIGURE 11.17 Schematic of mass spectrometer used for stratospheric measurements (IG = ion getter pump, PS = pressure sensor) (adapted from Arnold and Hauck, 1985).

laser photoionization (see Letokhov (1987) and Pfab (1995) for reviews). Trace gases can be ionized if sufficient energy in the form of light is pumped in; for example, polycyclic aromatic hydrocarbons (PAH; see Chapter 10) in combustion mixtures have been measured by two-photon ionization at 248 nm (e.g., Castaldi and Senkan, 1998).

In practice, for application to ambient air, efficient photoionization requires the use of pulsed lasers and multiphoton absorption methods. The terms "multiphoton ionization," or MPI, and "resonance-enhanced multiphoton ionization," or REMPI, are used to describe these processes.

Figure 11.18 illustrates the principles of application of REMPI to NO (discussed in more detail later). The electronically excited states of NO are shown in Fig. 11.18a and some potential ionization schemes in Fig. 11.18b (Pfab, 1995). Pulsed tunable lasers with wavelengths from ~190 to 1000 nm and spectral resolutions of 0.1 $cm^{-1}$ are readily available. To ionize NO, the absorption of two, three, or four photons is needed. The first photon excites the NO into an intermediate state from which it is ionized using a second or, in some cases, two more photons. The transitions are described as an $(n + m)$ transition, where $n$ is the number of photons that need to be absorbed simultaneously to reach the intermediate state and $m$ is the number of photons to ionize the molecule from that state. The wavelength/energies of the photons involved in the various steps may be the same, which is referred to as a "one-color" process, or different, a "two-color" process. In the two-color case, the second photon is primed to indicate it is a different wavelength than the first photon. For example, in Fig. 11.18b, ionization via the A state can occur either by a (1 + 1) process using 226 nm or by a (1 + 1′) process, where the A state is reached using 226 nm and ionization from this state occurs using 308 nm (Pfab, 1995; Hippler and Pfab, 1995). (The dashed arrows show transitions used for detecting NO by laser-induced fluorescence; see Section A.4a(1).)

The high spectral resolution of laser radiation provides selectivity. For example, Figure 11.19 shows the REMPI spectrum of the NO X (0,0) → A band using a (1 + 1′) process with 226- and 308-nm light to photoionize NO (e.g., see Pfab, 1995; and Lee *et al.*, 1997). As the laser is tuned into resonance with a particular rotational transition in this band, ions are generated and detected using a conventional electron multiplier. Clearly, high selectivity is possible by tuning on and off

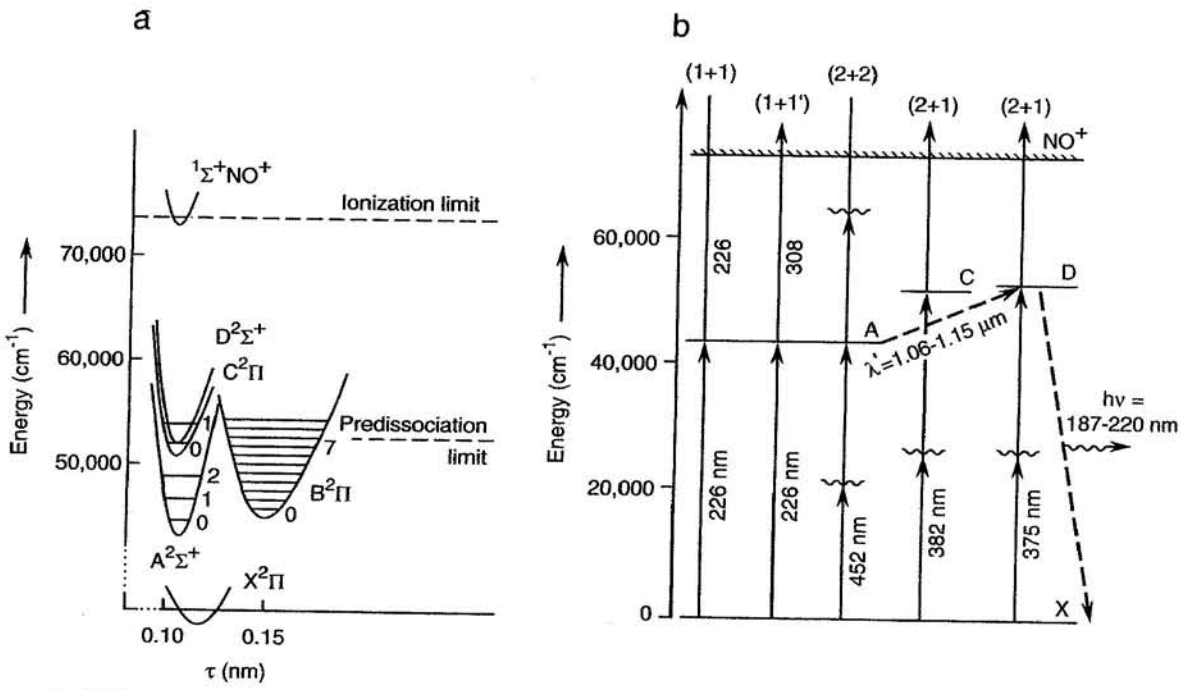


**FIGURE 11.18** (a) Potential energy diagram and (b) REMPI schemes for the excitation and ionization of NO (adapted from Pfab, 1995). The ~~~ indicates a virtual state. The dashed arrows show other transitions used to detect NO in the atmosphere by laser-induced fluorescence (see Section A.4.a(1)).

the rotational transitions. (Note, however, as discussed later, interferences may result if NO is generated by photolysis of other species such as $NO_2$ in the laser beam.)

Pumping low-lying Rydberg states as the resonant intermediate is generally preferred over excitation of higher valence states because the latter often predissociate, undergo rearrangement, or intersystem cross before the subsequent absorption of photons can form ions. The Rydberg region can be reached by the simultaneous absorption of two or three photons, but with a loss of sensitivity (the absorption cross sections for two-photon absorption are of the order of $10^{-50}$ cm$^4$ compared to $10^{-18}$ cm$^2$ for one-photon absorption). On the other hand, pulse energies from conventional excimer or Nd:YAG pumped tunable laser systems are one to two orders of magnitude higher, since no second harmonic generation stages are required.

Other interferences from the use of two- or three-photon resonant excitation compared to $(1 + n)$ processes are photolysis of the analyte at the energy of the first (or second) photon and broadening of the absorption spectra due to the higher photon fluxes employed.

Table 11.5 summarizes some potential REMPI processes for the measurement of species of atmospheric interest (Pfab, 1995). This ionization technique clearly has a great deal of potential, although to date it has not been applied extensively to measurements in ambient air.

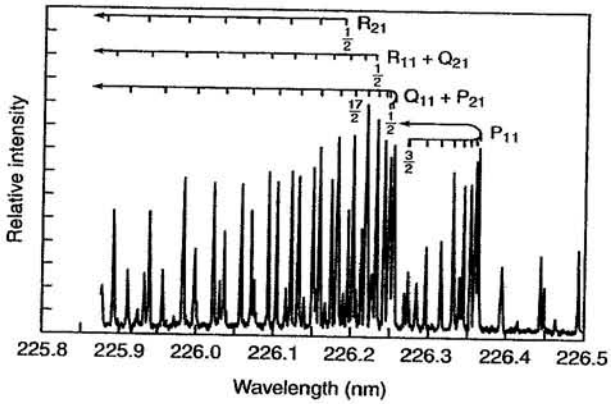


**FIGURE 11.19** Two-color (1 + 1') REMPI spectrum of the NO ($X^2\Pi$, $v' = 0 \rightarrow A^2\Sigma^+$, $v' = 0$) band at 300 K (adapted from Pfab, 1995).

### *c. Mass Filters*

Two types of mass analyzers have been used extensively in atmospheric applications: quadrupole mass filters and time-of-flight (TOF) instruments. The use of ion traps is also being increasingly explored for this application. For the fundamental principles of mass

TABLE 11.5 Some Potential REMPI Transitions for Ionization of Molecules of Atmospheric Interest[a]

| | Type of process | Resonant transition | Excitation wavelength (nm) |
|---|---|---|---|
| NO | 1 + 1 | X → A | 226 |
| | 1 + 1′ | X → A | 226 + 308[b] |
| | 1 + 1′ | X → B, C, D | 191 + 355 or 226 |
| | 2 + 1 | X → C | 380 |
| CO | 1 + 1′ | X → B | 115 + 345 |
| | 2 + 1 | X → B | 229–231 |
| | 2 + 1 | X → E | 215 |
| $NO_2$ | 1 + 1′ + 1 | 3*p* Rydberg + | 484 + 248 + 484[c] |
| | 1 + 1′ + 1″ | 3*p* Rydberg + | e.g., 482 + 275 + 460[d] |
| $N_2O$ | 2 + 1 | 3*p* Rydberg + | 230–250 |
| $NH_3$ | 2 + 1 | $\tilde{X} \rightarrow \tilde{B}$ | 340–355 |
| | | $\tilde{X} \rightarrow \tilde{D}$ | 286–289 |
| $CH_3CHO$ | 2 + 1 | $n \rightarrow 3s$ | 346–365 |
| $CH_3COCH_3$ | 2 + 2 | $n \rightarrow 3s$ | 372–392 |
| | 2 + 1 | $n \rightarrow 3p$ | 322–342[e] |
| $C_6H_6$ | 1 + 1 | $S_0 \rightarrow S_1$ | 259[f] |
| Toluene | 1 + 1 | $S_0 \rightarrow S_1$ | 267 |
| Naphthalene | 1 + 1 | $S_0 \rightarrow S_1$ | 270–310 |

[a] Adapted from Pfab (1995).
[b] Hippler and Pfab (1995).
[c] Benter *et al.* (1995).
[d] Campos *et al.* (1990).
[e] McDiarmid and Sabljić (1988).
[f] Boesl *et al.* (1980).

separation using these techniques, see standard analytical chemistry texts such as Skoog *et al.* (1998).

A potential limitation in the application of MS to near-surface measurements is the tremendous number of compounds in the atmosphere, particularly organics, and hence the increased complexity of interpretation of the single mass spectrum. In the MS ion source, the use of particular ion–molecule reactions to form the ions of interest or the ionization of one selected compound through resonant multiphoton absorption discussed earlier provides one means of specificity. A second method applied in the analyzer region is tandem mass spectrometry.

Figure 11.20, for example, is a schematic diagram of a tandem MS used for both surface and airborne measurements in the troposphere (Spicer *et al.*, 1994a). Air is drawn into the sample inlet and ions are formed by a corona discharge generated by high voltage be-

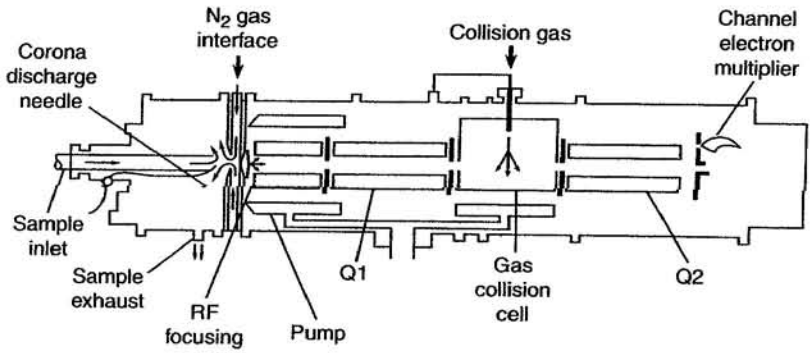


FIGURE 11.20 Schematic diagram of tandem mass spectrometer (adapted from Spicer *et al.*, 1994a).

tween a needle and plate. Ions such as $H_3O^+(H_2O)_n$ are generated and undergo the ion–molecule reactions with trace gases (T) as described earlier. The ions then enter the interface, where water is stripped from the cluster by a stream of dry $N_2$, leaving the ion $TH^+$. Negative ions are generated and sampled by reversing the voltages on the needle and plate.

After being focused, the ions enter the first quadrupole (Q1), which can be used as a single mass spectrometer. However, the peaks observed using Q1 may not be parent ions. While the degree of fragmentation of ions formed using chemical ionization is generally much less than that using electron impact, it does occur. Hence observation of a particular peak corresponding to $TH^+$ in the positive ion mode, for example, does not guarantee that the trace gas T is responsible for the signal at this mass rather than a fragment from a larger molecule.

Tandem MS provides a powerful approach to this problem. In this mode, an ion exiting Q1 enters a cell containing a low pressure of a gas such as Ar or $N_2$ where it is collisionally dissociated. The fragments are then detected using the second quadrupole (Q2). The fragments are characteristic of the ion selected using Q1 and provide confirmation of the identity of the parent ion.

Figure 11.21, for example, shows the MS–MS of the peaks at $m/e$ 70, 72, and 74, respectively, when a calibration sample of $Cl_2$ is sampled into the instrument shown in Fig. 11.20. The peak at $m/e$ 70 fragments only to 35 amu, that at $m/e$ 72 to both 35 and 37 amu, and that at $m/e$ 74 only to 37 amu. Clearly, such fragmentation is consistent with the peaks in the Q1 scan being attributable to $Cl_2$ with isotopes $^{35}Cl$ and $^{37}Cl$.

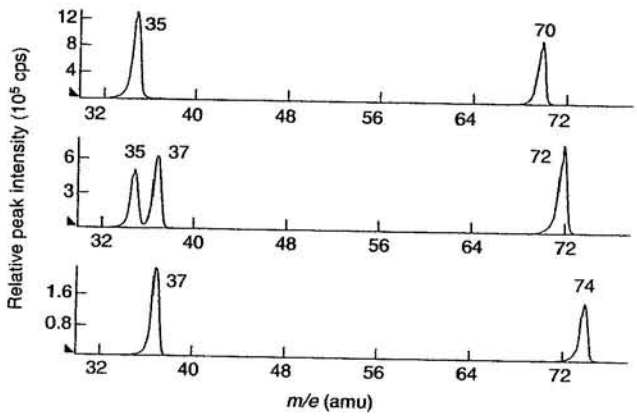


FIGURE 11.21 MS–MS of peaks at $m/e$ 70, 72, and 74 due to $Cl_2$ (spectra taken by K. Oum).

The instrument can be run in various combinations of fixed or scanning modes for Q1 and Q2 (e.g., see Johnson and Yost, 1985). Particularly useful is the continuous mode, where particular peaks in the Q1 scan and certain fragments in the Q2 mass spectrometer are followed, rather than scanning one (or both) of the quadrupoles. Indeed, this method has been used to measure $Cl_2$ specifically in the marine boundary layer (Spicer *et al.*, 1998). In these studies, $Cl_2^-$ was generated as described earlier and the mass combinations (Q1/Q2) for 70/35, 72/35, 72/37, and 74/37 were followed. The combination of MS–MS and the isotope ratios provided unique confirmation that the species being measured was indeed $Cl_2$. Concentrations down to 15 ppt $Cl_2$ could be measured using this approach, with slightly better sensitivity for $Br_2$.

Table 11.6 shows some compounds that can be measured using this technique and estimated detection limits (Spicer *et al.*, 1994a).

### *d. Detectors*

The detectors used in mass spectrometers for atmospheric applications are essentially the same as for other MS applications and are commonly electron multipliers, either channeltrons or multichannel plate

TABLE 11.6 Estimated Detection Limits for Some Species of Atmospheric Interest by Atmospheric Pressure Ionization Mass Spectrometry[a]

| Class | Example | Estimated detection limit (ppt) |
|---|---|---|
| Alcohols | Methanol | 500 |
| Aldehydes | Benzaldehyde | 10 |
| Alkaloids | Nictone | 0.3 |
| Amides | Dimethylformamide | 20 |
| Amines | Pyridine | 2 |
| | Ammonia | 1 |
| Carboxylic acids | Acetic acid | 20 |
| Esters | Ethyl butyrate | 300 |
| Ethers | Diethyl ether | 50 |
| Inorganic acids | Sulfuric acid | 10 |
| | Hydrogen chloride | 20 |
| Ketones | Acetone | 40 |
| Nitriles | Benzonitrile | 4 |
| Nitrosamines | Dimethylnitrosamine | 10 |
| Organometallics | Trimethylarsine | 1 |
| Pesticides | Sulfotep | 100 |
| Sulfur compounds (organic) | Dimethyl sulfoxide | 10 |
| | Dimethyl sulfide | 2 |
| Sulfur compounds (inorganic) | Sulfur dioxide | 10 |
| Terpenes (terpene-like compounds) | Linalool | 500 |

[a] Adapted from Spicer *et al.* (1994a).

(MCP) detectors, respectively. The latter are preferred in TOF instruments since the area of detection is much larger and space charge distortions within the separated ion packets can be minimized.

In short, mass spectrometry is a powerful analytical tool that has been used successfully for a number of years at high altitudes and is now seeing increasing use in the troposphere, including at the earth's surface. A number of different approaches have been developed, including systems that are designed to measure species such as OH, NO, and $HNO_3$. They are described in more detail in the sections on measurement techniques for the individual species.

## 3. Filters, Denuders, Transition Flow Reactors, Mist Chambers, and Scrubbers

A variety of methods have been used to collect gases for subsequent quantification by techniques such as ion chromatography or colorimetric or other (e.g., electrochemical) analyses. These include filter methods, denuders, transition flow reactors, and scrubbers. Sampling must be carried out for sufficient periods of time to collect measurable amounts of the species of interest. From the total volume of air sampled and the amount of the analyte measured, the average concentration of the species in air over the collection period can be calculated. These techniques do not provide real-time analyses, although collection periods as short as ~0.5 h provide sufficient sample for analysis in some cases.

### *a. Filters*

Air is drawn through a filter that consists of, or is coated with, a substance that takes up the species of interest. The filter is then extracted and the ions of interest are measured. For most species of interest, care must be taken to avoid interference from particles. For example, as discussed later, filter collection of $HNO_3$ will have a contribution from particulate nitrate if particles are not removed first. Figure 11.22 shows a typical filter pack used to measure gaseous $HNO_3$ and $NH_3$ (Anlauf *et al.*, 1988).

As discussed below with respect to measurement techniques for individual compounds, the filter material is optimized for the compound of interest. For example, nylon has been found to be effective for the adsorption of gaseous $HNO_3$ (Spicer, 1977). However, care must be taken that the filter does not also remove other gases simultaneously that are measured downstream of the filter. For example, $SO_2$ has been shown to be taken up by nylon filters, forming sulfate, with the extent of conversion being quite variable (e.g., Chan *et al.*, 1986). In addition, changes in the characteristics of what is ostensibly the same filter material with time have been reported in the literature; for example, Cadle and Mulawa (1987) reported that nylon manufactured prior to May 1984 did not retain $SO_2$ to a significant extent (< 4%), whereas that manufactured at later times retained as much as 70% of gaseous $SO_2$.

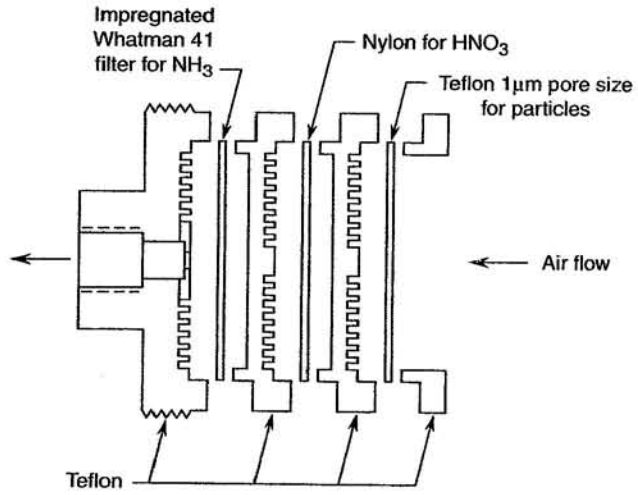


FIGURE 11.22 Schematic diagram of a typical filter pack used to measure gaseous $HNO_3$, particulate matter, and gaseous $NH_3$ (adapted from Anlauf *et al.*, 1988).

In short, the performance of filter media must be carefully assessed prior to field deployment.

### *b. Denuders*

Denuders (also known as diffusion denuders) are based on differences in the diffusion properties of gases compared to particles. The principle is illustrated in Fig. 11.23. A laminar flow of air is pulled through a tube. The inertia of the particles carries them through the tube, while the relatively high diffusivity of gases means that they will strike the walls of the tube a number of times while passing through it. If the walls are coated with a substance that will take up a particular compound, or group of compounds, from the gas phase, then these substances are removed from the gas stream. As discussed in detail by Durham *et al.* (1987), the depletion of the gas as a function of distance, $x$, as it travels along the tube is given by the Gormley–Kennedy equation:

$$\frac{C_x}{C_0} = 0.819e^{(-11.49Dx/Q)}. \qquad \text{(I)}$$

This holds for values of $C_x/C_0$ less than 0.819, where the gas is collected with 100% efficiency. $C_0$ and $C_x$ are the mass concentrations of the gas at the entrance to

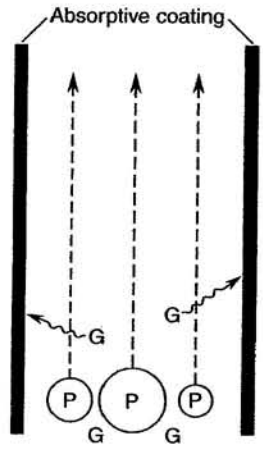


FIGURE 11.23 Schematic of principle of operation of denuders. G = gas, P = particles.

the tube and at distance $x$, respectively, $D$ is the diffusion coefficient of the gas in air, and $Q$ is the volumetric flow rate.

There are a variety of denuder designs, for example, ones incorporating a number of separate tubes in parallel or annular denuders in which the air is pulled through the annular space between two concentric tubes (e.g., Hering *et al.*, 1988; Krieger and Hites, 1992; Koutrakis *et al.*, 1993; Eatough *et al.*, 1993). In a variant of this method, the "coating" is a stream of water that continuously flows along the walls of the denuder and is collected for analysis (Buhr *et al.*, 1995), or, alternatively, a parallel plate with NaOH as the absorbing agent can be used (Simon and Dasgupta, 1995). The opposite approach is used in a diffusion separator developed for semivolatile organic compounds. In this case, the air containing the aerosol and gases flows along the outer walls of a tube, in the center of which is a core flow of clean air; only gases diffuse sufficiently rapidly to penetrate into the central core of clean air, which is sampled at the end of the tube onto a solid sorbent (Turpin *et al.*, 1993). However, despite differences in design in each case, the fundamental principle of using rapid gas diffusion to separate gases and particles is common to all methods.

Denuders have been used in several different ways. One is to extract the walls of the denuder and measure the adsorbed gas directly by ion chromatography. Denuders have also been used as "difference denuders." For example, in nitric acid measurements, the combination of gas-phase $HNO_3$ and particle nitrate has been measured using a nylon filter or Teflon–nylon filter combination in one sampling train. In a parallel sampling train, particulate nitrate alone is measured by first passing the airstream through a denuder to remove gaseous $HNO_3$. The difference between the two gives gaseous $HNO_3$.

As discussed with respect to the measurement of individual compounds, different coatings are used for the collection and measurement of different compounds. The criteria used to choose these coatings and interferences that can occur in the application of denuders to ambient air measurements are discussed by Perrino *et al.* (1990).

### *c. Transition Flow Reactors (TFRs)*

These operate in a manner similar to that of denuders except that the gas flow is in the transition regime rather than being laminar flow and only a fraction ($F$) of the gas of interest is trapped at the walls. As described by Durham *et al.* (1986), TFRs can be treated as if there is a stagnant film of air adjacent to the wall and a core of turbulent air passing through the center of the tube. Uptake of the gas can be thought of as molecular diffusion through the stagnant air film. The fraction of the gas taken up is then given by

$$F = 1 - e^{(-2\pi rDx/Q\lambda)}, \qquad \text{(J)}$$

where $x$, $D$, and $Q$ are as defined in Eq. (I), $r$ is the radius of the tube, and $\lambda$ is the thickness of the stagant air film at the wall. $F$ is typically about 10% and in practice is determined by independent calibrations. The advantages of this sampler are that it has a high gas transfer coefficient and samples a greater volume of air (Durham *et al.*, 1986).

However, in at least one intercomparison study using diffusion denuders and transition flow reactors, different results were obtained for some important atmospheric gases such as $SO_2$, $HNO_3$, and $H^+$, where the TFR values were about 30, 80, and 85% higher, respectively, than those from the denuder system (Sickles *et al.*, 1989); the researchers attributed these differences to biases in the TFR measurements.

### *d. Mist Chambers and Scrubbers*

Air is passed through a chamber where a mist of water or other aqueous solution is used to scrub out species of interest. The solution is then analyzed for the corresponding ions. As discussed shortly, this method has been used for several atmospheric gases, including $HNO_3$, carboxylic acids, and carbonyl compounds.

It has also been applied to measure inorganic chlorine gases and to differentiate HCl from other inorganics such as $Cl_2$ and HOCl (Keene *et al.*, 1993; Pszenny *et al.*, 1993). In this case, the first chamber has an acidic solution that scrubs out HCl, some $Cl_2$ and HOCl, and other chlorine-containing species such as ClNO,

$ClNO_2$, and $ClONO_2$. The air then passes into a second chamber with an alkaline scrubbing solution, which absorbs most of the $Cl_2$ and some HOCl. The two solutions are analyzed for chloride ion by ion chromatography. Differences in the chloride ion concentrations in the acid compared to the alkaline solutions provide a measure of chlorine-containing inorganics other than HCl.

## 4. Methods for, and Tropospheric Levels of, Specific Gases

### *a. NO, $NO_2$, $NO_x$, and $NO_y$*

As we have seen in earlier chapters, NO is the major form of nitrogen oxides emitted from combustion processes, but in the atmosphere it is oxidized to $NO_2$ and other oxides of nitrogen. The term $NO_x$ is used for the sum of (NO + $NO_2$). The term $NO_y$ denotes the sum of NO, $NO_2$ (i.e., $NO_x$), plus all other oxides of nitrogen where the nitrogen is in an oxidation state of +2 or greater:

$$NO_y = NO + NO_2 + HNO_3 + NO_3 + 2N_2O_5 + HONO + PAN + \text{higher peroxynitrates} + \text{alkyl nitrates} + \text{particulate nitrate} \ldots \quad (K)$$

*The term $NO_z$ is also occasionally used in the literature.* In these cases, it is defined by

$$NO_z = NO_y - NO_x. \quad (L)$$

Operationally, $NO_y$ is defined by the measurement method used to measure it, as discussed in more detail in Section A.4.a(2). Since NO, $NO_y$, and $NO_x$ are commonly measured simultaneously using variants of the same techniques, these are discussed together in the following sections, and in that order, for reasons that will become apparent.

*(1) NO* Nitric oxide is most commonly measured using the chemiluminescence from its reaction with $O_3$ described earlier. One such instrument designed for high-sensitivity (1- to 2-ppt detection limit in 10 s) is described by Ridley and Grahek (1990).

A second method is a two-photon laser-induced fluoresence (TP-LIF) technique (Bradshaw *et al.*, 1985; Sandholm *et al.*, 1990, 1997). Figure 11.18b illustrates the basis of this method. Ground-state NO ($X^2\Pi$) is pumped at 226 nm using a Nd:YAG pumped dye laser into the $A^2\Sigma$ state. This molecule is further excited by a second photon, $\lambda'$, in the 1.06- to 1.15-$\mu$m range into the $D^2\Sigma$ electronically excited state, from which it fluoresces, returning to the ground state. Because the fluorescence occurs at higher energies and shorter wavelengths (187–220 nm) than the two pumping steps, interference from the excitation lasers is minimal. While the simplest approach is to carry out the second step using a fixed (1.1 $\mu$m) wavelength (Sandholm *et al.*, 1990), there are advantages to being able to tune the IR laser, such as increasing the selectivity of the measurements and optimizing the pumping efficiency from the $A^2\Sigma$ state to the $D^2\Sigma$ state (Bradshaw *et al.*, 1985). The sensitivity of this method is ~20 ppt for a 1-s integration time and 0.4 ppt for 100-s integration time at a signal-to-noise of 2:1 (Sandholm *et al.*, 1990, 1997).

Intercomparison studies of these two measurement methods for NO generally show good agreement for levels of 25 ppt and greater (e.g., Hoell *et al.*, 1987a; Gregory *et al.*, 1990; Crosley, 1996). For example, Fig. 11.24 shows the results of one aircraft study in which the chemiluminescence method and the TP-LIF method were compared (Crosley, 1996). The slope of the plot in Fig. 11.24 was 0.94, with an intercept of $-0.1 \pm 0.8$ ppt and $r^2 = 0.90$. For the data <25 ppt, although the slope was 0.989, the correlation was poorer, $r^2 = 0.66$.

A technique that has been used in laboratory studies for oxides of nitrogen and shows promise for field measurements is resonance-enhanced multiphoton ionization (REMPI) (Guizard *et al.*, 1989; Lemire *et al.*, 1993; Simeonsson *et al.*, 1994). For example, Akimoto and co-workers (Lee *et al.*, 1997) have reported a REMPI system in which a (1 + 1) two-photon absorption of light at 226 nm by NO results in ionization (vide supra). They report a detection limit of ~16 ppt in their laboratory studies. Other oxides of nitrogen such as $NO_2$ and $HNO_3$ can also photodissociate in the

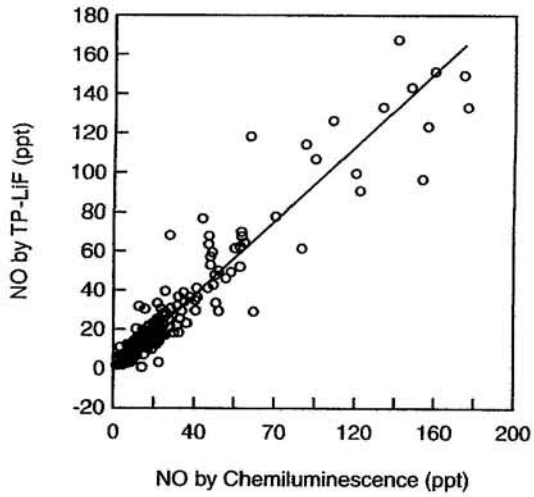


FIGURE 11.24 Measured NO concentrations using TP-LIF and chemiluminescence during one series of aircraft flights (adapted from Crosley, 1996).

laser beam to generate NO, causing interference in the NO measurement. However, since the ionization of NO is a two-photon process, the signal is expected to vary with the square of the laser power ($P$). On the other hand, since the production of NO from other compounds such as $NO_2$ requires three photons to generate and then photoionize NO, the dependence of the signal on the laser power is steeper. For example, Lee *et al.* (1997) report that the signal varies with $P^{1.75}$ for NO but $P^{2.4}$ for $NO_2$.

Figure 11.25 is a schematic diagram of one such REMPI system currently under development for ambient air analysis (Schmidt *et al.*, 1999). The ions are generated in a two-photon process and then separated using time-of-flight mass spectrometry (TOF-MS), which provides an additional means of selectivity. For NO in laboratory air, the current detection limit using this system is 1 ppt. It has also been applied to the measurement of CO and $CH_3CHO$ in laboratory systems using a (2 + 1′) two-color ionization process, with detection limits in synthetic air in laboratory studies of 10 and 1 ppt, respectively.

*(2) $NO_y$* $NO_y$ is measured by passing the airstream containing NO and the other oxides of nitrogen over a catalyst to convert all of the other oxides of nitrogen into NO, which is then measured by one of the techniques just discussed. The resulting measurement is taken as the total oxides of nitrogen present.

The most common catalysts used are MoO at 375–400°C or Au at 300°C with added CO or $H_2$. The mechanism of reduction at the surfaces is not clear. Reaction of the various oxides of nitrogen on the metal surfaces may leave a surface oxide, which is then removed by reaction with the CO, forming $CO_2$, or with the $H_2$, forming $H_2O$ (e.g., Kliner *et al.*, 1997, and references therein).

This method of measurement of total oxides of nitrogen means that $NO_y$ is defined operationally in terms of compounds that can be reduced to NO over these catalysts. It had been generally accepted that under typical operating conditions, species such as HCN, $CH_3CN$, $N_2O$, $NH_3$, and amines are not significantly reduced and hence did not contribute to $NO_y$ (e.g., see Crosley, 1996). However, Kliner *et al.* (1997) showed that HCN, $CH_3CN$, and $NH_3$ can be converted to NO with high efficiencies under some conditions. For example, 85% of the HCN was converted using $H_2$ and 100% using CO with an Au catalyst at 300°C. Weinheimer *et al.* (1998) measured conversion efficiencies for HCN using three "outwardly identical" gold converters at 300°C with added CO. The conversion efficiency was 5–7% for ambient air sampled during aircraft flights with or without added water for two of the converters, with the efficiency doubled when synthetic air was sampled on the ground. The third converter had efficiencies for HCN of ~30% under all conditions. Bradshaw *et al.* (1998) reported conversion efficiencies ranging from 6 to 100% for HCN in gold converters. High conversion efficiencies were also found for organic nitrates, with the efficiencies being larger for the smaller nitrates such as nitroethane; differences were also noted between pure gold and gold-plated

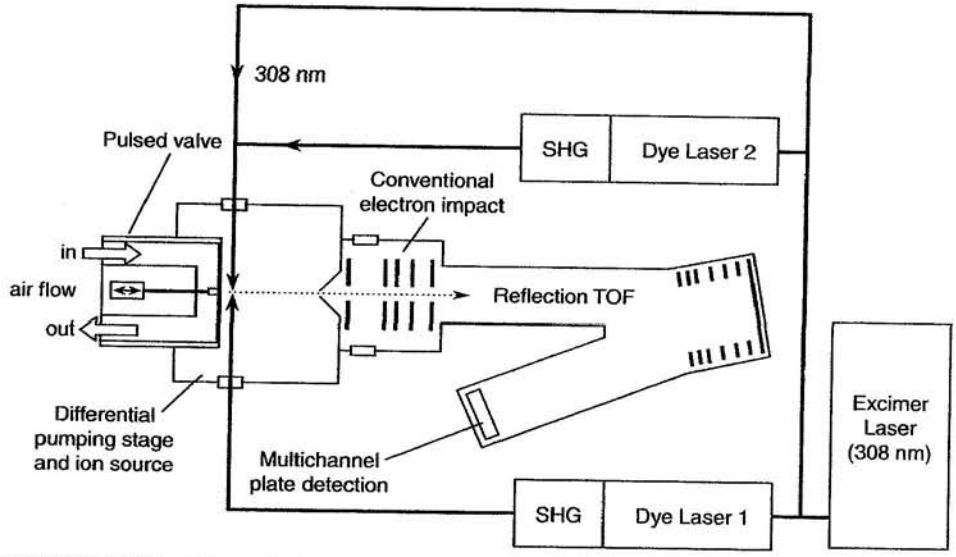


FIGURE 11.25 Schematic of REMPI-TOF. The conventional electron impact ionization source is just used for ion beam focusing (adapted from Schmidt *et al.*, 1999).

converters, and in the latter case, depended on previous cleaning of the converter.

In short, it is clear that the conversion efficiencies have to be tested for each converter under conditions in which the field measurements are made.

With HCN concentrations of ~170 ppt in the stratosphere and upper troposphere (Coffey *et al.*, 1981; Cicerone and Zellner, 1983; Zander *et al.*, 1988; Schneider *et al.*, 1997), and up to ~900 ppt at times (Rinsland *et al.*, 1998), HCN could contribute significantly to $NO_y$, depending on the conversion efficiency. The same is true of acetonitrile, $CH_3CN$, whose concentrations are less well known; it has been measured over Europe at concentrations in the range of 150–200 ppt (e.g., Hamm *et al.*, 1989) and in the lower stratosphere at concentrations of 110–160 ppt (Schneider *et al.*, 1997). However, much smaller concentrations, of the order of a few tens of ppt, have also been reported in the atmosphere (Knop and Arnold, 1987a, 1987b). High concentrations of $NH_3$ are quite common in the troposphere, particularly near sources such as cattle feedlots (vide infra).

In addition to the potentially varying contributions of compounds such as HCN and $NH_3$ to $NO_y$, there are a number of other variables that can impact the measured values. One of the most important is the effect of the sampling lines, which can adsorb and desorb various gases. Nitric acid in particular is well known to be "sticky," readily adsorbing to various surfaces in a manner that is not reproducible and depends on such factors as the amount of water present on the surface. It is therefore not surprising that the agreement between various methods of measuring $NO_y$ is not as good as for NO. Figure 11.26, for example, shows the $NO_y$ measurements made during the flights for which the NO data are shown in Fig. 11.24 (Crosley, 1996). The slope of the regression line is $1.18 \pm 0.04$, with an $r^2$ value of only 0.37 for the scattered data.

In principle, if each of the compounds contributing to $NO_y$ is individually measured, their concentrations should sum up to the measured $NO_y$. While this is sometimes the case, in many field studies the sum has been found to be less than the measured $NO_y$ (e.g., Fahey *et al.*, 1986; Ridley *et al.*, 1990a; Atlas *et al.*, 1992; Parrish *et al.*, 1993; Sandholm *et al.*, 1994; Nielsen *et al.*, 1995; Williams *et al.*, 1997). Cases where the sum of the individual components is significantly less than the $NO_y$ measured simultaneously are often referred to as "missing $NO_y$."

Table 11.7, for example, summarizes measurements of the components of $NO_y$ made at Niwot Ridge, Colorado, in mid-1987 (Ridley *et al.*, 1990a). The sum of $NO_x$ ($NO + NO_2$), $HNO_3$, particulate nitrate, PAN,

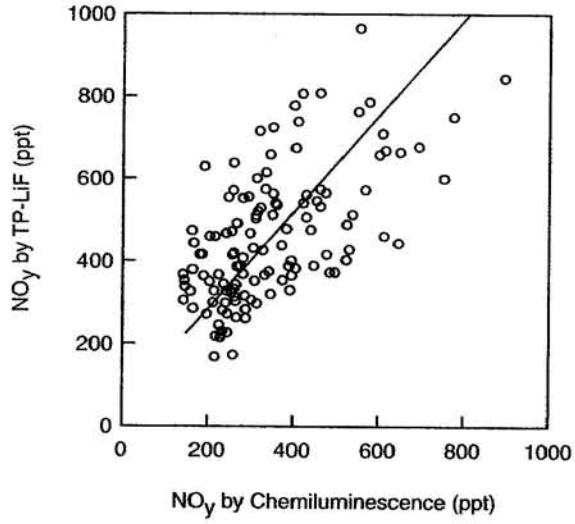


FIGURE 11.26 Measured $NO_y$ concentrations using catalytic converters and TP-LIF or chemiluminescence to measure the NO produced in the same flights as NO data in Fig. 11.24 (adapted from Crosley, 1996).

PPN (peroxypropionyl nitrate), methyl nitrate, *n*-propyl nitrate, and 2-butyl nitrate was, on average, $76 \pm 13\%$ of the measured $NO_y$.

Figure 11.27 summarizes the ratio of the sum of the individual components of $NO_y$ to the total $NO_y$ measured using conversion to NO (Parrish *et al.*, 1993). These data summarize measurements of NO, $NO_2$, PAN, $HNO_3$, and particulate nitrate as well as total $NO_y$ at Whiletop Mountain (Tennessee), Bondville (Illinois), Scotia (Pennsylvania), and Egbert (Ontario, Canada). The median value (which is less influenced by extremes) of the percentage $NO_y$ that can be accounted for ranges from 75 to 94%, with all but the Bondville site being within experimental error of 100%.

TABLE 11.7 Measured Components of $NO_y$ at Niwot Ridge, Colorado, in Mid-1987[a]

| Compound | Percentage of $NO_y$ |
|---|---|
| $NO_x + HNO_3 + NO_3^- + PAN$ | 74 |
| $NO_x$ | 32 |
| PAN | 24 |
| PPN[b] | 1.2 |
| (NPN + 2BN)[c] | 0.5 |
| MN[d] | <0.2 |
| Sum | $76 \pm 13$ |

[a] Adapted from Ridley *et al.* (1990a).
[b] PPN = peroxypropionyl nitrate.
[c] NPN = *n*-propyl nitrate; 2BN = 2-butyl nitrate.
[d] MN = methyl nitrate.

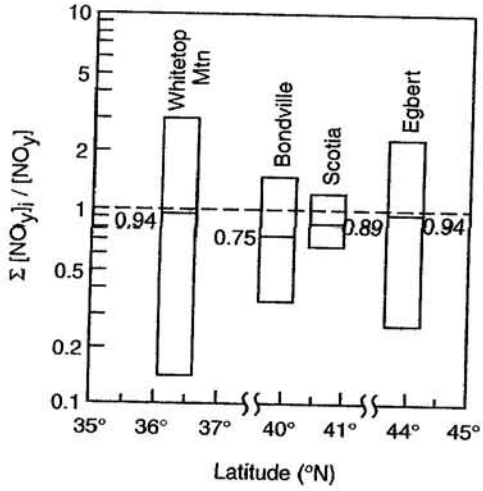


FIGURE 11.27 Ratio of the sum of ($NO + NO_2 + PAN + HNO_3$ + particulate nitrate) measured individually to total measured $NO_y$ at three sites in the United States (Whitetop Mountain, Tennessee; Bondville, Illinois; and Scotia, Pennsylvania) and one in Canada (Egbert, Ontario). The bars represent the range of results and the mid-range lines the median values (adapted from Parrish *et al.*, 1993).

As discussed by Parrish *et al.* (1993), the Bondville $HNO_3$ data may be artificially low, so that the apparent "missing $NO_y$" of 25% may be an overestimate. Given the difficulty in measuring individual components of $NO_y$ such as $HNO_3$ (vide infra) at the very low levels found in the atmosphere, these data suggest that extent of the "missing $NO_y$" is relatively small on average. However, note the wide range of total $NO_y$ that could be accounted for in Fig. 11.27. As discussed by Parrish *et al.* (1993), values above 100% must be due to systematic errors whereas those below 100% may reflect either systematic errors or true "missing $NO_y$."

Figure 11.28 shows similar data for measurements made at Idaho Hill, Colorado, in the fall of 1993 (Williams *et al.*, 1997). Measurements were made of NO, $NO_2$, PAN, PPN, $HNO_3$, and particulate nitrate, as well as total $NO_y$. Two sets of meteorological conditions were encountered, one where the wind was downslope and from the west where there were few sources nearby, and one where the wind was upslope, carrying pollutants from urban areas to the east. Figure 11.28a shows that for upslope air masses from the east with relatively fresh emissions, the sum of the measured compounds accounts, within experimental error, for the total $NO_y$. The average ratio of $\Sigma NO_y$/total $NO_y$ was $1.06 \pm 0.15$. On the other hand, during periods with cleaner, downslope air from the west (which has also had more time to react), the sum of the individual compounds frequently does not add up to the total measured $NO_y$ (Fig. 11.28b). The deficit ranges from 0 to 50% of the measured total $NO_y$.

The average contributions of the various oxides of nitrogen to $NO_y$ for the two conditions are shown in Fig. 11.29 (Williams *et al.*, 1997). The mean total $NO_y$ measured under the more polluted conditions was 4.3 $\pm$ 2.4 ppb, with essentially all of it accounted for by the measured individual compounds. Under the cleaner

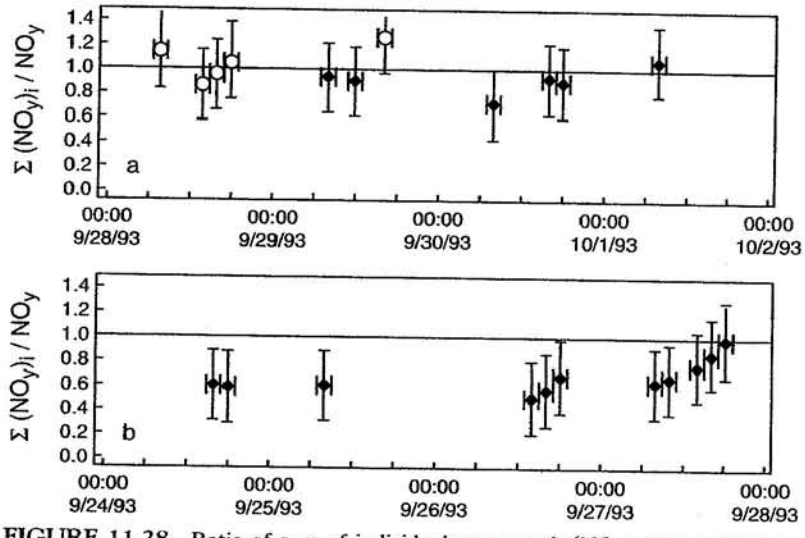


FIGURE 11.28 Ratio of sum of individual compounds ($NO + NO_2 + PAN + PPN + HNO_3$ + particulate nitrate) to total measured $NO_y$ under two types of overall meteorological conditions: (a) episodes with winds from the south and east with fresh emissions and (b) winds primarily from the west with cleaner but more aged air (adapted from Williams *et al.*, 1997).

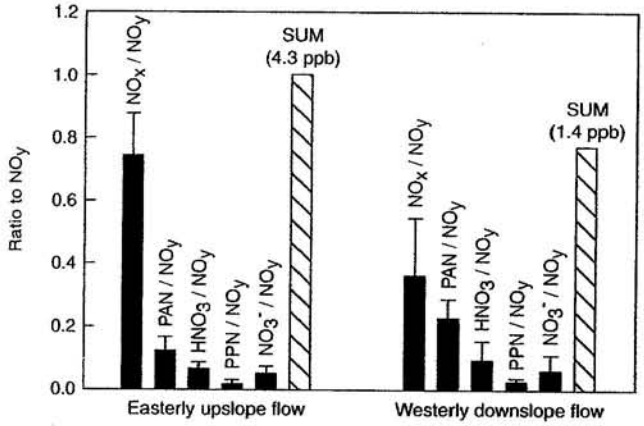


FIGURE 11.29 Ratio of measured individual compounds of $NO_y$ to total $NO_y$ at Idaho Hill, Colorado, with easterly winds (more polluted air) and with westerly winds (cleaner but more aged air), respectively (data from Williams *et al.*, 1997).

conditions of westerly flow (but where the air was more aged), the total $NO_y$ was smaller, $1.4 \pm 0.4$ ppb, but only 77% was accounted for by the individual compounds. Interestingly, the deficit appeared to correlate with $O_3$, suggesting the compounds responsible are photochemically generated. A similar observation has been made in Denmark by Nielsen *et al.* (1995, 1998), who also report that the fraction of total $NO_y$ that is in the form of particulate nitrate is small (0.17–0.28%). The deficit in accounting for $NO_y$ at Idaho Hill also decreased as the air temperature decreased, which may reflect a correlation of temperature with the age of the air mass and/or that the species responsible for the missing $NO_y$ are thermally unstable (Williams *et al.*, 1997).

As seen from the VOC–$NO_x$ chemistry in Chapter 6, organic nitrates are among the expected products of the oxidation of hydrocarbons in air containing $NO_x$. Williams *et al.* (1997) have considered the possible contribution of simple alkyl nitrates but, based on other measurements of these species, indicate that it is unlikely they are responsible for a significant portion of the "missing $NO_y$."

Multifunctional organics are also possible contributors. Nielsen *et al.* (1998) have examined the possible contribution of multifunctional compounds to "missing $NO_y$" in both the gas and particle phases. As discussed in Chapter 9, compounds with sufficiently high vapor pressures ($> 2\times10^{-5}$ Torr) exist essentially completely in the gas phase, those with low vapor pressures ($<2 \times 10^{-9}$ Torr) in the condensed phase (i.e., on or in particles), and those in between the two extremes as both gases and particles. Nielsen and co-workers have developed a relationship between the expected vapor pressure of a multifunctional compound and its structure:

$$\begin{aligned}\log P = &-(0.4069 \pm 0.0057)(\text{no. of C})\\ &-(2.144 \pm 0.070)(\text{no. of nitrate groups})\\ &-(1.961 \pm 0.057)(\text{no. of OH groups})\\ &-(1.130 \pm 0.071)(\text{no. of carbonyl groups})\\ &+(4.466 \pm 0.077). \qquad \text{(M)}\end{aligned}$$

This relationship is based on data for 183 compounds, including $C_7$–$C_{29}$ hydrocarbons, $C_1$–$C_{18}$ alcohols, $C_2$–$C_{10}$ diols, $C_5$–$C_{18}$ carbonyls, $C_1$–$C_{20}$ alkyl nitrates, and $C_2$–$C_3$ hydroxynitrates and dinitrates. Based on this analysis, Nielsen *et al.* (1998) suggest that the organic nitrates found in particles are probably bi- and multifunctional compounds and that they may also contribute to gas-phase $NO_y$ and $NO_z$.

Such multifunctional compounds, however, are very difficult to collect, identify, and quantify and, in fact, need to be specifically targeted if they are of interest for a particular study. As a result, such compounds usually go undetected but may be responsible for some of the "missing $NO_y$."

In addition, given that the efficiency of conversion of compounds such as HCN and $NH_3$ over the catalysts may be higher than thought under some conditions (e.g., Kliner *et al.*, 1997; Weinheimer *et al.*, 1998; Bradshaw *et al.*, 1998), these compounds may also be responsible for a substantial portion of the "missing $NO_y$." However, Williams *et al.* (1998) argue that such interferences, if they exist in their measurements, are too small to account for the magnitude of the "missing $NO_y$" in their studies.

Because of the sensitivity of $NO_y$ measurements to the particular catalyst used, its recent exposure, cleaning, etc., agreement between various measurements of $NO_y$ and between $NO_y$ and the sum of individual compounds would not necessarily be expected, especially in aged air masses and/or other types or air masses where compounds other than NO and $NO_2$ contribute significantly to $NO_y$. Indeed, this is the case (e.g., see discussion by Bradshaw *et al.* (1998) and Williams *et al.* (1998)). Agreement is generally reasonably good at higher concentrations and when $NO_x$ is a major portion of $NO_y$, e.g., in urban and suburban areas (Williams *et al.*, 1998).

***(3) $NO_x$ and $NO_2$*** $NO_x$ is defined as the sum of ($NO + NO_2$). NO can be measured by the techniques described earlier. $NO_2$ is one of the compounds contributing to $NO_y$ and in a relatively "young" air mass is often the primary contributor. However, separating out its contribution from other compounds contributing to $NO_y$ obviously requires a different approach.

One approach that has been used is to photolyze the $NO_2$ at wavelengths below 400 nm to form NO and then measure the NO using chemiluminescence or TP-LIF as discussed earlier (Kley and McFarland, 1980; Ridley *et al.*, 1988; Gao *et al.*, 1994). The reactions are as follows:

$$NO_2 + h\nu \xrightarrow{k_p} NO + O, \quad (8)$$

$$NO + O_3 \xrightarrow{k_{9a}} NO_2^* + O_2 \text{ (in gas phase)}, \quad (9a)$$

$$\xrightarrow{k_{9b}} NO_2 + O_2 \text{ (on cell wall)}. \quad (9b)$$

From the differential equations for the change in $NO_2$ and NO with time, i.e., $d[NO_2]/dt$ and $d[NO]/dt$, based on reactions (8), (9a), and (9b), it can be shown that the fractional conversion of $NO_2$ to NO is given by Eq. (N) (Kley and McFarland, 1980; Gao *et al.*, 1994):

$$\text{Fractional conversion} = \frac{k_p(1 - e^{-(k_p + k_9[O_3])\tau})}{k_p + k_9[O_3]}. \quad (N)$$

$k_p$ is the photolysis rate constant for $NO_2$, reaction (8), $k_9 = k_{9a} + k_{9b}$, and $\tau$ is the residence time of the air in the photolysis cell. Fractional conversions of up to ~0.65 have been observed ((Kley and McFarland, 1980; Ridley *et al.*, 1988; Gao *et al.*, 1994). Photolysis of $NO_2$ at 353 nm using a XeF excimer laser has also been used (Sandholm *et al.*, 1990). Measurement precision and detection limits are determined by a number of factors, including an artifact due to desorption of $NO_x$ from the walls of the reaction vessel during irradiation. Gao *et al.* (1994) report the latter is equivalent to ~20–40 ppt using synthetic air in the laboratory, but in ambient air, may limit measurements of concentrations below 100 ppt.

As discussed earlier, TDLS can be used to measure $NO_2$. The detection limit cited for a path length of 33.5 m in a ground-based study is ~150 ppt (Mackay *et al.*, 1988) and 25 ppt in an aircraft study (Schiff *et al.*, 1990). The detection limit for DOAS with a path length of 800 m is ~4 ppb (Biermann *et al.*, 1988).

Finally, matrix isolation combined with electron spin resonance has been used for $NO_2$ as well as for other free radicals such as $HO_2$, $RO_2$, and $NO_3$ (Mihelcic *et al.*, 1985, 1990, 1993; Zenker *et al.*, 1998). Trace gases in a sample of air (typically about 8 L) are trapped in a $D_2O$ matrix at 77 K and the ESR spectrum obtained. Any paramagnetic species present has a characteristic ESR spectrum that can be used to identify it and, using reference spectra, obtain its concentration. Since $NO_2$ is the paramagnetic species present in the largest concentration, it is easily detected and measured.

Several intercomparison studies for $NO_2$ have been carried out (e.g., Fehsenfeld *et al.*, 1990). At concentrations of $NO_2$ above 400 ppt, measurements using the photolysis of $NO_2$ and chemiluminescence for the NO generated by photolysis were in reasonably good agreement with TDLS measurements. At levels above about 300 ppt, the photolysis and luminol method corrected for ozone and PAN agreed reasonably well, with the slope of the corrected luminol versus photolysis data being 1.09 (Fehsenfeld *et al.*, 1990).

An airborne intercomparison study (Gregory *et al.*, 1990a) was also carried out using two photolysis methods (the 353-nm laser photolysis with TP-LIF detection of NO and a Xe arc lamp photolysis with chemiluminescence detection of NO) as well as TDLS. Overall, for $NO_2$ up to 200 ppt, the techniques agreed with the average values of all three by 20% or better and with each other to within 30%. However, below 50 ppt, there was very little correlation between the various measurement techniques (Gregory *et al.*, 1990a).

An informal intercomparison study of $NO_2$ measurements was carried out in a remote atmosphere at Izaña, Tenerife (Zenker *et al.*, 1998). Three techniques were used: TDLS, photolysis with a chemiluminescence detector, and matrix isolation–ESR. Agreement between the three methods was good, with plots of data from one technique against the others having slopes within experimental error of unity. For example, TDLS and the photolysis technique plotted against the matrix isolation measurements had slopes of $0.90 \pm 0.47$ and $1.04 \pm 0.34$, respectively, over a range of $NO_2$ concentrations from ~100 to 600 ppt.

In summary, there are a variety of methods of measuring $NO_2$ that are reasonably accurate for higher concentrations, particularly those found in polluted areas. However, at smaller concentrations found in the remote troposphere, there are significant discrepancies between the various methods.

In addition to these techniques, there are passive samplers for $NO_2$ that have been used for unique situations such as indoor measurements. For example, in the Palmes Tube, $NO_2$ diffuses through to a surface coated with triethanolamine and is trapped in the form of $NO_2^-$. The nitrite is subsequently measured colorimetrically (e.g., see Boleij *et al.*, 1986; Miller, 1988; and Krochmal and Górski, 1991). As with most, if not all, such wet chemical methods, interferences can arise, for example, from PAN (Hisham and Grosjean, 1990) and HONO (Spicer *et al.*, 1993b).

***(4) Typical levels of NO, $NO_2$, and $NO_y$*** Figure 11.30 shows a summary of measurements of surface concentrations of NO, $NO_x$, and $NO_y$ made at a variety of remote to rural sites in North America and Europe (Emmons *et al.*, 1997). The bars encompass the central 90% of the values and the medians and means are

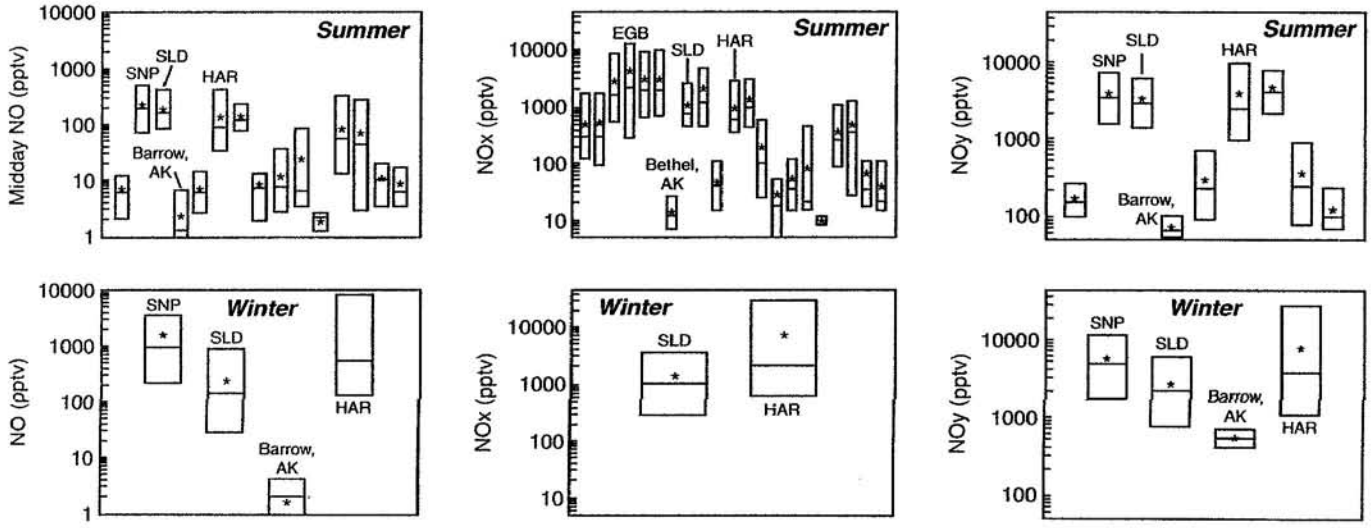


FIGURE 11.30 Range of surface concentrations of NO, $NO_x$, and $NO_y$ at a variety of Northern Hemisphere locations. The asterisk is the mean and the horizontal line the median. The bar represents the central 90% of measured values. SNP, Shenandoah National Park, Virginia; SLD, Schauinsland, Germany; EGB, Egbert, Ontario, Canada; and HAR, Harvard Forest, Massachusetts. (Adapted from Emmons *et al.*, 1997.)

shown by the horizontal lines and asterisks, respectively. The identity of some of the specific sites at which measurements were made are indicated. As expected, remote regions such as Barrow, Alaska, have the smallest concentrations of NO, typically less than 10 ppt. The most polluted (but still rural) areas have concentrations that in the winter are in the ppb range.

Similar conclusions hold for $NO_x$ and $NO_y$. $NO_x$ concentrations range from median values of 25 ppt in Alaska (remote) to 2.3 ppb at Egbert, a rural area in Ontario, Canada, in the summer. $NO_y$ ranges from 69 ppt at Barrow, Alaska, to 5.0 ppb at Shenandoah National Park in Virginia (Emmons *et al.*, 1997). Data from a number of studies are archived electronically and can be accessed as described by Carroll and Emmons (1996).

In urban areas, the concentrations can of course be much greater. For example, in Paris in late September 1997, $NO_2$ concentrations exceeded 210 ppb (*Environmental Science & Technology*, 1997). In metropolitan Toronto, Canada, peak 30-min average concentrations of ~40 ppb have been reported (Schiff *et al.*, 1986). In the Los Angeles area, maximum 1-h concentrations of about 200 ppb are encountered (Air Quality Management District summary data; see Appendix IV).

Measurements of NO, $NO_x$, $NO_y$, PAN, $HNO_3$, and $O_3$ in the free troposphere obtained from 1985 to 1995 are summarized by Thakur *et al.* (1999) and can be obtained electronically as described in that paper.

***(5) $HNO_3$*** Analysis of $HNO_3$ at the low levels typically found in the atmosphere is difficult, in large part due to its tendency to adsorb very readily to surfaces. As a result, sampling $HNO_3$ in an artifact-free manner is often the limiting aspect in making accurate measurements.

Several different methods exist for measuring $HNO_3$, most commonly FTIR and TDLS, which were described earlier. Other techniques commonly used include filters, denuders, transition flow reactors, and scrubbers, followed by analysis of the collected material for nitrate, e.g., by ion chromatography. A modification of the luminol method has also been used. Finally, mass spectrometric methods look very promising as a sensitive and specific method of detection and measurement. A brief description of each of these methods that have not yet been treated follows.

*Filters.* $HNO_3$ is efficiently trapped out on nylon filters. Typically, two or more filters are connected in series. A schematic of such a filter pack was shown in Fig. 11.22 (Anlauf *et al.*, 1988). A Teflon filter first removes particles from the airstream and a nylon filter then removes gaseous $HNO_3$. In this particular system, a third filter (Whatman 41 impregnated with an aqueous solution of glycerol and citric acid) was used to trap $NH_3$. After sample collection, each of the filters is extracted separately and nitrate, ammonium, and additional particle components collected on the Teflon filter are measured by ion chromatography. The sensitivity of this method for nitric acid and the other species is determined in part by filter blank values (i.e., nitrate on unexposed filters) and by the total amount collected and hence the sampling time used. Times of

4–6 h are often used, but can be as short as 0.5–2 h (Fehsenfeld *et al.*, 1998).

Other filters have also been used to collect nitric acid, such as Whatman 41 filters impregnated with NaCl (e.g., Anlauf *et al.*, 1986).

Potential interferences in the measurement of nitric acid using this method include removal of gaseous $HNO_3$ on the Teflon particle filter and/or volatilization of particle nitrate collected on this Teflon filter. As discussed in Chapter 7, $NH_4NO_3$ is a common particle component, but exists in equilibrium with gas-phase $NH_3$ and $HNO_3$:

$$NH_4NO_{3(s,aq)} \leftrightarrow NH_{3(g)} + HNO_{3(g)}. \quad (10, -10)$$

Shifts to the right, e.g., due to a temperature increase, release $HNO_3$ and $NH_3$, which are then collected on the nylon filter and Whatman impregnated filters, respectively, and measured as gas-phase nitric acid and ammonia. This was hypothesized to be responsible for higher filter pack values compared to those measured by mass spectrometry under some conditions, particularly at colder air temperatures (<15°C), where the equilibrium (10, −10) favors relatively larger amounts of ammonium nitrate in air (Fehsenfeld *et al.*, 1998). Talbot *et al.* (1990) observed higher $HNO_3$ concentrations by the nylon filter technique compared to a mist chamber (vide infra) and hypothesized that unknown (perhaps organic) nitrogenous compounds were also being collected on the nylon, forming nitrate. They also showed that $O_3$ at typical concentrations found in the troposphere could react with some unknown substance(s) on the nylon filter to generate a positive artifact. This artifact was significantly reduced by prewashing the nylon to remove water-soluble adsorbed species.

*Denuders.* A variety of denuder wall coatings have been used to collect $HNO_3$ (Perrino *et al.*, 1990). These include nylon fiber mats (e.g., Durham *et al.*, 1987), MgO (e.g., Solomon *et al.*, 1988, 1992), $Na_2CO_3$/glycerol (e.g., Ferm, 1986; Koutrakis *et al.*, 1988), and tungsten oxide ($WO_3$) (e.g., see Fox *et al.*, 1988). A variant of this is the tungstic acid technique. Air containing the $HNO_3$ is passed through tubes coated with tungstic acid. When the tube is subsequently heated, the $HNO_3$ decomposes and desorbs as NO or $NO_2$.

*Transition flow reactors.* TFRs have also been used to measure gaseous $HNO_3$ (e.g., Hering *et al.*, 1988). When operated in the configuration used by Durham *et al.* (1986), where the TFR is upstream of the Teflon particle filter, the problems of adsorbing gaseous $HNO_3$ on the particle filter or of evaporation of $HNO_3$ from the collected particles onto the gaseous $HNO_3$ sampler are avoided.

*Scrubbers.* Mist chamber scrubbers have also been used for $HNO_3$. The airstream passes through a Teflon filter to remove particles and then encounters a mist of water that scrubs the $HNO_3$ out of the air. The nitrate concentration is measured in the aqueous scrubbing solution using ion chromatography (Talbot *et al.*, 1990).

*Luminol method.* As described earlier, $NO_2$ undergoes a chemiluminescent reaction with luminol, and this has been used to measure $NO_2$. This has also been used to measure $HNO_3$ by difference. One airstream passes through a Teflon filter to remove particles, while another passes through a Teflon–nylon filter combination to remove both particles and gaseous $HNO_3$. The air is then passed over hot glass beads to convert NO and $HNO_3$ to $NO_2$, which is measured using the luminol method. The difference in signal between the two filtering methods then gives gaseous $HNO_3$ (Hering *et al.*, 1988).

All of these methods have potential interferences, some of which have been described in conjunction with the individual methods. For example, whenever a Teflon prefilter for particles is used, gaseous $HNO_3$ can be taken up on this filter, particularly when it has a high particle loading, leading to a negative artifact. Volatilization of ammonium nitrate particles collected on the Teflon filter can also occur, giving a positive artifact. Uptake and conversion of other nitrogen-containing compounds to nitrate gives a positive artifact (e.g., see Koutrakis *et al.*, 1988). In addition, as mentioned at the beginning, $HNO_3$ is notoriously "sticky," and the use of short (or ideally, no) sampling lines made of materials such as Teflon that minimize its adsorption are necessary to avoid negative artifacts when it is adsorbed and positive artifacts when it later desorbs. Finally, they are not "real-time" methods in that sampling for periods of time of the order of hours is typically required.

Given these considerations, it is perhaps not surprising that intercomparison studies have shown significant disagreements between the various techniques. Figure 11.31, for example, shows some data from one such intercomparison (the so-called "nitric acid shootout"), in which filter pack (FP), difference denuder (DD), annular denuder (AD), TDLS, and FTIR measurements were all taken simultaneously. It is seen that the filter pack measurements were consistently higher, and the annular denuder and TDLS consistently lower, than the FTIR measurements, which were used as the standard for comparison. While most measurements in this period were within the wide error bars for the FTIR measurements, note that the range of concentrations from the different methods spans more than a factor of two! In addition, there were significant differences in some of the methods from day to night.

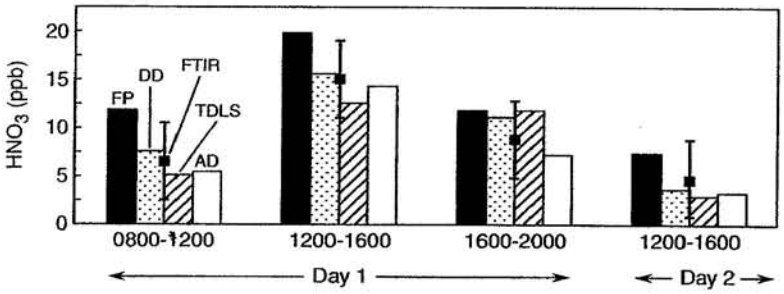


FIGURE 11.31 Comparison of gaseous $HNO_3$ measurements made simultaneously in Claremont, California, on two different days using FT-IR shown as ■; with error bars and by a filter pack (FP), a difference denuder (DD), an annular denuder (AD), and tunable diode laser spectroscopy (TDLS) (adapted from Hering *et al.*, 1988).

These studies were carried out in a polluted urban atmosphere where the concentrations are relatively high; it might be expected that the agreement (or lack thereof) would certainly not improve at the much smaller concentrations found in rural and remote regions. Similar disagreements have been observed in other intercomparison studies (e.g., Anlauf *et al.*, 1985; Gregory *et al.*, 1990b; Huebert *et al.*, 1990), even in synthetic atmospheres (e.g., Fox *et al.*, 1988).

Because of such problems, spectroscopic methods, where available, are generally preferred. However, the sensitivity of long-path FTIR (4 ppb at a 1.15-km path length) is insufficient except for the most polluted atmospheres. TDLS measurements have better sensitivity (75 ppt) but it is still not sufficient for measurements in remote atmospheres. As a result, there continues to be a need for accurate, specific, and very sensitive methods of measurement of $HNO_3$ that also have good time resolution (seconds or better). Recent efforts using mass spectrometry look promising in this regard.

*Mass spectrometry.* Several instruments based on chemical ionization mass spectrometry (CIMS) have been developed and applied to ambient air (Huey *et al.*, 1998; Mauldin *et al.*, 1998). Figure 11.32 shows two such instruments that have undergone an informal intercomparison study between themselves and a filter pack (nylon) method (Fehsenfeld *et al.*, 1998).

The first CIMS method (Fig. 11.32a) uses the equilibrium $HNO_3$ adduct with $HSO_4^-$ to measure gaseous $HNO_3$ (Mauldin *et al.*, 1998):

$$HNO_3 + HSO_4^- \overset{K_{11,-11}}{\longleftrightarrow} HSO_4^- \cdot HNO_3. \quad (11, -11)$$

From equilibrium considerations,

$$[HNO_3] = [HSO_4^- \cdot HNO_3]/K_{11,-11}[HSO_4^-], \quad (O)$$

and the ratio of the adduct and reagent ions is measured to obtain the concentration of $HNO_3$. Sampling and ionization of $H_2SO_4$ to generate the reagent $HSO_4^-$ ion using a radioactive $^{241}Am$ source occur at atmospheric pressure. The ions are transported into the mass spectrometer through a free jet expansion of dry $N_2$, which helps to strip water clustered to the ions, as well as through a collisional dissociation chamber where the collisional energies have been adjusted so that $HSO_4^-(H_2O)_n$ clusters are dissociated but the adduct $HSO_4^- \cdot HNO_3$ is not. Figure 11.33a shows a typical mass spectrum of air using this approach. The strong reagent $HSO_4^-$ ion and the adduct are clearly visible. Detection limits for a 1-s integration time are reported to be 1–3 ppt in clean air but higher in polluted air due to increased background signals (Mauldin *et al.*, 1998).

In the second CIMS instrument, shown in Fig. 11.32b, air is drawn through a small orifice into a flow tube at ~20 Torr pressure where it is mixed with $SiF_5^-$ reagent ions (Huey *et al.*, 1998). These ions are generated by alpha particle ionization where electrons attach to small amounts (~30 ppb) of $SF_6$ in the $N_2$ carrier gas, forming $SF_6^-$, $SF_5^-$, and $F^-$. These species react with $SiF_4$, present at ~300 ppb, forming $SiF_5^-$. The $SiF_5^-$ reagent ions react with gaseous $HNO_3$, setting up an equilibrium with the adduct (Huey and Lovejoy, 1996):

$$SiF_5^- + HNO_3 + M \overset{K_{12,-12}}{\longleftrightarrow} SiF_5^- \cdot HNO_3 + M. \quad (12, -12)$$

A typical mass spectrum taken in air is shown in Fig. 11.33b. The reagent ion and the adduct are clearly visible, as are adducts with other species, including formic acid. As discussed by Huey *et al.* (1998), the latter should permit the same method to be used to measure HCOOH, but with a sensitivity that is likely to be about two orders of magnitude less than that for

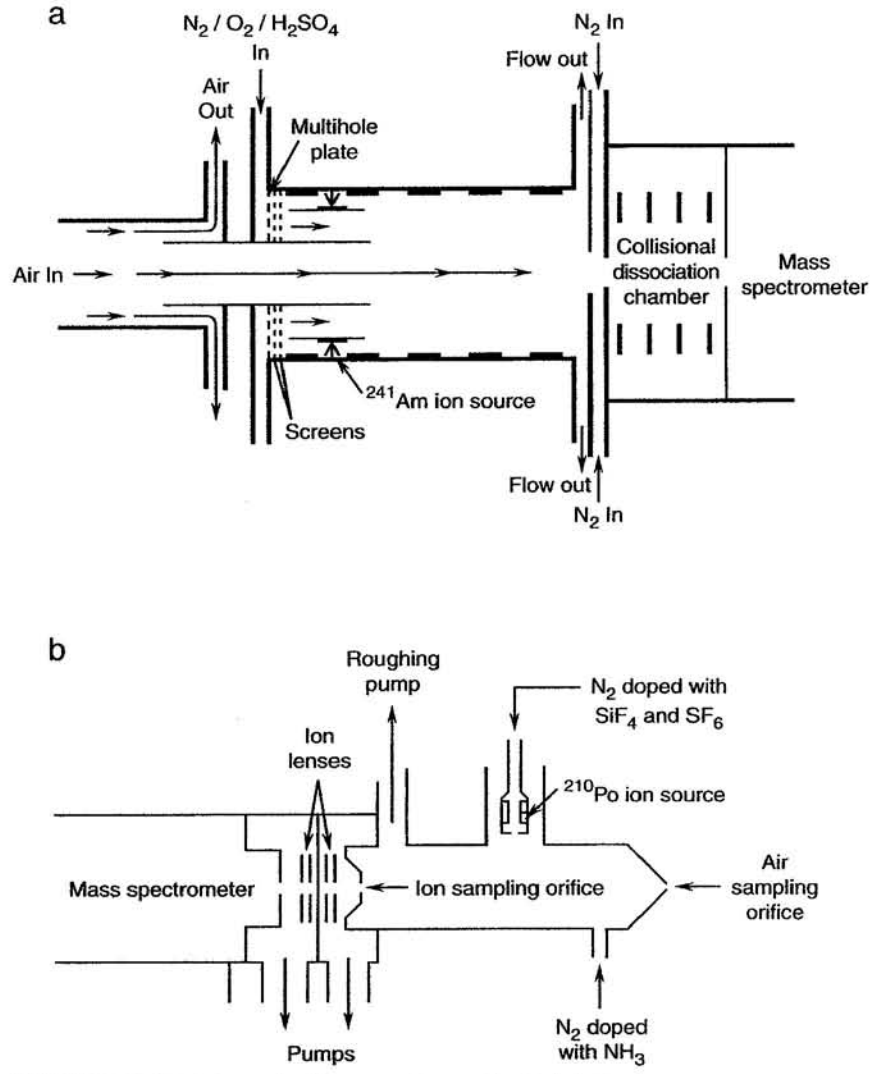


FIGURE 11.32 Schematic diagrams of two chemical ionization mass spectrometers used to measure $HNO_3$ (adapted from Mauldin *et al.*, 1998; and Huey *et al.*, 1998).

$HNO_3$ because of differences in the equilibrium constants for adduct formation. Since reaction (12, −12) is at equilibrium, the $HNO_3$ concentration is given by

$$[HNO_3] = [SiF_5^- \cdot HNO_3]/K_{12,-12}[SiF_5^-] \quad \text{(P)}$$

and measuring $HNO_3$ requires measuring the ratio of the adduct and reagent ions. Background signals occur from desorption of $HNO_3$ from the flow tube walls and from formation of radicals in the ionization region that generate $HNO_3$. The addition of small amounts of $NH_3$ was found to decrease the first signal but not react with $HNO_3$ in the air under the flow tube conditions. Detection limits were 5–50 ppt (depending on the background, which was larger at higher $HNO_3$ concentrations) for a 1-s measurement time.

An informal intercomparison of these two CIMS methods with a filter pack method shows generally excellent agreement between the mass spectrometric approaches and often, but not uniformly, good agreement with the filter pack method (Fehsenfeld *et al.*, 1998). The latter was often high, which was attributed to interference from decomposition of ammonium nitrate to $HNO_3 + NH_3$ on the Teflon particle prefilter, followed by absorption of the $HNO_3$ by the nylon filter.

In short, these chemical ionization mass spectrometry methods appear to be quite promising for the measurement of $HNO_3$, especially at the low levels found in the remote trosposphere.

*Typical tropospheric concentrations of $HNO_3$.* Given the difficulties in measuring atmospheric nitric acid,

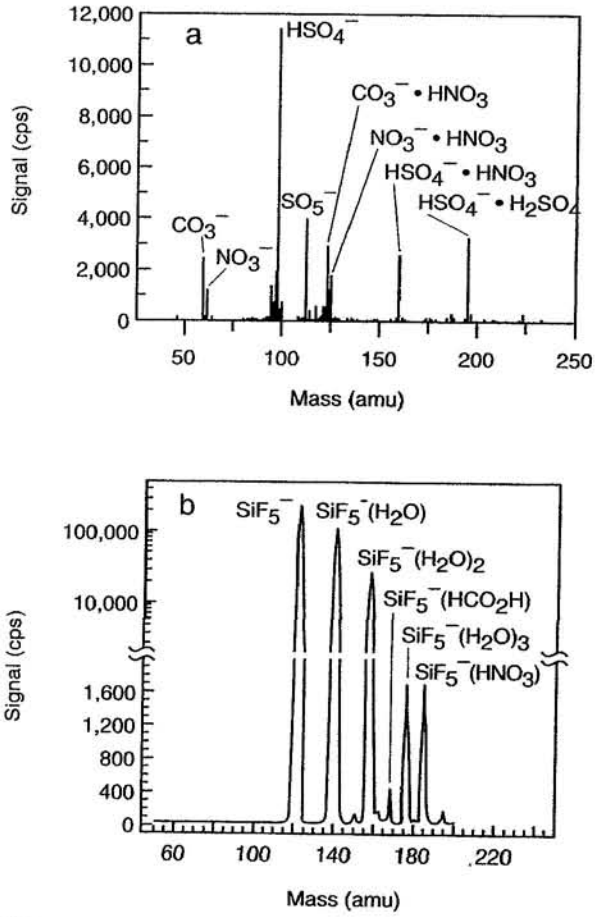


FIGURE 11.33 Typical chemical ionization mass spectra taken using (a) $HSO_4^-$ as the chemical ionization reagent or (b) $SiF_5^-$ as the CI reagent. Note the change to a logarithmic scale in (b) above ~ 2000 counts per second (CPS) (adapted from Mauldin *et al.*, 1998; and Huey *et al.*, 1998).

there is not a large data base of measurements in a variety of locations and types of air masses that is believed to accurately portray its concentrations, particularly in remote atmospheres. However, the intercomparison studies described by Hering *et al.* (1988) suggest that concentrations in polluted urban areas are as high as 25 ppb for 4- to 6-h averages, levels that have also been measured over much shorter time periods using FTIR (Biermann *et al.*, 1988). Similar ppb levels (up to ~5 ppb) have been measured near Vienna, Austria, in the summer (Piringer *et al.*, 1997).

A brief informal intercomparison study of the mass spectrometry methods with a nylon filter pack method near Boulder, Colorado, gave average levels of 0.38–1.6 ppb when the wind carried air from the direction of the greater metropolitan Denver urban area and 0.14–0.56 ppb when the wind was downslope and westerly, where there are fewer emissions sources; previous filter pack measurements at this site gave concentrations ranging from a few ppt, characteristic of remote regions, to several ppb, characteristic of polluted urban areas (Fehsenfeld *et al.*, 1998).

Measurements of $HNO_3$ in the marine boundary layer are typically of the order of tens to hundreds of ppt. For example, Heikes *et al.* (1996) reported average concentrations of 160 ppt, with a range from 30 to 280 ppt. In the middle and upper troposphere, concentrations of ~100–400 ppt have been reported (e.g., Singh *et al.*, 1998).

*(6) $NO_3$* As discussed earlier, the nitrate radical can be measured using visible spectroscopy and its absorption bands, particularly the one at 662 nm. As a result, visible absorption spectroscopy has been the method of measurement used most extensively for $NO_3$. As discussed shortly, a matrix isolation technique has also been applied with success in some studies.

Noxon *et al.* (1978) were the first to report the detection of $NO_3$ and to estimate its column abundance in the atmosphere, using its absorption at 662 nm and the moon as the light source. Their initial hypothesis was that most of the $NO_3$ was in the stratosphere. However, Noxon *et al.* (1980) subsequently showed using the moon as the light source, or alternatively a surface-based lamp with a 10-km path length at the Fritz Peak Observatory in Colorado, that $NO_3$ was also present in the troposphere at concentrations up to a few hundred ppt. About the same time, $NO_3$ was also detected and measured in the polluted troposphere by Platt *et al.* (1980b). Since then, there have been a number of measurements of its column abundance and concentrations at specific locations in the troposphere (e.g., see Platt, 1994; and Plane and Smith, 1995), all of which are at night or at sunset or sunrise due to the rapid photolysis of $NO_3$ during the day.

Vertical profiles, and in particular the amounts of tropospheric $NO_3$, have been extracted from measurements of the column abundance as a function of solar zenith angle at sunrise using either the moon or scattered sky light as the light source (e.g., Smith and Solomon, 1990; Smith *et al.*, 1993; Weaver *et al.*, 1996; Aliwell and Jones, 1996a, 1996b, 1998). As the sun rises, the column abundance of $NO_3$ decreases due to photolysis. During the night, the sun is sufficiently below the horizon that the atmosphere is in darkness throughout the stratosphere and troposphere. As it rises to a solar zenith angle of ~97°, altitudes down to 40 km are exposed to direct sunlight, and by the time the solar zenith angle is 93°, only the region below 10 km is not exposed to direct sunlight. Because the photolysis of $NO_3$ is so fast, under these conditions any signal remaining must be attributable to tropospheric

$NO_3$ (e.g., Smith and Solomon, 1990; Weaver *et al.*, 1996; Aliwell and Jones, 1998).

Using this approach in various locations, it has been shown that the relative contributions of stratospheric and tropospheric $NO_3$ vary considerably. For example, in the Antarctic in spring, essentially all of the $NO_3$ was in the stratosphere (Smith *et al.*, 1993), whereas at Fritz Peak, Colorado, in the summer, about equal amounts were in the troposphere and stratosphere (Weaver *et al.*, 1996). Assuming that this tropospheric $NO_3$ was in a 1-km-thick bounday layer, the average $NO_3$ radical concentration in this layer at sunrise was about 20 ppt. Aliwell and Jones (1998) using a similar approach at Cambridge, England, suggest the average concentration could be as high as 89 ppt.

Surface measurements of $NO_3$ have been made using folded light paths and a light source such as a Xe arc lamp (Platt, 1994; Plane and Smith, 1995). Concentrations as high as ~350 ppt have been observed in polluted urban areas (Platt *et al.*, 1980b, 1981; Platt and Janssen, 1995), although many times even in polluted areas, the concentrations are below 20 ppt (Biermann *et al.*, 1988). This likely reflects the balance between sources and sinks. For example, since $NO_3$ reacts rapidly with NO, significant concentrations of $NO_3$ will not be observed close to NO emission sources.

A second technique, matrix isolation–electron spin resonance (ESR), described earlier for $NO_2$ measurements, has also been used to measure $NO_3$ in the atmosphere (Mihelcic *et al.*, 1985, 1990, 1993). Because there is a large concentration of $NO_2$ in air compared to other paramagnetic species, this dominates the spectra. However, the contribution of $NO_2$ can be subtracted using a reference spectrum and the residual then matched using the simultaneous fit of other contributing species (Mihelcic *et al.*, 1990) to derive the contributions of species such as $NO_3$, $HO_2$, and $RO_2$. A sample spectrum containing contributions from all of these species is shown later (Fig. 11.53) in the discussion of $HO_2$ and $RO_2$ measurements. The detection limit of this method for $NO_3$ is 3 ppt (Mihelcic *et al.*, 1993). The disadvantage is that it is not a "real-time" method, and as with any sampling of free radicals, care must be taken not to destroy the radicals before they are trapped and/or measured.

*Typical tropospheric concentrations.* Studies carried out in a remote region, at Izaña de Tenerife in the Canary Islands, showed average nighttime $NO_3$ concentrations in clean air from the mid-Atlantic to be ~8 ppt, with a maximum of ~20 ppt (Carslaw *et al.*, 1997b), and the concentrations are often below the detection limits (e.g., <3 ppt at Loop Head, Ireland; Platt and Janssen, 1995).

In rural–suburban areas, concentrations between these two have been observed. For example, in central California peak concentrations were typically about 30 ppt, with a maximum value of ~80 ppt (Smith *et al.*, 1995), and at Kap Arkona in the Baltic Sea, the average nighttime concentrations were 8 ppt (Heintz *et al.*, 1996). However, even in such rural–suburban areas, high concentrations can occur, e.g., 280 ppt at Deuselbach, Germany (Platt *et al.*, 1981; Platt and Janssen, 1995).

In short, the concentration of $NO_3$ in the troposphere can vary from very small, low-ppt concentrations to several hundred ppt, depending on the particular air mass. As discussed in Chapters 7 and 10, at typical tropospheric levels, it is believed to play a major role in nighttime chemistry, in some cases rivaling daytime OH for the net oxidation of certain organics, particularly alkenes (e.g., see Aliwell and Jones, 1998) as well as certain gaseous PAH.

*(7) **HONO*** Because of its importance as an OH source by photolysis at dawn, particularly in polluted areas, there have been a number of measurements reported for HONO. The two methods used most commonly have been DOAS and denuder methods. In addition, diffusion scrubber and photofragmentation—laser-induced fluorescence methods have been developed, although they have not seen widespread use.

*DOAS.* As discussed earlier, HONO has been measured at the earth's surface at a number of sites around the world by DOAS using its characteristic absorption bands in the 340- to 380-nm region. Because this is a spectroscopic method, it has high selectivity as well as sensitivity. The disadvantage is that it requires a unique set of equipment and, more importantly, skilled experimentalists to accurately extract the HONO signal from others present in air, particularly that of $NO_2$, which is essentially always present simultaneously.

*Denuders.* The principle behind denuders has been discussed earlier with respect to $HNO_3$. Several types of wall coatings have been used for trapping HONO, including $Na_2CO_3$ (Ferm and Sjödin, 1985) and a triple denuder coated first with tetrachloromercurate to remove $SO_2$ and $HNO_3$, followed by two $Na_2CO_3$-coated tubes (Febo *et al.*, 1993; Febo and Perrino, 1995; Febo *et al.*, 1996). A wet diffusion denuder using NaOH as the absorbing agent has also been described (Simon and Dasgupta, 1995). The nitrite ion is then extracted and measured, most commonly using ion chromatography but, in some cases, using colorimetric methods (e.g., Ferm and Sjödin, 1985).

Figure 11.34 shows one set of measurements of HONO made in Milan, Italy, using DOAS and a denuder method, respectively (Febo *et al.*, 1996). In this

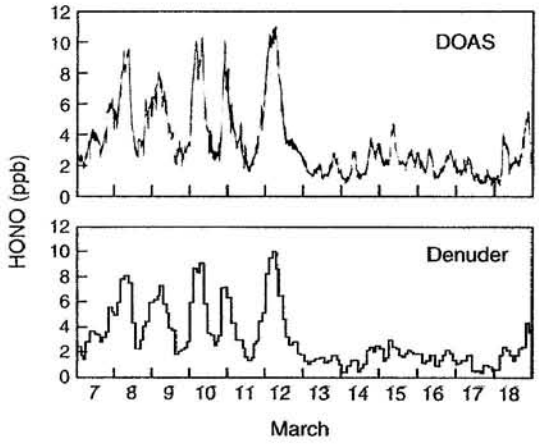


FIGURE 11.34 HONO measurements at Milan, Italy, using DOAS or denuders, respectively, in March 1994 (adapted from Febo *et al.*, 1996).

particular study, the DOAS and denuder methods are in reasonably good agreement, although this is not always the case.

As is the case for denuder methods in general, artifacts are possible and this is particularly the case for nitrite, which can be oxidized relatively easily to nitrate. Positive artifacts due to high concentrations of $NO_2$ and PAN can occur, and $SO_2$ can also interfere (Perrino *et al.*, 1990). For example, HONO has been reported during the day using denuders at levels much higher than would be expected given its rapid photolysis, suggesting the presence of significant positive artifacts (e.g., see Lammel and Cape, 1996).

*Diffusion scrubber.* In one such approach, air containing the HONO flows past a microporous membrane through which a flow of water is pumped. HONO (and other gases) diffuse through the membrane and are "scrubbed" into the water and measured by ion chromatography (Večeřa and Dasgupta, 1991). A second approach involves reducing the absorbed nitrite ion to NO using ascorbic acid and then measuring the NO by chemiluminescence (Kanda and Taira, 1990; Harrison *et al.*, 1996). Since there is often significant NO present, HONO must be determined using difference methods.

*Photofragmentation–laser-induced fluorescence.* In an approach similar to that which has been applied to $HNO_3$, HONO can be photolyzed to generate OH and the OH measured using laser-induced fluorescence (Rodgers and Davis, 1989):

$$\text{HONO} + h\nu(355\text{ nm}) \rightarrow \text{OH}(\text{X}^2\Pi)_{v''=0} + \text{NO}, \quad (13)$$

$$\text{OH}(\text{X}^2\Pi)_{v''=0} + h\nu(282\text{ nm}) \rightarrow \text{OH}(\text{A}^2\Sigma)_{v'=1} \xrightarrow{\text{M}} \text{OH}(\text{A}^2\Sigma)_{v'=0}, \quad (14)$$

$$\text{OH}(\text{A}^2\Sigma)_{v'=0} \rightarrow \text{OH}(\text{X}^2\Pi) + h\nu(309\text{ nm}). \quad (15)$$

The detection of OH and the uncertainties associated with it are discussed in detail shortly. The detection limit is a few tens of ppt for a measurement time of 15 min (Rodgers and Davis, 1989).

Atmospheric pressure ionization mass spectrometry has also been used to meaure HONO in indoor air enviroments (Spicer *et al.*, 1993a) and outdoors from a research aircraft (Berkowitz *et al.*, 1998). In this case, HONO does not have a parent peak in either positive or negative ion modes, so that adduct formation must be used to form a parent ion. In this case, $CCl_4$ was introduced into the corona discharge region, forming $Cl^-$, which forms an adduct with HONO. Peaks at $m/e$ 82 and 84 corresponding to the $^{35}Cl^-$ and $^{37}Cl^-$ adducts are observed in the negative ion mode and their collisionally induced fragmentation to $m/e$ 46 followed.

*Typical surface concentrations of HONO.* Because it is so readily photolyzed, HONO builds up at night and its concentrations rapidly drop at dawn. Figure 11.35 summarizes the range of measured tropospheric HONO concentrations and their average values in remote to polluted urban regions (Lammel and Cape, 1996). The highest concentrations are generally found in polluted areas where there are higher concentrations of precursor $NO_2$ (see Chapter 7). Concentrations up to 10 ppb have been observed in Milan, Italy (Febo *et al.*, 1996), and the Los Angeles area (Platt *et al.*, 1980a; Harris *et al.*, 1982; Atkinson *et al.*, 1986; Winer and Biermann, 1994). Peak values of several ppb have been observed in many other urban locations, including, for example, Ispra, Italy (Andrés-Hernández *et al.*, 1996), and Göteborg, Sweden (Sjödin, 1988).

***(8) $NH_3$*** A number of measurement techniques have been used for ammonia, including a spectroscopic method, denuder methods, and filter packs.

*Photofragmentation–laser-induced fluorescence (PD-LIF).* This spectroscopic method is based on the photofragmentation of $NH_3$ in a two-photon process using 193-nm radiation, followed by laser-induced fluorescence of the NH fragment (Schendel *et al.*, 1990). The processes are as follows:

$$\text{NH}_3 + 2h\nu(193\text{ nm}) \rightarrow \text{NH}(\text{b}^1\Sigma^+)_{v''=0} + \text{H}_2 \text{ or } 2\text{H}, \quad (16)$$

$$\text{NH}(b^1\Sigma^+)_{v''=0} + h\nu(450\text{ nm}) \rightarrow \text{NH}(\text{c}^1\Pi)_{v'=0}, \quad (17)$$

$$\text{NH}(c^1\Pi)_{v'=0} \rightarrow \text{NH}(\text{a}^1\Delta)_{v''=0} + h\nu(325\text{ nm}). \quad (18)$$

Selectivity is obtained by tuning the NH excitation laser to a specific rotational transition and following specific fluorescence transitions. Detection limits of ~5 ppt for

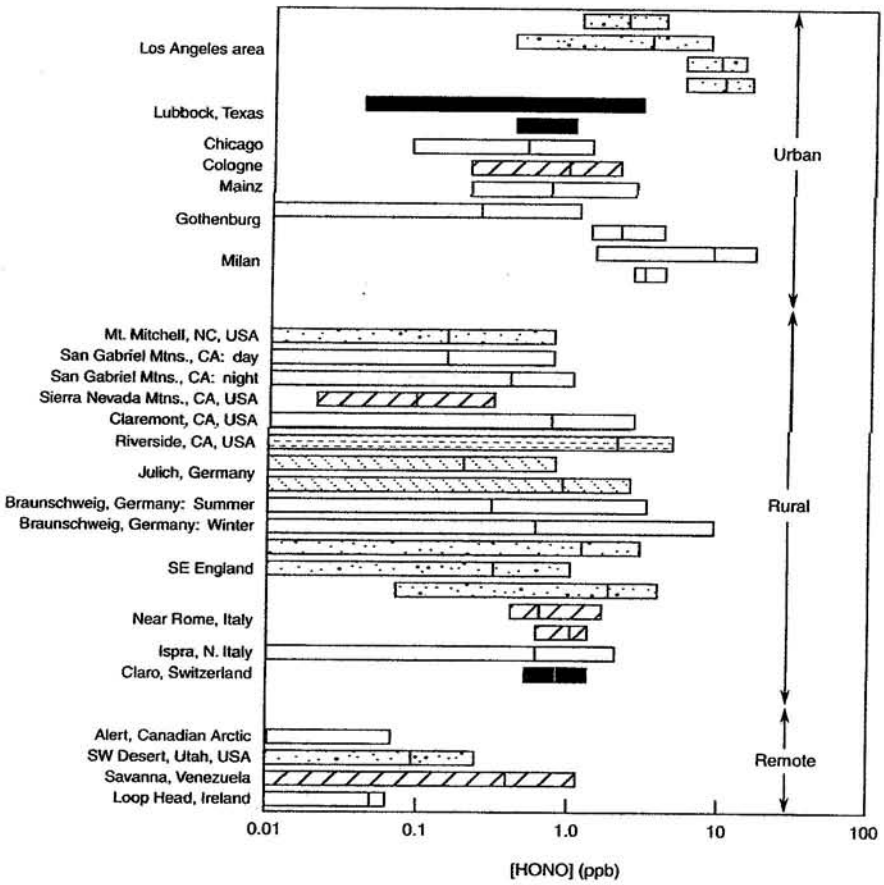


*FIGURE 11.35* *Range of tropospheric HONO concentrations observed in remote to* polluted areas. The averages are shown by the vertical bars. Note the scale is logarithmic (adapted from Lammel and Cape, 1996).

an integration time of 5 min have been reported (Williams *et al.*, 1992).

*Denuder methods.* As described earlier for $HNO_3$, diffusion denuders are also used for $NH_3$. For example, tungstic acid coated denuders take up both $HNO_3$ and $NH_3$. The ammonia is then thermally desorbed (as $NH_3$), oxidized to NO, and measured using chemiluminescence (Braman *et al.*, 1982; Hering *et al.*, 1988). In practice, since $HNO_3$ desorbs in the form of NO and $NO_2$, the $NH_3$ from the thermal desorption is usually first readsorbed on a second $WO_3$-coated tube to separate it from the $HNO_3$ signal, and a second thermal desorption followed by conversion to NO used for the measurement of $NH_3$.

Other denuder coatings for $NH_3$ include molybdenum oxide, from which ammonia is thermally desorbed and converted to NO for measurement as in the tungstic acid method; with $MoO_3$ as the coating, some of the $NH_3$ thermally desorbs directly in the form of NO (Langford *et al.*, 1989). In addition, oxalic acid has been used as a coating and the $NH_3$ collected as ammonium ion is obtained by extracting the tube and measuring $NH_4^+$ by ion chromatography (Ferm, 1979).

*Filter packs.* As shown in Fig. 11.22, $NH_3$ can be collected on impregnated filters in filter packs designed to collect particles and gas-phase nitric acid. Oxalic acid or citric acid on Whatman filters is often used to absorb the gaseous ammonia, which is then measured by extraction into aqueous solution and ion chromatography or by a colorimetric method (e.g., see Anlauf *et al.*, 1988; and Williams *et al.*, 1992).

Williams *et al.* (1992) have carried out an intercomparison of PD-LIF with three denuder methods and one filter pack technique using both laboratory-prepared samples and ambient air. All methods agreed to within 10% when measuring an ammonia standard. When a measured amount of $NH_3$ was introduced as a spike into filtered air, the agreement was not as good. The PF-LIF and citric acid denuders gave 87 and 93% response, respectively, but the recoveries using the tungstic acid denuder, the molybdenum oxide annular denuder, and the filter pack were only 68, 37, and 22%,

discussed earlier. Sachse *et al.* (1987), for example, applied TDLS to measure CO using the P(5) line at 4.7 $\mu$m (2128 $cm^{-1}$). Measurements could be made in 1 s with an accuracy of $\pm 1.4$ ppb.

The application of a commercial NDIR instrument to ambient CO measurements is described by Parrish *et al.* (1994); precision ($1\sigma$) of $\sim 2$ ppb with 1-h averaging times could be obtained. A similar detection principle has been used to measure middle-tropospheric CO from the space shuttle (Reichle *et al.*, 1990).

Finally, gas chromatography can be used to separate CO from the other constituents in air. Various detection methods have been used, including conversion of CO to $CH_4$ and measurement of $CH_4$ by flame ionization detection (e.g., Porter and Volman, 1962). A unique method is also used for CO in which it reacts with hot HgO, releasing Hg vapor, which is measured by atomic absorption of light from a mercury lamp, known as the GC–HgO method (e.g., see Greenberg *et al.*, 1996). Intercomparisons of chromatographic measurements and TDLS have shown that the two approaches are in good agreement (e.g., see Hoell *et al.*, 1985, 1987b). Intercomparisons of the GC–HgO methods with NDIR have also been carried out using a round-robin approach on prepared CO standards (Novelli *et al.*, 1998a); while agreement was good in many cases, the uncertainties associated with the NDIR method were larger by a factor of about 5 at low CO levels, $\sim 50$ ppb. Differences in the accuracy between laboratories were also noted, even among those using the same method. These were traced in some cases to inaccurate calibrations, but other factors such as nonlinearity in the GC–HgO detectors over the full range of atmospheric concentrations were also suggested as possible contributing factors.

*Typical ambient levels.* Typical levels of CO range from $\sim 50$–$150$ ppb in remote areas (e.g., see Parrish *et al.*, 1991, 1994; Novelli *et al.*, 1992, 1998a, 1998b; and Derwent *et al.*, 1998) to $\sim 1000$ ppb in rural–suburban areas up to $\sim 10$ ppm in very polluted areas such as Mexico City (e.g., Riveros *et al.*, 1998). It is interesting that the values that appear to be representative of clean, remote areas are about the same as those found using ice cores for the preindustrial era; for example, Haan *et al.* (1996) report preindustrial values of about 92 ppb for a Greenland ice core and $\sim 55$–$60$ ppb for an Antarctic ice core.

Figure 11.36, for example, shows the zonally averaged CO concentrations in the Northern and Southern Hemispheres, respectively, from 1990 to 1995 (Novelli *et al.*, 1998b). Concentrations are higher in the Northern than in the Southern Hemisphere, but both show a decreasing trend with time, $-2.6 \pm 0.3$ ppb $yr^{-1}$ in the Northern Hemisphere and $-1.9 \pm 0.1$ ppb $yr^{-1}$ in the Southern Hemisphere. The seasonal trends observed in both hemispheres reflect an anticorrelation with OH that removes CO from the atmosphere. CO in the NH, for example, peaks in March/April and is a minimum in July.

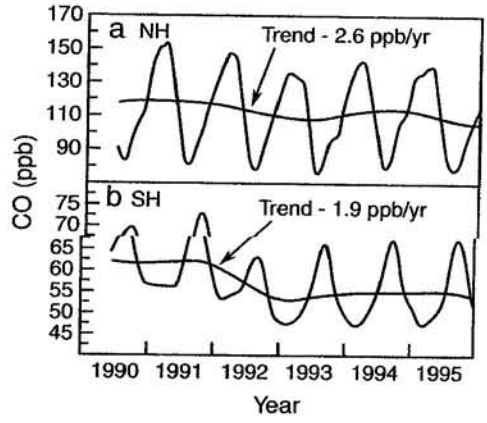


FIGURE 11.36 Zonal average concentrations of CO in (a) the Northern Hemisphere and (b) the Southern Hemisphere (adapted from Novelli *et al.*, 1998b).

### *d. $SO_2$*

*Detection techniques.* As shown in Table 11.1, common techniques for measuring $SO_2$ include UV fluorescence, DOAS, and a wet chemical (pararosaniline) technique in which $SO_2$ undergoes the Schiff reaction with pararosaniline, HCHO, and HCl to form a red-violet product whose absorbance at 560–580 nm is measured (West and Gaeke, 1956; Dasgupta and Gupta, 1986). Filter packs (e.g., Ferek and Hegg, 1993), diffusion scrubbers (e.g., Lindgren and Dasgupta, 1989), and denuders (e.g., see Pui *et al.*, 1990) have also been used for $SO_2$.

Infrared techniques, including TDLS (Schiff *et al.*, 1994b) and matrix isolation FTIR (Griffith and Schuster, 1987), have been applied to $SO_2$, with detection limits of 500 and 10 ppt, respectively.

Several chemiluminescence methods have also been developed for $SO_2$. For example, $SO_2$ has been shown to enhance the chemiluminescence signal from the luminol–$NO_2$ reaction so that the enhancement can be used as a measure of $SO_2$ at a fixed $NO_2$ concentration (Zhang *et al.*, 1985). Another method involves the formation of SO in a hydrogen flame followed by reaction with $O_3$ to generate electronically excited $SO_2$ whose emission is followed at 340 nm (e.g., see Benner and Stedman, 1990).

Gas chromatography with various detectors such as flame photometry have been applied in a number of studies; flame photometry involves the generation of

electronically excited $S_2$ in a hydrogen-rich flame, and the emission at 394 nm is followed. The signal is proportional to the square of the concentration of the sulfur compound. Since all compounds containing sulfur will form $S_2$ in the flame, a separation technique such as GC must be used to differentiate $SO_2$ from other sulfur compounds.

Another GC method, isotope dilution GC–MS, involves the addition of an isotopomer of the analyte of interest to the sampling manifold (e.g., see Bandy *et al.*, 1993; and Blomquist *et al.*, 1993). In the case of $SO_2$, where the ambient $SO_2$ consists mainly of $^{16}O$ and $^{32}S$, $SO_2$ containing the $^{34}S$ isotope is used. This labeled $SO_2$ at mass 66 is used as internal standard and has a number of additional advantages such as minimizing the loss of the analyte in the sampling system (Bandy *et al.*, 1993). The air with the added isotopomer is trapped cryogenically and then sampled into a GC–MS for analysis.

The results of intercomparison studies suggest that measuring $SO_2$, particularly at low concentrations found in remote areas, is difficult. For example, Gregory *et al.* (1993) evaluated five techniques for measuring $SO_2$ in air: GC with flame photometric or mass spectrometric detection, a chemiluminescence method using reaction with $KMnO_4$, and a filter method with either the $KMnO_4$ chemiluminescence or ion chromatographic detection. Above ~200 ppt, agreement between pairs of techniques varied from about 30% to several orders of magnitude. At concentrations below this, there was no correlation between the measurements made using these five methods! Kok *et al.* (1990) compared a filter pack, diffusion denuder, and a commercial pulsed fluorescence analyzer over the range of 0.1–1 ppb. The results for this intercomparison were also quite scattered, although they did show some correlation with each other.

*Typical ambient levels.* Concentrations of $SO_2$ in remote areas are quite low, ~10–50 ppt (e.g., Bandy *et al.*, 1993), since the only source is oxidation of biogenically produced organic sulfur compounds such as dimethyl sulfide (see Chapter 8.E). In rural–suburban areas, concentrations of ~1–20 ppb (e.g., Luria *et al.*, 1987; Boatman *et al.*, 1988) are common and in polluted urban areas, levels up to several hundred ppb are observed (e.g., Bennett *et al.*, 1986).

### *e. NMHC and VOC*

As discussed in detail in Chapters 6 and 16, organic compounds play a key role in the formation of ozone, particles, and other species of interest. While some of the individual species are of concern from the point of view of health effects (e.g., the carcinogens benzene and 1,3-butadiene), for most VOC it is because of their central role in the formation of ozone and associated pollutants that their emissions are regulated.

As discussed in Chapter 16.B, methane reacts relatively slowly with OH ($k^{298K} = 6.3 \times 10^{-15}$ cm$^3$ molecule$^{-1}$ s$^{-1}$), with a lifetime with respect to this reaction of about 5 years at an OH concentration of $1 \times 10^6$ cm$^{-3}$. It is because of this long lifetime in the troposphere that methane is the only hydrocarbon to survive long enough to reach the stratosphere and participate in chemistry there. However, in terms of generating $RO_2$ radicals that convert NO to $NO_2$ on time scales of a few hours to days, $CH_4$ is not important compared to larger hydrocarbons (see Chapter 16.B for a discussion of reactivity and data in Table 16.8). This is the case even though its concentrations in air are much higher than those of other organics, 1.8 ppm versus a few ppb or less. Because of this, the regulatory focus has traditionally been on "non-methane hydrocarbons" (NMHC). (See Chapter 14 for a discussion of the role of $CH_4$ in global climate.)

However, it is not only hydrocarbons, but a wide variety of organics, that participate in the chemistry. Indeed, as discussed in Chapter 16, some of these such as the carbonyl compounds can be much more reactive than the parent hydrocarbon. As a result, the term "volatile organic compounds" (VOC) is often used to encompass all of the individual reactive organics in the troposphere, and we shall use this term here. Other terms used synonymously are ROG ("reactive organic gases") and NMOG ("non-methane organic gases").

There are two approaches to measuring VOC: measuring the total without segregating into individual species, or measuring the individual organics that contribute to VOC. The former is commonly used for routine monitoring purposes whereas the latter is clearly of interest from the point of view of understanding the details of atmospheric reactions.

***(1) Sampling and measurement techniques for VOC***

*Total NMOC.* Total non-methane organics (NMOC) as a group (i.e., nonspeciated) are commonly measured by cryotrapping the air sample, e.g., in liquid argon, which does not trap $CH_4$. The contents of the trap can then be thermally desorbed directly into a flame ionization detector (FID) (McElroy *et al.*, 1986).

In a second approach, $CH_4$ is separated and measured independently and NMOC obtained by difference. This can be accomplished using gas chromatography to separate the $CH_4$ or, alternatively, oxidizing all of the organics except $CH_4$ to $CO_2 + H_2O$ and measuring the $CH_4$ remaining by FID, which does not respond to $CO_2$ and water vapor. [Note, however, that water affects the GC baseline so that care must be

Camel and Caude (1995) and Matisová and Škrabáková (1995).

As might be expected, these sorbents can have different efficiencies for the uptake of individual organics, so that results from trapping on one sorbent may not be the same as that on another one. For example, a comparison of Tenax-TA with a combination of Carbotraps B and C on a test atmosphere containing a number of compounds of atmospheric interest showed good agreement for most compounds; however, ethanethiol was not well retained by the Carbotrap, whereas these carbon sorbents were more effective for chlorodifluoromethane and 1,2-dichlorotetrafluoroethane (McCaffrey *et al.*, 1994). A combination of adsorbents in one trap is often used to overcome such problems (e.g., see Helmig and Greenberg, 1994). The sorbents are arranged so that lightest organics pass through to the last layer and are trapped there, so that the most highly absorbing sorbent is the last one exposed to the airstream. The direction of the flow is reversed during thermal desorption (Matisová and Škrabáková, 1995).

Even for compounds that are efficiently trapped by a particular sorbent, care must be taken not to pass so much sample through the adsorbent that it becomes overloaded and hence "breakthrough" of the organic occurs (e.g., see Brown and Purnell (1979) for data on a variety of organics using Tenax-GC). Care must also be taken to investigate and, where possible, avoid artifacts when such sorbents are used. These can arise from desorption of organics such as benzene, either from the sorbent itself or from uptake of organics on it during storage (e.g., see Cao and Hewitt, 1994). To overcome such problems, the sorbents are cleaned prior to use, which is commonly done either by heating under a flow of gas or by extracting the solid with a solvent or combination of solvents followed by storage in a cold, organic-free container (Helmig, 1996).

Artifacts can also arise from reaction of the sorbent with components of the airstream, such as $O_3$ and $NO_2$. For example, Clausen and Wolkoff (1997) observed a number of products from the reactions of $O_3$ with Tenax, such as acetophenone, decanal, and benozic acid. Interestingly, 2,6-diphenyl-*p*-hydroquinone was generated when limonene was also present and was suggested to arise from the reaction with the Tenax of the radicals or the Criegee biradical generated in the ozone–limonene reaction. They also observed reactions of $NO_2$ with the Tenax sorbent.

Reaction of adsorbed organics with other components of the airstream during sampling, particularly ozone, is well known, leading to artificially low levels of the organic and, in some cases, the appearance of new species that are products of these artifact reactions (see Helmig (1997) for a review of these interferences). This is particularly the case for reactive compounds such as the unsaturated biogenics. It should be noted that such interferences due to ozone also occur with cryotrapping (Helmig, 1997). In this case, reactions between ozone and the organics can occur as the trap is warmed to desorb the organics onto the GC column. For example, Goldan *et al.* (1995) examined the effects of 100 ppb $O_3$ on a synthetic mixture of *n*-pentane, isoprene, 2,2-dimethylbutane, benzene, *m*-xylene, and $\alpha$-pinene. Figure 11.37 shows the chromatograms of this mixture in the absence of $O_3$, in the presence of 100 ppb $O_3$ with no ozone trap, and finally, with a $Na_2SO_3$ scrubber for ozone upstream of the cryotrap. The presence of 100 ppb $O_3$ essentially completely removes $\alpha$-pinene and most of the isoprene, and new peaks corresponding to oxidation products (methacrolein and methyl vinyl ketone) appear. However, this is not a problem if an ozone trap is used (Fig. 11.37c). Similar results have been reported for a series of terpenes, where $O_3$ at 8 ppb had no effect but at 61–125 ppb reduced the measured terpene concentrations and decreased the precision of the measurements (Larsen *et al.*, 1997).

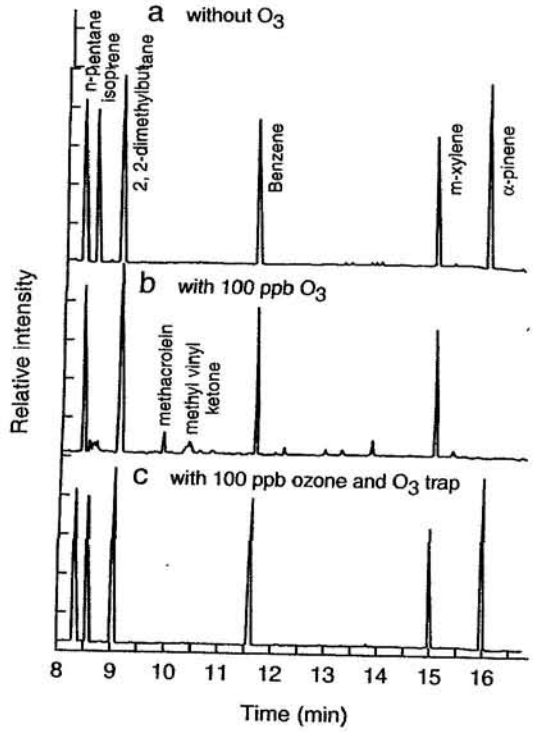


FIGURE 11.37 Chromatograms of a synthetic mixture of *n*-pentane, isoprene, 2,2-dimethylbutene, benzene, *m*-xylene, and $\alpha$-pinene in synthetic air which are cryotrapped (a) in the absence of $O_3$, (b) in the presence of 100 ppb $O_3$, and (c) same as (b) but with an ozone scrubber upstream (from Goldan *et al.*, 1995).

The severity of these problems is quite sensitive to the nature of the particular organic, as expected, and likely to the particular sampling configuration and conditions as well. For example, Calogirou *et al.* (1997) showed that saturated oxygenated terpenes adsorbed on Tenax were not affected by the presence of ~100 ppb $O_3$ whereas as much as 80–90% of the most reactive, unsaturated compounds reacted. Indeed, no α-terpinene was observed when ozone was present. On the other hand, Koppmann *et al.* (1995) report no significant interference problems with $O_3$ for the $C_2$–$C_4$ hydrocarbons which were sampled using a heated stainless steel inlet line, which destroys as much as half of the initial ozone, and then cryotrapped.

Because of these problems, removal of ozone prior to trapping the organics is highly desirable. A variety of approaches have been used, including the use of heated inlet lines as just described (Koppmann *et al.*, 1995), annular denuders coated with inorganics that react rapidly with $O_3$ such as KI (e.g., Williams and Grosjean, 1990), scrubbers containing $O_3$-reactive substances such as KI, crystalline $Na_2SO_3$, $Na_2CO_3$, or $MnO_2$, or polymeric sulfur scrubbers such as polyphenylene sulfide in which $O_3$ oxidizes the –S– group to =S(O)– without the formation of gas-phase products that could interfere with the analysis (e.g., Calogirou *et al.*, 1997). Titration of the $O_3$ with NO (e.g., Sirju and Shepson, 1995) has also been used. These and other techniques are reviewed in detail by Helmig (1997).

*Collection of air samples in stainless steel canisters* whose surfaces have been passivated is another common collection technique for VOCs. (Aluminum has also been used but the stability of polar organics in them is poor; Gholson *et al.*, 1990.) Indeed, this method is used not only for sampling air but in medical applications as well, where they have been used to sample organics in a single breath (Pleil and Lindstrom, 1995). Passivation of the canisters is often carried out using a process called SUMMA and hence referred to as "SUMMA canisters." The canisters also have to be thoroughly cleaned before use; an example of one such procedure is described by Blake *et al.* (1994). The sample is then typically preconcentrated by transfer to a cold trap prior to injection onto the GC column (e.g., see Blake *et al.*, 1994).

Loss of some organics to the walls of the canisters can occur, and these can subsequently desorb. Such negative changes depend on the nature, past use, and pretreatment of the canister surface, the nature of the compound, the canister pressure, the storage temperature, and interestingly, the water vapor present. The loss of organics to the walls is generally less in the presence of water, which has been attributed to water occupying active sites on the metal surface that would otherwise adsorb organics (e.g., Pate *et al.*, 1992; Apel *et al.*, 1994). The nature of the compound is particularly important, as might be expected, since highly reactive organics can react with other species such as ozone in the canister itself (Apel *et al.*, 1994). In addition, characteristics of the compound such as its vapor pressure, solubility in water, and polarity determine how readily it is taken up onto the canister surfaces or into a thin film of water on the surface. In fact, positive changes in some VOCs have been observed in canisters and attributed to uptake into a film of water on the canister surface. As samples are removed from the canister and the pressure reduced, the amount of surface water decreases, causing a release of dissolved organic into the gas phase. This appears then as a positive change with time.

Zielinska *et al.* (1996) and Kelly and Holdren (1995) have summarized the stability in canisters of organics, some of which are U.S. EPA designated HAPs (hazardous air pollutants). Kelly and Holdren propose that for compounds whose stability in canisters is not known, estimates can be made based on species of similar physical and chemical characteristics. These characteristics include their vapor pressure, polarizability, water solubility, Henry's law coefficient in water, and estimated lifetimes with respect to reactions in air and in the aqueous phase.

While these methods are most commonly used for sampling and analysis of ambient air, others have been applied as well, particularly in laboratory studies or source sampling. For example, flexible chambers made from thin films of Teflon or Tedlar are often used to store organics prior to sampling. The advantage is that as sample is removed, they collapse so that their pressure remains at atmospheric while the volume decreases. However, again some losses of organics can occur in these chambers, either on the walls or on the attached sampling hardware (e.g., see Wang *et al.*, 1996).

Passive samplers are used for specific applications such as for indoor air environments or as passive dosimeters. In this approach, the air containing the organic diffuses to and adsorbs on a solid sorbent without active pumping. The organics are subsequently thermally desorbed or extracted from the sorbent using a solvent (e.g., see Shields and Weschler, 1987).

***(2) Intercomparison studies*** Because of the importance of accurate measurement of individual organics in air, there have been several intercomparison studies carried out in which a number of different laboratories have analyzed common samples, either synthetic or ambient air. In one such study (Apel *et al.*, 1994), a

16-component synthetic mixture was distributed to about three dozen laboratories for analysis. Of the 28 laboratories completing this analysis, 12 identified all 16 components correctly. Figure 11.38 shows the percentage difference for each component from the gravimetric values used in the mixture preparation averaged over all participating laboratories as well as the percent standard deviation for all of the measurements. Clearly, the accurate identification and analysis of individual hydrocarbons found in ambient air remains a difficult problem.

Figure 11.39 shows the results of another such intercomparison (Bernardo-Bricker *et al.*, 1995). Some of the problems encountered and the approaches taken to solve them are also discussed by Bricker and coworkers. As seen in Fig. 11.39, the precision of the measurement of compounds present at concentrations less than 5 ppbC is much worse than for species present in higher concentrations, as might be expected. However, some of these compounds, such as limonene, are notoriously difficult to measure accurately even at higher concentrations, so that it is likely a combination of the small concentrations and nature of the compound that contributes to the poor precision seen in some cases.

***(3) Typical atmospheric concentrations*** A large number of field studies have been carried out in which organics as well as a number of associated species such as $NO_x$, $NO_y$, and $O_3$ have been measured simultaneously, both at the earth's surface and at various altitudes. For the sake of brevity, we focus here primarily on surface measurements and, of necessity, cite only a few of the many studies that have been carried out. The accuracy of the absolute values in any case should be interpreted in light of the results of intercomparison studies such as those already described. However, it is clear that there are major differences in the concentrations, depending on where the sample is taken. Table 11.8 summarizes a few typical ranges of concentrations measured in regions that can be characterized as covering the range from remote to highly polluted urban areas.

### *f. Aldehydes, Ketones, Alcohols, and Carboxylic Acids*

As discussed in Chapter 6, carbonyl compounds are particularly important in atmospheric chemistry because of their absorption of light in the 290- to 400-nm region that generates free radicals. With the increasing use of alcohol fuels (see Chapter 16) as well as the recognition that there are biogenic emissions of alcohols (see Chapter 6.J.1), the measurement of these compounds has also become of interest. Finally, carboxylic acids are now known to contribute significantly to the total acid burden and hence acid deposition in the atmosphere (Chapter 8.D). In this section, techniques for measuring these oxygenated compounds and some typical levels found in the troposphere are discussed.

***(1) Aldehydes and ketones*** *Spectroscopic techniques* have proven particularly useful for the smaller aldehydes, which have distinct infrared and UV–visible absorption bands. As seen in Table 11.2 and discussed earlier, HCHO has been measured by FTIR in polluted urban areas as well as by TDLS and matrix isolation spectroscopy. In addition, as seen in Table 11.3, DOAS has high sensitivity for HCHO due to its strongly banded absorption in the 300- to 400-nm region (see Chapter 4.M).

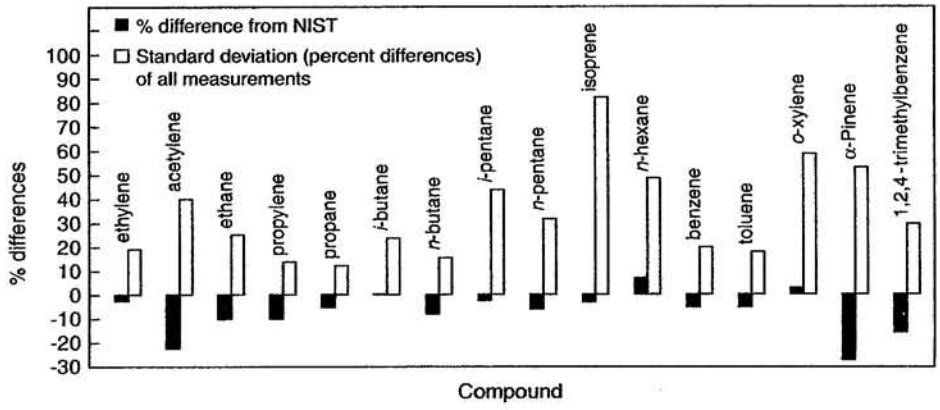


FIGURE 11.38 Average percent differences from the NIST standards for all participating laboratories (■) and the percent standard deviation of all measurements (□) (adapted from Apel *et al.*, 1994).

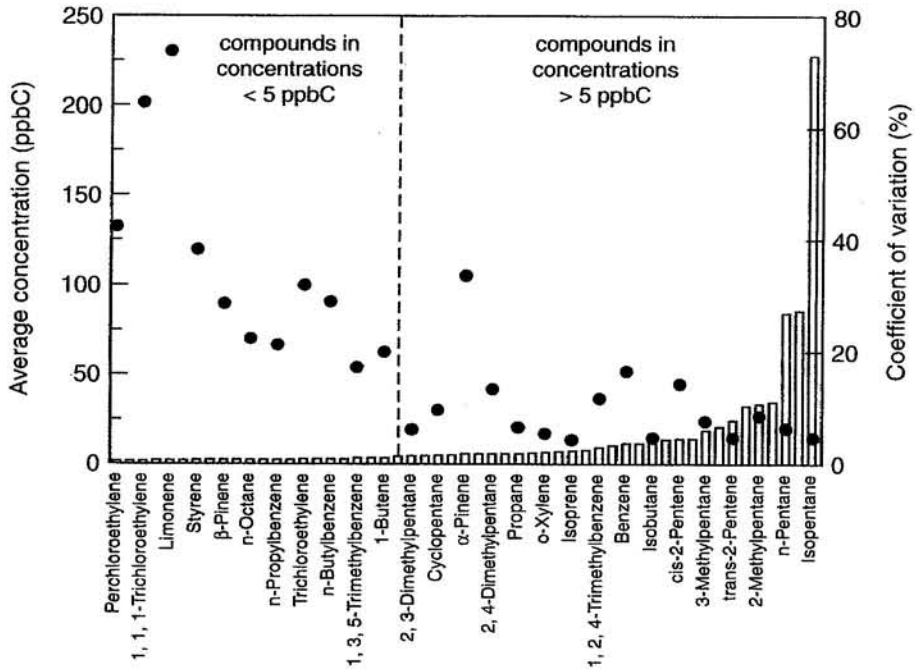


**FIGURE 11.39** Results of intercomparison study of a mixture of organics found in ambient air. The concentrations (in ppbC) are shown as unfilled bars, along with the coefficient of variation (●) for these measurements (adapted from Bernardo-Bricker *et al.*, 1995).

In addition to the spectroscopic methods, there are a number of *derivatization methods*, in which a derivative of the carbonyl compound that can be easily separated and measured is formed. The most common of these is the use of 2,4-dinitrophenylhydrazine (DNPH), which reacts to form the hydrazone:

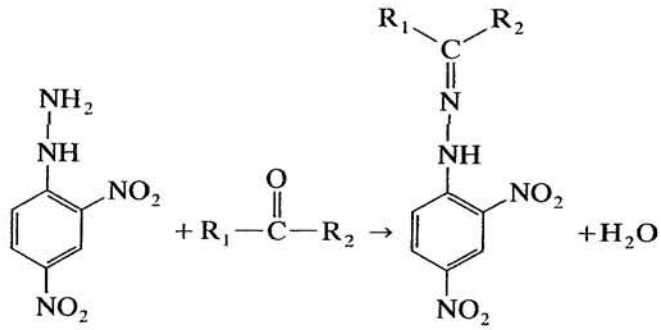


The mixture of hydrazones formed from the reactions of the set of carbonyl compounds commonly found in air can then be separated using HPLC and detected using light absorption at 254 or ~365 nm (e.g., see Kuntz *et al.*, 1980; Lipari and Swarin, 1982; and Kuwata *et al.*, 1983).

The aldehydes and ketones can be collected in several different ways. One of the most common is the use of solid sorbents such as silica gel, Florisil, or $C_{18}$ cartridges that are coated with DNPH (e.g., see Lipari and Swarin, 1985; Arnts and Tejada, 1989; Zhou and Mopper, 1990; Sirju and Shepson, 1995; and Kleindienst *et al.*, 1998). Some care must be taken to avoid artifacts due to reactions of $O_3$, which has been shown to give positive interferences for $C_{18}$ cartridges but negative interferences when silica gel is used as the sorbent (e.g., see Arnts and Tejada, 1989; Rodler *et al.*, 1993; Sirju and Shepson, 1995; Kleindienst *et al.*, 1998; Gilpin *et al.*, 1997; and Apel *et al.*, 1998b). The DNPH technique has also been used in passive samplers for HCHO (e.g., see Levin *et al.*, 1989; and Grosjean and Williams, 1992). However, with care, concentrations in the 30- to 500-ppt range (depending on the particular carbonyl) can be measured using this technique and a 156-L air sample (Grosjean *et al.*, 1996a).

Other approaches to collection of the carbonyl compounds include the use of impingers containing the DNPH in a solvent such as acetonitrile (e.g., Grosjean and Fung, 1982; Lipari and Swarin, 1982), scrubbers (e.g., Dasgupta *et al.*, 1988, 1990; Lee and Zhou, 1993), mist chambers (e.g., Cofer and Edahl, 1986; Munger *et al.*, 1995; Khare *et al.*, 1997), and condensation collectors (Dawson and Farmer, 1988).

Alternate derivatization techniques have also been used. These include dansylhydrazine with fluorescence or chemiluminescence detection of the hydrazone (e.g., Nondek *et al.*, 1992; Rodler *et al.*, 1993), 3-methyl-2-

TABLE 11.8 Some Typical Concentration Ranges Measured for Some Small Hydrocarbons from Remote to Urban Areas (ppb)

| | Type of air mass | | |
|---|---|---|---|
| | Urban | Rural–suburban | Remote |
| Compound | Brazil,[a] Denmark,[b] India,[c] Japan,[d] Greece,[e] U.K.,[f] U.S.,[i,k,q] Canada,[l,o] Sweden,[m,n] France,[w] Italy,[x] Mexico[y] | Brazil,[a] Denmark,[b] U.S.,[i,k,q] Canada[l,o] Sweden,[m,n] France[w] | U.S.,[i,k,q] Canada,[l,o] France,[w] Antarctic,[p,s] North Atlantic[t] |
| Ethane | 0.6–29 | 0.4–4 | 0.4–2 |
| Ethene | 0.7–168 | 0.1–3 | 0.07–0.4 |
| Acetylene | 0.7–44 | 0.1–3 | 0.01–0.7 |
| Propane | 0.4–221 | 0.2–2 | 0.04–0.9 |
| Propene | 0.1–39 | 0.02–2 | 0.02–0.2 |
| *n*-Butane | 0.02–96 | 0.1–1 | 0.1–0.75 |
| Isobutane | 0.3–45 | 0.04–0.6 | 0.003–0.2 |
| 1-Butene | 0.2–7 | 0.01–0.04 | 0.005–0.014[w] |
| 2-Methyl propene | 3–18 | 0.04–0.16 | — |
| 2-Butene (*cis* and *trans*) | 0.10–4 | 0.008–0.06 | 0.006–0.024[w] |
| *n*-Pentane | 0.7–67 | 0.07–0.4 | 0.007–0.19 |
| Isopentane | 2–90 | 0.1–0.6 | 0.008–0.2 |
| Benzene | 0.9–26 | 0.1–0.6 | 0.008–0.2 |
| Toluene | 2–39 | 0.05–0.8 | 0.01–0.25 |
| *o*-Xylene | 0.4–6 | 0.02–0.2 | 0.001–0.03 |
| *m*- and *p*-Xylene | 0.3–30 | 0.02–0.12 | 0.002–0.008 |
| 1,3-Butadiene | 0.1–6 | 0.03–0.6 | 0.02–0.13 |
| Isoprene | 0.1–2 | 0.005–5.5 | |

[a] Grosjean *et al.* (1998a, 1998b); Port Alegre, Brazil.

[b] Hansen *et al.* (1998); Copenhagen.

[c] Rao *et al.* (1997); measurements made close to industrial regions in Bombay.

[d] Morikawa *et al.* (1998); monthly means for Osaka.

[e] Moschonas and Glavas (1996); Athens in early morning.

[f] Dollard *et al.* (1995); range of annual means for eight sites in seven cities (Birmingham, Cardiff, Edinburgh, Bristol, Middlesbrough, Belfast, and two sites in London).

[g] Evans *et al.* (1992); 24-h medians in five cities (Boston, Chicago, Houston, Seattle, Tacoma).

[h] Edgerton *et al.* (1989); daily medians in nine cities (Phoenix, Chicago, Denver, Houston, Los Angeles, Philadelphia, Pittsburgh, San Jose, St. Louis).

[i] Zielinska and Fujita (1994); range for two sets of samples collected from 6:00 to 8:00 a.m. and 10:00 a.m. to noon, respectively, in downtown Los Angeles in 1991.

[j] Fraser *et al.* (1998); Los Angeles during severe smog episode in 1993.

[k] Gong and Demerjian (1997); Whiteface Mountain, New York.

[l] Bottenheim and Shepherd (1995); monthly means at four locations (Saturna Island, British Columbia; Egbert, Ontario; Lac la Flamme, Quebec; Kejimkujik National Park, Nova Scotia).

[m] Lindskog and Moldanova (1994); annual average based on monthly means at Rörvik on the west coast of Sweden for all but 1,3-butadiene and isoprene; for the latter, the ranges during the period April 23–27, 1990, at Rörvik from Lindskog *et al.* (1992) are reported.

[n] Hewitt *et al.* (1995); typical concentrations from forested sites in the United States, Europe, and Brazil.

[o] Blake *et al.* (1994); measured in northern Quebec and Ontario.

[p] Rudolph *et al.* (1989); either yearly average or range is given.

[q] Singh *et al.* (1988); average concentrations measured in lower troposphere over the land and ocean in Colorado and California.

[s] Clarkson *et al.* (1997); annual averages at Baring Head, New Zealand, and Scott Base, Antarctica, between 1991 and 1996.

[t] Penkett *et al.* (1993); range represents summer minimum to winter maximum over the North Atlantic Ocean with air mainly of polar marine origins.

[u] Mowrer and Lindskog (1991); mean concentrations measured at Rörvik from February 21 to April 8, 1989.

[v] Rappenglück *et al.* (1998); means of 20-min samples in two locations in Athens.

[w] Boudries *et al.* (1994); monthly average concentrations at Porspoder on the west coast, Brittany. Remote air masses were of oceanic origin. Those under "rural–suburban" were identified as being of continental origin.

[x] Possanzini *et al.* (1996); range measured in Rome from 0600 to 0900 hours.

[y] D. R. Blake and F. S. Rowland, personal communication, 1998; concentrations measured at various locations throughout the day in Mexico City in 1993.

benzothiazolinone hydrazone, which has been used for post-HPLC column derivatization (Igawa *et al.*, 1989), and *O*-(2,3,4,5,6-pentafluorobenzyl)hydroxylamine hydrochloride derivatization, which has been used in combination with GC–MS (Lacheur *et al.*, 1993; Yu *et al.*, 1995, 1998).

There are some methods that are specific to HCHO. For example, the Hantzsch reaction of HCHO, collected with a diffusion scrubber, with ammonium acetate, acetic acid, and acetylacetone to form diacetyldihydrolutidine, which is measured using its fluorescence at 470 nm, has been applied to air measurements (Dasgupta *et al.*, 1988, 1990; Kleindienst *et al.*, 1988a,b; Lawson *et al.*, 1990; Khare *et al.*, 1997). Reaction with 1,3-cyclohexanedione and ammonium acetate to form a dihydropyridine derivative that is measured by fluorescence has been used in conjunction with a diffusion scrubber (Fan and Dasgupta, 1994). Enzymatic methods have been used in which formaldehyde dehydrogenase catalyzes the oxidation of HCHO to HCOOH in the presence of $\beta$-nicotinamide adenine dinucleotide, $NAD^+$, which is reduced to NADH. The latter is measured by fluorescence at 450 nm (Lazrus *et al.*, 1988; Ho and Richards, 1990).

Finally, cryotrapping followed by GC–MS analysis has been used for a variety of carbonyl compounds, with the exception of HCHO, which is removed on surfaces (e.g., see Goldan *et al.*, 1995; and Leibrock and Slemr, 1997).

These spectroscopic and derivatization techniques have largely supplanted earlier wet chemical techniques such as that employing chromotropic acid (Altshuller and McPherson, 1963).

A number of intercomparison studies of the various methods of measurement of HCHO have been carried out. As might be expected given the specificity of spectroscopic methods, the results of FTIR, DOAS, and TDLS are generally in good agreement, within 15% of their mean value in one study in a polluted atmosphere (Lawson *et al.*, 1990). During the same study, the diacetyldihydrolutidine derivative method and the DNPH method were lower by ~15–25% than the spectroscopic mean, whereas the enzymatic method was higher by ~25%.

In another intercomparison using TDLS, several DNPH methods, the 1,3-cyclohexanedione diffusion scrubber, and the enzymatic method were compared using both spiked samples and ambient air. The TDLS was used as a standard for comparison. For ambient air measurements, results obtained with the 1,3-cyclohexanedione diffusion scrubber were about 30% higher than those obtained with TDLS, whereas results for the enzymatic method were about 35% lower. The DNPH cartridge measurements were quite variable, which may reflect in part the problem with interference by ozone reactions mentioned earlier. However, in an earlier study, the slope of a plot of TDLS measurements against DNPH on silica gel cartridges was within the relatively large scatter unity ($0.95 \pm 0.36$), whereas that for the enzymatic method against TDLS was about 30% low, with a slope of $0.71 \pm 0.09$ (Kleindienst *et al.*, 1988b). Similarly, Sirju and Shepson (1995) showed that if $O_3$ was removed to avoid interference, TDLS and DNPH cartridge measurements were in agreement. Benning and Wahner (1998) compared DNPH cartridge measurements with $O_3$ removal with DOAS measurements of HCHO; there was reasonable overall agreement between the two, although there was significant scatter in individual measurements on a plot of DOAS concentrations against those measured using DNPH.

TDLS and DOAS measurements of HCHO were intercompared in a rurul region in Colorado (Harder *et al.*, 1997b). The DOAS measurements were made over a 10.3-km path and the TDLS essentially at a point at one end of the DOAS path length (Fried *et al.*, 1997). When anthropogenic influences were thought to be small, the two techniques were in excellent agreement, to within 5%. At other times, higher concentrations were obtained using DOAS due to anthropogenic influences that did not affect the TDLS measurements.

In short, the spectroscopic methods appear to be reliable and specific for HCHO. The derivatization methods are generally in reasonable overall agreement with the spectroscopic methods where intercomparisons have been carried out, but there can be very large discrepancies in individual measurements. Part of the reason for these discrepancies may be related to the fact that some of the spectroscopic methods average over long distances whereas the derivatization methods sample at a point. On the other hand, the latter methods involve collecting the sample over a period of time, usually several hours, whereas the spectroscopic methods are real-time measurements. Finally, variations in collection efficiencies and possible interferences must be taken into account for the derivatization methods.

*Typical tropospheric concentrations.* Table 11.9 shows some typical concentrations of the major aldehydes and ketones measured near the earth's surface. Formaldehyde is usually present in the highest concentration, followed by acetaldehyde and then, at significantly smaller concentrations, higher aldehydes and ketones. Figure 11.40, for example, shows the percentages of the total carbonyl compounds due to each of the simple straight-chain aldehydes measured in one study in the Los Angeles area in which 23 different carbonyl compounds were identified and measured (Grosjean *et al.*, 1996a). These percentages are in terms of ppb of each

TABLE 11.9 Some Typical Concentrations of Aldehydes and Ketones in Ambient Air (ppb)

| | Type of air mass | | |
|---|---|---|---|
| | Urban | Rural–suburban | Remote |
| Compound | Denver,[a] Los Angeles,[b] Albuquerque,[c] various U.S. Cities,[d] Rome,[e] Copenhagen,[f] Paris,[g] Mexico City[h] | Germany,[i,k] Denmark,[l] U.S.,[i,o,p,s,u,x] Canada,[m] Venezuela[n] | Canada,[q] Caribbean Sea[r] |
| HCHO | 1–60 | 0.1–10 | 0.3–2 |
| $CH_3CHO$ | 1–18 | 0.1–4 | 0.1–1 |
| $CH_3CH_2CHO$ | 0.1–3 | 0.004–0.2 | 0–0.2 |
| $CH_3CH_2CH_2CHO$ | 0.2–1.4 | 0.1–0.3 | — |
| $CH_3C(O)CH_3$ | 0.2–9 | 0.2–8 | 0–1 |
| $CH_3C(O)CH_2CH_3$ | 0.3–8 | 0.1–0.5 | 0–0.18 |
| Benzaldehyde | 0.1–1 | — | < 0.01–0.5 |
| Acrolein | <0.04–1 | ~0.6[t] | — |
| Crotonaldehyde | 0.1–0.5[o] | 0.2–0.3[o] | ~0.09[r] |
| Methacrolein | <0.7[c] | 0.02–1.7 | — |
| Methyl vinyl ketone | — | 0.2–1.5 | |

[a] Anderson *et al.* (1994, 1996).
[b] Grosjean *et al.* (1996a).
[c] Gaffney *et al.* (1997).
[d] Salas and Singh (1986).
[e] Possanzini *et al.* (1996).
[f] Granby *et al.* (1997a).
[g] Kalabokas *et al.* (1988).
[h] Báez *et al.* (1989).
[i] Lee *et al.* (1995).
[j] Benning and Wahner (1998).
[k] Slemr *et al.* (1996).
[l] Granby *et al.* (1997).
[m] Shepson *et al.* (1991).
[n] Trapp and Serves (1995).
[o] Grosjean *et al.* (1996).
[p] Harder *et al.* (1997a,b); Fried *et al.* (1997).
[q] Tanner *et al.* (1996).
[r] Zhou and Mopper (1990, 1993).
[s] Goldan *et al.* (1995).
[t] Leibrock and Slemr (1997).
[u] Apel *et al.* (1998b).
[v] Riemer *et al.* (1998).

compound (not as ppbC). There were also 19 carbonyls whose identity could not be confirmed but likely included hydroxycarbonyl aliphatic and aromatic compounds. Nondek *et al.* (1992), for example, have tentatively identified biogenic emissions of *p*-hydroxybenzaldehyde in a forest.

Dicarbonyl compounds such as glyoxal (CHOCHO) and methylglyoxal ($CH_3C(O)CHO$) have also been measured in tropospheric air, in rural areas at small concentrations, and in polluted urban areas. For example, Munger *et al.* (1995) report an average concentration of 44 ppt glyoxal in central Virginia, and Lee *et al.* (1995) measured average glyoxal concentrations of 18–83 ppt and average methylglyoxal concentrations of 31–88 ppt at a rural site in Georgia. Higher concentrations are found in urban air, e.g., $0.78 \pm 0.85$ ppb glyoxal and $1.0 \pm 0.6$ ppb methylglyoxal in the Los Angeles area (Grosjean *et al.*, 1996a).

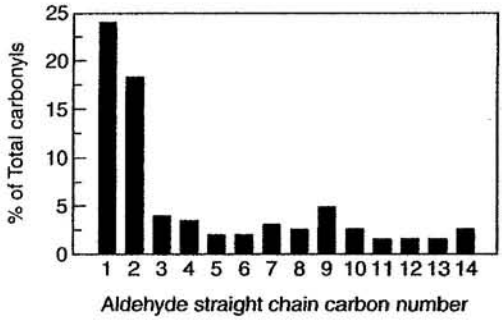


FIGURE 11.40 Percentage of total carbonyl compounds due to each of the straight-chain aldehydes in the Los Angeles area (adapted from Grosjean *et al.*, 1996a).

***(2) Alcohols*** There are far fewer measurements of alcohols than there are of the aldehydes and ketones. They are typically measured using GC–FID or GC–MS (e.g., see Goldan *et al.*, 1995; Leibrock and Slemr, 1997; and Grosjean *et al.*, 1998a,b,c). Measuring alcohols is difficult because of their polar nature and tendency to stick to surfaces. For example, Apel *et al.* (1998a) reported that GC measurements of methanol, ethanol, and *n*-butanol in calibration gas mixtures had higher variability than aldehydes and ketones.

Methanol and ethanol are the primary simple alcohols that have been identified in air, with concentrations of methanol in the ~1- to 20-ppb range and

ethanol in the ~0.1- to 1-ppb range in rural areas (Goldan *et al.*, 1995; Leibrock and Slemr, 1997; Riemer *et al.*, 1998). In areas where ethanol is used as a fuel, the concentrations can be much higher. For example, in Porto Alegre, Brazil, ethanol concentrations up to 68 ppb have been measured (Grosjean *et al.*, 1998b). Higher alcohols such as *n*-butanol have also been reported to be present in air in smaller concentrations; for example, Riemer *et al.* (1998) reported concentrations of ~55 ppt at a rural site in the southeastern United States.

As discussed in Chapter 6.J.1, there are also biogenic emissions of multifunctional alcohols, which are treated in that section.

*(3) Carboxylic acids* The smallest carboxylic acid, formic acid, can be measured using infrared spectroscopy (Table 11.2), since it has characteristic absorption bands. As discussed earlier and seen in Fig. 11.33b, mass spectrometry with chemical ionization using $SiF_5^-$ also revealed HCOOH in an indoor environment (Huey *et al.*, 1998). However, since the sensitivity in these initial studies was about two orders of magnitude less than that for $HNO_3$, the detection limit may be about the same as that for FTIR and TDLS. Formic and acetic acids have been monitored continuously from aircraft (Chapman *et al.*, 1995) and their surface flux determined by eddy correlation (Shaw *et al.*, 1998) using atmospheric pressure ionization mass spectrometry. Detection limits are about 30 ppt.

Gas-phase carboxylic acids have been sampled using mist chambers (e.g., Andreae *et al.*, 1987; Talbot *et al.*, 1988), condensates (Dawson and Farmer, 1988), filters coated with alkaline compounds such as KOH, NaOH, $K_2CO_3$, and $Na_2CO_3$ (e.g., Grosjean *et al.*, 1990; Nolte *et al.*, 1997), and denuders coated with NaOH (Keene *et al.*, 1989). The acid anions are then separated and detected using ion chromatography. It should be noted that interferences have been reported for some of these methods. For example, the conversion of formaldehyde to formic acid and PAN to acetate on alkaline filters has been observed (Andreae *et al.*, 1987; Keene *et al.*, 1989; Grosjean and Parmar, 1990), and with some ion chromatography columns, coelution of several anions can be a problem (e.g., see Jaffrezo *et al.*, 1998). The results of one intercomparison study (Keene *et al.*, 1989) suggest that artifacts in these measurement methods occur episodically and that care should be taken in their application.

A promising method involves derivatization by reaction with pentafluorobenzyl bromide (Chien *et al.*, 1998). Carboxylic acids (RC(O)OH) react to form the esters, $RC(O)OCH_2C_6F_5$, which can be measured by GC–MS. This method has the advantage of increased sensitivity and selectivity.

Formic and acetic acids are found primarily (>98%) in the gas phase (e.g., Andreae *et al.*, 1987; Talbot *et al.*, 1988). Concentrations of gas-phase HCOOH and $CH_3COOH$ in rural areas are typically ~0.3–3 and ~0.5–2 ppb, respectively (Andreae *et al.*, 1987; Talbot *et al.*, 1988; Dawson and Farmer, 1988; Sanhueza *et al.*, 1996; Nolte *et al.*, 1997; Granby *et al.*, 1997a,b), although higher concentrations, up to 32 ppb for $CH_3COOH$, have been observed in wood-burning areas (Gaffney *et al.*, 1997). In urban areas, HCOOH and $CH_3COOH$ concentrations are about the same, typically in the range of ~1–10 ppb (e.g., see Tuazon *et al.*, 1981; Dawson and Farmer, 1988; Grosjean, 1990; Grosjean *et al.*, 1990; Khare *et al.*, 1997; Granby *et al.*, 1997a; Nolte *et al.*, 1997; and Gaffney *et al.*, 1997).

Multifunctional acids containing a carbonyl group such as pyruvic acid [$CH_3C(O)COOH$] are typically measured using the derivatization techniques used for aldehydes and ketones, such as the DNPH method (e.g., see Lee *et al.*, 1995).

### *g. PAN, Other Peroxynitrates, and Alkyl Nitrates*

The formation and fate of peroxyacyl nitrates, $RC(O)OONO_2$, were discussed in Chapter 6.I. These compounds are almost universally measured using gas chromatography with electron capture detection (GC-ECD), although a luminol chemiluminescence detector has also been used in which PAN is thermally decomposed to $NO_2$ at the end of the column and the $NO_2$ measured (Burkhardt *et al.*, 1988; Blanchard *et al.*, 1990; Gaffney *et al.*, 1998). In polluted atmospheres where the concentrations are higher, FTIR has also been used (Table 11.2). For a summary of methods, see reviews by Gaffney *et al.* (1989) and Kleindienst (1994).

Of the peroxyacyl nitrates, the most prevalent compound is peroxyacetyl nitrate, $R = CH_3$, with peroxypropionyl nitrate (PPN, $R = C_2H_5$) typically being present at the next highest concentration. Because they are formed in the VOC–$NO_x$ photochemical cycles, the highest levels of PAN are often seen downwind of urban areas rather than in the center. For example, in the Los Angeles area, some of the highest concentrations have been measured at a mountain site about 35 km northeast of Los Angeles (Grosjean *et al.*, 1993a, 1996b).

Peak concentrations of PAN in or downwind of major urban areas during periods of high photochemical activity can reach levels as high as ~35 ppb (e.g., see Tuazon *et al.*, 1981; Tanner *et al.*, 1988; Grosjean *et al.*, 1993a, 1996b; Altshuller, 1993; Williams *et al.*, 1993; Kleindienst, 1994; Suppan *et al.*, 1998; and Gaffney *et al.*, 1998, 1999). In rural areas, peak concen-

trations up to about a ppb are typical (e.g., see Corkum *et al.*, 1986; Andersson-Sköld *et al.*, 1993; Ridley *et al.*, 1990a; Gaffney *et al.*, 1993, 1997; Hastie *et al.*, 1996; Nouaime *et al.*, 1998; and Roberts *et al.*, 1998). However, in remote areas where NO and $NO_x$ levels are small (vide supra), a few tens of ppt to ca. several hundred ppt are common (e.g., see Rudolph *et al.*, 1987; Singh *et al.*, 1990; Ridley *et al.*, 1990b, 1998; Perros, 1994; Talbot *et al.*, 1994; Heikes *et al.*, 1996; Beine *et al.*, 1996, 1997; Solberg *et al.*, 1997; and Singh *et al.*, 1998).

As might be expected from the chemistry common to the formation of $O_3$ and PAN, the two are often highly correlated both temporally and geographically. Figure 11.41, for example, shows the median values for the diurnal variation of ozone and PAN at one site in Athens, Greece, during meteorological conditions conducive to photochemical smog formation (Suppan *et al.*, 1998). Both increase about 9 a.m. and continue at relatively high levels until late in the afternoon.

Smaller concentrations of higher members of the series have also been observed. In and downwind of polluted urban areas, peak concentrations of PPN of ~0.4–4 ppb have been reported (e.g., see Grosjean *et al.*, 1993a, 1996b; and Williams *et al.*, 1993), whereas the concentrations in rural areas are about an order of magnitude smaller (e.g., Ridley *et al.*, 1990a). For example, typical average PPN levels in the southeastern United States have been reported to be ~50 ppt, with the PPN/PAN ratio being about 0.15 in air masses impacted by anthropogenic emissions (Nouaime *et al.*, 1998; Roberts *et al.*, 1998). Peroxy-*n*-butyryl nitrate ($n$-$C_3H_7C(O)OONO_2$) and peroxymethacroyl nitrate (MPAN, $CH_2=C(CH_3)C(O)OONO_2$) have been measured at concentrations up to ~1–2 ppb (Williams *et al.*, 1993; Grosjean *et al.*, 1993a, 1993b; Gaffney *et al.*, 1999). Since MPAN is an oxidation product of isoprene (see Chapter 6), it is found primarily in forested areas having significant isoprene emissions. For example, in rural areas near Nashville, Tennessee, the average concentration was about 30 ppt (Nouaime *et al.*, 1998), with a typical MPAN/PAN ratio of 0.10–0.17 (Roberts *et al.*, 1998).

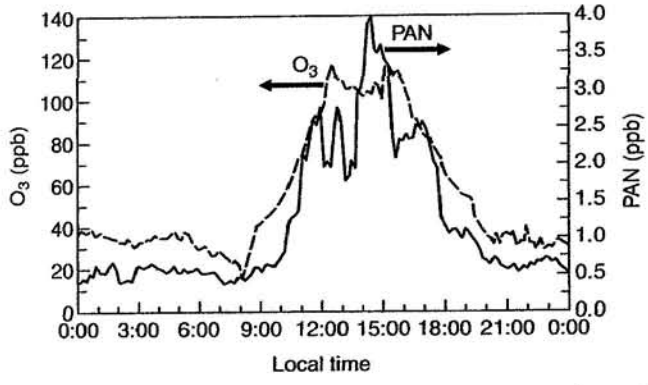


FIGURE 11.41 Diurnal variation of median concentrations of PAN and $O_3$ at a monitoring site in Athens, Greece, during periods of high photochemical activity (adapted from Suppan *et al.*, 1998).

Simple alkyl nitrates are also commonly measured using GC-ECD, usually with preconcentration either by cryotrapping or using a solid sorbent (e.g., Atlas and Schauffler, 1991; Ridley *et al.*, 1997). Another approach is GC with an $NO_y$ detector as described earlier (e.g., Flocke *et al.*, 1998). In this approach, the compounds are converted to NO over a catalyst as they emerge from the GC column, and the NO measured by its chemiluminescence reaction with $O_3$.

A number of alkyl nitrates have been observed in the troposphere, including methyl nitrate and ethyl nitrate, as well as all of the isomers of the higher alkyl nitrates up to $C_5$ (e.g., see Buhr *et al.*, 1990; Ridley *et al.*, 1990a; O'Brien *et al.*, 1995; and Flocke *et al.*, 1998). Although the specific isomers were not identified, the $C_6$–$C_8$ alkyl nitrates have also been measured (O'Brien *et al.*, 1995; Flocke *et al.*, 1998). A summary of the measurements through about 1998 is found in Flocke *et al.* (1998).

Of the simple alkyl nitrates, methyl nitrate is present in the highest concentration. For example, in measurements made in Schauinsland, a rural area in Germany, concentrations of $CH_3ONO_2$ up to 216 ppt were measured. The median value, however, was only 19 ppt (Flocke *et al.*, 1998). In the same studies, the median concentrations for ethyl nitrate, *n*-propyl nitrate, 2-propyl nitrate, and 1-butyl nitrate were 9, 3, 12, and 2 ppt, respectively. The sum of the $C_1$–$C_8$ alkyl nitrates averaged 120 ppt, which is only ~3% of the $NO_y$. Similarly, in rural Ontario, Canada, 17 different organic nitrates were identified in air, but their sum was only 0.5–3% of $NO_y$ (O'Brien *et al.*, 1995). In aircraft measurements over the Pacific Ocean near Hawaii, average values for methyl nitrate near the surface were ~6 ppt and the sum of $C_1$–$C_5$ alkyl nitrates was <5% of the total $NO_y$ (Ridley *et al.*, 1997).

In short, a variety of alkyl nitrates are present in air, but at relatively small concentrations compared to the peroxyacyl nitrates and to $NO_y$.

### *h. $H_2O_2$ and Organic Peroxides*

There are a variety of methods for collecting and measuring $H_2O_2$ and organic peroxides in air. $H_2O_2$ is especially water soluble and hence partitions between the gas phase and clouds and fogs (e.g., Macdonald *et al.*, 1995). While the collection techniques for air versus clouds and fogs are different, the analytical techniques are the same.

Collection of air for peroxide analysis has been accomplished using a number of approaches, including mist chamber sampling, diffusion scrubbers (e.g., see Dasgupta *et al.*, 1988), impingers, and cryogenic trapping (e.g., see Sakugawa and Kaplan, 1987). Artifacts have been observed with many of the sampling systems. For example, Sakugawa and Kaplan (1987) reported that $H_2O_2$ collected by impingers was higher than by cryotrapping and attributed this to generation of $H_2O_2$ by aqueous-phase reactions in the bubbler. Indeed, the generation of $H_2O_2$ in water when $O_3$ is bubbled into it has been observed (e.g., Zika and Saltzman, 1982; Heikes, 1984). On the other hand, artifact formation of $H_2O_2$ and hydroxymethyl hydroperoxide during cryogenic trapping of air was reported by Staffelbach *et al.* (1995, 1996) and attributed to reactions of alkenes with $O_3$ in the traps. In addition, $H_2O_2$ is a sufficiently "sticky" molecule that it is readily lost to surfaces in sampling systems, so that such surfaces prior to scrubbing into solution must be minimized (e.g., Lee *et al.*, 1991, 1993). Differences in collection efficiencies for different hydroperoxides must also be taken into account (e.g., de Serves and Ross, 1993).

Various techniques for measuring peroxides in air are reviewed by Gunz and Hoffmann (1990) and Sakugawa *et al.* (1990). $H_2O_2$ can be measured spectroscopically by FTIR and by TDLS (e.g., Slemr *et al.*, 1986), although the FTIR detection limit is too high to be of value except for relatively rare, extremely large concentrations (see Table 11.2). More common are derivatization methods, and of these, one using *p*-hydroxyphenylacetic acid (POPHA) has been applied extensively to ambient air.

The POPHA method is based on the oxidation of horseradish peroxidase in the +3 state to its +5 state (Lazrus *et al.*, 1985, 1986; Kok *et al.*, 1986). This oxidized form is then reduced by electron transfer from POPHA, generating the POPHA free radical. The POPHA free radicals self-react to produce the dimer, which, upon excitation at 320 nm, fluoresces at 405 nm. The overall reaction is

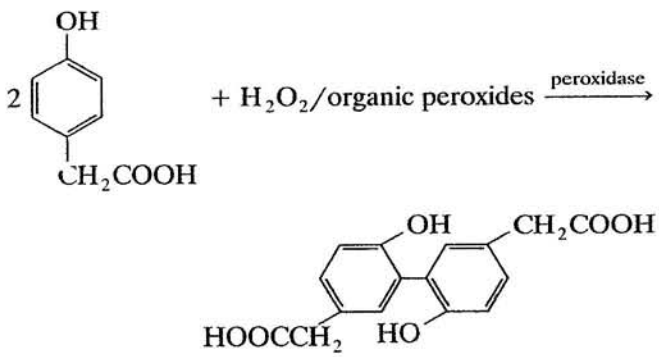


Since both $H_2O_2$ and organic peroxides carry out this reaction, this method measures total peroxides. However, the contribution of $H_2O_2$ can be separated by adding catalase, which decomposes $H_2O_2$ but not the organic peroxides. The instruments therefore usually have two channels, one in which catalase is added to give the organic peroxides, and one in which it is not, giving total peroxides. The difference between the two channels gives $H_2O_2$. Another approach involves using the different solubilities of $H_2O_2$ and organic peroxides (Staffelbach *et al.*, 1996).

The organic peroxides can be separated by HPLC prior to detection (Kok *et al.*, 1995). Sauer *et al.* (1996, 1997), for example, used HPLC with a POPHA detector to measure peroxides in air and in rainwater in Germany and at a marine coastal site in France. Although no organic peroxides were found in air, several were identified in some rainwater samples, including hydroxymethyl hydroperoxide ($HOCH_2OOH$) and 1-hydroxyethyl hydroperoxide ($CH_3CH(OH)OOH$). Hydroxymethyl hydroperoxide is expected to be formed in the atmosphere from the reaction of the one-carbon Criegee biradical ($\cdot CH_2OO\cdot$) with water, i.e., from the reaction of ethene and terminal alkenes with $O_3$ in air (see Chapter 6.E.2) and perhaps from the reaction of $HOCH_2OO\cdot$ radical with $HO_2$ (see Chapter 6.E.2).

Fels and Junkermann (1994) reported both hydroxymethyl hydroperoxide and $CH_3OOH$ in air in a rural area in Germany, with these two compounds comprising more than 90% of the total organic hydroperoxides. Ethyl hydroperoxide and peroxyacetic acid were also detected in some samples. Methyl hydroperoxide is expected in low-$NO_x$ environments from the reaction of $CH_3O_2$ with $HO_2$ (see Chapter 6). The organic hydroperoxides were about 10–40% of the $H_2O_2$ concentrations measured simultaneously. This is similar to the observations of Tremmel *et al.* (1994), who found that organic hydroperoxides in air over the northeastern United States were typically about half that of $H_2O_2$.

Other hydroperoxides have also been detected at small concentrations in air. For example, Hewitt and Kok (1991) reported the presence of 1-hydroxyethyl hydroperoxide as well as an unidentified compound, perhaps hydroxybutyl hydroperoxide, in air in rural Colorado.

In remote areas, $CH_3OOH$ is generally the major, and often the sole detectable, organic hydroperoxide present (e.g., see Staffelbach *et al.*, 1996). This is not surprising, since $CH_4$ is often the major organic in such regions, and hence the $CH_3O_2 + HO_2$ reaction is important.

A three-channel approach was developed by Lee *et al.* (1993) to distinguish $H_2O_2$ from hydroxymethyl hydroperoxide and total peroxides. In this approach, one channel is used to scrub the air sample into a POPHA solution to obtain total peroxides. In a second channel, the air sample is scrubbed into Fenton reagent solution at a pH of 3. This converts the $H_2O_2$ into OH radicals:

$$Fe(II) + H_2O_2 \rightarrow Fe(III) + OH^- + OH.$$

The OH radicals are trapped by reaction with benzoic acid, forming hydroxybenzoic acid, which is measured by fluorescence. Organic peroxides ROOH form RO + $OH^-$, but the derivatives of benzoic acid formed by the reaction of the RO radicals do not fluoresce under the conditions chosen to measure $H_2O_2$. Thus, in principle, this second channel measures $H_2O_2$. However, in practice, it was found to give about a 30% response to hydroxymethyl hydroperoxide as well, so that the results from this channel must be corrected for this contribution (Lee *et al.*, 1993).

In the third channel of this instrument, air is scrubbed into a solution containing Fenton reagent at a pH of 9. At this high pH, hydroxymethyl hydroperoxide is rapidly hydrolyzed to give $H_2O_2$. Thus the third channel gives the sum of $H_2O_2$ and hydroxymethyl hydroperoxide and the difference between this and the second channel (corrected) gives hydroxymethyl hydroperoxide.

An intercomparison of TDLS, POPHA, and a luminol chemiluminescence method for $H_2O_2$ was carried out using zero air, irradiated VOC–$NO_x$ mixtures, and ambient air (Kleindienst *et al.*, 1988a). The TDLS and two POPHA methods using different sampling approaches (continuous scrubbing and a diffusion scrubber, respectively) were in reasonably good agreement. However, the luminol method exhibited positive and negative interferences under different conditions and hence has not since been applied extensively to ambient air measurements.

Another intercomparison was carried out at the Mauna Loa Observatory in 1991 and 1992 (Staffelbach *et al.*, 1996). TDLS was used to measure $H_2O_2$. In addition, the POPHA method with catalase was used to distinguish between $H_2O_2$ and organic peroxides, the POPHA method with aqueous solubility differences was employed to discriminate between these compounds, and HPLC was used to separate and detect different hydroperoxides. For $H_2O_2$, while the measurements using the wet chemical methods and TDLS showed similar trends, there was a significant amount of scatter in individual measurements. For example, the correlation coefficients for plots of the TDLS versus the two POPHA techniques varied from 0.20 to 0.60. HPLC showed that $CH_3OOH$ was the only organic hydroperoxide present. However, individual measurements of $CH_3OOH$ made using this method compared to those using POPHA with catalase only had a correlation coefficient of 0.14 in wet air and 0.49 in dry air, whereas the corresponding correlation coefficients for the two POPHA measurements of organic hydroperoxides were 0.33 and 0.48, respectively.

In short, while wet chemical techniques are valuable for measurement of $H_2O_2$ and organic hydroperoxides, the absolute accuracy and precision remain a subject of concern and research.

*Typical tropospheric concentrations.* Measurements of $H_2O_2$ in air up to approximately 1990 are summarized by Gunz and Hoffmann (1990) and Sakugawa *et al.* (1990). Concentrations of $H_2O_2$ observed in air near the earth's surface are typically about 1–5 ppb (e.g., Daum *et al.*, 1990; Van Valin *et al.*, 1990; Claiborn and Aneja, 1991; Tremmel *et al.*, 1993; Lee *et al.*, 1993; Das and Aneja, 1994; Tanner and Schorran, 1995; Macdonald *et al.*, 1995; Staffelbach *et al.*, 1996; Sanhueza *et al.*, 1996; Ridley *et al.*, 1997; Martin *et al.*, 1997; Balasubramanian and Husain, 1997; Weinstein-Lloyd *et al.*, 1998). Although it may initially appear surprising, concentrations in remote and rural areas are not tremendously different from those in more polluted urban areas. For example, Heikes *et al.* (1996) reported levels of 0.3–5 ppb in the marine boundary layer, and Weinstein-Lloyd *et al.* (1998) measured concentrations of 1–4 ppb in the continental boundary layer midday in a rural area in the southeastern United States. The reason is that although there is a great deal more photochemical activity in the polluted regions, which might be expected to lead to $H_2O_2$, there is also more NO. Since $H_2O_2$ is formed by the $HO_2 + HO_2$ self-reaction and since $HO_2$ also reacts rapidly with NO, higher NO levels tend to inhibit the formation of the peroxide.

In addition to $H_2O_2$, methyl hydroperoxide has also been measured. For example, in air over Hawaii, concentrations of ~0.1–0.5 ppb were typical, although concentrations as high as 1.6 ppb have been observed in remote areas (Staffelbach *et al.*, 1996; Heikes *et al.*, 1996; Sanhueza *et al.*, 1996; Ridley *et al.*, 1997). Weinstein-Lloyd *et al.* (1998) measured concentrations up to ~2.5 ppb in the rural continental boundary layer. There are insufficient studies to firmly establish the relative contribution of $CH_3OOH$ and perhaps other organic hydroperoxides to the total atmospheric levels, but the data available indicate that $H_2O_2$ is the major hydroperoxide present in air. For example, Tanner and Schorran (1995) found that $H_2O_2$ typically comprised about 90% of the total peroxides in the Grand Canyon area of the United States and Ayers *et al.* (1996) found

in a limited set of measurements at Cape Grim, Tasmania, that $H_2O_2$ was ~60% of the total. Similarly, the median concentration of $CH_3OOH$ measured by Weinstein-Lloyd *et al.* (1998) in the rural continental boundary layer was 1.7 ppb, representing about a third of the total measured hydroperoxides.

Hydroxymethyl hydroperoxide has also been identified and measured in rural continental areas as well as in the marine boundary layer. For example, Lee *et al.* (1993) report concentrations as high as 5 ppb in rural Georgia, and Heikes *et al.* (1996) measured concentrations from 0.6 to 1.6 ppb in the marine boundary layer over the south Atlantic Ocean. The median value in the rural continental boundary layer in the southeast United States was reported to be 0.97 ppb, with individual measurements ranging from ~0.2 to 3 ppb (Weinstein-Lloyd *et al.*, 1998).

In summary, $H_2O_2$ is ubiquitous in air throughout the troposphere. $CH_3OOH$ and $HOCH_2OOH$ have also been observed, generally at smaller concentrations than $H_2O_2$. There is at present little evidence for significant contributions of larger organic peroxides.

### *i. $HO_x$ Free Radicals*

As seen throughout this book, OH and $HO_2$ are central to the chemistry of both the lower and upper atmosphere. As a result, accurate measurement of their concentrations is critical to a quantitative understanding of atmospheric chemistry.

*(1) OH* Estimates of globally averaged OH concentrations have been obtained by applying a mass balance type of approach to certain compounds whose major removal from the atmosphere is believed to be reaction with OH. For example, the emissions of methylchloroform, $CH_3CCl_3$, are well known and its concentrations have been measured at a number of locations around the world. Using 3-D models, one can calculate the concentrations of OH and their geographical distribution that remove $CH_3CCl_3$ at appropriate rates to generate the measured concentrations (e.g., see Altshuller review, 1989; Spivakovsky *et al.*, 1990; Prinn *et al.*, 1992, 1995; and Krol *et al.*, 1998). A similar approach has been taken using $^{14}CO$ (Brenninkmeijer *et al.*, 1992).

In particular air masses, estimates of OH concentrations have also been derived from the relative rates of decay of a series of hydrocarbons in the air mass whose rate constants for reactions with OH are well known (e.g., Blake *et al.*, 1993). Alternatively, organics can be added as tracers; criteria for the choice of suitable compounds are discussed by Davenport and Singh (1987). However, such approaches can be complicated by the effects of transport and mixing of the air mass with ones of different composition (e.g., McKeen *et al.*, 1990) and by the possible contribution of oxidants other than OH to the decay of the organic (e.g., Blake *et al.*, 1993). In addition, average OH concentrations rather than point or local measurements are derived from such data, and both this and the mass balance approach are indirect. However, Ehhalt *et al.* (1998) have proposed an alternate approach to using hydrocarbon concentrations to determine OH, which minimizes the assumptions inherent in this method.

Clearly, direct techniques for measuring OH are needed that provide concentrations either at a point or over relatively restricted spatial scales. Two (absorption and laser-induced fluorescence) are direct, spectroscopic methods and two others (mass spectrometry and a radiocarbon method) rely on conversion of OH to another species that is measured. Each of these approaches and some of the intercomparisons that have been carried out are discussed briefly in the following sections. A good overview of these methods is found in a review by Eisele and Bradshaw (1993) and articles by Crosley (1994, 1995a, 1995b) and papers in a special issue of the *Journal of the Atmospheric Sciences* [52 (19), October 1, 1995].

*Absorption spectroscopy.* OH undergoes an allowed transition between its $X^2\Pi$ ground state and the first electronically excited $A^2\Sigma^+$ state. Because it is a small species, absorption lines due to the individual vibrational and rotational transitions can be resolved experimentally. As a result, it has a very characteristic banded absorption structure around 308 nm whose features make it an ideal candidate for DOAS measurements.

Atmospheric OH has been measured for a number of years using its absorption. For example, vertical column abundances of OH have been measured in a number of studies using the sun as a light source (e.g., Burnett and Burnett, 1981, 1996; Burnett *et al.*, 1988; Burnett and Minschwaner, 1998). Over the past several decades, beginning with the measurements of Perner *et al.* (1976), absorption spectroscopy has been used to make measurements of OH over much shorter paths in the troposphere. The fundamental principles behind this technique have been described earlier in the discussion of DOAS spectrometry. Here we briefly discuss some of the aspects of the measurements that are unique to OH, as well as some typical applications.

Figure 11.42a shows an energy level diagram and some of the allowed lines in the $v'' = 0$ level of $X^2\Pi$ to the $v' = 0$ level of $A^2\Sigma^+$ (Mount, 1992). Figure 11.42b shows the absorption spectrum of OH obtained using a butane flame as the source in this case. The emission of a frequency-doubled dye laser whose full width at half-maximum is 0.41 nm is also shown (Dorn *et al.*, 1995a). The laser emission is sufficiently broad

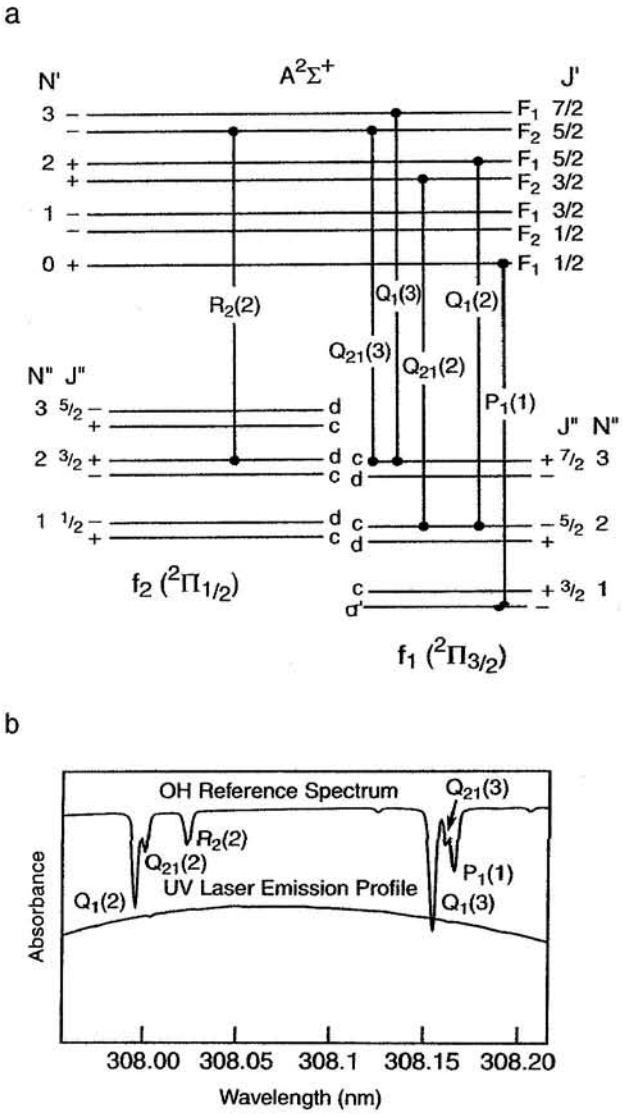


FIGURE 11.42 (a) Energy levels and some allowed transitions for the OH($X^2\Pi \rightarrow A^2\Sigma^+$) absorption, (b) a typical broadband laser emission line profile, and an OH reference spectrum with absorption lines in this region. (Adapted from Mount, 1992; and Dorn *et al.*, 1995a.)

compared to the OH linewidth that six different OH lines can be measured simultaneously using a high-resolution spectrograph and linear photodiode array. In an open multipass White cell with base path of 38.5 m and a total path length of 1.85 km, a detection limit for OH of $8.7 \times 10^5$ radicals $cm^{-3}$ can be obtained (Brandenburger *et al.*, 1998).

Open-beam double-pass instruments using a retroflector array to return the light beam back to the spectrograph are also in use (e.g., Mount, 1992; Mount and Harder, 1995; Harder *et al.*, 1997a). Another variation is the use of a fast-scanning technique with picosecond pulse lengths and a photomultiplier detector, rather than the use of a photodiode array. For example, Armerding and co-workers (Armerding *et al.*, 1994, 1995, 1996, 1997) tune the laser wavelength rapidly over the region of interest, covering up to $\sim 13$ $cm^{-1}$ in spectral width in 0.1 ms. Multiple scans, taken with a repetition rate of 1.3 kHz, are averaged to improve the signal-to-noise ratio.

A typical example of such measurements was shown in Fig. 11.15.

A major advantage of this approach is that the fundamental spectroscopic parameters for OH, including the absorption cross sections for various transitions, are well known (e.g., see Mount, 1992; Dorn *et al.*, 1995b), so that absolute concentrations of OH can be calculated based solely on the absorption spectra. Another major advantage is that the laser beams are expanded so that generation of OH in the beam itself by photolysis of ozone is not the problem that it has been in LIF measurements (vide infra).

A disadvantage is that the use of long paths gives average concentrations over the whole distance, over which there could be considerable variability. Folded paths using White cells provide a more restricted measurement distance, but reflection losses on the mirrors preclude increasing the total path length and hence detection sensitivity beyond a certain point. Whether such a system can be made sufficiently stable for aircraft use is also not clear. Finally, the sensitivity of such systems is in the $10^5$ to low $10^6$ radical $cm^{-3}$ range. While this is sufficient for daytime measurements when there are significant photolytic sources of OH, it is not adequate for nighttime measurements where much lower concentrations (likely of the order of $10^4$ $cm^{-3}$ or less) are generated by such processes as PAN decomposition.

*Laser-induced fluorescence (LIF).* Laser-induced fluorescence measurements have been applied to the atmosphere since the suggestion of Baardsen and Terhune in 1972 that this method should be feasible. Figure 11.43 shows the energy levels and transitions involved in LIF measurements. OH is excited from its ground $X^2\Pi$ state into the first electronically excited $A^2\Sigma$ state. The $v'' = 0$ to $v' = 0$ transition is around 308 nm and the $v'' = 0$ to $v' = 1$ at 282 nm. Two schemes have been used: excitation using 282 nm into $v' = 1$ of the upper electronic state, or excitation using 308 nm into $v' = 0$ of the upper state. Collisional quenching deactivates some of the $v' = 1$ into $v' = 0$ in competition with fluorescence, mainly in the (1,1) band of the electronic transition (that is, from $v' = 1$ of the upper state into $v'' = 1$ of the lower state). Collisional deactivation of $v' = 0$ then occurs in competition with fluorescence in the (0,0) band at 308 nm

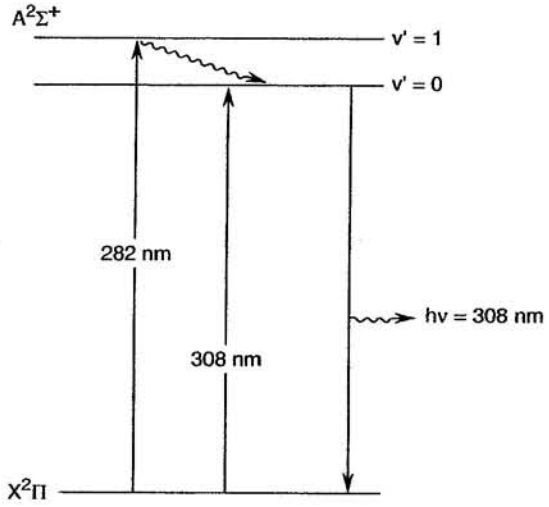


FIGURE 11.43 Schematic diagram of OH energy levels used in LIF measurements.

(e.g., see Copeland *et al.*, 1985; Copeland and Crosley, 1986; Crosley, 1989).

The major problem with LIF measurements in the past has been what might be called the "atmospheric uncertainty principle;" i.e., in the act of carrying out the measurement, the system is perturbed and artifact formation of OH can occur (e.g., see Smith and Crosley, 1990; and Hard *et al.*, 1992b). This is primarily due to the photolysis of $O_3$ to generate $O(^1D)$, which in the presence of water vapor forms OH:

$$O_3 + h\nu(\lambda < 350 \text{ nm}) \rightarrow O(^1D) + O_2,$$
$$O(^1D) + H_2O \rightarrow 2OH,$$
$$+ M \rightarrow O(^3P) + M.$$

This artifact formation of OH is less severe when the excitation is at 308 nm, rather than 282 nm, since both the absorption cross sections and quantum yields for ozone photolysis decrease rapidly with wavelength in this region (see Chapter 4.B). Another advantage is that the absorption cross section for the (0,0) transition is about a factor of four larger than for the (0,1) transition, increasing the amount of excited OH. As a result, most LIF systems now use 308-nm excitation (e.g., Chan *et al.*, 1990; Stevens *et al.*, 1994; Hard *et al.*, 1995; Holland *et al.*, 1995). The disadvantage is a larger background signal at the fluorescence wavelength due to scattered laser light.

A second approach to minimizing the artifactual formation of OH in these measurements has been to sample the air through a nozzle into a low-pressure region operated at ~4 Torr. This was pioneered by O'Brien, Hard, and co-workers (Hard *et al.*, 1984; Chan *et al.*, 1990; Hard *et al.*, 1995) and is known as the FAGE technique (*f*luorescence *a*ssay with *g*as *e*xpansion). The advantage is that the rate of generation of OH from the $O(^1D) + H_2O$ reaction is smaller, providing less *in situ* generation of OH in the laser beam. While the OH concentration in air is reduced proportionately with the pressure, collisional quenching of the electronically excited OH is as well; the result is that the OH LIF signal does not change substantially on reducing the pressure.

The "zero" signal in such instruments is usually established by adding an organic such as isobutane (e.g., Hard *et al.*, 1992b) or $C_6F_6$ (Stevens *et al.*, 1994; Dubey *et al.*, 1996) that reacts rapidly with the OH. The difference in signal when the compound is added compared to when it is not is then a measure of the OH present. Another approach is to tune the laser on and off resonance with the OH absorption, permitting measurement of the background signal, which can be subtracted (e.g., Hofzumahaus *et al.*, 1996).

Figure 11.44 is a schematic diagram of one LIF instrument (Stevens *et al.*, 1994; Brune *et al.*, 1998). An air-cooled copper-vapor laser pumps a dye laser whose output at 616 nm is doubled to generate the 308-nm exciting radiation. An OH reference cell in which OH is generated from the thermal dissociation of water

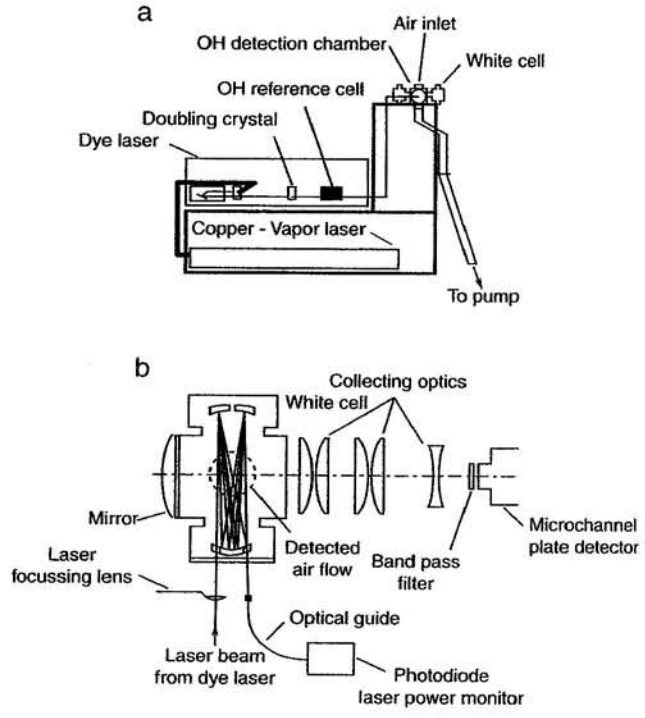


FIGURE 11.44 (a) Overall schematic diagram of an LIF instrument used for OH and $HO_2$ and (b) sample chamber in this instrument. (Adapted from Stevens *et al.*, 1994.)

provides the reference for tuning the dye laser into resonance with the OH absorption. The beam is directed into a multipass cell with White cell optics as shown in Fig. 11.44b.

One disadvantage of LIF compared to absorption measurements is the need for field calibration. It is a nontrivial issue to generate known concentrations of OH under ambient conditions for this purpose. A variety of approaches are used. These include photolysis of water vapor at 185 nm where the $H_2O$ absorption cross section as well as that of $O_2$ are needed (e.g., Holland *et al.*, 1998). However, there has been considerable uncertainty associated with these absorption cross sections (e.g., see Lazendorf *et al.*, 1997; and Hofzumahaus *et al.*, 1997, 1998). Stevens *et al.* (1994) used an internal calibration by titration of known concentrations of $NO_2$ with an excess of H atoms which generates OH via $H + NO_2 \rightarrow OH + NO$ combined with external calibration using water vapor photolysis to account for transmission of OH through the sampling system. Sampling from a sample chamber in which a VOC–$NO_x$ mixture is irradiated and the rate of decay of the organics used to obtain the OH concentration has also been used (Hard *et al.*, 1984; Chan *et al.*, 1990).

As discussed later, LIF has also been used to measure $HO_2$ by conversion to OH by reaction with NO.

*Mass spectrometry.* Reaction of OH to form an ion, $HSO_4^-$, which can be measured by mass spectrometry was first demonstrated by Eisele and Tanner (1991). Figure 11.45 is a schematic diagram of this approach (Tanner *et al.*, 1997). Air is sampled through an inlet system described in detail by Eisele *et al.* (1997) and mixed with isotopically labeled $^{34}SO_2$, forming $H_2^{34}SO_4$ via reactions discussed in Chapter 8.C.2:

$$OH + {}^{34}SO_2 + M \rightarrow H^{34}SO_3 + M,$$

$$H^{34}SO_3 + O_2 \rightarrow HO_2 + {}^{34}SO_3,$$

$${}^{34}SO_3 + H_2O + M \rightarrow H_2{}^{34}SO_4 + M.$$

Sufficient $^{34}SO_2$ is added to convert more than 99% of the OH in air to the acid. The use of isotopically labeled $SO_2$ forms labeled $H_2SO_4$ which is not present in measurable quantities in air. Thus, labeled $H_2SO_4$ is equal to the initial OH and allows $H_2{}^{32}SO_4$ present in air to be measured simultaneously. Periodically during the measurements, propane is added simultaneously with the $^{34}SO_2$ at concentrations that will remove most of the OH, providing a background signal.

As discussed shortly, $HO_2$ and $RO_2$ react in the presence of NO to regenerate OH, which will lead to an overestimate of the OH concentration. To minimize this, propane is added downstream of the $^{34}SO_2$ injector to remove any of this regenerated OH. However, as discussed by Tanner *et al.* (1997), at high $NO_x$ concentrations, some regeneration does occur and the measurements must be corrected for that.

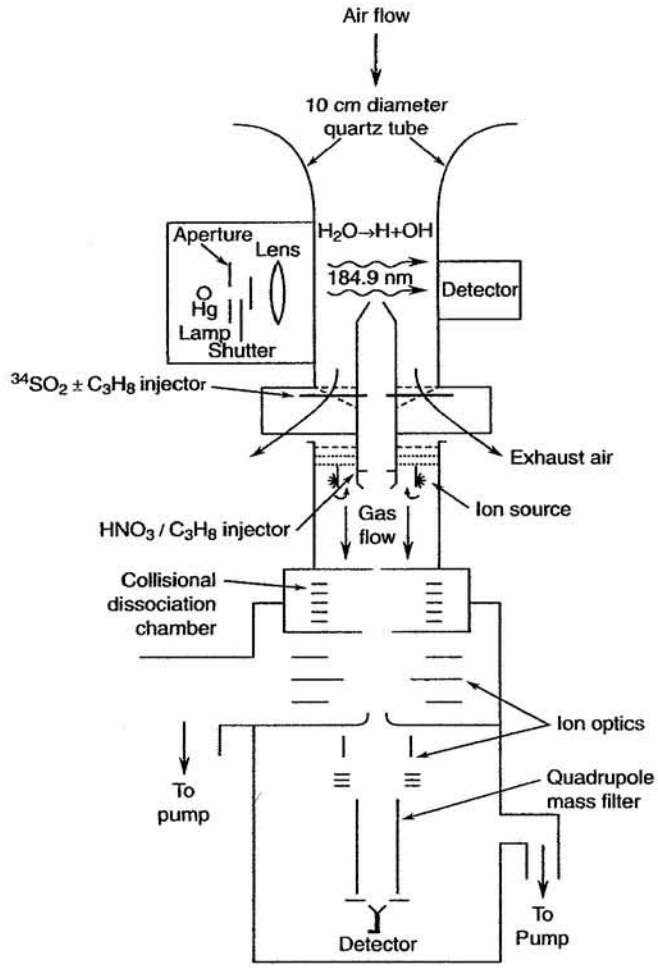


**FIGURE 11.45** Schematic diagram of mass spectrometer used for OH measurements using derivatization approach (adapted from Tanner *et al.*, 1997).

At this downstream port, $HNO_3$ is also added at concentrations such that the $NO_3^-(HNO_3)$ ion adduct is the major nitrate ion (see discussion of mass spectrometry in Section A.2). Since $H_2SO_4$ is a stronger acid, it proton transfers to the cluster:

$$H_2{}^{34}SO_4 + NO_3^-(HNO_3) \rightarrow H^{34}SO_4^-(HNO_3) + HNO_3.$$

Figure 11.46a shows a typical mass spectrum. In addition to the $NO_3^-(HNO_3)$ ionizing agent, smaller amounts of $NO_3^-$ and $NO_3^-(HNO_3)_2$ are present. The $HNO_3$ adducts of both the naturally occurring $^{32}S$ and the added $^{34}S$ isotopes of $HSO_4^-$ are seen as well as the corresponding $HSO_4^-$ ions. These ions then enter a

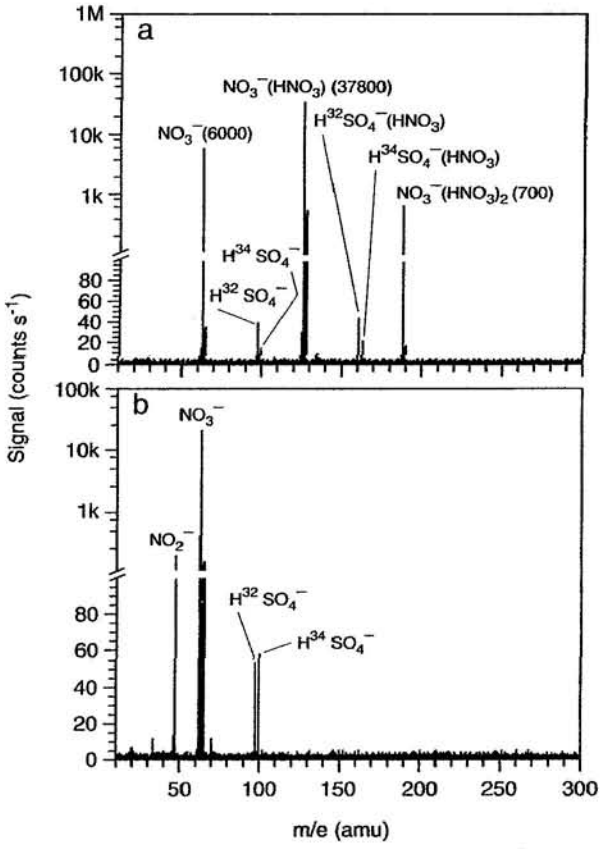


FIGURE 11.46 Typical mass spectra of ambient air (a) without collisional dissociation of the adducts and (b) with collisional dissociation. The counts for $NO_3^-$ and its adducts with $HNO_3$ are shown in parentheses in (a). Note changes in scale from linear to logarithmic (adapted from Tanner *et al.*, 1997).

collisional dissociation chamber where the $HNO_3$ adducts of $HSO_4^-$ are fragmented. Figure 11.46b shows a typical mass spectrum (not for the same conditions as Fig. 11.46a, however) after collisional dissociation. The $HSO_4^-$ ions are now the sole form of these ions and can be cleanly measured using mass spectrometry.

As is the case for LIF, calibration to obtain absolute concentrations is a challenge. In the instrument shown in Fig. 11.45, a calibration source based on the photolysis of water at 185 nm is installed in the inlet. From the absorption cross section of $H_2O$ gas at 185 nm, its concentration, the light intensity, and the sample flow rate, the concentration of OH generated by the photolysis can be calculated. However, not only is there significant uncertainty in the absorption cross section for $H_2O$ at 185 nm (e.g., see Lazendorf *et al.*, 1997; Hofzumahaus *et al.*, 1997, 1998; and Tanner *et al.*, 1997), but the measured calibration factor was highly variable from day to day, by as much as a factor of two (Tanner *et al.*, 1997).

In summary, the measurement of OH by reaction to form isotopically labeled $H_2{}^{34}SO_4$ and measurement of the latter by chemical ionization mass spectrometry is promising. As discussed later, measurements made using this technique compare well with those using UV absorption, and the sensitivity is good, $\sim 2 \times 10^5$ radicals cm$^{-3}$. With sufficiently long integration times, even much smaller nighttime concentrations in the range of low $10^4$ radicals cm$^{-3}$ have been measured (Tanner and Eisele, 1995). Figure 11.47, for example, shows OH measurements made throughout the night at the Mauna Loa Observatory in Hawaii in May 1992. Concentrations of OH just after sunset are in the low $10^5$ cm$^{-3}$ range and fall off during the night to levels indistinguishable from zero in this instrument.

The disadvantages are the need to correct for regeneration of OH in the instrument from $HO_2$ and $RO_2$ reactions at high ambient NO concentrations and, as with LIF, the uncertainty in the absolute calibration.

*Radiocarbon technique.* Campbell and Sheppard (Campbell *et al.*, 1979) developed a method for OH based on its oxidation of isotopically labeled $^{14}CO$ that is added to the air sample. Assuming that CO is oxidized to $CO_2$ by the reaction with OH, the rate of formation of $CO_2$ is given by

$$d[CO_2]/dt = k[CO][OH],$$

where $k$ is the rate constant for the OH + CO reaction under the appropriate conditions. The added $^{14}CO$ and reaction time are such that the $^{14}CO$ concentration remains essentially constant. Integration of this rate expression results in the following expression:

$$[OH] = \frac{[^{14}CO_2]}{[^{14}CO]} \frac{1}{kt}. \qquad (Q)$$

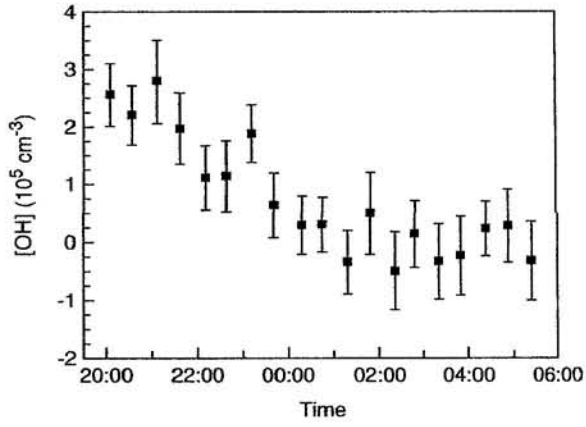


FIGURE 11.47 Nighttime measurements of OH at Mauna Loa Observatory, Hawaii, in May 1992 made by the mass spectrometry derivatization technique (adapted from Tanner and Eisele, 1995).

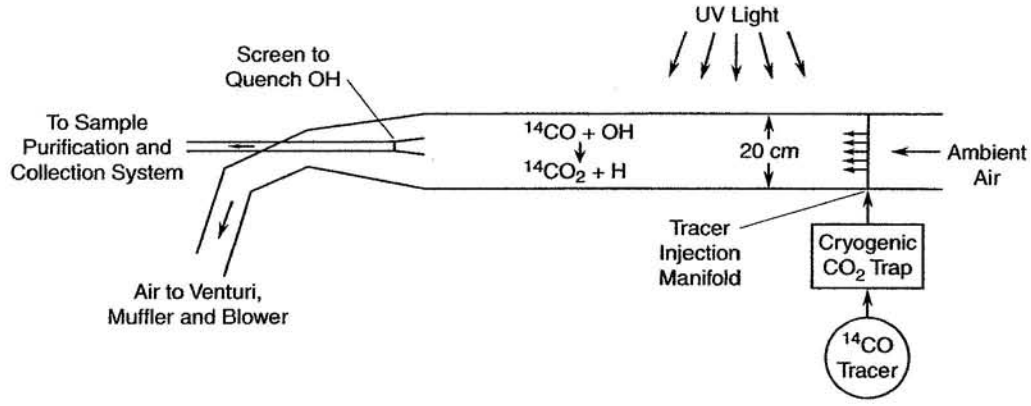


FIGURE 11.48 Schematic diagram of radiochemical OH measurement apparatus (adapted from Felton *et al.*, 1990).

Figure 11.48 is a schematic diagram of this apparatus (Felton *et al.*, 1990). Air is introduced into a sampling manifold consisting of a quartz tube where it is mixed with the $^{14}CO$. The air is collected downstream after a measured reaction time and analyzed for $^{14}CO_2$.

There are several assumptions inherent in this method (e.g., see Felton *et al.*, 1990, 1992). For example, the concentration of $^{14}CO_2$ in ambient air must be negligible compared to that formed in the reaction and the OH concentration in air is assumed to be unperturbed either by the addition of $^{14}CO$ or by the sampling system itself, e.g., by loss on the walls. While straightforward in principle, as discussed by Felton *et al.* (1990, 1992), it is experimentally challenging. For example, accurately measuring the small concentrations of $^{14}CO_2$ formed is difficult, imposing stringent requirements on the purity of the $^{14}CO$ tracer and on the purification techniques used for the product $^{14}CO_2$.

*Intercomparisons.* A number of intercomparison studies have been carried out for the different OH measurement techniques (e.g., see Beck *et al.*, 1987; Mount and Eisele, 1992; Eisele *et al.*, 1994; Campbell *et al.*, 1995; Brauers *et al.*, 1996; Mount *et al.*, 1997a, 1997b; and Hofzumahaus *et al.*, 1998). Overall, given the extreme difficulty in sampling and measuring this highly reactive free radical at the sub-ppt concentrations found in air, the agreement is generally quite good.

Figure 11.49, for example, shows measurements of the diurnal variation of OH made using LIF and UV absorption, respectively, on two different days in a rural area in Germany (Hofzumahaus *et al.*, 1998). The agreement is, in most cases, excellent. These data also illustrate a typical diurnal variation of OH, being below the detection limits of the instruments at night ($5 \times 10^5$ radicals cm$^{-3}$ for LIF and $1.5 \times 10^6$ radicals cm$^{-3}$ for DOAS) and rising to a peak of $\sim 10^7$ radicals cm$^{-3}$ at noon when photolysis of its precursors peaks. Similar diurnal behavior has been observed in remote areas such as the Mauna Loa Observatory (e.g., Eisele *et al.*, 1996) and in more polluted areas as well (e.g., Felton *et al.*, 1990; Hard *et al.*, 1995; Mount *et al.*, 1997b). Typical peak OH concentrations are usually in the range of $\sim(2\text{–}10) \times 10^6$ radicals cm$^{-3}$.

Figure 11.50 shows for this particular intercomparison study a plot of OH measured by DOAS against those obtained simultaneously by LIF. The correlation coefficient is $r = 0.85$. Disagreement was greatest when the wind was from a particular direction, which gave higher DOAS readings. The reason for this is not clear, but Hofzumahaus and co-workers propose that it may

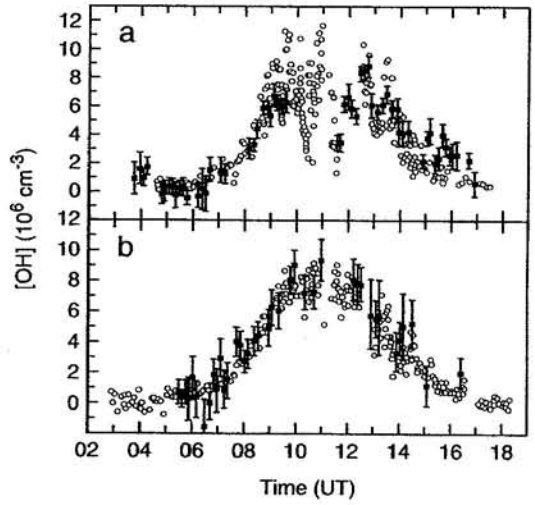


FIGURE 11.49 Diurnal variation of OH measured using LIF (○) and DOAS (●) in a rural area in Germany on the (a) 16th and (b) 17th of August 1994. (Adapted from Hofzumahaus *et al.*, 1998.)

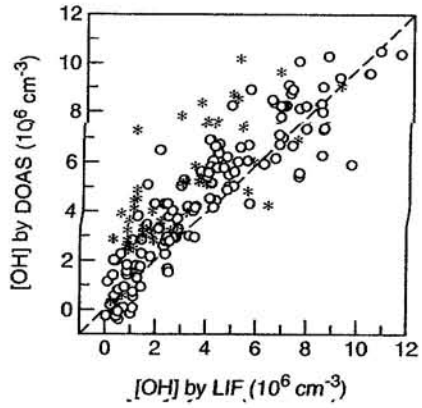


FIGURE 11.50 Correlation between OH measurements made by DOAS and by LIF in a rural area in Germany in August 1994. The data indicated by asterisks were measurements made when the wind was from a particular direction suggesting it might contain unrecognized OH sources affecting the long-path DOAS measurements (adapted from Hofzumahaus *et al.*, 1998).

be due to unrecognized OH sources that affected the long-path DOAS measurements more than the point measurements made by LIF. Exclusion of those data points improves the correlation ($r = 0.90$) and the slope of the line is $1.09 \pm 0.04$ with an intercept within experimental error of zero.

Similarly, agreement between UV absorption and the mass spectrometer technique is quite good. Figure 11.51 shows a plot of OH concentrations measured using the mass spectrometry derivatization technique compared to those measured using long-path UV absorption in a rural area in Colorado for clear days with $NO_x$ below 450 ppt measured by an *in situ* technique and $NO_2$ below 500 ppt averaged over the long path

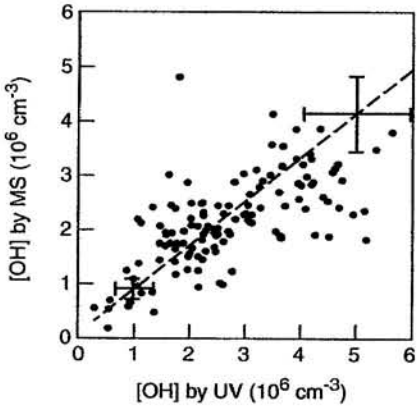


FIGURE 11.51 Correlation between measurements made by the mass spectrometry–derivatization technique and long-path UV absorption in rural Colorado for lower $NO_x$ conditions (adapted from Mount *et al.*, 1997a).

(Mount *et al.*, 1997a). The slope of the line is $0.82 \pm 0.06$; i.e., the mass spectrometer point measurements were about 20% lower than the UV measurements over a path length of 10.3 km. About 25% of the data were different by amounts outside the experimental errors. Such discrepancies may be due to comparing distance-averaged to point values and/or to calibration inaccuracies.

An intercomparison of the mass spectrometer method with an LIF instrument, however, was not as good. While the slope of the plot of LIF versus the MS measurements was 0.73, the $r$ value was only 0.26, in part due to poor laser performance in the LIF instrument during the studies (Mather *et al.*, 1997).

Extensive intercomparisons using the radiocarbon technique have not been carried out. Campbell *et al.* (1995) compared measurements using the radiocarbon technique to those from an LIF instrument (Chan *et al.*, 1990). The values obtained were frequently near the detection limits of the instruments, but despite that, were reasonably well correlated ($r^2 = 0.74$). However, the slope of a plot of the radiocarbon versus LIF absolute concentrations was 2.9, i.e., there was a difference of about a factor of three.

In short, given the challenges associated with measuring OH, the disagreement between the various methods is not surprising and the discrepancies appear to be improving as the methods are developed further.

***(2) $HO_2$ and $RO_2$*** There are three approaches that are used to measure $HO_2$ and/or $RO_2$: (1) conversion of $HO_2$ and/or $RO_2$ to OH and measurement of the latter using techniques already described, (2) a chemical amplifier method, and (3) matrix isolation ESR.

*Conversion of $HO_2$ to OH.* $HO_2$ can be measured by conversion into OH by its fast reaction with NO,

$$HO_2 + NO \rightarrow OH + NO_2,$$

followed by measurement of the OH by one of the methods described in the preceding section. For example, LIF detection of OH generated by reacting $HO_2$ with NO has been used to measure $HO_2$ at both remote and urban sites (Hard *et al.*, 1984, 1992a).

Another approach combines the mass spectrometric derivatization approach with chemical amplification (Reiner *et al.*, 1997, 1998). In this instrument, $HO_2$ and $RO_2$ are converted to OH through the reactions in the chemical amplifier approach discussed below, and the OH is then converted to $H_2SO_4$ by reaction with $SO_2$ and measured by chemical ionization mass spectrometry using $NO_3^-(HNO_3)$ clusters as described earlier. In this case, the use of isotopically labeled $SO_2$ is not necessary, since the ambient $H_2SO_4$ concentration is much smaller than that of the peroxy radicals.

Because $HO_2$ radical concentrations in the troposphere are typically about two orders of magnitude larger than those of OH, the contribution of ambient OH to the signal does not present a problem.

*Chemical amplifier method.* Another approach, known as the chemical amplifier method, pioneered by Cantrell and Stedman (Cantrell and Stedman, 1982; Cantrell *et al.*, 1984) has been used extensively to measure the combination of $HO_2$ and $RO_2$ (although the latter is not necessarily with 100% efficiency; vide infra). This method involves the conversion of $HO_2$ to OH in a chain reaction with a length of ~100–200. Figure 11.52 is a schematic diagram of one such instrument (Cantrell *et al.*, 1993). Air containing $HO_2$, $RO_2$, OH, and other species is sampled into the instrument, where it is mixed with NO, typically at ~3 ppm, and CO, at about 7–10% of the total flow. $HO_2$ reacts with NO as above to generate OH. In the presence of large concentrations of CO, $HO_2$ is regenerated:

$$OH + CO \xrightarrow{O_2} HO_2 + CO.$$

Thus, a chain reaction is set up in which $HO_2$ converts NO to $NO_2$ and is subsequently regenerated by the OH + CO reaction. The $NO_2$ is measured using techniques such as those described earlier; in the case of the system in Fig. 11.52, the luminol chemiluminescence technique is used. Termination of the chain occurs via reactions such as

$$OH + NO + M \rightarrow HONO + M,$$
$$HO_2 + NO_2 + M \rightarrow HO_2NO_2 + M,$$
$$HO_2 \rightarrow \text{Wall loss}.$$

The $HO_2$ concentration is given by

$$[HO_2] = \Delta NO_2/\text{chain length},$$

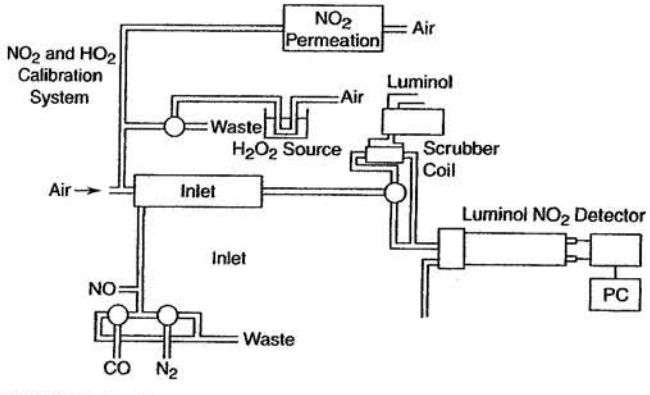


FIGURE 11.52 Schematic diagram of chemical amplifier apparatus for measurement of $HO_2$ and $RO_2$ (adapted from Cantrell *et al.*, 1993).

where the chain length is defined as the number of $NO_2$ molecules formed per initial $HO_2$ radical.

In addition to $HO_2$, organic peroxy free radicals are also measured, although not necessarily with 100% efficiency. For example, if $CH_3O_2$ is also present, the following reactions occur:

$$CH_3O_2 + NO \rightarrow CH_3O + NO_2,$$
$$CH_3O + O_2 \rightarrow HO_2 + HCHO.$$

The $HO_2$ then reacts as above in a chain reaction. While $CH_3O_2$ forms $HO_2$ in a straightforward series of reactions, larger $RO_2$ radicals may not. For example, as discussed in Chapter 6, a significant fraction of the reactions of larger $RO_2$ radicals with NO generates stable organic nitrates, $RONO_2$, rather than RO + $NO_2$. In addition, larger alkoxy radicals may not solely undergo reaction with $O_2$ to generate $HO_2$; indeed, as seen in Chapter 6, this is a minor path for some organic peroxy radicals, where decomposition and/or isomerization may predominate. As a result, the chemical amplifier measures $HO_2$ and some weighted fraction of $RO_2$ radicals.

For example, Cantrell and co-workers (1993) estimate the efficiency of conversion of simple alkyl peroxy radicals to vary from 0.93 for $CH_3CH_2O_2$ to 0.47 for $(CH_3)_2CO_2$, and it may be even less for larger alkyl peroxy radicals. This may be the reason that in some intercomparison studies, the matrix isolation–ESR technique (vide infra), which measures the sum of $RO_2$, gives some higher concentrations for some individual measurements than the chemical amplifier method (e.g., Zenker *et al.*, 1998).

Calibration has been carried out using known $HO_2/RO_2$ sources such as the thermal decomposition of PAN or $H_2O_2$ (e.g., Cantrell *et al.*, 1993), photolysis of $H_2O_2$ or water vapor (e.g., Schultz *et al.*, 1995), and the photolysis of $CH_3I$ in the presence of $O_2$ (e.g., Clemitshaw *et al.*, 1997). This in effect allows the chain length to be determined so that peroxy radical concentrations can be derived from the increase in $NO_2$ as given above. However, there appear to be some factors affecting the sensitivity that are not well understood. For example, the chain length has been shown to be sensitive to the concentration of water vapor in air in at least one instrument, for reasons that are not clear (Mihele and Hastie, 1998).

*Matrix isolation–electron spin resonance.* A third method used to measure $HO_2$ and $RO_2$ is matrix isolation with ESR (see earlier description of matrix isolation). Because $HO_2$ and $RO_2$ have distinct ESR signals, they can be differentiated (Mihelcic *et al.*, 1985, 1990, 1993). For example, Fig. 11.53, part A, shows the ESR spectrum obtained when approximately

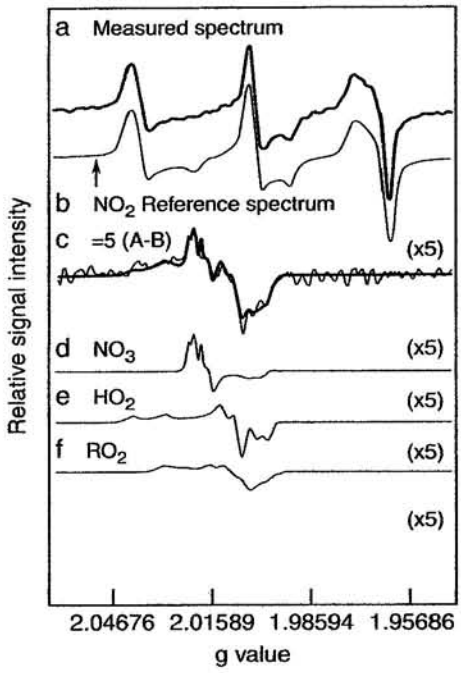


**FIGURE 11.53** Matrix isolation–ESR measurement of $NO_2$ (680 ppt), $NO_3$ (5.2 ppt), $HO_2$ (10 ppt), and $\Sigma RO_2$ (5 ppt) in Schavinsland, Germany, in August 1990 (adapted from Mihelcic *et al.*, 1993).

8 L of air in rural Germany was trapped in a polycrystalline matrix of $D_2O$ at 77 K (Mihelcic *et al.*, 1993). Spectrum b shows the ESR spectrum of $NO_2$; it can be seen that most of the observed ESR signals are due to $NO_2$, calculated from reference spectra to be present at a concentration of 0.68 ppb in this sample. Spectrum c is the difference between spectra a and b, magnified by a factor of five. Spectra d, e, and f are those of $NO_3$, $HO_2$, and $RO_2$, respectively, and their sum is shown by the heavy line through spectrum c. Clearly, the signals in spectrum c reflect contributions from these three radicals, at concentrations of 5.2 ppt $NO_3$, 10 ppt $HO_2$, and 5 ppt $RO_2$ in this particular sample. Detection limits for this method are 5 ppt for $HO_2$ and $RO_2$, respectively (Mihelcic *et al.*, 1993).

Fewer intercomparison studies have been carried out for peroxy radicals than for OH. Two chemical amplification methods were compared during a measurement campaign in Brittany, France (Cantrell *et al.*, 1996). Although the measurements tended to track one another, there is more scatter than might be expected, given the similar nature of the instruments. For example, a plot of the data from one instrument against those from the second had a slope of 0.71 but a correlation coefficient of only $r = 0.36$. In another study (Zenker *et al.*, 1998), comparison of three chemical amplifier techniques to matrix isolation–ESR gave agreement to within 25% for two of the chemical amplifier methods and the ESR approach. The third chemical amplifier technique gave on average values that were about 65% of the matrix isolation–ESR values.

Measurements using the chemical amplifier technique were also carried out at the same time as the mass spectrometer derivatization method was used, with titration of the $HO_2$ to OH (Cantrell *et al.*, 1997a). The chemical amplifier values were a factor of 2–3 times higher than those measured using the mass spectrometer approach, possibly because the latter measured $HO_2$ whereas the former measured $HO_2$ and some weighted fraction of $RO_2$. Finally, comparison of chemical amplifier measurements to those using matrix isolation–ESR (Volz-Thomas *et al.*, 1995; cited by Cantrell *et al.*, 1997b) shows agreement within about 40% for clean or moderately polluted air masses. For more heavily polluted air, the chemical amplifier was systematically lower, suggesting that there were significant concentrations of larger $RO_2$ radicals to which the chemical amplifier was less sensitive.

*Typical tropospheric concentrations.* Figure 11.54 shows the diurnal variation of average typical peroxy radical concentrations made using the chemical amplifier technique in Cape Grim, Tasmania, and Mace Head, Ireland (Carpenter *et al.*, 1997). As is the case for OH, $HO_2$ and $RO_2$ typically peak around noon, when photolysis is maximum, and are much smaller at night, particularly in low-$NO_x$ environments where there is little nighttime $NO_3$ (e.g., Monks *et al.*, 1996; Carslaw *et al.*, 1997a; Stevens *et al.*, 1997). Peak concentrations are in the $10^8$–$10^9$ $cm^{-3}$ range in remote areas (e.g., Carpenter *et al.*, 1997; Fischer *et al.*, 1998), with higher concentrations in polluted areas. For example, in downtown Denver, peak concentrations of $3 \times 10^9$ radicals $cm^{-3}$ have been measured (Hu and Stedman, 1995).

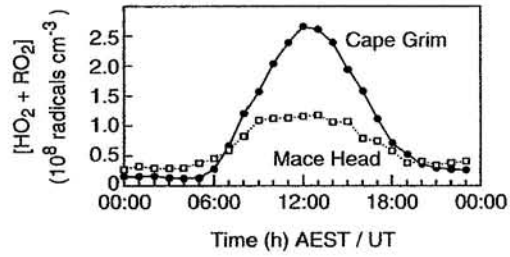


**FIGURE 11.54** Diurnal profile of average ($HO_2$ + $RO_2$) concentrations measured at Cape Grim, Tasmania (●), and at Mace Head, Ireland (■), under clean air conditions using a chemical amplification technique. (Adapted from Carpenter *et al.*, 1997.)

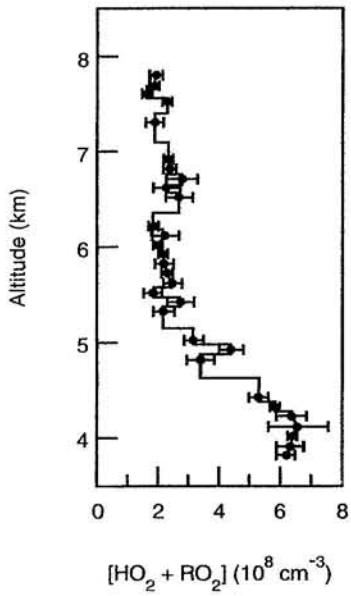


FIGURE 11.55 Altitude profiles for $HO_2 + RO_2$ in the free troposphere over southern Germany determined by conversion to OH and measuring OH by the mass spectrometric derivatization technique (adapted from Reiner *et al.*, 1998).

Figure 11.55 shows an altitude profile for peroxy radicals measured above the boundary layer over southern Germany using chemical amplification with the mass spectrometric derivatization measurement of OH (Reiner *et al.*, 1998). Concentrations are again seen to be in the range of $10^8$–$10^9$ $cm^{-3}$.

In summary, $HO_2$ and $RO_2$ radical concentrations are substantially greater than those of OH, typically by several orders of magnitude. There are several different approaches to measuring these peroxy radicals, and the results from these are in overall agreement as to the magnitude of the concentrations and their diurnal variation. However, there have not been a significant number of intercomparison studies of these methods, so evaluation of the absolute accuracies will require further work.

## 5. Generation of Standard Gas Mixtures

As seen throughout this discussion of the measurement of gases in the atmosphere, a critical component is the accurate calibration of the technique for the gas(es) of interest. This clearly requires sources of such calibration gases, which however, vary depending on the particular gas.

In the simplest case, the gas of interest can be purchased in a gas cylinder with known concentration provided by the supplier. In the United States, NIST has some mixtures relevant to atmospheric measurements. This approach has been used, for example, for simple hydrocarbons that are readily available and relatively stable. Preparation of standards in cylinders can also be carried out by the individual laboratory (e.g., see Apel *et al.*, 1998a). Such standards are frequently at higher concentrations than those to be measured in air. In this case, dynamic dilution systems are used to dilute the cylinder mixtures to the desired concentration range.

Caution must be exercised in using cylinder gases in some cases, however. For example, $NO_2$ in air from cylinders commonly contains a few percent $HNO_3$ as an impurity, and nickel carbonyls are present in CO stored in cylinders.

In other cases, the species cannot be preprepared as a mixture in air and hence flow systems must be used to generate them. For example, $HNO_3$ strongly adsorbs to surfaces and hence it is not possible to make a stable calibration mixture that can be stored. Some larger organics also do not have long-term stability when stored in gas cylinders.

In such cases, permeation tubes or diffusion cells are commonly used to generate the species in a flow of air, which can then be introduced into the measuring device. Permeation tubes are permeable tubes whose ends are sealed off and which contain the species of interest as a liquid in equilibrium with its vapor. The vapor permeates through the walls of the device at a rate that depends on temperature. The rate of permeation at a given temperature is normally supplied by the manufacturer and can be determined independently by weighing the permeation tube before and after use. From a knowledge of the flow rate of the gas passing over the tube, which entrains the vapor, the concentration of the species of interest in the air flow can be calculated. This approach is commonly used for species such as $HNO_3$, $Cl_2$, and HCl.

A similar approach is the use of diffusion cells. In this case, the liquid is held in a container that has a capillary of fixed length and diameter through which the vapor over the liquid diffuses. The vapor exiting the capillary is swept into a flow of gas to provide the gas mixture; this approach has been used to prepare mixtures of terpenes in air, for example (Larsen *et al.*, 1997). The concentration of the gas can be varied by using capillaries of varying internal diameter and length.

In some cases, the compound itself is sufficiently unstable that it cannot be purchased and must be synthesized. This is the case for compounds such as $O_3$ and HONO. Ozone at ppb to ppm concentrations in air is generated either by photolyzing $O_2$, e.g., using a low-pressure mercury lamp, or by a discharge in $O_2$;

when discharges are used, care must be taken to exclude air from the discharge region to avoid the simultaneous formation of oxides of nitrogen. In the case of HONO, a flow of gaseous HCl over $NaNO_2$ salt is often used to generate this compound in a flow system (Febo *et al.*, 1995). For other more "exotic" species such as $ClONO_2$ and $ClNO_2$, synthesis of the compounds is more involved and the literature should be consulted for methods of synthesis.

## B. PARTICLES

With the increasing epidemiological evidence for significant health impacts of particles (see Chapter 2.A.5), measurement of particle characteristics has taken on new urgency. With particles, both the chemical composition and size distribution of each component are important, and a wide range of sizes from ultrafine particles to coarse particles must be analyzed. While there is no fixed definition of "ultrafine" particles, those with diameters $<10$ nm are often referred to as ultrafine (although in some cases, up to 100 nm has been included in this description). In addition, the chemical components encompass almost the entire periodic table and include inorganic and organic as well as elemental and complex molecular species. Hence the area of particle characterization is a very challenging one.

Traditionally, particles have been collected and then analyzed for the distribution of mass and chemical composition. Various size ranges, or "bins," have been used, ranging from simple cutoffs at 10 $\mu$m, for example, to multibin analyses in which particles in six or more size ranges are collected and analyzed individually. Such approaches have produced the vast majority of the data in the literature, and the techniques used are summarized briefly in the following sections.

However, one might clearly expect significant variations in chemical composition between particles even within one range, and hence analysis of individual particles by size and composition is important. In addition, measuring such size-resolved properties in real time is desirable to elucidate sources, the atmospheric chemistry of particles, and the processes involved in their formation and fate. While techniques are now becoming available that address these concerns, this area of real-time and single-particle measurement could be considered to be in its infancy. Some of the instrumental techniques that have been successfully applied to ambient air are described in the following sections, along with some promising new approaches.

### 1. Sampling and Collection of Particles

The first steps in traditional analysis of the physical and chemical properties of atmospheric particulate matter are sampling, that is, obtaining a representative sample over the desired size range, and collection, that is, separating the particles from air. During sampling and collection, such parameters as humidity, temperature, and particle concentration must be controlled to maintain the sample integrity.

Sampling of particles presents some different considerations compared to sampling of gases. The larger mass of particles results in a much greater inertia, so that when the gas flow curves sharply, the particles tend to go straight ahead. High or low inlet velocities as well as bends in tubing used to sample for particles can thus lead to significant particle size bias and should be avoided. In addition, the sampling lines should be as short as possible to minimize particle loss by gravitational settling and turbulent deposition. Losses can also occur on the sampling surfaces if an electrostatic charge is allowed to build up.

Because it is particles in the smaller size range, $\lesssim 2.5$ $\mu$m ($PM_{2.5}$), that are of greatest interest with respect to health effects, inlet systems are normally used that exclude larger particles. These size exclusion inlets are usually based on filters, cyclone collectors, or impactors, the principle behind which is discussed shortly. Inlet cutoff diameters from 2.2 to 15 $\mu$m are achieved in commercial instruments using these techniques (Chow, 1995).

Collection of particles is based on filtration, gravitational and centrifugal sedimentation, inertial impaction and impingement, diffusion, interception, or electrostatic or thermal precipitation (e.g., see Spurny, 1986, Chapter 3). The choice of method depends on a number of parameters such as the composition and size of the particles, the purpose of the sample, and acceptable sampling rates. Table 11.10 summarizes some of the commonly used methods and the size ranges over which they are effective.

#### *a. Filters*

Filters collect liquid and solid particles by mechanisms including diffusion, impaction, interception, electrostatic attraction, and sedimentation onto the filter while allowing the gas to pass through. The types commonly used in atmospheric particulate collection are membranes, fibrous mats, or porous sheets. Different filter materials are used depending on the particular type of measurement being carried out, including Teflon, quartz fiber, nylon, silver, cellulose filters, glass fibers, and polycarbonate. The characteristics of each are summarized by Chow (1995).

TABLE 11.10 Some Commonly Used Methods of Collecting Atmospheric Particles

| Method | Approximate range of diameters[a] ($\mu$m) |
|---|---|
| Filters | >0.03 |
| Sedimentation collectors | |
| Gravitational | ≥10 |
| Centrifugal | 0.1–10 |
| Impactors | |
| Atmospheric pressure | ≥0.5 |
| Low pressure | ≥0.05 |
| Precipitators | |
| Electrostatic | 0.05–5 |
| Thermal | 0.005–5 |

[a] The upper size ranges are usually related to inlet losses that prevent large particles from reaching the sampling surface.

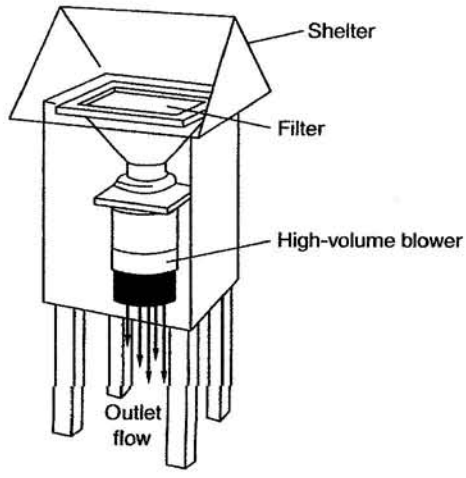


FIGURE 11.56 Schematic of Hi-Vol particulate sampler (adapted from Lawrence Berkeley Laboratory, 1979).

Different filters have unique characteristics, which include the collection efficiency as a function of particle size, the pressure drop at a given flow velocity, and types of reactions that occur on the filter surfaces. Perhaps somewhat surprisingly, sieving action is not the only filtration mechanism. The major filtering action is due to forces that bring the particles into contact with the filter surface where they may stick; these include impaction, interception, diffusion, sedimentation, and electrostatic attraction. At larger particle diameters and high flows, impaction is efficient, whereas at smaller diameters and flows, collection by diffusion to the surface is important; this increased efficiency at large and small diameters results in a minimum at $\sim 0.3\ \mu$m in the curve of collection efficiency against particle diameter at the usual sampling rate per unit surface.

Fibrous mat type filters include the frequently used paper (cellulose) fiber filter, for example, the Whatman paper filter, and glass fiber filters. A common fibrous mat filter used for sample collection and air cleaning is known as the HEPA filter (*h*igh *e*fficiency *p*articulate *a*ir filter) and is made of a combination of cellulose and mineral fibers. A widely used type of fibrous mat filter is the *high-volume* filter, commonly referred to as *Hi-Vol*, shown in Fig. 11.56. A modification of the Hi-Vol filter to increase the total air flow allows the collection of sufficient particulate matter in relatively short time periods (e.g., 2 h) to carry out chemical analysis; this is important for studies of the diurnal variation of various chemical components of the aerosol as well as for minimizing sampling artifacts (Fitz *et al.*, 1983).

Porous materials and membranes used as filters have a number of small, often tortuous, pores. This type of filter includes sintered glass filters, organic membrane filters, and silver membrane filters. Two types of membrane filters are Nucleopore and Millipore filters, named after their principal manufacturers. Nucleopore filters are thin films with smooth surfaces and straight, uniform cylindrical pores made by irradiating a thin polycarbonate plastic sheet in contact with a uranium sheet with slow neutrons. The neutrons cause fission of $^{235}$U and the resulting fragments produce ionization tracks through the plastic; these tracks are then chemically etched to a desired and uniform size using a sodium hydroxide solution.

Millipore filters have twisted, interconnecting pores that are much more complex than those in Nucleopore filters. They are available in different materials such as Teflon, polycarbonate, quartz, silver, and cellulose acetate.

Membrane filters are particularly useful when surface analytical techniques, such as optical and electron microscopy and X-ray fluorescence analysis, are to be used subsequent to collection, because most of the particles remain on the surface of the filter.

Filter sampling is also accompanied by potential reactions of pollutant gases with the particles on the filter or with the filter medium (including binders that are used in some filters) during sampling and the absorption of water from humid air. In the first case, conversion of gaseous $SO_2$ and $HNO_3$ to particulate sulfate and nitrate, respectively, has been observed on some filters. Some filters, especially paper filters, are hygroscopic and thus tend to adsorb water vapor from humid air. Glass fiber filters are relatively (but not entirely) insensitive to humidity, which is a major reason they have been used in the Hi-Vol reference method. However, even here the particulate matter

collected on the filter may be hygroscopic and adsorb or desorb water. To minimize this problem, Hi-Vol filters are equilibrated at temperatures between 15 and 35°C and in air with a relative humidity $\leq 50\%$ for 24 h prior to weighing before and after sampling.

Other problems with collection using filters, such as interference of impurities contained in the filter itself with chemical analysis of the collected particles, are discussed by Chow (1995).

***b. Impactors***

Impactors are based on the principle that particles in an airstream will tend to continue in a straight line due to their inertia when the flow of air bends sharply; if a surface to which they can adhere is present, they will impact on it and may stick. In practice, a collection plate is placed in the flow of air, causing the gas flow to stream around the obstacle; particles, however, may strike the plate and stick. Obviously, the larger the particle, the greater its inertia and the greater the impaction on the plate.

The impaction efficiency ($\eta$) for particles depends directly on the particle diameter ($D$), the flow velocity of the air ($V$), and the particle density ($\rho$); it varies inversely with the gas viscosity ($\mu$) and with a parameter ($D_b$) that is representative of the impactor's physical dimensions (e.g., the inlet nozzle diameter) and that is related to the curvature of the airstream.

$$\eta = D^2 V \rho / 18 \mu D_b. \qquad \text{(R)}$$

Thus, the impaction efficiency should be greatest for larger, denser particles and higher flow velocities. The factors involved in particle impaction on surfaces are discussed in detail by John (1995).

There are two overall types of impactors in widespread use: cascade and virtual impactors.

*Cascade impactors.* Impactors have been used to obtain different size fractions of ambient particles in the range of diameters $\sim 0.5$–$30$ $\mu$m. The range can be extended down to 0.05 $\mu$m by operating some of the later stages at reduced pressures (Hering *et al.*, 1978, 1979). The cascade impactor, as its name implies, is a series of impactor plates connected in series or in parallel (Fig. 11.57). The diameters of the nozzles or slits above each impactor plate become increasingly smaller as the air moves through the impactor so that the air moves increasingly faster through these orifices and smaller and smaller particles impact on the plates [see Eq. (R)].

Impactors with various designs as well as different types of impaction surfaces are in use (e.g., see Chow, 1995). Examples include the Lundgren impactor, the Anderson sampler, the Mercer impactor, and the University of Washington Mark III impactor. An impactor that is in wide use is the MOUDI (*M*icro*o*rifice *U*niform *D*eposit *I*mpactor) (Marple *et al.*, 1991). This device collects particles down to 0.056 $\mu$m in aerodynamic diameter and, as the name implies, gives a uniform particle deposit on the plates. This uniform deposit helps in carrying out chemical analysis by such techniques as X-ray fluorescence. The uniformity in deposition is obtained by using multiple nozzles located at specific distances from the center of the impactor plates and rotating the plates beneath the nozzles.

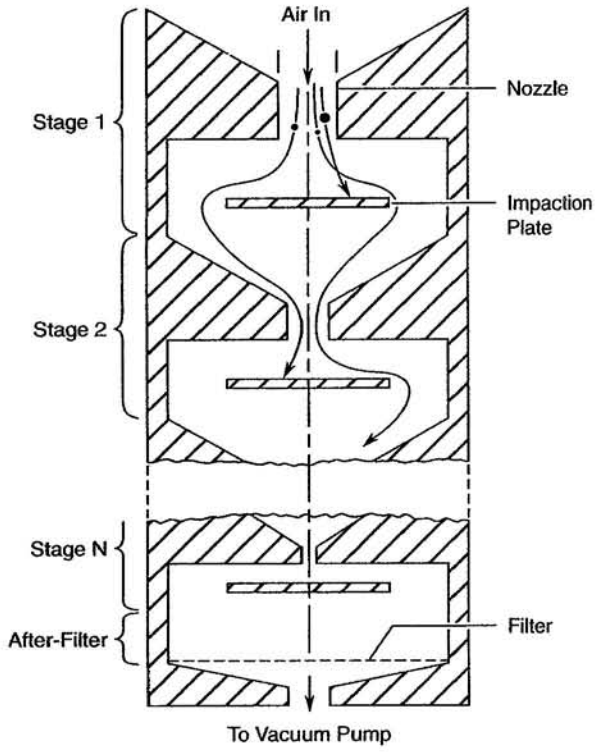


**FIGURE 11.57** Principle of operation of cascade impactor (adapted from Marple and Willeke, 1979).

Two problems with particle collection by impactors are bounce-off and reentrainment (John, 1995). Reentrainment is the resuspension of a previously collected particle from the surface into the gas flow due either to the motion of the air over the surface or to impact of an incoming particle. When a particle strikes a surface, if it does not stick, it can bounce off back into the gas steam, break into fragments, or cause a previously adsorbed particle to be knocked off into the gas stream; in all three cases the collection efficiency is lowered and the net effect is referred to as bounce-off. To minimize these problems, the surface of the impactor is often coated with a soft, energy-absorbing substance such as oil, water, grease, resin, or paraffin, which helps

to absorb the kinetic energy of the striking particle; a summary of the types of agents used to minimize bounce-off and reentrainment is given by Marple and Willeke (1979), Cahill (1979), and Turner and Hering (1987).

While the use of soft surfaces would seem to be mandated by the foregoing discussion of bounce-off problems, there are a number of disadvantages to coating the impactor surfaces with a substance such as grease. For example, it makes accurate mass determinations difficult and can introduce such a large background of certain chemicals that the chemical analysis of these elements in the particles becomes difficult. In addition, with such surfaces one cannot use chemical analytical techniques that only probe the upper surface layer because the coating surrounds some of the collected particles.

*Virtual impactors.* The virtual impactor is a modified type of impactor, an example of which is shown in Fig. 11.58; one commonly used type of virtual impactor is known as the dichotomous sampler. The basis of virtual impactors is that the airstream impacts against a mass of relatively still air rather than against a plate. The inertia of the particles carries them into the still air mass, which is slowly withdrawn through a filter to collect the particles. This type of impactor avoids the problem of particle reentrainment from the impaction surface caused by air motion over the collected particles or by dislodging due to collisions of incoming particles with the impactor surface. It also avoids the problem of bounce-off or of using greases that may interfere with subsequent chemical analysis.

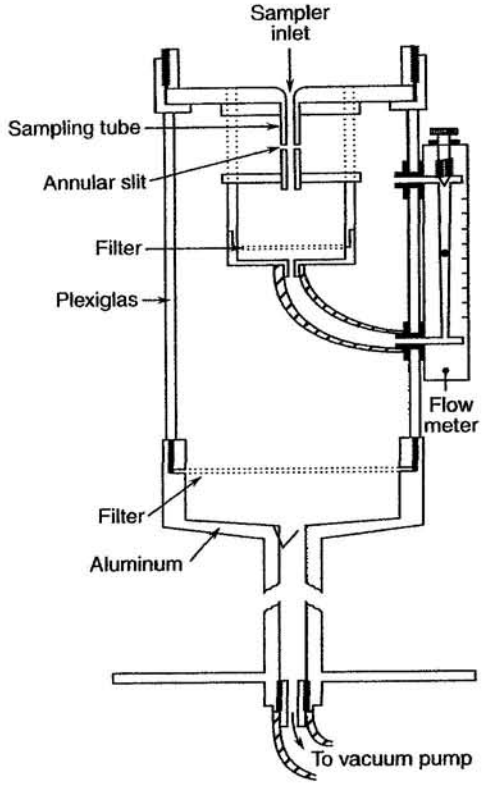


FIGURE 11.58 Schematic diagram of a virtual impactor (adapted from Conner, 1966).

### *c. Electrostatic Precipitators*

Electrostatic precipitators operate on the principle of the attraction of a charged particle for an oppositely charged collector. They have been used for both collecting particles for further analysis and for controlling particulate emissions from sources. In one common design, the particles in air can be charged if introduced into a cylindrical chamber containing a wire down the axis of the cylinder that is at a high negative voltage (e.g., 5–50 kV) relative to the walls of the chamber. A corona discharge is set up around the wire and this produces ions; the negatively charged ions are attracted to the positively charged outer walls. These ions collide with the particles in the air, charging them and causing them to move to the outer walls to be captured there. In place of the corona discharge, ions may also be generated using radioactive bombardment of the particles.

While electrostatic precipitators have relatively high collection efficiencies (99–100%) over a wide range of particle sizes ($\sim$0.05–5 $\mu$m), there are a number of disadvantages. These include the lack of size information, particle reentrainment due to sparking, and practical problems such as high cost and shock hazards. As a result, they have not been widely used in ambient air studies.

An example of a study in which this approach was applied involved the use of a transmission electron microscopy (TEM) grid as the collector plate in the electrostatic precipitator (Witkowski *et al.*, 1988). After sample collection, analysis by TEM (vide infra) could then be carried out.

A related area is that of single-particle levitation, which has been used in a number of studies to isolate a single particle and study its properties (e.g., see papers by Tang and co-workers in Chapter 9). A review of this area is given by Davis (1997).

### *d. Sedimentation Collectors*

These collectors are used primarily for large particles ($\gtrsim$2.5 $\mu$m), that is, those in the coarse particle range. They include collection by gravitational sedimentation (e.g., dustfall jars) as well as by centrifugal

sedimentation, which allows collection in the submicrometer range (e.g., centrifuges and cyclone collectors).

Gravitational sedimentation only collects the large particles that settle out of the atmosphere fairly quickly. This *dustfall* generally consists of particles that are relatively large and, as such, are not particularly relevant to the focus of this book. Thus dustfall collectors will not be discussed further.

The principle of centrifugal collection is, of course, well known. Collection of particles using centrifugation involves passing the aerosol at a controlled rate through a rapidly spinning air mass. Collection of particles in ranges as small as ~0.1–1 $\mu$m has been reported using this technique. The cyclone collector, a modification of the centrifuge technique, is based on bringing the air samples into a stationary cylindrical vessel at high velocity; a vortex is formed by the entry of the air tangential to the length of the vessel and particles in this vortex are subjected to a centrifugal force that depends on their size (Fig. 11.59). As a result, particles of different sizes are deposited at different locations along the length of the cyclone separator. Although cyclone collectors have been applied to size distribution measurements by using a series of cyclones in parallel, each having a different cut size, they are most commonly used as precollectors to remove larger particles (~3- to 30-$\mu$m diameter) before the air sample enters a device such as an impactor designed for the measurement of particles in smaller size ranges.

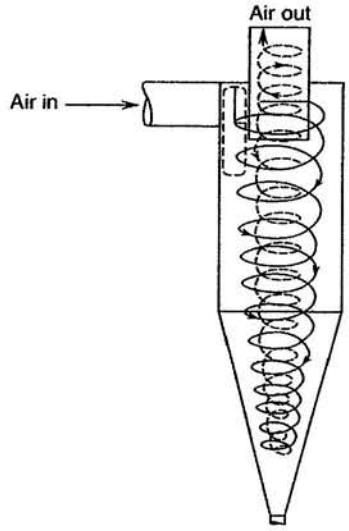


FIGURE 11.59 Schematic diagram of one type of cyclone collector (adapted from Ayer and Hochstrasser, 1979).

## 2. Measurement of Physical Characteristics: Mass and Size

### *a. Mass*

The total mass of particles per unit volume of air is one of the major parameters used to characterize particles in air and, along with size, is the basis of air quality standards for particulate matter (see Chapter 2). Methods of mass measurement include gravimetric methods, $\beta$-ray attenuation, piezoelectric devices, and the oscillating microbalance.

***(1) Gravimetric methods*** The most straightforward method of determining the particle loading of the atmosphere is to weigh a collection substrate such as a filter before and after sampling. However, care must be taken to be sure that both temperature and relative humidity are carefully controlled when weighing both the loaded and clean substrate. As discussed earlier, some filters and/or the collected particles are hygroscopic and unless care is taken to equilibrate them at a fixed temperature and relative humidity, the change in water content may completely mask the change in mass due to the particles. In addition, problems such as forces due to static electricity on the filter that interfere with accurate weight measurements must be controlled. Finally, particulate loading can change the sampling air flow rate and lead to large errors in determining the actual volume of air sampled.

***(2) $\beta$-Ray attenuation*** $\beta$-Particle beams (electrons) emitted from a radioactive source are attenuated when they pass through a filter on which particulate matter has been collected. ($\beta$-particle beams rather than $\alpha$-particle beams or $\gamma$-rays are used because $\alpha$ particles do not penetrate typical thicknesses of filter well and $\gamma$-rays are too penetrating and hence would require large sample thicknesses.) Figure 11.60 shows a

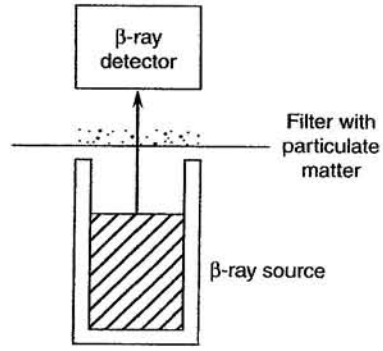


FIGURE 11.60 Schematic diagram of a typical $\beta$-ray attenuation device for measuring particulate mass.

schematic of a $\beta$-ray attenuation device, which consists essentially of a $\beta$ source such as $^{14}C$, a $\beta$ detector, and a means of positioning the filter paper containing the particulate matter between the two. The ratio of the transmission of $\beta$-rays through a clean and loaded portion of the filter, respectively, is related to the particle loading via a Beer–Lambert type of relationship:

$$I/I_0 = e^{-\mu X}. \qquad \text{(S)}$$

$I_0$ and $I$ are the intensities of the $\beta$-rays that have passed through the clean and loaded portions of the filter, respectively, $X$ is the thickness of the deposit, and $\mu$ is an attenuation constant that is approximately proportional to the density ($\rho$) of the material deposited. The mass per unit area deposited on the filter, given by $\rho X$, is the parameter desired in this measurement. Rearranging Eq. (S), one obtains

$$\ln(I_0/I) = (\mu/\rho)\rho X. \qquad \text{(T)}$$

The parameter $\mu/\rho$ is a constant known as the *mass absorption coefficient*; with the assumption that this is independent of the type of absorbing particles (an assumption that generally holds well enough to cause $\lesssim 10\%$ uncertainty), the value of $\ln(I_0/I)$ is directly related to the parameter of interest, $\rho X$ = mass per unit area.

Such measurements can be carried out on filters with different cutoff sizes to obtain size resolution as well (e.g., see Spagnolo and Paoletti, 1994).

***(3) Piezoelectric microbalance*** The piezoelectric microbalance is a resonant frequency device. The piezoelectric effect is the development of a charge on some crystals such as quartz when a stress is applied; the stress may be mechanical (e.g., added weight) or electrical. Such crystals may be used as part of a resonance circuit to provide very stable, narrow-band frequencies; the quartz crystal is plated on two sides with a thin conducting layer and leads are connected to the resonance circuit so the crystal replaces an $LC$ network. The obtained frequency of vibration ($v_0$) depends on a number of parameters of the crystal but is usually ~5–10 MHz. However, if a mass ($\Delta m$) becomes attached to one side of the crystal, it changes the resonant frequency by an amount $\Delta v_0$ such that

$$\Delta v_0/v_0 = \Delta m/m \qquad \text{(U)}$$

as long as the increase in mass $\Delta m$ is much smaller than the mass ($m$) of the active part of the crystal.

Particulate matter from ambient air can be deposited on the crystal in various ways, for example, by using it as an impaction device. The mass of the collected particles can then be determined by following the change in the frequency. Alternatively, a reference crystal held at the same temperature and pressure as the crystal on which the particles are collected can be used, and the difference in frequencies between the two crystals can be determined.

The piezoelectric microbalance is very sensitive, capable of detecting $\sim 10^{-8}$–$10^{-9}$ g. The particles collected on the crystal surface can be chemically analyzed after collection using surface-sensitive techniques. One limitation is possible overloading of the crystal; thus when the collected mass reaches ~0.5–1% of the mass per unit of the crystal, the surface must be cleaned.

***(4) Oscillating microbalance*** The tapered-element oscillating microbalance is based on a similar principle to the piezoelectric microbalance. A hollow glass piece is mounted with the wider end fixed and a filter attached to the narrower end. The tip oscillates at a particular frequency in an applied magnetic field. As particles are collected on the filter, the resonant frequency of the glass tends to decrease. A feedback is used to maintain the oscillation frequency and provides a measurement of the collected mass (e.g., see Patashnick and Rupprecht, 1991). Good agreement has generally been observed between measurements made using the tapered-element oscillating microbalance and Hi-Vol filter methods (e.g., Eldering and Glasgow, 1998).

### *b. Size*

There are several different approaches that are commonly used to determine particle size distributions in air. One of them, impaction, has been discussed earlier. Multistage impactors with different cut points are used extensively to obtain both mass and chemical composition data as a function of size for particles with diameters $\gtrsim 0.2$ $\mu$m. Others, including methods based on optical properties, electrical or aerodynamic mobility, and diffusion speeds, are described briefly in the following section. The condensation particle counter (CPC) is used as a detector in combination with some of these size-sorting methods.

The reader is cautioned to keep in mind that atmospheric particles are not all spherical nor even necessarily simple in shape. Thus, as discussed in Chapter 9.A, the term *size* cannot be uniquely defined for atmospheric particles. As a result, a measurement of the distribution of sizes using an impactor that is based on inertial characteristics, for example, may not give the same results as a size measurement based on optical techniques that use light scattering. With this caveat in mind, let us examine the most commonly used

methods of determining the size distribution of atmospheric particles.

***(1) Optical methods*** Optical counters, optical microscopy, and electron microscopy fall under this heading. A review of optical methods is given by Baron *et al.* (1993).

*Single-particle optical counters.* These instruments are used to measure particles in the ~0.1- to 10-$\mu$m range by measuring the amount of light scattered by a single particle (Martens and Keller, 1968). As discussed in Chapter 9.A.4, the amount of this Mie scattering depends not only on the refractive index but also on the radius of the particle; hence the intensity of scattered light is a measure of the particle size. Assuming that the particles are spherical, smooth, and of known refractive index, one can calculate, using Mie theory, the intensity of scattered light of wavelength $\lambda$ at various angles ($\theta$) to the incident beam for a particle of a given size. Integrating over all scattering angles and wavelengths (since "white" incandescent sources are normally used in these instruments), one obtains the theoretical response of the single-particle counter, that is, the curve of scattered light intensity as a function of the particle diameter. Typical theoretical response curves are shown in Fig. 11.61 (Cooke and Kerker, 1975).

Calibration of these single-particle counters is usually carried out using monodisperse polystyrene latex or polyvinyl latex spheres, which are available in sizes from ~0.1 to 3 $\mu$m and have a refractive index of 1.6; alternatively, aerosols with lower refractive indices may be generated from liquids such as dioctyl phthalate ($m$ = 1.49). Whitby and Willeke (1979) discuss the importance of instrument calibration using standardized aerosols with an index of refraction as close as possible to the sample being measured; since the refractive index of atmospheric particles varies from 1.33 for water to 1.7 for minerals, they recommend using a calibration aerosol with $m \cong 1.5$. Because light scattering is very dependent on the particle shape, when measuring irregularly shaped particles such as coal dust, one should calibrate the instrument with aerosols generated from the same material. Figure 11.62, for example, shows the instrument response as a function of particle diameter for an ideal calibration aerosol of dioctyl phthalate and for coal dust particles.

Potential problems with using single-particle counters in ambient measurements and ways to minimize these are discussed in detail by Whitby and Willeke (1979).

Optical counters allow relatively rapid measurements of the size distribution and, unlike some of the other methods of size fractionation, include volatile particles in the measurement. However, some care must be taken in interpreting the detailed shape of the size distribution spectrum because of some anomalies that have been observed; for example, around the 1-$\mu$m region, interference from light that is reflected or refracted from the front and back of the particle gives a "knee" in many calibration curves of number of particles versus their diameter (LBL, 1979).

*Electron and optical microscopies.* Counting the particles and measuring their sizes can be done by optical or electron microscopy, the former for particles with diameters from ~0.4 $\mu$m to several hundred microns,

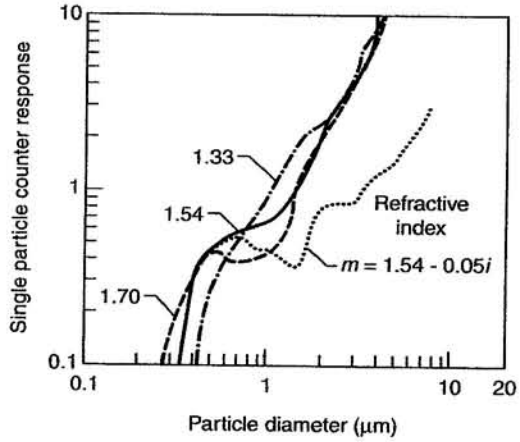


FIGURE 11.61 Theoretical response of a typical single-particle counter (adapted from Whitby and Willeke, 1979; data from Cooke and Kerker, 1975).

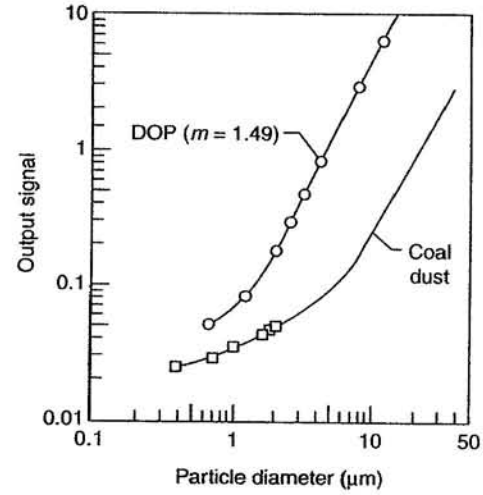


FIGURE 11.62 Experimental calibration curves for a commercial single-particle counter and two types of calibration aerosols: dioctyl phthalate (DOP) and coal dust (adapted from Whitby and Willeke, 1979).

and the latter for particles from ~0.001 $\mu$m and larger. The particles must be on the surface of the substrate and form less than a monolayer to minimize overlap of the particles. For electron microscopy, the sample and substrate must also be able to be subjected to high vacuum, heat, and electron bombardment without degradation over a period of time sufficient to make the measurement.

Because of the instrumental requirements, these are usually not routine monitoring techniques. However, unlike other methods, they give detailed information on particle shapes. In addition, chemical composition information can be obtained using transmission electron microscopy (TEM) or scanning electron microscopy (SEM) combined with energy-dispersive spectrometry (EDS). The electron beam causes the sample to emit fluorescent X-rays that have energies characteristic of the elements in the sample. Thus a map showing the distribution of elements in the sample can be produced as the electron beam scans the sample.

For example, Fig. 11.63 shows the TEM image of an NaCl crystal (Fig. 11.63A) and of the same crystal after exposure to gaseous $HNO_3$ (Fig. 11.63B) and then small amounts of water vapor (Fig. 11.63C) (Allen *et al.*, 1996). After the crystal is dried, the formation of new microcrystallites attached to the NaCl is observed. These can be shown using EDS to be crystals of $NaNO_3$. Thus Fig. 11.64b shows the EDS spectra obtained from the larger, original NaCl crystal (but after exposure to $HNO_3$ and water vapor) and of small microcrystallites attached to it (Fig. 11.64a). Only Na and Cl are seen in the first case, but Na, N, and O in the second, and in the correct ratio for $NaNO_3$. The $HNO_3$ has reacted with the NaCl surface to generate metastable surface nitrate ions. Exposure to water vapor generates a mobile quasi-liquid layer on the surface that contains $Na^+$, $Cl^-$, and $NO_3^-$ ions. On drying, the ions segregate to form separate microcrystallites of $NaNO_3$ and a fresh NaCl crystal (Allen *et al.*, 1996).

The combination of SEM with EDS has also been applied to atmospheric particles (e.g., Pósfai *et al.*, 1995; Anderson *et al.*, 1996; McMurry *et al.*, 1996; Ganor *et al.*, 1998). For example, individual sea salt particles were analyzed using TEM combined with EDS as well as selected-area electron diffraction (SAED) by Pósfai *et al.* (1995) and Anderson *et al.* (1996). The crystal shapes correlated well with the chemical composition determined using EDS and SAED. For example, cubic crystals of NaCl were observed. Sulfate occurred in either rod-shaped crystals, which had significant concentrations of (Mg + K + Ca) compared to Na, or tubular crystals, with much smaller concentrations of these three metals. In the latter case, the EDS showed

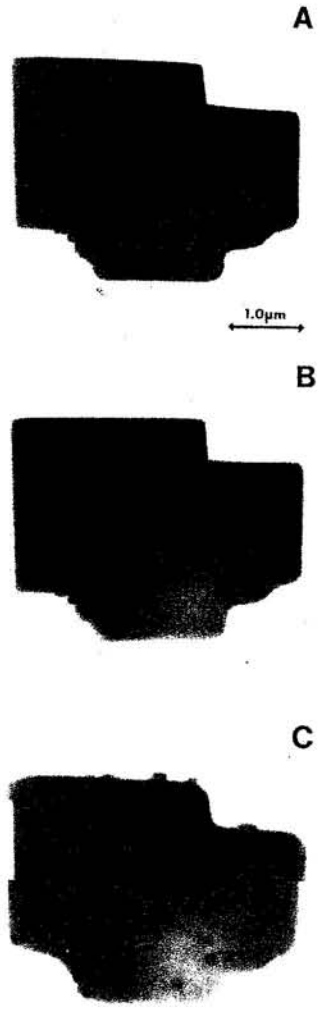


**FIGURE 11.63** TEM images of an NaCl crystal (A) before reaction and (B) after reaction with gaseous $HNO_3$ ($1.2 \times 10^{15}$ $cm^{-3}$ for 15 min) and then (C) exposure to water vapor (<15 Torr) followed by drying (adapted from Allen *et al.*, 1996).

spectra with large contributions from Na, O, and S, and the SAED patterns were similar to that of $Na_2SO_4$.

It should be noted that as with all analytical techniques that involve subjecting the sample to vacuum conditions before and/or during the analysis, separation of components via selective crystallization is expected (e.g., Ge *et al.*, 1998a). Hence these particles may not have actually existed in these crystalline forms at relative humidities above their deliquescence points in the atmosphere, although the various constituents observed were clearly present.

***(2) Atomic force microscopy (AFM) and scanning tunneling microscopy (STM)*** These methodologies for probing the morphological details of a surface down to

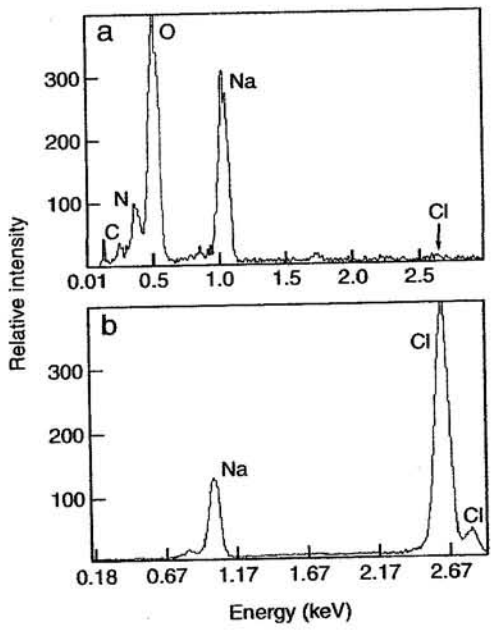


FIGURE 11.64 Energy-dispersive spectroscopy light-element spectra acquired from (a) one of the small microcrystallites attached to NaCl after exposure to gaseous $HNO_3$ (see Fig. 11.63C) and (b) an adjacent area of the NaCl crystal (adapted from Allen *et al.*, 1996).

the atomic scale have been used extensively in many laboratory studies to map atomic and molecular structures. In STM, which is used with electrically conducting materials, a probe with a very fine metal tip scans over the surface of the sample, which is held at a potential relative to the tip. When the tip is very close to the surface, there is a tunneling current between the tip and the sample, whose magnitude depends exponentially on the distance between the tip and the sample. The tip is kept at a constant distance from the sample using a feedback circuit to measure and maintain the tunneling current at a constant value. The tip thus moves up and down with the surface topography. For insulating surfaces, AFM accomplishes similar topographical mapping. In this case, the force acting between the surface and a fine tip attached to a cantilever is kept constant and the deflections of the cantilever required to do this are monitored, for example using optical means.

AFM has been used in only a few studies to explore the sizes and morphology of airborne particles (e.g., Friedbacher *et al.*, 1995; Pósfai *et al.*, 1998). In this case, atomic scale resolution is not used, but rather much lower resolution that provides information on particle sizes and shapes in the micron and submicron size range under ambient conditions. This has the advantage that effects due to the application of vacuum to the particles do not occur, as is the case for TEM (vide supra). AFM combined with TEM has been applied by Pósfai *et al.* (1998), for example, to explore the loss of water from particles upon exposure to vacuum conditions.

***(3) Electrical mobility analyzers*** Several types of instruments for measuring particle sizes in the atmosphere depend on the mobility of charged particles in an electric field (e.g., see Yeh (1993) and Flagan (1998) for a review and history of the development of this field). The electrical mobility analyzer developed by Whitby and co-workers at the University of Minnesota, in particular, has been used extensively to measure particles in the range $\sim$0.003 to $\sim$1 $\mu$m (Whitby and Clark, 1966; Eisele and McMurry, 1997).

Figure 11.65a illustrates the principles of the electrical aerosol analyzer. The essential components are the aerosol charger, the mobility analyzer, and the detector (shown in Fig. 11.65a as the current-collecting filter). The air containing the particulate matter is first introduced into the aerosol charger, where a corona discharge generates positive ions for particle charging. The positively charged particles are introduced as a thin layer around the outside of the tubular mobility analyzer. Clean air flows down the central portion of the tube between the layer of ambient aerosol at the walls and the charged collection rod in the center of the tube. A negative voltage is applied to the collection rod, causing the positively charged particles to move from the outer wall through the clean air to the collection rod.

The particles with the highest mobilities reach the collection rod first and are removed from the gas stream; those that do not reach the rod before the flow passes out of the region of the electric field pass through to a detector and are measured. Increasing the voltage on the collection rod increases the number of charged particles that reach it before passing out of the field and hence decreases the number reaching the detector. The relationship of the particle count at the detector to the voltage in the analyzer is thus dependent on the particle mobility in the analyzer, which depends on particle size. Thus size distributions can be obtained by studying the detector output as a function of collection rod voltage. The detector may be a current-sensing device, as in Fig. 11.65a, or other type such as a condensation nuclei counter (vide infra).

Details of the calibration, use, performance, and artifactual problems are given in a proceedings entitled *Aerosol Measurement* (Lundgren *et al.*, 1979); this also shows data for the mobility distribution for monodisperse aerosols.

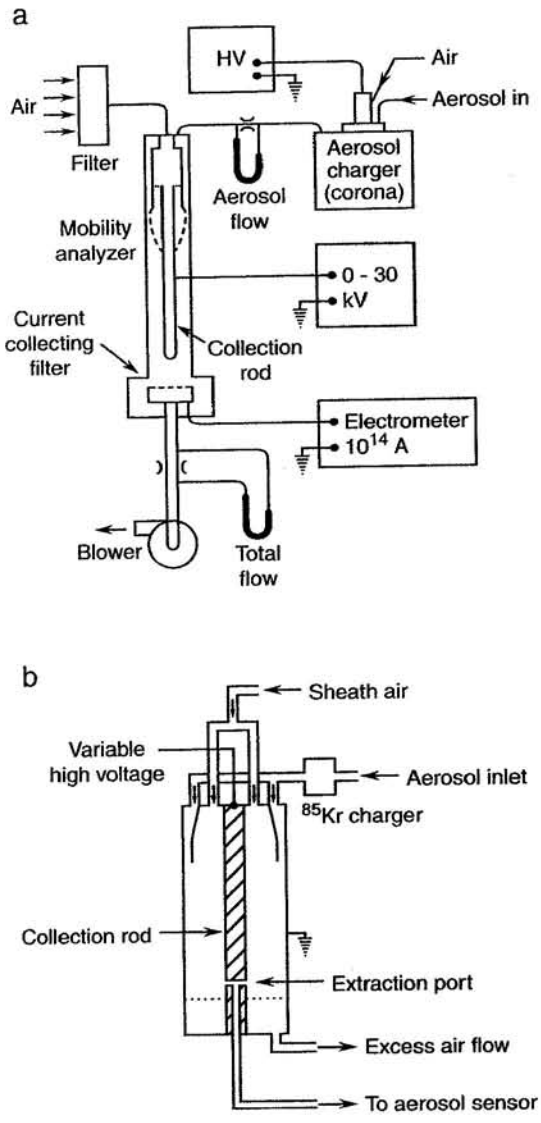


FIGURE 11.65 (a) Electrical aerosol analyzer (adapted from Whitby and Clark, 1966). (b) Schematic diagram of differential mobility analyzer (adapted from Yeh, 1993).

A widely used form of the electrical mobility analyzer now in use is called a differential mobility analyzer (DMA), which operates on the same principle. Figure 11.65b is a schematic diagram of a DMA. Charging is carried out using a radioactive source such as $^{85}$Kr, $^{90}$Sr, $^{210}$Po, or $^{241}$Am to produce ions of both signs that become attached to the particles. In this case, an extraction port is located in the center rod. Smaller particles of opposite electrical charge to the center rod and having higher electrical mobilities strike the central rod before this port and are removed; larger particles are carried beyond the extraction port and out with the major flow. Only a narrow range of particles will strike the extraction port, providing a narrow range of particle sizes at the aerosol outlet. This monodisperse aerosol exiting the mobility analyzer is then directed to a measuring device such as a condensation particle counter (CPC; see later) or a Faraday cup electrometer (e.g., Winklmayr *et al.*, 1991). A modified version that extends the range down to 1 nm, approaching molecular ions, has also been developed (Rosell-Llompart *et al.*, 1996).

Results of particle size distributions in air using different methods tend to be in reasonably good agreement when the different sampling times are taken into account. For example, Hoff *et al.* (1996) made particle size measurements in a rural area in Ontario, Canada, using a DMA, an eight-stage impactor and light scattering instruments. The number size distributions obtained using each technique were in excellent agreement, assuming for the impactor samples that the composition of the particles had a density of 2 g cm$^{-3}$.

***(4) Diffusion separators*** As discussed in Chapter 9.A.3, small particles with diameters $\lesssim 0.05$ $\mu$m undergo diffusion via Brownian motion sufficiently rapidly that this can be used to separate particles. Thus the aerosol can be passed through a tube in which the smaller particles diffuse more rapidly to the walls and are removed there, leaving the larger, more slowly diffusing particles to pass through. Variation of residence time in the tubes by varying the flow rates and tube lengths leads to different size cutoffs (but not high resolution). Hence size fractionation of small particles can be achieved using such diffusion separators. The particles exiting the tube can be measured using techniques such as the CPC. The design and testing of a typical diffusion battery-CPC apparatus are described by Raes and Reineking (1985).

***(5) Aerodynamic particle size*** This technique is based on measuring the velocity lag of particles in accelerating air flows (Wilson and Liu, 1980; Baron *et al.*, 1993). A laser beam is split into two coherent beams using a beam splitter, and these two beams are then focused onto a point, forming an interference pattern. When a particle passes through this interference pattern, it scatters light, with the scattered light intensity oscillating as the particle passes through the interference fringes. The frequency of the oscillation of the scattered light multiplied by the spacing of the fringes gives the velocity of the particle perpendicular to the fringes. From the particle velocity, the size can be obtained.

***(6) Condensation particle counter (CPC)*** Very small particles in the Aitken range act as condensation nuclei for the formation of larger particles in a supersaturated

vapor. If these very small particles are injected into air that is supersaturated with water or another vapor such as an alcohol, the vapor condenses on them to form droplets. In the condensation particle counter (CPC), supersaturation of the air containing these particles is achieved by passing them through a higher temperature region saturated with the vapor and then into a lower temperature region in which the alcohol vapor condenses on the nuclei to form larger droplets. These can be counted as is done in absolute nuclei counters, for example, by measuring the pulses of scattered light by a single droplet as it passes through the viewing volume. Alternatively, the particles can be measured using techniques such as total light extinction or scattering. In this case (sometimes called photoelectric nuclei counters), calibration against some other reference is required. CPCs are applicable in the size range from $\sim 3$ to 1000 nm. Note that a 10-nm particle contains $\sim 10^4$ molecules, whereas a 2.7-nm particle contains only $\sim 10^2$ molecules (Eisele and McMurry, 1997). Hence these very small ultrafine particles are approaching molecular clusters.

Measurement of ultrafine particles, those $\lesssim 10$ nm in diameter, has become of increasing interest due to their importance in acting as cloud condensation nuclei (see Chapter 14) and in elucidating rates and mechanisms of homogeneous nucleation. Methods based on the foregoing principles have been developed and applied for these very small particles (e.g., see Stolzenburg and McMurry, 1991; McDermott *et al.*, 1991; Wiedensohler *et al.*, 1993, 1994; Saros *et al.*, 1996; Marti *et al.*, 1996; and Weber *et al.*, 1998). For example, CPCs have been used in conjunction with pulse height analysis to measure particles with diameters in the 3- to 15-nm range. Higher supersaturations of the alcohol vapor are required to grow the smaller particles into the light-scattering range, and hence these particles travel further in the measuring system before activation occurs. As a result, for particles less than 15 nm, the final size of the light-scattering particles formed from smaller particles is smaller as well, whereas above 15 nm, the final particle size is relatively independent of the initial particle size (Saros *et al.*, 1996). For particles in this smaller size range, the height of the detector pulses produced by the scattered light decreases with particle size. Thus, for ultrafine particles, pulse height analysis provides a means of determining particle size (e.g., Stolzenburg and McMurry, 1991; Saros *et al.*, 1996; Marti *et al.*, 1996; Weber *et al.*, 1998).

*(7) **Summary*** In summary, no one technique is capable of measuring the size distribution of atmospheric aerosols from the smallest to the largest diameters of interest, a range covering approximately five orders of magnitude. However, a combination of methods can be used to provide information over this range. Figure 11.66 summarizes the size ranges covered by the various techniques.

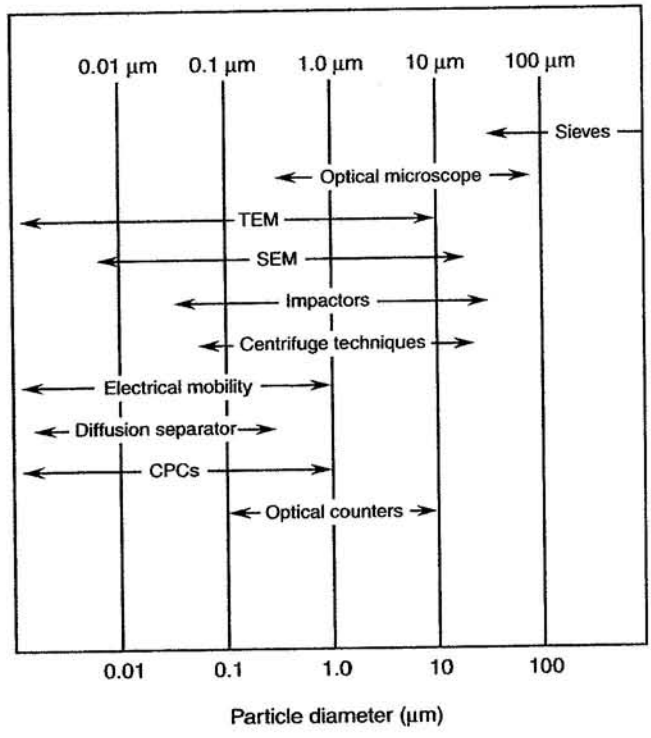


FIGURE 11.66 Summary of size ranges covered by various analytical techniques for atmospheric aerosols. TEM, transmission electron microscopy; SEM, scanning electron microscope (adapted from Hinds, 1982).

### *c. Typical Particle Concentrations in the Atmosphere*

Given the complexity of particle size distributions in the atmosphere (see Chapter 9.A), as well as the large number of chemical components (Chapter 9.C) that are not distributed equally throughout the various sizes, characterizing a "typical" collection of particles in the atmosphere is not possible. However, some indication of particle levels in the atmosphere is provided by mass measurements of $PM_{10}$ (i.e., total mass less than 10 $\mu$m in diameter), for which extensive measurements have been made for regulatory purposes.

Concentrations of $PM_{10}$ in urban areas around the world as high as $\sim 300$ $\mu g\ m^{-3}$ have been reported (e.g., Reponen *et al.*, 1996; Kasparian *et al.*, 1998; Morawaska *et al.*, 1998; Lam *et al.*, 1999). In extreme situations such as the fires in Indonesia, 24-h average concentrations of $PM_{10}$ as high as $\sim 900$ $\mu g\ m^{-3}$ were

measured (Brauer and Hisham-Hashim, 1998). More typical mass concentrations in cities are ~20–100 $\mu g\ m^{-3}$ (e.g., Berico *et al.*, 1997; Brook *et al.*, 1997; Harrison *et al.*, 1999). In suburban-rural areas, peak concentrations are about an order of magnitude lower (e.g., Reponen *et al.*, 1996; Eldering and Glasgow, 1998). For example, studies of $PM_{10}$ at 28 sites in 10 countries in Europe reported median concentrations in rural Scandinavia of 11 $\mu g\ m^{-3}$ (Hoek *et al.*, 1997).

With the new regulations on $PM_{2.5}$, there are also increasing data on this smaller particle fraction as well. In rural areas, maximum 24-h average concentrations typically range from ~1 to 50 $\mu g\ m^{-3}$ (e.g., Hoff *et al.*, 1996; Sweet and Gatz, 1998). Because a significant fraction of the smaller particles is formed by reactions in air rather than by direct emissions, and as we have seen such reactions occur during transport, differences in concentrations between rural and urban areas may not be extremely large (Sweet and Gatz, 1998).

Thus, typical concentrations of $PM_{2.5}$ in urban areas are ~50–80 $\mu g\ m^{-3}$ (Sweet and Gatz, 1998). For example, Lam *et al.* (1999) report median $PM_{2.5}$ levels of ~70–150 $\mu g\ m^{-3}$ in Hong Kong, and levels up to ~200 $\mu g\ m^{-3}$ have been observed in Mexico City (Vega *et al.*, 1997). 1-h average concentrations of $PM_3$ measured in Pocatello, Idaho, during January 1996 were from 0 to about 45 $\mu g\ m^{-3}$ (Eldering and Glasgow, 1998). The mean concentration of $PM_{2.5}$ in 19 locations in Canada was reported to be 13.9 $\mu g\ m^{-3}$, with a standard deviation of 9.5 $\mu g\ m^{-3}$ (Brook *et al.*, 1997); in these studies, the ratio of $PM_{2.5}$ to $PM_{10}$ was quite variable, ranging from 0.36 to 0.65, with ratios similar to the high end of this range reported for Birmingham, U.K., by Harrison *et al.* (1999).

Concentrations in remote areas are, of course, generally much smaller, as indicated by the much higher visual range in these areas (see Chapter 9).

## 3. Measurement of Chemical Composition

As discussed in Chapter 9.C, ambient particulate matter contains inorganic elements and ions, including trace metals, as well as graphitic (elemental) carbon and a wide variety of organic compounds and water. Techniques in common use to measure these species are discussed very briefly here. For further details of the principles behind these techniques, the reader should consult instrumental analysis texts (e.g., Skoog *et al.*, 1998). Specific applications of various methods to particles in the atmosphere are described in the book edited by Spurny (1986) as well as the references at the end of this chapter.

### *a. Inorganic Elements*

Table 11.11 summarizes the major methods used to measure the inorganic elements in atmospheric particulate matter.

*Colorimetry.* Colorimetric methods, that is, wet chemical methods in which reagents are added to generate a light-absorbing species whose absorbance can

TABLE 11.11 Some Common Methods Used to Measure Inorganic Elements in Atmospheric Particles

| Element | Analytical methods |
|---|---|
| Aluminum | XRF,[a] PIXE,[b] AA,[d] NA,[e] ICP[j] |
| Antimony | Col,[c] AA, XRF, NA, ASV,[f] ICP |
| Arsenic | Col, AA, XRF, NA, ASV, MS,[g] PIXE, ICP |
| Beryllium | Col, AA, ES,[h] ICP |
| Bismuth | AA, ASV, ICP |
| Bromine | XRF, NA, MS, PIXE |
| Cadmium | Col, AA, XRF, NA, ASV, MS, ES, ICP |
| Calcium | XRF, PIXE, NA, AA, ICP |
| Chlorine | XRF, NA, MS, PIXE |
| Chromium | AA, XRF, NA, MS, ES, PIXE, ICP |
| Cobalt | AA, NA, XRF, ICP, ES |
| Copper | AA, XRF, NA, ASV, MS, ES, PIXE, ICP |
| Gallium | XRF, NA, AA, PIXE, ICP |
| Iodine | NA, MS |
| Iron | Col, AA, XRF, NA, PIXE, ASV, MS, ES, ICP |
| Lead | Col, AA, XRF, ESCA,[i] ASV, MS, ES, PIXE, ICP |
| Magnesium | NA, PIXE, AA, ICP |
| Manganese | Col, AA, XRF, NA, MS, ES, PIXE, ICP |
| Mercury | Col, AA, XRF, NA, ES, ICP |
| Molybdenum | Col, AA, ES, MS, XRF, PIXE, ICP |
| Nickel | AA, XRF, NA, MS, ES, PIXE, ICP |
| Nitrogen | ESCA |
| Potassium | XRF, PIXE, NA, AA |
| Rubidium | XRF, NA, PIXE |
| Selenium | Col, AA, NA, ASV, ES, XRF, PIXE, MS, ICP |
| Silicon | XRF, PIXE, AA, ICP |
| Sodium | NA, AA, PIXE, ICP |
| Strontium | XRF, NA, PIXE, AA, ICP |
| Sulfur | NA, XRF, ESCA, MS, PIXE, ICP |
| Tin | AA, XRF, MS, ES, ICP |
| Titanium | AA, XRF, NA, ES, PIXE, ICP |
| Vanadium | AA, XRF, NA, MS, ES, PIXE, ICP |
| Zinc | AA, XRF, NA, ASV, MS, ES, PIXE, ICP |

*Source:* Adapted from LBL (1979) and Chow (1995).

[a] XRF = X-ray fluorescence analysis.

[b] PIXE = particle-induced X-ray emission.

[c] Col = colorimetry.

[d] AA = atomic absorption spectrometry.

[e] NA = neutron activation analysis.

[f] ASV = anodic stripping voltammetry.

[g] MS = mass spectrometry.

[h] ES = emission spectrometry.

[i] ESCA = electron spectroscopy for chemical analysis; also known as XPS = X-ray photoelectron spectroscopy.

[j] ICP = inductively coupled plasma spectroscopy.

be quantified using conventional absorption spectroscopy, have been used rather extensively in the past. An example is the measurement of $Cl^-$ in aerosols from remote regions by the mercury thiocyanate method (Huebert and Lazrus, 1980). In this technique, chloride ions react with $Hg(SCN)_2$ in a dioxane–ethanol solution to form $HgCl_2$, $HgCl_4^{2-}$, and $SCN^-$. Upon addition of $Fe^{3+}$ in a nitric acid solution, an orange solution due to $FeSCN^{2+}$ results, whose absorbance can be measured at its 460-nm peak (Iwaski *et al.*, 1956).

While colorimetric methods have the advantages of being relatively inexpensive, simple to carry out, and applicable to a large number of elements, they are increasingly being replaced by other physical techniques. The major reason for this is that, as discussed earlier in this chapter, wet chemical methods are more likely to suffer from unrecognized interferences, particularly in complex environmental samples. However, when the aerosol composition is sufficiently well known that one can be confident of the absence of interfering species, colorimetric methods are useful.

*X-ray fluorescence (XRF).* The sample is irradiated with monochromatic X-rays that eject electrons from the inner shells of the elements. When an electron from an outer shell of the ion drops into the vacancy, it emits characteristic X-rays whose wavelength is used to identify the element and whose intensity is related to the amount present. XRF is used primarily for elements heavier than magnesium because of the weak fluorescence of lighter elements and absorption of the X-rays within the particles. The combination of transmission or scanning electron microscopy (TEM/SEM) with X-ray fluorescence, also known as energy-dispersive spectrometry (EDS), was discussed in Section B.2b.

*Particle-induced X-ray emission (PIXE).* Elements heavier than sodium can be analyzed using PIXE. In this method, the sample is bombarded with a beam of particles, usually protons, that excites the elements in the sample in a manner similar to that for XRF, causing them to emit X-rays at wavelengths characteristic of the elements (Johansson *et al.*, 1975). Closely related methods of analysis use other ions such as $\alpha$ particles to bombard the sample and induce the X-ray emission. As in the case of XRF, the lighter elements (hydrogen through fluorine) cannot be easily measured with this technique; however, backscattering of $\alpha$ particles used to bombard the sample can be measured, and the energy lost in the nuclear recoil can be used to identify the scattering element for these lighter species. These ion-excited X-ray analytical techniques (IXA) are reviewed by Cahill (1980, 1981a, 1981b) and by Traxel and Wätjen (1986). An example of the application to $PM_{10}$ and $PM_{2.5}$ in Brisbane, Australia, is discussed by Chan *et al.* (1997).

*Atomic absorption spectrometry (AA).* This is a standard laboratory analytical tool for metals. The metal is extracted into a solution and then vaporized in a flame. A light beam with a wavelength absorbed by the metal of interest passes through the vaporized sample; for example, to measure zinc, a zinc resonance lamp can be used so that the emission and absorbing wavelengths are perfectly matched. The absorption of the light by the sample is measured and Beer's law is applied to quantify the amount present.

*Emission spectrometry (ES).* Emission spectrometry is based on the excitation of an element to an upper electronically excited state, from which it returns to the ground state by the emission of radiation. As discussed in Chapter 3, the wavelength emitted is characteristic of the emitted species, and, under the approximate conditions, the emission intensity is proportional to its concentration. Means of excitation include arcs and sparks, plasma jets (see ICP), and lasers.

*Inductively coupled plasma spectroscopy (ICP).* ICP has become a well-established analytical technique for a variety of trace metals. The sample is introduced into a plasma formed by a rf discharge in a gas such as argon. Ions and electrons generated in the plasma are induced to travel in annular paths by interaction with a fluctuating magnetic field generated by the rf induction coil. Elements in the plasma are excited and emit at their characteristic wavelengths. The particular elements can thus be identified from the emission wavelengths and the amounts of each from the emission intensity.

ICP can also be coupled with mass spectrometry (ICP–MS) for very high sensitivity and is finding increasing use for elemental analysis (e.g., Skoog *et al.*, 1998).

*Neutron activation (NA).* The sample is bombarded with neutrons and the radioactivity induced in the sample is then measured. Both $\beta$ and $\gamma$ radiation can be monitored, but $\gamma$ radiation is more frequently used because of the discrete wavelengths associated with emission that can be used to identify the emitter.

*Anodic stripping voltammetry (ASV).* This is an electrochemical technique in which the element to be analyzed is first deposited on an electrode and then redissolved, that is, "stripped," from the electrode to form a more concentrated solution. For example, a drop of mercury hanging from a platinum electrode in a solution containing the species to be measured has been used as the deposition electrode. A potential slightly more negative than the half-wave potential for the ion of interest is applied to deposit the element on the electrode. After deposition of the metal for a given

time period, stirring of the solution is stopped and the voltage decreased at a constant rate toward the anodic potential while the anodic current is measured. The peak anodic current, corrected for the residual current, is proportional to the elemental concentration under controlled conditions, for example, fixed deposition time.

*Mass spectrometry (MS).* Mass spectrometry is a common method for detecting and measuring organics (vide infra), but it has also been used for certain inorganic elements and ions as well. For example, Schuetzle *et al.* (1973) volatilized ambient particulate matter into the source region of a high-resolution mass spectrometer by heating the sample continuously from 20 to 400°C. The elements sulfur, cadmium, and iodine were identified and measured using their masses, ion intensities, and vaporization temperatures. In combination with ICP, MS provides a powerful analytical technique for trace metals.

Secondary ion mass spectrometry (SIMS) and secondary neutral mass spectrometry (SNMS) have also been used for the surface analysis of atmospheric particles. In the SIMS approach, the sample is collected and bombarded with high-energy (keV) atoms or molecules, typically $Ar^+$, causing ejection of material from the surface of the particles into the gas phase. The emitted species include positive and negative ions that are then measured by mass spectrometry. In the SNMS method, the sample is located behind an orifice that contains an rf plasma, for example in argon. The sample holder is held at negative potential, which extracts $Ar^+$ from the plasma and accelerates them toward the sample where they eject surface materials. Neutral species ejected from the surface become partially ionized as they travel back through the plasma, and these are then detected by mass spectrometry (SNMS). The depth analyzed is typically a few monolayers. The application of these techniques to atmospheric particles is described by Klaus (1986) and, as discussed in more detail below, in a series of papers by Goschnick and co-workers (Goschnick *et al.*, 1994a,b; Bentz *et al.*, 1995a, 1995b; Faude and Goschnick, 1997).

Mass spectrometry has also been shown to be a promising method for differentiating the oxidation states of some metals. This is important because the oxidation state in some cases determines the toxicity of the element. For example, Cr(VI) is a carcinogen whereas Cr(III) is not. Laser ionization mass spectrometry studies of the oxides of chromium and arsenic suggest that some cluster ions are characteristic of the oxidation state. For example, Neubauer *et al.* (1995) have shown using single-particle laser ionization mass spectrometry (vide infra) that the ratios of ions such as $Cr_3O_9^-/Cr_2O_6^-$, $HCr_2O_7^-/Cr_2O_6^-$, and $Cr_2O_5^-/Cr_2O_6^-$ can be used to determine the relative amounts of Cr(III) and Cr(VI). However, the relative signal intensities also depended on a number of other parameters such as particle size, water content, laser irradiance, and counterions. As a result, at present this approach is applicable only to well-controlled situations such as process analysis rather than ambient air.

Similarly, Allen *et al.* (1996) have used laser ionization mass spectrometry to differentiate the oxidation states of arsenic. In this case, a bulk sample was collected on a sampling stage and inserted into the instrument (rather than using single particles). $As_2O_3$, i.e., As(III), was shown to give a characteristic $As_3O_5^-$ ion whereas $As_2O_5$, i.e., As(V), gave an $As_3O_8^-$ ion. This approach has also been shown to be promising for some organics. For example, it has been used to screen for the presence of nitro-PAHs (see Chapter 10) in diesel exhaust particles (Bezabeh *et al.*, 1997). Quantification was not possible due to such factors as matrix effects.

While these techniques are promising for ambient air analysis, this is clearly going to be complex due to the many different species present in air and the many parameters that affect the ionization process.

*Electron spectroscopy for chemical analysis (ESCA / X-ray photoelectron spectroscopy (XPS).* The sample is irradiated with X-rays of a fixed frequency, causing ejection of electrons whose kinetic energy is measured. Conservation of energy dictates that the kinetic energy of the electron plus its binding energy must equal the energy of the exciting photon; since the latter is known and the kinetic energy of the electron is measured, the binding energy can be calculated. Since the binding energies are characteristic of each element, this can be used for elemental analysis. In addition, the binding energies of inner-shell electrons are influenced to some extent by the bonding electrons that determine the oxidation state of the element. For example, ESCA was used by Novakov and co-workers (1972) to elucidate the forms of nitrogen and sulfur in atmospheric particulate matter. Similarly, Faude and Goschnick (1997) used XPS to identify a variety of components of aerosol particles in the upper Rhine Valley in Germany, including sulfate and chlorine. Nitrogen in the form of ammonium and organo-nitrogen compounds (but, interestingly, not nitrate) was observed and carbon in organic or elemental as well as in oxidized forms attached to oxygen was noted. Other atmospheric applications are discussed in the review of Cox and Linton (1986).

*Intercomparison studies.* A number of intercomparison studies have been carried out to determine the accuracy and precision of measurements of various elements found in particles. For example, Nejedly *et al.*

(1998) compared the analysis of ambient air particles using ion chromatography, PIXE, and X-ray fluorescence. Two samplers operated side-by-side with PIXE analysis of the filters to assess precision were generally in excellent agreement, to within ~10% for a series of elements including Na, Mg, Ti, Cu, Al, Si, Mn, Fe, Ca, Zn, and S as well as for mass of $PM_{2.5}$ and the light absorption coefficient.

In another portion of the study, filters were analyzed both by X-ray fluorescence and by PIXE for samples collected in a remote area and in an urban area. The normalized percentage difference compared to the mean of the two was $\leq 10\%$ for the elements S, K, Ca, Mn, Fe, and Zn. However, at small concentrations of sulfur, the X-ray fluorescence data were about 20–30% higher than the PIXE analyses for unknown reasons. The agreement for Si was poorer, perhaps due to the greater absorption of X-rays by Si and/or matrix effects.

In the third portion of the study, the results using five different sampler and analytical method combinations were compared. When obvious outliers were excluded from the data, the normalized percentage differences compared to the mean value for sulfur varied from −21 to +23%. Pairwise comparisons for other elements showed similar variability. The agreement overall for X-ray fluorescence compared to PIXE was good, although there was scatter in the individual measurements, perhaps due to differences in sampling (Nejedly *et al.*, 1998).

Similarly, the concentrations of 17 elements in particles sampled using a variety of methods at Mace Head, Ireland, were compared (Francois *et al.*, 1995). Sampling was carried out using a Hi-Vol sampler, a stacked filter unit, Nucleopore filters, and cascade impactors. Analytical techniques included AA, ICP, NA, PIXE, and X-ray fluorescence. Concentrations obtained using the Hi-Vol sampler were higher, which was attributed to differences in collection efficiencies, particularly of larger particles. Ratios of the concentrations of elements determined using cascade impactors compared to stacked filter units ranged from $0.48 \pm 0.12$ for Na to $1.31 \pm 0.19$ for Ti, but for most elements were in good agreement. A comparison of two different cascade impactors with PIXE analysis gave relatively good agreement for the total elemental concentrations, although the size distributions in the smaller size range differed for S and Pb. The latter may reflect differences in cutoff diameters for the states in the two impactors and/or bounce and particle reentrainment problems (Francois *et al.*, 1995).

In summary, there is relatively good agreement overall between different methods of elemental analysis for atmospheric particles, with many of the observed discrepancies due to differences in sampling rather than analysis.

### *b. Inorganic Ions*

Inorganic ions such as $NH_4^+$, $SO_4^{2-}$, and $NO_3^-$ are major components of ambient particulate matter and a wide variety of methods have been used to measure their concentrations. A few of the methods most commonly used are summarized in Table 11.12 and discussed briefly in the following sections.

*Colorimetry.* A variety of colorimetric techniques have been used to measure ions such as $NH_4^+$, $SO_4^{2-}$, and $NO_3^-$ in ambient particles. For example, nitrate can be measured by reduction to nitrite using hydrazine in the presence of a copper catalyst, followed by its conversion to a colored azo dye, which can be measured by its absorbance at 524 nm (Mullin and Riley, 1955). Sulfate has been determined using an exchange reaction between sulfate and a barium–nitrosulfonazo(III) chelate in aqueous acetonitrile; the chelate has an absorbance peak at 642 nm and hence the decrease in this peak can be followed as a measure of the amount of sulfate present that has exchanged with the chelate (Hoffer *et al.*, 1979). Similarly, $NH_4^+$ can be measured by the indophenol blue method (Weatherburn, 1967).

*Ion chromatography (IC).* Ion chromatography has become one of the most widely used methods for the determination of ion concentrations in ambient particles. As the name implies, ions are separated using ion exchange chromatography and are detected usually using electrical conductivity. For example, sulfate and nitrate can be separated on a column containing a strong basic resin using a carbonate solution as the eluant. To overcome the high conductivity of the eluant, which would mask the signal due to the sulfate and

TABLE 11.12 Some Common Methods of Measuring the Major Inorganic Ions in Atmospheric Particles

| Ion | Analytical methods |
|---|---|
| $NH_4^+$ | Col,[a] ESCA,[b] IC,[c] SIE,[d] IR[e] |
| $SO_4^{2-}$ | Col, ESCA, IC, IR |
| $NO_3^-$ | Col, ESCA, SIE, IC, CC,[f] IR |

*Source:* Adapted from LBL (1979).

[a] Col = colorimetry.

[b] ESCA = electron spectroscopy for chemical analysis.

[c] IC = ion chromatography.

[d] SIE = selective ion electrodes.

[e] IR = infrared spectroscopy.

[f] Chemical conversion followed by detection of the product of the $NO_3^-$ reaction.

nitrate, the solutions then pass into a suppression column that contains a strong acid resin; this converts the carbonate into $CO_2 + H_2O$, which has a low conductivity, and the sulfate and nitrate into their acids, which have high conductivities and hence can be easily detected against the suppressed eluant background (Mulik *et al.*, 1976). This *eluant suppression* was the key to the development of IC to measure sulfate and nitrate. Since this first application of IC in ambient aerosols, a variety of anions and cations in ambient aerosols have been separated and measured using this technique. An example of its application to the measurement of nitrate, sulfate, chloride, and ammonium in $PM_{10}$ in Taiwan is discussed by Tsai and Perng (1998).

*Selective ion electrodes (SIE).* Selective ion electrodes are essentially variants of the well-known pH meter. They are membrane indicator types of electrodes in which a potential is developed across a membrane in the presence of the ion; the size of the potential is related to the concentration and hence can be used to quantitatively detect and measure the species. However, instead of a glass membrane, as in the pH meter, the membranes consist of organics that are immersible in water. For example, anion-sensitive electrodes use a solution of an anion exchange resin in an organic solvent; the liquid can be held in the form of a gel, for example, in polyvinyl chloride. The ion reacts with the organic membrane, setting up an equilibrium between the free ion in solution and the ion bound to the membrane, generating a potential difference, which is measured.

Membrane electrodes used to measure species such as $NH_4^+$ that are in equilibrium with the gaseous form (i.e., $NH_3$) in solution are known as gas-sensing electrodes. In this case, the solution to be analyzed is separated from the analyzing solution by a gas-permeable membrane. The gas in the solution to be analyzed diffuses through the membrane and changes the pH of the internal solution, which is monitored using a standard glass electrode.

*Infrared and Raman spectroscopy.* Stephens and Price (1970, 1972) used infrared spectroscopy to examine both ambient and laboratory-generated aerosols. They identified sulfate, nitrate, and ammonium ion absorption bands in ambient particles as well as bands indicating the presence of organics in diesel exhaust (C–H) and oxidized organics in irradiated hydrocarbon–$NO_x$ mixtures. Since then, many studies using IR have been carried out and a variety of species identified, including $CO_3^{2-}$, $PO_4^{3-}$, and $SiO_4^{4-}$. See Chapter 9.C.2 and Figs. 9.49, 9.50, and 9.51 for some typical FTIR spectra of atmospheric particles.

A variety of infrared approaches have been used, including transmission IR, photoacoustic IR, diffuse reflectance IR, and attentuated total reflectance. The principles behind these methods and their application to atmospheric aerosols have been reviewed by Allen and Palen (1989).

Raman spectroscopy (reviewed by Schrader, 1986) has also been applied to single particles in laboratory systems. For example, Fung and Tang (1991, 1992a, 1992b) and Fung *et al.* (1994) have applied resonance Raman spectroscopy to particles containing nitrate and sulfate, both very common constituents of atmospheric particles. The detection limits for nitrate and sulfate in aqueous droplets of 15-$\mu$m diameter were reported to be about 0.0025 M (Fung *et al.*, 1994), suggesting that this method might prove applicable to ambient particles as well.

A variant of Raman spectroscopy that has been used to probe interfaces in large aqueous particles (e.g., of the order of several hundred microns) in laboratory studies is nonlinear morphology-dependent stimulated Raman scattering (e.g., Zhang and Aker, 1993; Aker and Zhang, 1994). In this method, light generated inside the particle in effect undergoes internal reflections at the interface; when the wavelength of the light is an integral factor times the circumference of the particle, it gets "trapped," in effect increasing the optical path length and hence the net absorption by species dissolved in the particle. As with resonance Raman, this technique has not yet been applied to particles in ambient air.

*Mass spectrometry.* Laser microprobe mass spectrometry (LMMS) has also been applied to atmospheric particles to measure primarily inorganic elements and ions (e.g., see Bruynseels *et al.*, 1985; Kaufmann, 1986; Wieser and Wurster, 1986; Dierck *et al.*, 1992; and Hara *et al.*, 1996). The particles are collected using techniques such as impactors described earlier and subsequently analyzed. A laser pulse, e.g., at 266 nm, is used to volatilize a selected particle or a group of particles and the gaseous fragments produced are analyzed by mass spectrometry. Both positive and negative ions can be analyzed. The mass spectra of ambient particles can be quite complex and include many fragments as well as clusters. It is because of the extensive fragmentation that specific organic compounds cannot be identifed, although clusters of carbon atoms from soot, for example, can be seen. As discussed shortly, this method has been applied more recently to single particles suspended in air, and typical positive and negative ion spectra are shown in Section B.4a.

### c. Total Carbon: Organic versus Graphitic (Elemental)

The separate determination of organic and elemental carbon in atmospheric particles has been addressed in a number of ways by many workers over a period of

years; despite this, there is still no accepted accurate and reliable standard method of sampling and analysis for these important aerosol species.

Four major methods have been used to separate the organic elemental carbon: thermal methods, digestion, extraction, and optical techniques. These are discussed in detail in the volume on particulate carbon edited by Wolff and Klimisch (1982) and in the article by Cadle *et al.* (1983).

In the thermal methods, the sample is heated to increasingly higher temperatures, with most steps being carried out in the presence of $O_2$. The basis of this method is that volatile organics will vaporize first and then other organic compounds will be oxidized. Only at the highest temperatures will graphitic carbon oxidize. The carbon thus ejected into the vapor phase at various temperatures is detected in the form of $CO_2$ or, alternatively, after catalytic reduction, as $CH_4$.

For example, in one thermal method, shown in Fig. 11.67, the sample is oxidized and volatilized with an $O_2$–He mixture at 350°C; the volatilized carbon is oxidized to $CO_2$ in an $MnO_2$ bed and reduced to $CH_4$ so it can be measured using the sensitive technique of flame ionization detection (FID) (e.g., Huntzicker *et al.*, 1982; Japar *et al.*, 1984; Huffman, 1996). The purge gas is then replaced by pure He and the temperature is raised to 600°C; in this step the remaining organic carbon is volatilized, oxidized to $CO_2$ by the $MnO_2$ catalyst, and reduced to $CH_4$ for measurement. Finally, elemental carbon is determined by heating in an $O_2$–He mixture from 400 to 600°C. In this particular apparatus, a light pipe, He–Ne laser, and photocell are used to monitor the reflectance of the filter as an indication of the changes in graphitic carbon on the filter (vide infra).

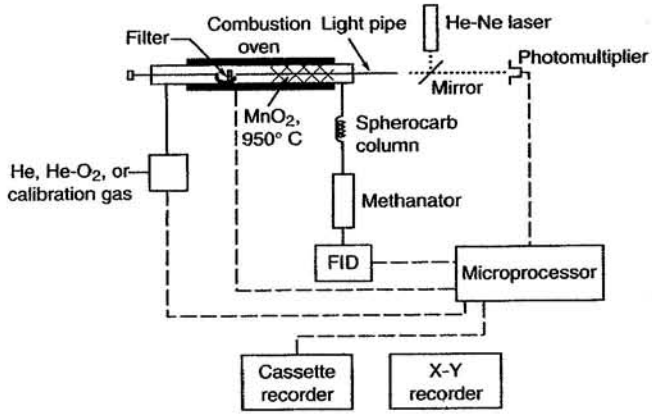


FIGURE 11.67 Schematic diagram of one type of thermal analyzer for organic and graphite carbon (adapted from Huntzicker *et al.*, 1982).

Although relatively fast and simple, such thermal methods can suffer from the possibility of carbonization of organics during heating in an inert atmosphere; thus elemental carbon can be formed from organic carbon during the analysis, leading to significant errors. Corrections for this can be applied by following the sample reflectance during the heating (e.g., Huffman, 1996). Fung (1990) suggests that this error can be minimized by using another approach in which the sample is oxidized by $MnO_2$ during rapid heating to a maximum of 525°C, during which organic carbon is oxidized but elemental carbon is not. Heating to 850°C then leads to oxidation of elemental carbon by $MnO_2$.

A second approach to analyzing organic and elemental carbon has been to digest the sample in a strongly oxidizing solution (e.g., nitric acid) to remove the organics. The remaining carbon on the filter is then measured using standard methods with the assumption that only graphitic carbon remains on the filter after digestion. Organic carbon is then the difference between the total carbon on the filter before and after digestion, respectively. However, it has been shown that during digestion, some elemental carbon is removed, in addition to organic carbon (Cadle *et al.*, 1983). Thus digestion has no clear advantages over thermal methods.

Extraction of the organics from filters using various solvents has also been used. Total carbon analysis of portions of the filter after extraction gives graphitic carbon directly, and organic carbon is obtained by the difference between this and total carbon before extraction (e.g., Japar *et al.*, 1984). As with thermal and digestion techniques, there are problems in establishing that the organics and elemental carbon are clearly and accurately separated.

There are a variety of optical methods used to measure graphitic carbon alone, the most widely used being visible light absorption or reflectance techniques. Visible light absorption is the basis of what is known as the integrating plate method (IPM) (Lin *et al.*, 1973), shown schematically in Fig. 11.68. Particles are collected on a Nucleopore filter and inserted between the light source and the detector; the light transmitted through the filter is compared to that transmitted through a clean filter, that is, one not containing particles. Opal glass is placed between the filter and the detector to transmit an isotropic light flux from scattered and transmitted light through the filter. Scattering of light by the particles, which would interfere with an absorption measurement, is minimized by using a filter with a refractive index approximately equal to that of the particles.

As might be expected for a measurement based on simple light absorption in a complex sample, there are

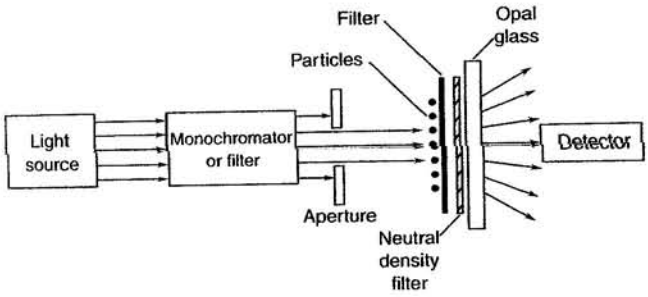


FIGURE 11.68 Schematic of integrating plate method (IPM) for measuring graphite carbon (adapted from Weiss and Waggoner, 1982).

a number of potential problems. For example, there may be other light-absorbing organics or other species present in the sample (e.g., Huffman, 1996); in addition, it is not clear what value should be used for the absorptivity of combustion-derived carbon particles. Thus, Horvath (1997) showed that the light absorption coefficient of carbon measured using the integrating plate method was systematically high and that this is expected theoretically for measurements made using a combination of transmission and integration of the scattered light.

Reflectance techniques, like the IPM, are based on the absorption of visible light by graphitic carbon. However, rather than measuring the decrease in light transmitted through a filter due to absorption, the decrease in light reflected from the carbon-containing surface is measured; the higher the elemental carbon, the more light will be absorbed and the less reflected. Thus $\log(R_0/R)$, where $R_0$ is the reflectance in the absence of carbon and $R$ the reflectance in its presence, has been shown to be linearly related to the elemental carbon concentrations (Delumyea *et al.*, 1980). Because this is a light absorption/reflectance measurement, it suffers from the same types of problems as the IPM. However, it has an advantage in terms of its simplicity. In addition, in some urban areas there are historical records of filter sample reflectances that can be calibrated against more recent methods to examine historical trends in graphitic carbon (e.g., see Cass *et al.*, 1983).

Although carbonate has been observed in some ambient samples (e.g., see Cunningham *et al.*, 1984), it is generally believed to be present at insignificant concentrations compared to organic and graphitic carbon.

Although it has been generally assumed that elemental carbon is the only component of particles that absorbs visible light, as discussed in Chapter 9, this may not be the case. Instrumentation for measuring total light absorption by all particle components based on the heating of the surrounding gas caused by the absorbed energy is discussed by Moosmüller *et al.* (1997).

### *d. Speciation of Organics*

As seen in Chapter 9.C.2, a very wide variety of organics are found in particles in ambient air and in laboratory model systems. The most common means of identification and measurement of these species is mass spectrometry (MS), combined with either thermal separation or solvent extraction and gas chromatographic separation combined with mass spectrometry and/or flame ionization detection. For larger, low-volatility organics, high-performance liquid chromatography (HPLC) is used, combined with various detectors such as absorption, fluorescence, and mass spectrometry. For applications of HPLC to the separation, detection, and measurement of polycyclic aromatic hydrocarbons, see Wingen *et al.* (1998) and references therein.

Thermal desorption was described earlier with respect to differentiating organic and elemental carbon. Once organics have been desorbed by heating, they can be identified and measured individually using chromatographic techniques. While this technique works well for a number of organics, as discussed shortly, some compounds are thermally unstable and decompose during the desorption process. In addition, it may not completely vaporize high molecular weight compounds of low volatility.

Solvent extraction of the sample is also frequently used in the analysis of particulate matter. Through the appropriate choice of solvents, the organics can be separated into acid, base, and neutral fractions, polar and nonpolar fractions, and so on. This grouping of compounds according to their chemical properties using extraction techniques simplifies the subsequent analysis. Each fraction can then be analyzed by GC–MS, with the GC retention time and the mass spectrum used for identification and measurement.

A more recent extraction technique involves the use of supercritical fluids such as $CO_2$. This has a number of advantages (e.g., see Skoog *et al.*, 1998) in that it avoids the use of large quantities of solvent and the need to concentrate the extract during which losses of the analyte may occur. Because the extracting fluid under atmospheric conditions is a gas, separating the fluid from the analyte only requires lowering the total pressure to release the "solvent" as a gas. In addition, it is quite fast since the rate of extraction depends on the rate of diffusion in the supercritical fluid and its viscosity, both of which are faster than for liquid extractions (e.g., minutes to hours versus hours to days). Low temperatures can be used for many supercritical fluids such as $CO_2$, minimizing thermal decomposition

and/or reactions that may occur using thermal desorption techniques.

Supercritical fluid extraction (SFE) has been applied to ambient air particles with some success. For example, Hansen *et al.* (1995) developed a technique in which particles collected on a filter were extracted online using $CO_2$ and simultaneously transferred to the cooled head of a GC column, a process that took only 20 min. Recovery of long-chain alcohols and carboxylic acids spiked onto filters was much better for SFE than for thermal desorption but about the same or worse for some compounds such as nicotine. For a sample of urban aerosol particles, SFE detected some compounds not seen by thermal desorption such as larger alcohols. This was attributed to a lack of volatilization of these compounds with the temperatures used in the thermal desorption method and/or to decomposition during heating. On the other hand, some compounds such as benzaldehyde and the alkene 1-nonacosene were observed using thermal desorption but not using SFE. The alkene was thought not to be present in the aerosol, but rather was produced by thermal decomposition of some other compound and hence would not be generated during SFE. The amount of benzaldehyde may have been below the detection limit of the SFE–GC system.

Two types of ionization sources are in widespread use—electron impact and chemical ionization. The traditional means of ionization by electron impact often causes extensive fragmentation of molecules so that only peaks corresponding to the fragments are seen in the mass spectrum. Particularly in a complex environmental sample, this may preclude positive compound identification. Chemical ionization complements electron impact mass spectra and is particularly useful for establishing the molecular weight of the compound. In chemical ionization sources, an electron beam is used to ionize a reagent gas such as $CH_4$. The sample is then ionized by collisions with the ionized fragments from $CH_4$. This often results in relatively strong peaks at masses one greater or one less than the parent peak, MH, through reactions such as the following:

$$CH_5^+ + MH \rightarrow MH_2^+ + CH_4,$$
$$C_2H_5^+ + MH \rightarrow M^+ + C_2H_6.$$

Other types of mass spectrometry have also been used to examine ambient particulate samples. One such technique is secondary ion mass spectrometry (SIMS) in which the surface of the sample is bombarded with a beam of ions or neutral atoms that cause ejection of fragments from the surface. The fragments may be neutral atoms or molecules, positively or negatively charged species, electrons, or photons. The charged species, that is, the secondary ions, can be analyzed using MS, generating a SIMS spectrum. Elements such as potassium and sodium as well as functional groups such as COOH, sulfates, and nitrates can be detected by SIMS.

### *e. Artifacts*

It is evident from the earlier discussion of sampling and collection of bulk samples of atmospheric particles that there is ample opportunity for the formation of artifacts, which can be either positive or negative, depending on the particular species measured and the techniques used. These can arise from a variety of processes such as the following: reactions of collected particles with other particle components or with gases (e.g., of NaCl with gaseous $HNO_3$), volatilization of compounds from collected particles (e.g., $NH_4NO_3$), adsorption and/or reactions of gases on filters or on the particles previously collected [e.g., $SO_2$ uptake and oxidation on particles (Eatough *et al.*, 1995) and adsorption of gas-phase organics on quartz fiber filters (e.g., Appel *et al.*, 1989; McDow and Huntzicker, 1990; Turpin *et al.*, 1994)], and reactions of gases with the filter medium, as discussed earlier for $SO_2$ on nylon filters, for example (e.g., Chan *et al.*, 1986; Cadle and Mulawa, 1987). In addition, the particle composition may change during collection due to shifts in gas-particle equilibria from changes in temperature, pressure drop across the collecting medium, or composition of the sampled air (e.g., Zhang and McMurry, 1987, 1991; Kaupp and Umlauf, 1992).

In addition to these chemical artifacts, physical artifacts can also occur. For example, the problems of particle bounce (e.g., see Wedding *et al.*, 1986) and reentrainment in impactors were discussed earlier. In addition, air turbulence is known to have a significant effect on the overall sampling efficiency of particle inlets (e.g., Wiener *et al.*, 1988; Francois *et al.*, 1995).

In short, care must be taken in sampling and analysis of airborne particles, as well as in the data interpretation, to minimize or at least recognize potential artifact problems. Such problems, along with a need to understand not only the bulk composition of a collection of airborne particles but also that of individual particles, have contributed to the development of real-time and single-particle analysis techniques discussed in the following section.

## 4. Real-Time Monitoring Techniques for Particles

Efforts to develop and apply real-time monitoring techniques for particles have been underway for more

than two decades. Early approaches typically involved the impaction of particles on a hot filament, surface, or oven that volatilized and ionized the species in the particles, with the ions detected by mass spectrometry (e.g., Myers and Fite, 1975; Davis, 1977a, 1997b; Allen and Gould, 1981; Stoffels, 1981a,b; Stoffels and Lagergren, 1981; Sinha *et al.*, 1982, 1985; Sinha and Friedlander, 1986; Stoffels and Allen, 1986). Laser ionization was also investigated (Sinha, 1984). The ions produced were measured by mass spectrometry. Since many species volatilized but did not ionize, neutrals were detected in some studies by electron impact ionization subsequent to volatilization (e.g., Allen and Gould, 1981; Sinha *et al.*, 1982). More recent developments of this approach (e.g., Tobias *et al.*, 1999; Jayne *et al.*, 1999) are discussed later in this section.

While the early studies paved the way for further development of real-time and single-particle monitoring techniques, their application to ambient air was limited by a number of factors. These included the fact that the burst of ions produced was very short, <10 ms, so that scanning mass spectrometric methods such as quadrupoles could not scan sufficiently rapidly to capture the large mass range of interest. As a result, only a single mass or very limited number of masses could be recorded for each scan. Other limitations included extensive fragmentation of organics and a dependence of the efficiency of ionization on the composition of the particles. The use of time-of-flight mass spectrometry proposed by Allen and Gould in 1981 has helped to overcome the first problem. As we shall see, the fragmentation and variable ionization efficiencies continue to present challenges.

### *a. Single-Particle Laser Ionization Techniques*

Since the first use of laser ionization by Sinha in 1984 to detect single particles, there has been a great deal of activity and development of this method for application to the atmosphere (see Johnston and Wexler (1995) for a review). In the early work, Sinha (1984) developed a method for simultaneous sizing of particles in which the particle first scattered light from one He–Ne laser, followed by a second He–Ne laser. The time interval between the two was used to obtain the speed of the particle and hence its size. The Nd:YAG ionizing laser was collinear with the second He–Ne laser and was fired at a set delay time after the particle was detected by the first He–Ne laser. Only particles of a given size whose speed is such that they reach the ionizing laser as it fired were detected. Particles of different sizes could be detected by varying the delay time between the scattering and ionizing lasers.

Subsequently, Marijnissen *et al.* (1988) proposed a single-particle system in which the amount of scattered light could be used along with the index of refraction of the particle to calculate its size. Shortly thereafter, McKeown *et al.* (1991) demonstrated the analysis of single particles using this approach, combined with time-of-flight mass spectrometry.

Since then, there has been a substantial development of such instruments. For example, Hinz *et al.* (1994) reported the first real-time monitoring of ambient particles in laboratory air using this technique of laser ionization combined with time-of-flight mass spectrometry. Carbon peaks from soot, metals attributed to abrasion of laboratory devices, and nicotine after "enriching the ambient air with tobacco smoke" were observed. Prather *et al.* (1994) and Mansoori *et al.* (1994) reported the application to inorganic and organic particles prepared in the laboratory, and Dale *et al.* (1994) and Yang *et al.* (1995a) reported analysis of organics adsorbed to the surface of particles of silicon carbide generated in the laboratory, using laser desorption combined with ion trap mass spectrometry. Reilly *et al.* (1998) have used laser ablation with an ion trap MS to identify polycyclic aromatic hydrocarbons in the particles from diesel engines.

Subsequently, Carson *et al.* (1995) and Neubauer *et al.* (1996, 1997) reported the ability to provide speciation of some aerosol components such as ammonium sulfate, ammonium sulfite, and methanesulfonic acid through control of the ionizing laser pulse energy, and Reents *et al.* (1995) showed that parent peaks could be obtained even for components such as $SiO_2$ that are difficult to ionize. Hinz *et al.* (1996) reported the simultaneous detection of both positive and negative ions produced by laser ionization of a single particle using a dual TOF system.

Prather and co-workers (Prather *et al.*, 1994; Noble *et al.*, 1994; Nordmeyer and Prather, 1994) introduced a significant improvement in particle size measurement and determining which particles are ionized. Light from the first laser is scattered by the particle and detected by a photomultiplier. It then travels a known distance where it encounters and scatters light from a second laser, which is also detected. The delay time between the two scattered light pulses is determined by the speed, i.e., the size, of the particle. This delay time is used to trigger the ionizing laser located further downstream at exactly the time that the particle should be in its optical line of sight. This use of three lasers allows both the determination of particle size and synchronization between detection of the particle and its ionization.

As illustrated below, the mass spectra of particles in ambient air can be (not surprisingly) quite complex. The use of tandem mass spectrometry would therefore be quite valuable, and indeed, such an instrument has

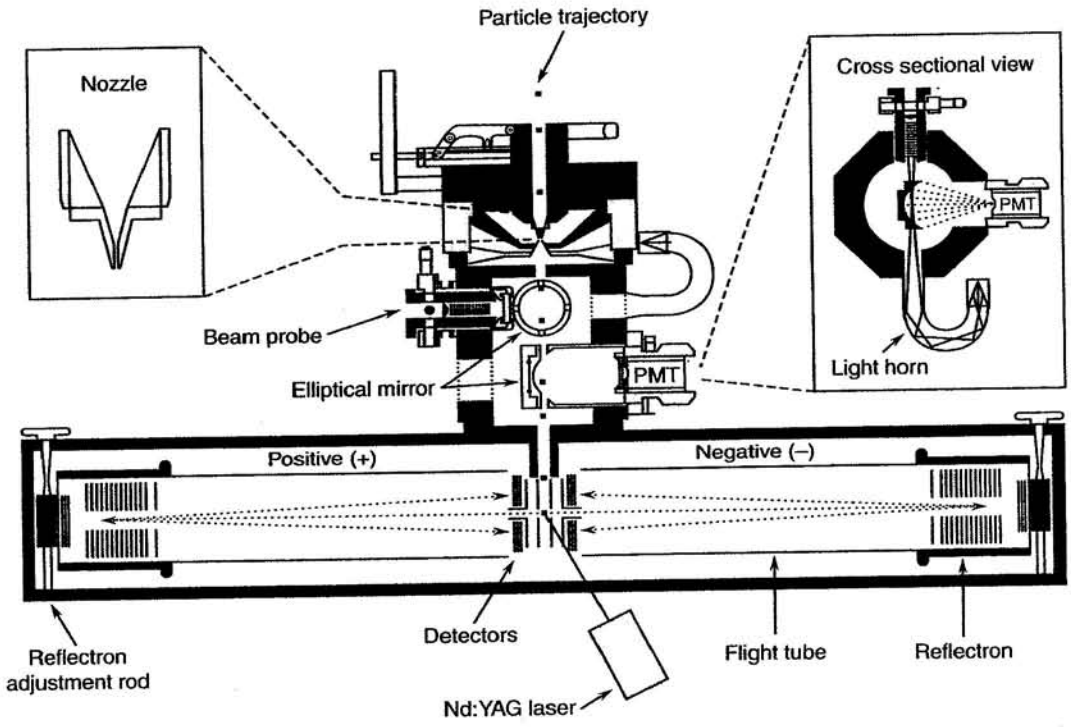


FIGURE 11.69 Schematic diagram of single-particle laser ionization mass spectrometer (adapted from Gard *et al.*, 1997).

been developed using an ion trap mass spectrometer (March, 1992). Its application to aerosols generated in the laboratory has been explored for relatively simple systems (Yang *et al.*, 1995a, 1996) and looks promising, although application to ambient air awaits further investigation.

Figure 11.69 is a schematic diagram of a single-particle laser ionization mass spectrometer with the particle sizing and ionization synchronization scheme of Prather and co-workers (Gard *et al.*, 1997). Ionization is produced using light at 266 nm using a Nd:YAG laser and both positive and negative ions from the single particle are detected using a dual-ion coaxial set of TOF mass spectrometers. Figure 11.70 shows both the positive and negative mode mass spectra acquired from a single particle that was generated in the laboratory from wood burning. Hydrocarbon fragments are seen in both positive and negative ion modes, with potassium also present in the positive ion spectrum and $HSO_4^-$ in the negative ion spectrum.

Figure 11.71 shows some single-particle mass spectra obtained in the positive ion mode in a rural area in Colorado using a laser ionization single-particle mass spectrometer (Murphy and Thomson, 1995, 1997a,b). Figure 11.71a is an example of a mass spectrum of a particle containing organics with fragments occurring up to higher amu; indeed, there are peaks appearing at most masses, suggesting a complex mixture. On the other hand, the spectrum in Fig. 11.71b shows mainly peaks due to $C_n$, which has been assigned to elemental carbon (soot particles). Figure 11.71c shows evidence for ammonium ions, perhaps due in part to ammonium nitrate as seen from the peaks in this mass spectrum.

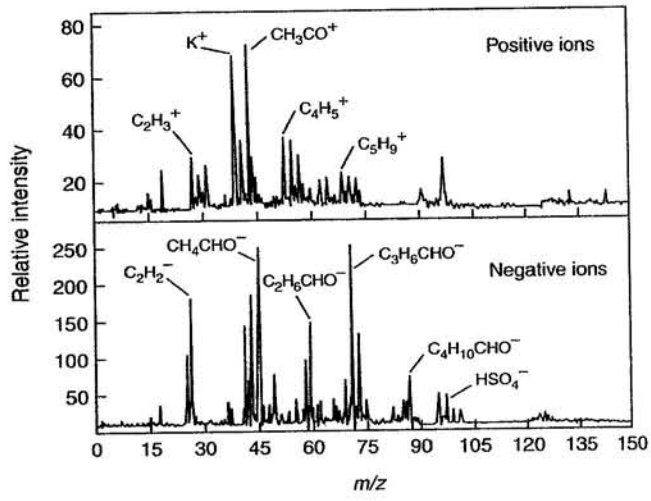


FIGURE 11.70 Positive and negative ions detected in a single particle from wood smoke generated in the laboratory (adapted from Gard *et al.*, 1997).

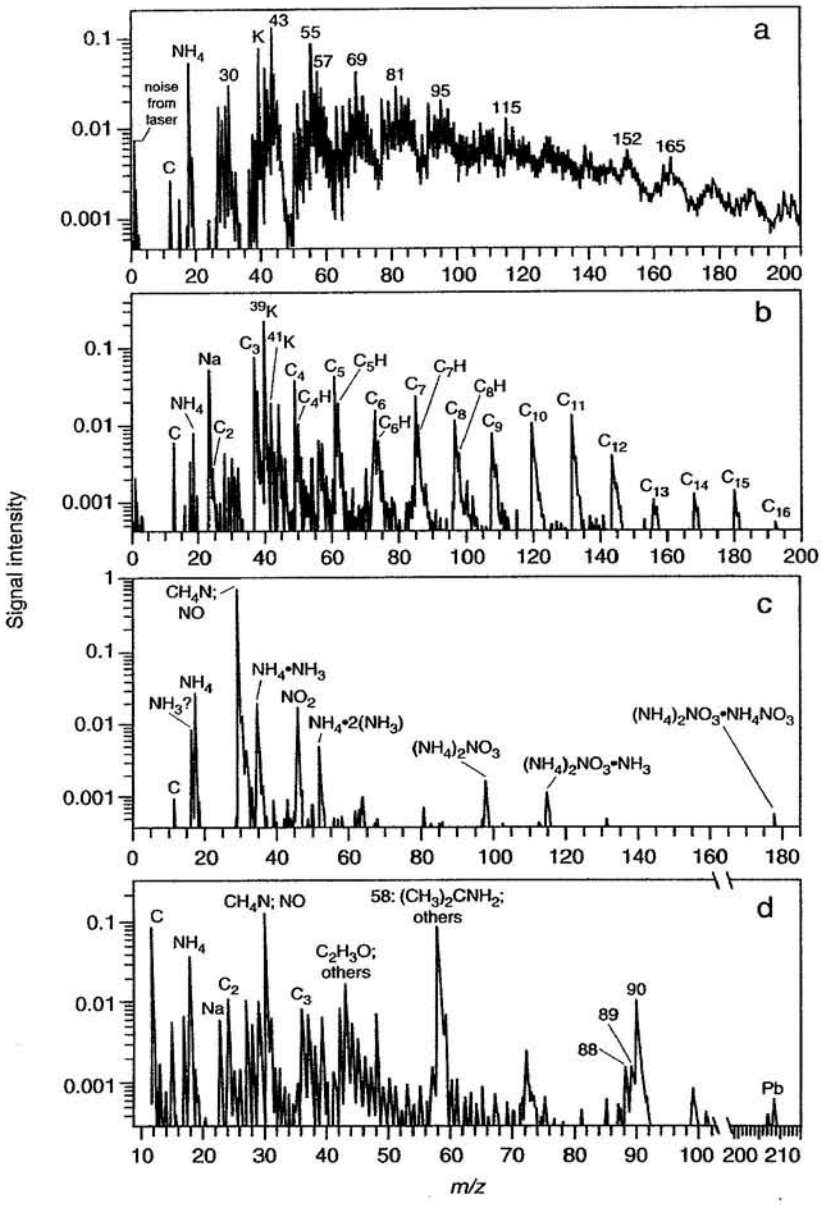


**FIGURE 11.71** Typical laser ionization positive ion mass spectra of single particles in rural Colorado (adapted from Murphy and Thomson, 1997a,b).

Clearly, laser ionization–TOF mass spectrometry is a promising tool for real-time single-particle analysis. However, there are some important aspects of particle characterization on which data are not provided by these techniques at the present time. For example, while the identification and grouping of elements in single particles in ambient air using principal-component analysis provide insight into their sources (e.g., see Noble and Prather, 1996; Liu *et al.*, 1997; Murphy and Thomson, 1997a, 1997b; Middlebrook *et al.*, 1997; and Wood and Prather, 1998), independent quantification has not yet been achieved. Indeed, it may prove to be elusive due to the sensitivity of ion formation to the particular conditions, including the wavelength of the ionizing laser, the laser fluence, the chemical composition of the particle, etc. (e.g., see Thomson *et al.*, 1997; and Ge *et al.*, 1998b).

For example, Neubauer *et al.* (1998) have shown that the spectra can be very sensitive to the amount of water present and whether the particle is aqueous, i.e., above the deliquescence point, or solid (but holding adsorbed water on the surface). Figure 11.72 shows the

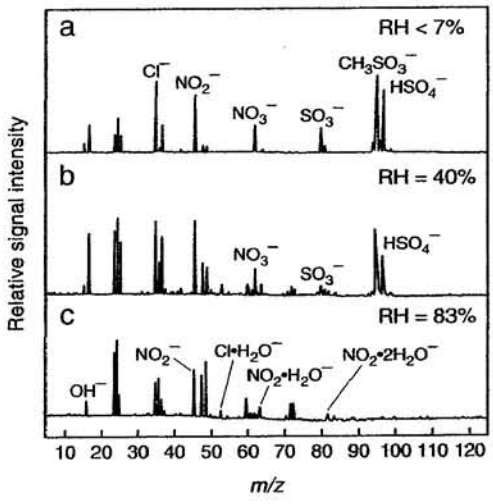


FIGURE 11.72 Negative ion laser ionization mass spectrometry of particles generated in the laboratory that contain equimolar amounts of NaCl, $NH_4NO_3$, $(NH_4)_2SO_4$, and $CH_3SO_3H$ at (a) 7%, (b) 40%, and (c) 83% relative humidity (adapted from Neubauer *et al.*, 1998).

negative ion mass spectra of particles containing equimolar amounts of NaCl, $NH_4NO_3$, $(NH_4)_2SO_4$, and methanesulfonic acid at relative humidities of <7, 40, and 83%, respectively. At the lowest relative humidity where the particle is a solid, peaks due to all of the salts appear, and the peak due to the anion of methanesulfonic acid is clear. At 83% RH, the latter has almost completely disappeared, as has that due to the sulfate.

However, relative peak intensities can be useful if the nature of the particles has not changed significantly. For example, Gard *et al.* (1998) followed peaks characteristic of chloride and nitrate in a coastal region in southern California and showed that they had an inverse correlation in single particles. Such behavior is expected from the well-known reaction of gaseous $HNO_3$ (and perhaps other gaseous oxides of nitrogen) with NaCl to give gaseous HCl and solid $NaNO_3$ (e.g., see De Haan *et al.*, 1999, and references therein).

A second issue is that while organics can be identified from $C_nH_m$ peaks, speciation is generally not possible. For example, although negative ions corresponding to organic acid anions were observed in particles in rural Colorado, Murphy and Thomson (1997b) indicate that these could be due to fragmentation from larger organics. Fragmentation patterns of specific organics can, however, provide clues to the presence of certain classes of compounds. For example, Fig. 11.71d shows the positive ion mass spectrum of a particle that Murphy and Thomson (1997a) attribute to the presence of amines or amides in the particle.

A third issue is illustrated by the mass spectrum in Fig. 11.71a, which, as described by Murphy and Thomson (1997a), appears to have a peak at almost every mass. Thus, in many instances in the atmosphere, particularly in polluted urban areas, the spectra may be so complex that only major classes of compounds may be discernible.

Finally, the approaches to sizing rely to date on light scattering. As discussed in Chapter 9.A.4, visible light scattering peaks in the 0.1- to 1-$\mu$m range so that particles smaller than this cannot be detected and hence measured using this approach. Although particles down to ~10 nm in size can be detected by free firing of the laser (e.g., Reents *et al.*, 1995; Carson *et al.*, 1997b), this clearly gives a rather random selection of particles detected and may not work at low particle concentrations typical of the atmosphere. New approaches for detecting smaller particles in such systems are needed.

### *b. Alternate Potential Mass Spectrometric Methods for Sizing and Chemical Composition*

Figure 11.73 is a schematic diagram of another approach to single-particle size and composition measurements that is applicable to volatile and semivolatile species over the size range from ~0.05 to 1 $\mu$m (Jayne *et al.*, 1999). This approach is similar in principle to that described by Allen and Gould (1981) and Sinha *et al.* (1982). Particles are sampled through an aerodynamic inlet that provides a narrow beam of particles with near unit efficiency (Liu *et al.*, 1995a, 1995b; Schreiner *et al.*, 1998). As the air containing the particle beam expands into the vacuum at the end of the inlet, the particles are accelerated, with smaller particles attaining higher speeds and vice versa. The beam of particles entering the sizing chamber is chopped to provide a time-of-flight

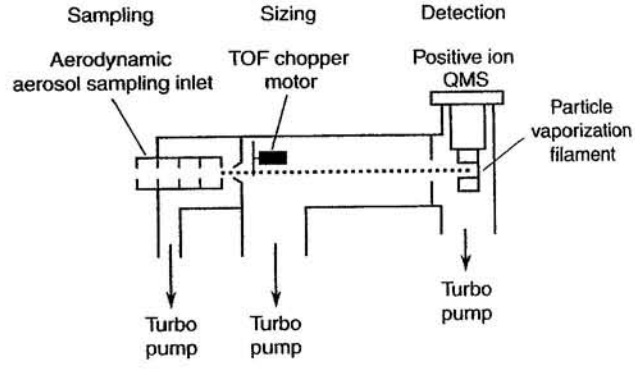


FIGURE 11.73 Schematic diagram of aerosol mass spectrometer for volatile and semivolatile particle sizing and composition measurement (graciously provided by J. Jayne, D. Worsnop, and C. Kolb, 1999).

measurement of the time for a particle to reach the detector, from which the particle size can be determined. In the third chamber, the particle collides with a heated surface that flash vaporizes volatile and semivolatile components. The vaporized species are ionized by electron impact and a quadrupole mass spectrometer is used to obtain the mass spectrum. The detection process is sufficiently sensitive to be able to detect single particles larger than 50 nm, so that the number of particles can be determined as a function of particle size.

At present, the full mass range cannot be scanned for one particle so that single-particle analysis is currently not possible with this approach; i.e., a complete mass spectrum cannot be obtained for one particle. Nonvolatile species are also not detected, so that important particle components in soil dust and soot cannot be measured. The advantages compared to single-particle laser ionization techniques are that some of the important volatile and semivolatile components such as ammonium sulfate and nitrate can be quantified. There is also much less fragmentation of organics. (However, given the complexity of the organic composition of particles in ambient air (see Chapter 9.C.2), it is not clear that specific organics in particles will be able to be identified.) Finally, the size and complexity of the instrument are significantly reduced without the need to incorporate a laser.

Figure 11.74 shows a similar approach to the measurement of a continuous beam of volatile and semivolatile particles with diameters as small as $\sim 0.02$ $\mu$m (Tobias *et al.*, 1999). Upon exiting the aerodynamic lensing system, the particles enter a small ($\sim 0.1$ cm$^3$) cell whose temperature can be regulated and is typically in the range of $\sim 100$–$200$°C. The particles vaporize in this cell and the vapors are sampled into a quadrupole mass spectrometer with electron impact ionization. The temperature of the vaporization cell can be optimized for particular compounds of interest, so that fragmentation of organic compounds, for example, can be minimized. Sizing of particles in this system can be provided by using a differential mobility analyzer prior to the aerodynamic lenses.

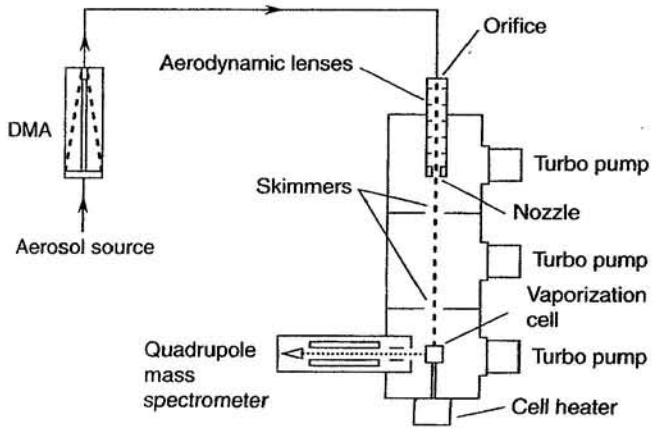


FIGURE 11.74 Schematic diagram of aerosol particle mass spectrometer for measurement of composition of continuous beams of volatile and semivolatile particles (graciously provided by P. Ziemann, 1998).

Both of these approaches are hence useful for a continuous stream of particles of similar composition where the mass spectrum can be continuously scanned, for example in laboratory environmental chamber studies.

In summary, the use of mass spectrometric methods, combined with various approaches to vaporizing and ionizing the particles, is gaining increasing popularity and interest for the analysis of continuous sources of particles or single particles. The problem of quantification of the components seen by single-particle laser ionization techniques remains to be solved. On the other hand, the vaporization approaches can provide quantitative data on some volatile and semivolatile components but cannot measure the nonvolatile species and, at present, do not provide a full mass spectrum for a single particle.

### *c. Depth Profiling of Particle Composition*

As seen in the preceding sections, the technology associated with particle measurement is developing from bulk analyses of chemical composition to that of single particles. Further "splitting hairs," one would like to be able to depth profile particle composition. For example, as discussed in Chapter 9, it is believed that some particles have an organic coating on them, which can affect the particle properties such as the uptake and evaporation of species between the particle and the gas phase. Another example is the surface reaction of NaCl in sea salt particles with gaseous oxides of nitrogen, generating $NaNO_3$. Whether the surface is coated with a layer of nitrate, preventing further oxidation of the underlying NaCl, or whether the nitrate recrystallizes into separate microcrystallites as suggested by laboratory studies (see Figs. 11.63 and 11.64, Vogt and Finlayson-Pitts (1994), and Allen *et al.* (1996)), leaving a fresh surface of NaCl that can react further, is of interest.

Depth profiling of solids is commonly carried out in surface science studies, for example, using sputtering of the surface with argon ions. Such methods have also been applied to bulk samples of collected atmospheric particles (e.g., Jach and Powell, 1984; Bentz *et al.*, 1994, 1995a, 1995b; Goschnick *et al.*, 1994a, 1994b; Faude and Goschnick, 1997). For example, Faude and

Goschnick (1997) applied a combination of X-ray photoelectron spectroscopy (XPS), secondary neutral mass spectrometry (SNMS), and secondary ion mass spectrometry (SIMS) to particles collected on a five-stage impactor in the upper Rhine Valley in Germany and found that the surface was enriched in organic compounds as well as ammonium sulfate and chloride. In a suburban area near Karlsruhe, Germany, SNMS and SIMS studies showed that in submicron particles, the cores consisted primarily of carbon (both elemental and organic), whereas the surface was enriched in ammonium sulfate; on the other hand, larger particles with diameters greater than 2 $\mu$m had cores of aluminosilicates surrounded by organics, carbonates, and nitrates and then a surface layer of ammonium sulfate and hydrogen-enriched organics (Bentz *et al.*, 1995a,b).

Depth profiling of single airborne particles has been reported by Carson *et al.* (1995, 1997a), who showed that the use of variable laser fluences in single-particle laser ionization mass spectrometry can be used to probe thin films on particles in laboratory systems. At low laser intensities, only the surface layer is volatilized and ionized, whereas the entire particle can be vaporized and detected at higher intensities.

Similarly, Ge *et al.* (1996, 1998a) have studied the composition of single particles formed from the crystallization of solutions of mixtures of salts such as KCl/NaCl and $(NH_4)_2SO_4/NH_4NO_3$ using single-particle laser ionization mass spectrometry. As the relative humidity decreases, the least soluble salt crystallizes out. With further decreases in the relative humidity, the other salt reaches its saturation and the two salts precipitate out together. The composition of the aqueous phase at this point is referred to as the eutonic composition. Thus, a solid core of the least soluble species surrounded by a mixture of the salts is expected. Ge *et al.* (1996) analyzed the relative peak heights due to individual components in single particles crystallized from solutions containing mixtures of salts as a function of the solution composition and laser fluence. They were able to establish that for a KCl/NaCl mixture, for example, the surface layer was enriched in the minor component relative to the original solution, as expected.

Emission of electrons from the particle surface has also been used in laboratory studies to probe surface composition. Electron emission has been induced by UV irradiation, for example, by Burtscher and Schmidt-Ott (1986) to probe perylene on the surface of carbon particles. In a series of laboratory studies, Ziemann *et al.* (1995, 1997, 1998) have demonstrated the potential utility of secondary electron yield measurements as a technique for probing particle surface composition. In this method, particles are bombarded with an electron beam and the change in the charge of the particles is measured using a Faraday cup. The number of secondary electrons emitted per primary electron incident on the particle, defined as the secondary electron yield, is characteristic of the chemical composition and of particle size. Figure 11.75, for example, shows the measured secondary electron yields for an 89-nm KCl particle, a 128-nm particle of the ester dioctyl sebacate (DOS), and KCl coated with DOS of various film thicknesses as a function of the energy of the bombarding electron beam (Ziemann and McMurray, 1998). Clearly, the yields are quite different for the organic and KCl and are a sensitive function of the thickness of the DOS film on the KCl.

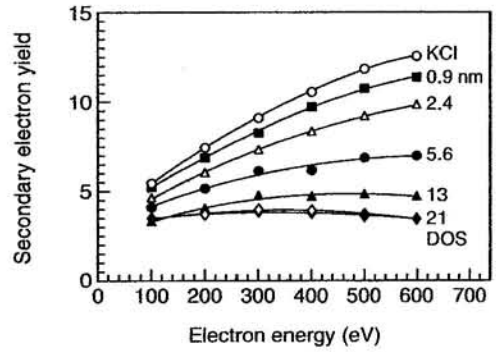


**FIGURE 11.75** Measured secondary electron yields from the electron bombardment of 89-nm KCl particles, 128-nm particles of dioctyl subacate (DOS), and KCl coated with DOS of film thickness (in nm) shown (adapted from Ziemann and McMurry, 1998).

Ziemann and McMurray (1998) also measured secondary electron yields and transport efficiencies of NaCl particles coated with octacosane upon exposure to relative humidities above the NaCl deliquescence point and then after drying. These data suggested that upon drying, the original organic film becomes localized on one side of the particle, giving it an irregular shape, in much the same manner as observed for the effect of water on surface nitrate (Figs. 11.63 and 11.64). Similarly, the secondary electron yields indicated that mixtures of NaCl and $NaNO_3$ crystallized heterogeneously whereas those of NaCl and $NH_4Cl$ were homogeneously mixed (Ziemann and McMurray, 1997).

## 5. Generation of Calibration Aerosols

Calibration of the instruments to measure the size distribution and chemical composition requires methods of generating aerosols of well-defined sizes and known composition. Generating aerosols of known

characteristics, both physical and chemical, is also necessary for carrying out studies of aerosol effects (e.g., on health or visibility) under well-defined experimental conditions.

A monodisperse aerosol is one with a narrow size distribution, which, for log-normal-distributed particles, usually means a geometric standard deviation of about 1.2 or smaller. Monodisperse particles are expected to have simple shapes and uniform composition with respect to size. A polydisperse aerosol, on the other hand, is one containing a wide range of particle sizes, but which may otherwise be homogeneous in terms of the basic physical and chemical properties that are not related to size. The term heterodisperse is also used occasionally; this describes aerosols varying widely in physical and chemical characteristics, as well as size.

As discussed in detail by Raabe (1976), an investigator's use of the terms monodisperse and polydisperse aerosols may depend on the particular properties of importance in the study; thus an aerosol may consist of particles of the same size, that is, be monodisperse with respect to size, but may vary in settling speed due to variations in density, that is, be polydisperse with respect to settling speed.

There are a number of techniques for generating aerosols, and these are discussed in detail in the LBL report (1979) and in volumes edited by Willeke (1980) and Liu *et al.* (1984). We briefly review here the major methods currently in use; these include atomizers and nebulizers, vibrating orifices, spinning disks, the electrical mobility analyzer discussed earlier, dry powder dispersion, tube furnaces, and condensation of vapors from the gas phase.

### *a. Atomizers and Nebulizers*

Aerosols may be produced by atomizing liquids or suspensions of solids in liquids. Nebulizers are a type of atomizer in which both large and small particles are initially produced but in which the large particles are removed by impaction within the nebulizer. As a result, only particles with diameters $\lesssim 10\ \mu$m exit most nebulizers.

There are two basic means of generating particles from liquids in nebulizers: compressed air or ultrasonic vibration. Figure 11.76 shows one relatively simple type of compressed air nebulizer. The compressed air shoots out of a small orifice at high velocity, creating a reduced pressure in the region of the orifice; a feed tube connected to the liquid through a small opening is subjected to this region of lowered pressure (the Venturi effect) and hence liquid is drawn up from the reservoir and exits as a thin stream. The flow of high-velocity air striking the liquid stream breaks it up into small droplets and carries this aerosol toward the exit.

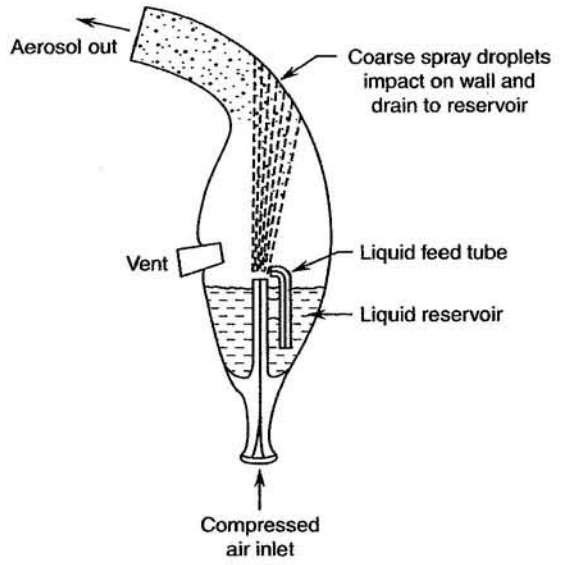


**FIGURE 11.76** Schematic diagram of compressed air nebulizer (from Hinds, 1982).

The larger droplets are removed by impaction on the curved wall, and the smaller particles exit the device. Detailed descriptions of other types of compressed air nebulizers that differ somewhat in design are found in Raabe (1976) and Hinds (1982).

These compressed air nebulizers produce polydisperse aerosols. After the aerosol is produced, the size distribution may change due to evaporation of liquid from the droplets. In addition, the particles may be electrically charged due to an ion imbalance in the droplets as they form; if such charges become further concentrated due to evaporation, the particle may break up into smaller particles. Thus electrical neutralization of the aerosol, for example, by exposure to a radioactive source, is usually necessary to prevent electrostatic effects from dominating the particle motion, coagulation, and other behavior.

Nebulization may be used to produce suspensions of liquid droplets in air by using the pure liquid as the fluid or by using liquids with low vapor pressures dissolved in volatile solvents that then evaporate off the particle. Suspensions of solid particles in air may also be generated using the nebulization of suspensions of insoluble materials (insoluble plastic particles suspended in organic solvents, aqueous colloidal suspensions, e.g., of ferric hydroxide, etc.) or of soluble materials dissolved in water (e.g., salts in water). Drying the aerosol after its generation is an important factor in the final aerosol produced since this may alter both the physical and chemical nature of the particles; for example, rapid drying may produce low-density particles that

are basically hollow shells formed by crystallization on the surface of the drying droplet.

Although these devices produce polydisperse aerosols, monodisperse aerosols can be generated by following the nebulizer with a size fractionating device such as an aerosol centrifuge or a differential mobility analyzer. Alternatively, nebulizers can be used to produce monodisperse aerosols of solid particles if suspensions of particles of one size are used as the generating fluid; for example, polystyrene and polyvinyltoluene latex beads of uniform size from 0.1 to 3.5 $\mu$m are commercially available in water suspensions. However, care must be taken to ensure that the vast majority of droplets formed contain only one sphere; otherwise, when the liquid evaporates, clusters of spheres will be formed. In addition, care must be taken to be sure they do not carry significant electrical charge (an anionic surfactant is added to the suspension to inhibit coagulation of the spheres). Finally, under some conditions, significant concentrations of other small particles may be simultaneously produced due to drying of empty droplets that contain impurities in the suspending liquid.

### *b. Vibrating-Orifice Generator*

Another common method of generating particles with diameters 0.5–50 $\mu$m is the Berglund–Liu (1973) vibrating-orifice generator shown schematically in Fig. 11.77. The solution to be aerosolized is pumped through a small orifice 5–20 $\mu$m in diameter. The orifice is oscillated by a piezoelectric crystal so that the liquid stream is broken on each oscillation, forming a small liquid particle that is carried away in a stream of air.

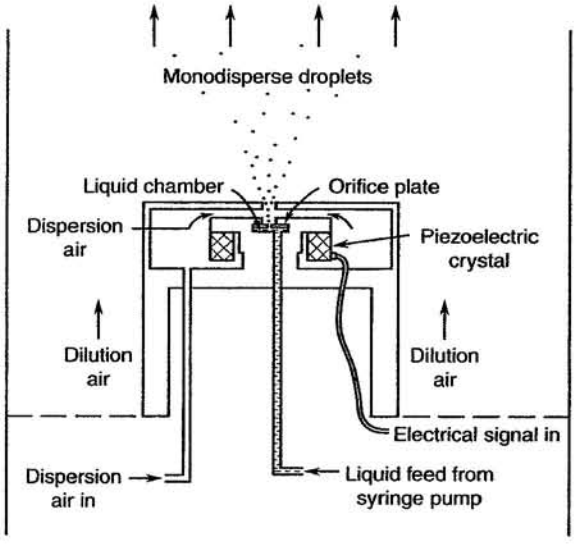


FIGURE 11.77 Schematic diagram of vibrating-orifice aerosol generator (from Hinds, 1982).

These droplets are then mixed with more air to dry the particles. The rate of droplet formation is equal to the oscillation frequency ($f$) of the piezoelectric crystal. From the volumetric flow rate of the liquid and the frequency $f$, the volume of the individual drops and particle diameter can be calculated.

### *c. Spinning-Disk Generator*

A third means of producing aerosols is the spinning-disk aerosol generator. The liquid is fed to the center of the spinning disk and then moves by centrifugal force to the outer edge. It accumulates at the edge until there is sufficient liquid that the centrifugal force exceeds the surface tension forces and a droplet of liquid is thrown off. Some smaller "satellite droplets" are also produced, but these are separated from the primary drops, which are thrown out further by using a flow of air. Monodisperse aerosols with diameters $\gtrsim 0.5$ $\mu$m, and more typically in the range $\sim$20–30 $\mu$m, are produced, the size being determined by the radius of the disk and the speed of the rotation (Hinds, 1982).

### *d. Dry Powder Dispersion*

When an aerosol consisting of solid particles is required, they are usually generated by the dispersion of a dry powder. One of the most common devices that is particularly effective for dry, hard materials such as silica is known as the Wright dust feed (Wright, 1950). The dust is packed into a plug and a sharp blade is used to scrape dust off the surface of the plug; the particles are then swept away by a stream of air along the outer edge of the scraper blade and exit through a jet onto an impactor to break up particle clusters. The aerosol produced has particle diameters $\leq 10$ $\mu$m. Variations on this type of aerosol generator are described in the LBL report (1979).

Fluidized beds have also been used for generating suspensions of solid particles with diameters in the range of $\sim$0.5–40 $\mu$m. Air flows through the fluidized bed, which contains beads kept suspended by the motion of the air; dust injected into the bed is broken up into small particles and carried out with the air flow (Raabe, 1976).

A device such as an impactor or cyclone is frequently used at the exit of these dry powder dispersion devices to eliminate the large particles. A charge neutralizer is usually used to reduce the electrostatic charges on the dispersed particles.

### *e. Tube Furnaces*

Monodisperse particles of salts, metals, metal oxides, and carbon have also been generated using electrically heated tube furnaces (e.g., Scheibel and

Porstendörfer, 1983; Ramamurthi and Leong, 1987). Salt particles, for example, can be generated by inserting the salt in a "boat" inside the tube furnace with a flow of $N_2$ passing over the salt. The salt vaporizes at the high temperatures and is carried downstream where the gas stream is cooled and the salt undergoes condensation into small particles.

Particles consisting of metals and metal derivatives such as the oxides can be generated in a two-step process. Primary aerosol particles are first generated using a vibrating-orifice generator and then dried by passing through a heated tube. This dried aerosol then passes into a tube furnace where the secondary aerosol is generated. For example, particles of nickel or nickel oxide can be generated from a primary aerosol of nickel formate using a tube furnace with $N_2$ or air as the carrier gas, respectively. Similarly, particles of ferric oxide or iron can be obtained from the thermal decomposition of ferrous sulfate heptahydrate in $N_2$ or in a mixture of $H_2/N_2$, respectively (Ramamurthi and Leong, 1987).

*f. Condensation*

When nuclei are present under conditions of supersaturation, condensation occurs on the nuclei, causing them to grow. If the particle radius is much less than the average distance between the particles, the growth rate of the particle with time is uniform, and since the nuclei are so much smaller than the final particles formed, nuclei of different initial sizes all give rise ultimately to particles of the same size, that is, a monodisperse aerosol, with diameters typically in the range 0.003–1.0 $\mu$m.

In practice then, a liquid having a low vapor pressure such as oleic acid or lubricating oils is carried by an inert gas to a heater where it vaporizes. As it leaves the heated area, it condenses to form the aerosol. Different generator designs based on condensation of a supersaturated vapor are discussed in the LBL report (1979).

However, care must be taken to ensure that seed nuclei are present on which condensation can occur. If a very clean system is used in which nuclei are not present, spontaneous nucleation may occur; this process is such that nuclei do not appear uniformly either in space or in time, and the initial particle growth rate depends on the degree of supersaturation. As a result, a polydisperse aerosol is produced under these conditions.

While condensation from a supersaturated vapor can be used to produce liquid particles, it is not as easily applied to the generation of solid particles except those that can be liquefied at modest elevated temperatures. However, these may be generated using different techniques. Methods used in the past have included the vaporization of wires or of salts fused onto wires, the use of "exploding" wires, and the use of electric arcs. For example, heating metal wires in an inert gas such as $N_2$ to a sufficiently high temperature produces small particles in the condensation nuclei and Aitken nuclei range. Thus tungsten wire at $\sim$1000–1200°C produces tungsten metal particles, whereas nichrome wire gives chromium particles.

Solid salt particles may be produced by fusing the salt onto the wire by immersing the wire in a saturated solution of the salt and passing an electrical current through it. When the wire is heated, salt particles are produced. Theoretical and practical considerations for such generators are described by Fuchs and Sutugin (1970).

The exploding wire method involves putting a large amount of energy into a wire suddenly, causing it to "explode." If $O_2$ is present, a metal oxide aerosol is produced, whereas particles of pure metal are formed in an inert atmosphere such as helium. Exploding wire generators and their size distribution characteristics have been discussed by Phalen (1972).

Finally, electric arcs have also been used in some cases to produce solid particles of the electrode material, such as graphite, as have argon plasmas at high temperatures which produce a finely divided aerosol on rapid cooling.

All these methods generally give ($\lesssim 1$ $\mu$m) polydisperse aerosols of the solid particles and, unless rapid air dilution is provided, coagulation leads to large agglomerates of the small primary particles.

Gas-phase reactions can also be used to produce products of low volatility that condense to give an aerosol. The reaction of gaseous $NH_3$ with HCl to form particles of solid ammonium chloride and the reaction of gaseous $SO_3$ with water vapor to form $H_2SO_4$ are typical examples. Such methods tend to give submicron particles.

## C. PROBLEMS

1. Chemiluminescence is useful as a monitoring technique in some cases. One of the requirements is that the excited state emit sufficiently fast that quenching does not completely overwhelm radiative processes.

a. Calculate the number of collisions per second of $NO_2$ in an excited state with air molecules at 1 atm pressure and 298 K. Assume the diameters of air and the excited state can both be taken as 0.40 nm.

b. Estimate the lifetime of the excited state if 10% of the excited molecules emit light rather than being

quenched by air and if the quenching occurs with a probability of one (i.e., on every collision).

c. What would your answer be for (b) if the quenching occurs with an efficiency of 1%?

2. Laser-induced fluorescence (LIF) is a technique commonly used to monitor OH in air. One approach discussed in this chapter to improving the signal-to-noise ratio is to lower the total pressure to reduce quenching of the excited OH. The lifetime of the emitting state of OH ($A^2\Sigma^+$) is about 700 ns and typical values (they depend on rotational level) of the quenching rate constants (in units of $10^{-10}$ $cm^3$ $molecules^{-1}$ $s^{-1}$) have been measured around room temperature to be 0.31 for $N_2$, 1.41 for $O_2$, and 4.1 for $CO_2$ (Copeland *et al.*, 1985; Copeland and Crosley, 1986; Crosley, 1989). What percentage of the excited OH emits rather than being quenched at 1 atm and 298 K? By what factor does this increase if the total pressure is $10^{-3}$ atm? Take all molecular diameters to be 0.40 nm.

3. (a) For the mixture of organics reported in Table 11.8 for urban atmospheres, what would you expect a total VOC analyzer to report for the organic concentration if the lowest values reported are used? What would it be if the highest values were used? (b) Repeat part (a) for the data given for remote areas and compare to your answer in (a).

4. Develop Eq. (N) starting from the differential equations for $NO_2$ and NO in the reaction system consisting of reactions (8) and (9).

5. As discussed in the chapter, UV–visible spectroscopy provides sensitive detection for many atmospheric gases. However, a criterion for applying DOAS is that the absorption have a banded structure. Why do so few molecules of interest have a detailed, banded structure in the UV–visible compared, for example, to their infrared spectra?

6. Reference infrared spectra are shown for $HNO_3$ and $NH_3$ in a 25-cm path cell in Fig. 11.4. By what factor are the concentrations increased over even the peak concentrations of these species observed in the ambient air spectra of Fig. 11.3?

7. Derive from first principles the expression for [OH] as a function of the measured $^{14}CO$ and $^{14}CO_2$ concentrations, OH + CO rate constant, and reaction time shown in Eq. (Q).

## References


Aker, P. M., and J.-X. Zhang, "Morphology-Dependent Stimulated Raman Scattering (MDSRS)," *J. Photochem. Photobiol. A: Chem., 80,* 381–388 (1994).

Alicke, B., K. Hebestreit, J. Stutz, and U. Platt, "Iodine Oxide in the Marine Boundary Layer," *Nature, 397,* 572–573 (1999).

Aliwell, S. R., and R. L. Jones, "Measurement of Atmospheric $NO_3$. 1. Improved Removal of Water Vapour Absorption Features in the Analysis for $NO_3$," *Geophys. Res. Lett., 23,* 2585–2588 (1996a).

Aliwell, S. R., and R. L. Jones, "Measurement of Atmospheric $NO_3$. 2. Diurnal Variation of Stratospheric $NO_3$ at Midlatitude," *Geophys. Res. Lett., 23,* 2589–2592 (1996b).

Aliwell, S. R., and R. L. Jones, "Measurements of Tropospheric $NO_3$ at Midlatitude," *J. Geophys. Res., 103,* 5719–5727 (1998).

Alkezweeny, A. J., G. L. Laws, and W. Jones, "Aircraft and Ground Measurements of Ammonia in Kentucky," *Atmos. Environ., 20,* 357–360 (1986).

Allen, D. T., and E. Palen, "Recent Advances in Aerosol Analysis by Infrared Spectroscopy," *J. Aerosol Sci., 20,* 441–455 (1989).

Allen, J., and R. K. Gould, "Mass Spectrometric Analyzer for Individual Aerosol Particles," *Rev. Sci. Instrum., 52,* 804–809 (1981).

Allen, T. M., D. Z. Bezabeh, C. H. Smith, E. M. McCauley, A. D. Jones, D. P. Y. Chang, I. M. Kennedy, and P. B. Kelly, "Speciation of Arsenic Oxides Using Laser Desorption/Ionization Time-of-Flight Mass Spectrometry," *Anal. Chem. A, 68,* 4052–4059 (1996).

Altshuller, A. P., and S. P. McPherson, "Spectrophotometric Analysis of Aldehydes in the Los Angeles Atmosphere," *J. Air Pollut. Control Assoc., 13,* 109–111 (1963).

Altshuller, A. P., "Ambient Air Hydroxyl Radical Concentrations: Measurements and Model Predictions," *JAPCA, 39,* 704–708 (1989).

Altshuller, A. P., "PANs in the Atmosphere," *J. Air Waste Manage. Assoc., 43,* 1221–1230 (1993).

Anderson, J. R., P. R. Buseck, and T. L. Patterson, "Characterization of the Bermuda Tropospheric Aerosol by Combined Individual-Particle and Bulk-Aerosol Analysis," *Atmos. Environ., 30,* 319–338 (1996).

Anderson, L. G., J. A. Lanning, and P. Wolfe, "Acetone in the Urban Atmosphere: A Study in Denver, Colorado," *Isr. J. Chem., 34,* 341–353 (1994).

Anderson, L. G., J. A. Lanning, R. Barrell, J. Miyagishima, R. H. Jones, and P. Wolfe, "Sources and Sinks of Formaldehyde and Acetaldehyde: An Analysis of Denver's Ambient Concentration Data," *Atmos. Environ., 30,* 2113–2123 (1996).

Andersson-Sköld, Y., J. Moldanova, and A. Lindskog, "Comparison of Simulated and Measured Concentrations of Ozone, PAN, and Organic Species—Influence of Chemical Activity and Emission Pattern," in *The Proceedings of EUROTRAC Symposium '92* (P. M. Borrel *et al.*, Eds.), pp. 433–436, SPB Academic Publishing BV, The Hague, The Netherlands, 1993.

Andreae, M. O., R. W. Talbot, and S.-M. Li, "Atmospheric Measurements of Pyruvic and Formic Acid," *J. Geophys. Res., 92,* 6635–6641 (1987).

Andrés-Hernández, M. D., J. Notholt, J. Hjorth, and O. Schrems, "A DOAS Study on the Origin of Nitrous Acid at Urban and Non-urban Sites," *Atmos. Environ., 30,* 175–180 (1996).

Anlauf, K. G., P. Fellin, H. A. Wiebe, H. I. Schiff, G. I. Mackay, R. S. Braman, and R. Gilbert, "A Comparison of Three Methods for Measurement of Atmospheric Nitric Acid and Aerosol Nitrate and Ammonium," *Atmos. Environ., 19,* 325–333 (1985).

Anlauf, K. G., H. A. Wiebe, and P. Fellin, "Characterization of Several Integrative Sampling Methods for Nitric Acid, Sulphur Dioxide, and Atmospheric Particles," *JAPCA, 36,* 715–723 (1986).

Anlauf, K. G., D. C. MacTavish, H. A. Wiebe, H. I. Schiff, and G. I. Mackay, "Measurement of Atmospheric Nitric Acid by the Filter Method and Comparisons with the Tuneable Diode Laser and Other Methods," *Atmos. Environ., 22,* 1579–1586 (1988).

Apel, E. C., J. G. Calvert, and F. C. Fehsenfeld, "The Nonmethane Hydrocarbon Intercomparison Experiment (NOMHICE): Tasks 1 and 2," *J. Geophys. Res., 99,* 16651–16664 (1994).

Apel, E. C., J. G. Calvert, R. Zika, M. O. Rodgers, V. P. Aneja, J. F. Meagher, and W. A. Lonneman, "Hydrocarbon Measurements during the 1992 Southern Oxidants Study Atlanta Intensive: Protocol and Quality Assurance," *J. Air Waste Manage. Assoc., 45,* 521–528 (1995).

Apel, E. C., J. G. Calvert, J. P. Greenberg, D. Riemer, R. Zika, T. E. Kleindienst, W. A. Lonneman, K. Fung, and E. Fujita, "Generation and Validation of Oxygenated Volatile Organic Carbon Standards for the 1995 Southern Oxidants Study Nashville Intensive," *J. Geophys. Res., 103,* 22281–22294 (1998a).

Apel, E. C., J. G. Calvert, D. Riemer, W. Pos, R. Zika, T. E. Kleindienst, W. A. Lonneman, K. Fung, E. Fujita, P. B. Shepson, T. K. Starn, and P. T. Roberts, "Measurements Comparison of Oxygenated Volatile Organic Compounds at a Rural Site during the 1995 SOS Nashville Intensive," *J. Geophys. Res., 103,* 22295–22316 (1998b).

Appel, B. R., W. Cheng, and F. Salaymeh, "Sampling of Carbonaceous Particles in the Atmosphere—II," *Atmos. Environ., 23,* 2167–2175 (1989).

Armerding, W., M. Spiekermann, and F. J. Comes, "OH Multipass Absorption: Absolute and *In Situ* Method for Local Monitoring of Tropospheric Hydroxyl Radicals," *J. Geophys. Res., 99,* 1225–1239 (1994).

Armerding, W., M. Spiekermann, J. Walter, and F. J. Comes, "MOAS: An Absorption Laser Spectrometer for Sensitive and Local Monitoring of Tropospheric OH and Other Trace Gases," *J. Atmos. Sci., 52,* 3381–3392 (1995).

Armerding, W., M. Spiekermann, J. Walter, and F. J. Comes, "Multipass Optical Absorption Spectroscopy: A Fast Scanning Laser Spectrometer for the *In-Situ* Determination of Atmospheric Trace Gas Components, in Particular OH," *Appl. Opt., 35,* 4206–4219 (1996).

Armerding, W., F. J. Comes, H. J. Crawack, O. Forberich, G. Gold, R. Ruger, M. Spiekermann, J. Walter, E. Cuevas, A. Redondas, R. Schmitt, and P. Matuska, "Testing the Daytime Oxidizing Capacity of the Troposphere: 1994 OH Field Campaign at the Izana Observatory, Tenerife," *J. Geophys. Res., 102,* 10603–10611 (1997).

Arnold, F., D. Krankowsky, and K. H. Marien, "First Mass Spectrometric Measurements of Positive Ions in the Stratosphere," *Nature, 267,* 30–31 (1977).

Arnold, F., and G. Hauck, "Lower Stratosphere Trace Gas Detection Using Aircraft-Borne Active Chemical Ionization Mass Spectrometry," *Nature, 315,* 307–309 (1985).

Arnold, F., K.-H. Wohlfrom, M. W. Klemm, J. Schneider, K. Gollinger, U. Schumann, and R. Busen, "First Gaseous Ion Composition Measurements in the Exhaust Plume of a Jet Aircraft in Flight: Implications for Gaseous Sulfuric Acid, Aerosols, and Chemiions," *Geophys. Res. Lett., 25,* 2137–2140 (1998).

Arnts, R. R., and S. B. Tejada, "2,4-Dinitrophenylhydrazine-Coated Silica Gel Cartridge Method for Determination of Formaldehyde in Air: Identification of an Ozone Interference," *Environ. Sci. Technol., 23,* 1428–1430 (1989).

Atkinson, R., A. M. Winer, and J. N. Pitts, Jr., "Estimation of Nighttime $N_2O_5$ Concentrations from Ambient $NO_2$ and $NO_3$ Radical Concentrations and the Role of $N_2O_5$ in Nighttime Chemistry," *Atmos. Environ., 20,* 331–339 (1986).

Atlas, E., and S. Schauffler, "Analysis of Alkyl Nitrates and Selected Halocarbons in the Ambient Atmosphere Using a Charcoal Preconcentration Technique," *Environ. Sci. Technol., 25,* 61–67 (1991).

Atlas, E. L., B. A. Ridley, G. Hubler, J. G. Walega, M. A. Carroll, D. D. Montzka, B. J. Huebert, R. B. Norton, F. E. Grahek, and S. Schauffler, "Partitioning and Budget of $NO_y$ Species during the Mauna Loa Observatory Photochemistry Experiment," *J. Geophys. Res., 97,* 10449–10462 (1992).

Ayer, H. E., and J. M. Hochstrasser, "Cyclone Discussion," in *Aerosol Measurement* (D. A. Lundgren, F. S. Harris, Jr., W. H. Marlow, M. Lippmann, W. E. Clark, and M. D. Durham, Eds.), pp. 70–79, University Presses of Florida, Gainesville, FL, 1979.

Ayers, G. P., S. A. Penkett, R. W. Gillett, B. Bandy, I. E. Galbally, C. P. Meyer, C. M. Elsworth, S. T. Bentley, and B. W. Forgan, "The Annual Cycle of Peroxides and Ozone in Marine Air at Cape Grim, Tasmania," *J. Atmos. Chem., 23,* 221–252 (1996).

Baardsen, E. L., and R. W. Terhune, "Detection of OH in the Atmosphere Using a Dye Laser," *Appl. Phys. Lett., 21,* 209–211 (1972).

Baez, A. P., R. D. Belmont, O. G. Gonzalez, and I. P. Rosas, "Formaldehyde Levels in Air and Wet Precipitation at Mexico City, Mexico," *Environ. Pollut., 62,* 153–169 (1989).

Balasubramanian, R., and L. Husain, "Observations of Gas-Phase Hydrogen Peroxide at an Elevated Rural Site in New York," *J. Geophys. Res., 102,* 21209–21220 (1997).

Bandy, A. R., D. C. Thornton, and A. R. Driedger III, "Airborne Measurements of Sulfur Dioxide, Dimethyl Sulfide, Carbon Disulfide, and Carbonyl Sulfide by Isotope Dilution Gas Chromatography/Mass Spectrometry," *J. Geophys. Res., 98,* 23423–23433 (1993).

Baron, P. A., M. K. Mazumder, and Y. S. Cheng, "Direct-Reading Techniques Using Optical Particle Detection," in *Aerosol Measurement: Principles, Techniques, and Applications* (K. Willeke and P. A. Baron, Eds.), pp. 381–409, Van Nostrand Reinhold, New York, 1993.

Beck, S. M., R. J. Bendura, D. S. McDougal, J. M. Hoell, Jr., G. L. Gregory, H. J. Curfman, Jr., D. D. Davis, J. Bradshaw, M. O. Rodgers, C. C. Wang, L. I. Davis, M. J. Campbell, A. L. Torres, M. A. Carroll, B. A. Ridley, G. W. Sachse, G. F. Hill, E. P. Condon, and R. A. Rasmussen, "Operational Overview of NASA GTE/CITE 1 Airborne Instrument Intercomparisons: Carbon Monoxide, Nitric Oxide, and Hydroxyl Instrumentation," *J. Geophys. Res., 92,* 1977–1985 (1987).

Beine, H. J., D. A. Jaffe, D. R. Blake, E. Atlas, and J. Harris, "Measurements of PAN, Alkyl Nitrates, Ozone, and Hydrocarbons during Spring in Interior Alaska," *J. Geophys. Res., 101,* 12613–12619 (1996).

Beine, H. J., D. A. Jaffe, J. A. Herring, J. A. Kelley, T. Krognes, and F. Stordal, "High-Latitude Springtime Photochemistry. Part I: $NO_x$, PAN, and Ozone Relationships," *J. Atmos. Chem., 27,* 127–153 (1997).

Benner, R. L., and D. H. Stedman, "Field Evaluation of the Sulfur Chemiluminescence Detector," *Environ. Sci. Technol., 24,* 1592–1596 (1990).

Bennett, M., C. Rogers, and S. Sutton, "Mobile Measurements of Winter $SO_2$ Levels in London, 1983–84," *Atmos. Environ., 20,* 461–470 (1986).

Benning, L., and A. Wahner, "Measurements of Atmospheric Formaldehyde (HCHO) and Acetaldehyde ($CH_3CHO$) during POPCORN 1994 Using 2,4-DNPH Coated Silica Cartridges," *J. Atmos. Chem., 31,* 105–117 (1998).

Benter, T., M. Liesner, V. Sauerland, and R. N. Schindler, "Mass Spectrometric *In-Situ* Determination of $NO_2$ in Gas Mixtures by Resonance Enhanced Multiphoton Ionization," *Fresenius' J. Anal. Chem., 351,* 489–492 (1995).

Bentz, J. W. G., M. Fichtner, J. Goschnick, and H.-J. Ache, "Depth-Resolved Speciation of Nitrogen Compounds in Environmental Solids," *Fresenius' J. Anal. Chem., 349,* 205–207 (1994).

Bentz, J. W. G., J. Goschnick, J. Schuricht, and H. J. Ache, "Depth-Resolved Investigation of the Element and Compound Inventory of Aerosol Particles from Outdoor Air," *Fresenius J. Anal. Chem., 353,* 559–564 (1995a).

Bentz, J. W. G., J. Goschnick, J. Schuricht, H. J. Ache, J. Zehnpfennig, and A. Benninghoven, "Analysis and Classification of Individual Outdoor Aerosol Particles with SIMS Time-of-Flight Mass Spectrometry," *Fresenius' J. Anal. Chem., 353,* 603–608 (1995b).

Berglund, R. N., and B. Y. H. Liu, "Generation of Monodisperse Aerosol Standards," *Environ. Sci. Technol., 7,* 147–153 (1973).

Berico, M., A. Luciani, and M. Formignani, "Atmospheric Aerosol in an Urban Area—Measurements of TSP and PM10 Standards and Pulmonary Deposition Assessments," *Atmos. Environ., 31,* 3659–3665 (1997).

Berkowitz, C. M., J. D. Fast, S. Springston, J. M. Hubbe, R. A. Plastridge, R. Larson, C. W. Spicer, and P. Doskey, "Formation Mechanisms and Chemical Characteristics of Elevated Photochemical Layers over the Northeast United States," *J. Geophys. Res., 103,* 10631–10647 (1998).

Bernardo-Bricker, A., C. Farmer, P. Milne, D. Riemer, R. Zika, and C. Stoneking, "Validation of Speciated Nonmethane Hydrocarbon Compound Data Collected during the 1992 Atlanta Intensive as Part of the Southern Oxidants Study (SOS)," *J. Air Waste Manage. Assoc., 45,* 591–603 (1995).

Bezabeh, D. Z., T. M. Allen, E. M. McCauley, P. B. Kelly, and A. D. Jones, "Negative Ion Laser Desorption Ionization Time-of-Flight Mass Spectrometry of Nitrated Polycyclic Aromatic Hydrocarbons," *J. Am. Soc. Mass Spectrom., 8,* 630–636 (1997).

Biermann, H. W., E. C. Tuazon, A. M. Winer, T. J. Wallington, and J. N. Pitts, Jr., "Simultaneous Absolute Measurements of Gaseous Nitrogen Species in Urban Ambient Air by Long Pathlength Infrared and Ultraviolet–Visible Spectroscopy," *Atmos. Environ., 22,* 1545–1554 (1988).

Blake, D. R., T. W. Smith, Jr., T.-Y. Chen, W. J. Whipple, and F. S. Rowland, "Effects of Biomass Burning on Summertime Nonmethane Hydrocarbon Concentrations in the Canadian Wetlands," *J. Geophys. Res., 99,* 1699–1719 (1994).

Blake, N. J., S. A. Penkett, K. C. Clemitshaw, P. Anwyl, P. Lightman, A. R. W. Marsh, and G. Butcher, "Estimates of Atmospheric Hydroxyl Radical Concentrations from the Observed Decay of Many Reactive Hydrocarbons in Well-Defined Urban Plumes," *J. Geophys. Res., 98,* 2851–2864 (1993).

Blanchard, P., P. B. Shepson, K. W. So, H. I. Schiff, J. W. Bottenheim, A. J. Gallant, J. W. Drummond, and P. Wong, "A Comparison of Calibration and Measurement Techniques for Gas Chromatographic Determination of Atmospheric Peroxyacetyl Nitrate (PAN)," *Atmos. Environ., 24A,* 2839–2846 (1990).

Blomquist, B. W., A. R. Bandy, D. C. Thornton, and S. Chen, "Grab Sampling for the Determination of Sulfur Dioxide and Dimethyl Sulfide in Air by Isotope Dilution Gas Chromatography/Mass Spectrometry," *J. Atmos. Chem., 16,* 23–30 (1993).

Boatman, J. F., M. Luria, C. C. Van Valin, and D. L. Wellman, "Continuous Atmospheric Sulfur Gas Measurements Aboard an Aircraft: A Comparison between the Flame Photometric and Fluorescence Methods," *Atmos. Environ., 22,* 1949–1955 (1988).

Boesl, U., H. J. Neusser, and E. W. Schlag, "Visible and UV Multiphoton Ionization and Fragmentation of Polyatomic Molecules," *J. Chem. Phys., 72,* 4327–4333 (1980).

Boleij, J. S. M., E. Lebret, F. Hoek, D. Noy, and B. Brunekreef, "The Use of Palmes Diffusion Tubes for Measuring $NO_2$ in Homes," *Atmos. Environ., 20,* 597–600 (1986).

Bottenheim, J. W., and M. F. Shepherd, "$C_2$–$C_6$ Hydrocarbon Measurements at Four Rural Locations across Canada," *Atmos. Environ., 29,* 647–664 (1995).

Boudries, H., G. Toupance, and A. L. Dutot, "Seasonal Variation of Atmospheric Nonmethane Hydrocarbons on the Western Coast of Brittany, France," *Atmos. Environ., 28,* 1095–1112 (1994).

Bradshaw, J. D., M. O. Rodgers, S. T. Sandholm, S. KeSheng, and D. D. Davis, "A Two-Photon Laser-Induced Fluorescence Field Instrument for Ground-Based and Airborne Measurements of Atmospheric NO," *J. Geophys. Res., 90,* 12861–12873 (1985).

Bradshaw, J., S. Sandholm, and R. Talbot, "An Update on Reactive Odd-Nitrogen Measurements Made during Recent NASA Global Tropospheric Experiment Programs," *J. Geophys. Res., 103,* 19129–19148 (1998).

Braman, R. S., T. J. Shelley, and W. A. McClenny, "Tungstic Acid for Preconcentration and Determination of Gaseous and Particulate Ammonia and Nitric Acid in Ambient Air," *Anal. Chem., 54,* 358–364 (1982).

Brandenburger, U., T. Brauers, H.-P. Dorn, M. Hausmann, and D. H. Ehhalt, "*In-Situ* Measurements of Tropospheric Hydroxyl Radicals by Folded Long-Path Laser Absorption during the Field Campaign POPCORN," *J. Atmos. Chem., 31,* 181–204 (1998).

Brassington, D. J., "Tunable Diode Laser Absorption Spectroscopy for the Measurement of Atmospheric Species," in *Spectroscopy in Environmental Science* (R. J. H. Clark and R. E. Hester, Eds.), pp. 85–148, Wiley, New York, 1995.

Brauer, M., and J. R. Brook, "Personal and Fixed-Site Ozone Measurements with a Passive Sampler," *Air Waste Manage. Assoc., 45,* 529–537 (1995).

Brauer, M., and J. Hisham-Hashim, "Fires in Indonesia: Crisis and Reaction," *Environ. Sci. Technol.,* 404A–407A, September 1 (1998).

Brauers, T., H.-P. Dorn, and U. Platt, in *Physico-Chemical Behaviour of Atmospheric Pollutants, Proceedings of the 5th European Symp., Varese, Italia* (G. Angeletti, Ed.), pp. 237–242, Kluwer Academic, Dordrecht, 1990.

Brauers, T., M. Hausmann, U. Brandenburger, and H.-P. Dorn, "Improvement of Differential Optical Absorption Spectroscopy with a Multichannel Scanning Technique," *Appl. Opt., 34,* 4472–4479 (1995).

Brauers, T., U. Aschmutat, U. Brandenburger, H.-P. Dorn, M. Hausmann, M. Beßling, A. Hofzumahaus, F. Holland, C. Plass-Dülmer, and D. H. Ehhalt, "Intercomparison of Tropospheric OH Radical Measurements by Multiple Folded Long-Path Laser Absorption and Laser Induced Fluorescence," *Geophys. Res. Lett., 23,* 2545–2548 (1996).

Brenninkmeijer, C. A. M., M. R. Manning, D. C. Lowe, G. Wallace, R. J. Sparks, and A. Volz-Thomas, "Interhemispheric Asymmetry in OH Abundance Inferred from Measurements of Atmospheric $^{14}CO$," *Nature, 356,* 50–52 (1992).

Brook, J. R., T. F. Dann, and R. T. Burnett, "The Relationship among TSP, $PM_{10}$, $PM_{2.5}$, and Inorganic Constituents of Atmospheric Particulate Matter at Multiple Canadian Locations," *J. Air Waste Manage. Assoc., 47,* 2–19 (1997).

Brown, R. H., and C. J. Purnell, "Collection and Analysis of Trace Organic Vapor Pollutants in Ambient Atmospheres. The Performance of a Tenax-GC Absorbent Tube," *J. Chromatogr., 178,* 79–90 (1979).

Brune, W. H., I. C. Faloona, D. Tan, A. J. Weinheimer, T. Campos, B. A. Ridley, S. A. Vay, J. E. Collins, G. W. Sachse, L. Jaeglé, and D. J. Jacob, "Airborne *In-Situ* OH and $HO_2$ Observations in the Cloud-Free Troposphere and Lower Stratosphere during SUCCESS," *Geophys. Res. Lett., 25,* 1701–1704 (1998).

Bruynseels, F., H. Storms, T. Tavares, and R. Van Grieken, "Characterization of Individual Particle Types in Coastal Air by Laser Microprobe Mass Analysis," *Int. J. Environ. Anal. Chem., 23,* 1–14 (1985).

Buhr, M. P., D. D. Parrish, R. B. Norton, F. C. Fehsenfeld, R. E. Sievers, and J. M. Roberts, "Contribution of Organic Nitrates to the Total Reactive Nitrogen Budget at a Rural Eastern U.S. Site," *J. Geophys. Res., 95,* 9809–9816 (1990).

Buhr, S. M., M. P. Buhr, F. C. Fehsenfeld, J. S. Holloway, U. Karst, R. B. Norton, D. D. Parrish, and R. E. Sievers, "Development of a Semi-Continuous Method for the Measurement of Nitric Acid Vapor and Particulate Nitrate and Suflate," *Atmos. Environ., 29,* 2609–2624 (1995).

Burkhardt, M. R., N. I. Maniga, D. H. Stedman, and R. J. Paur, "Gas Chromatographic Method for Measuring Nitrogen Dioxide and Peroxyacetyl Nitrate in Air without Compressed Gas Cylinders," *Anal. Chem., 60,* 816–819 (1988).

Burnett, C. R., and E. B. Burnett, "Spectroscopic Measurements of the Vertical Column Abundance of Hydroxyl (OH) in the Earth's Atmosphere," *J. Geophys. Res., 86,* 5185–5202 (1981).

Burnett, C. R., K. R. Minschwaner, and E. B. Burnett, "Vertical Column Abundance Measurements of Atmospheric Hydroxyl from 26°, 40°, and 65°N," *J. Geophys. Res., 93,* 5241–5253 (1988).

Burnett, C. R., and E. B. Burnett, "The Regime of Decreased OH Vertical Column Abundances at Fritz Peak Observatory, CO: 1991–1995," *Geophys. Res. Lett., 23,* 1925–1927 (1996).

Burnett, C. R., and K. Minschwaner, "Continuing Development in the Regime of Decreased Atmospheric Column OH at Fritz Peak, Colorado," *Geophys. Res. Lett., 25,* 1313–1316 (1998).

Burtscher, H., and A. Schmidt-Ott, "*In Situ* Measurement of Adsorption and Condensation of a Polyaromatic Hydrocarbon on Ultrafine C Particles by Means of Photoemission," *J. Aerosol Sci., 17,* 699–703 (1986).

Cadle, S. H., P. J. Groblicki, and P. A. Mulawa, "Problems in the Sampling and Analysis of Carbon Particulate," *Atmos. Environ., 17,* 593–600 (1983).

Cadle, S. H., and P. A. Mulawa, "The Retention of $SO_2$ by Nylon Filters," *Atmos. Environ., 21,* 599–603 (1987).

Cahill, T. A., "Comments on Surface Coatings for Lundgren-Type Impactors," in *Aerosol Measurement* (D. A. Lundgren, F. S. Harris, Jr., W. H. Marlow, M. Lippmann, W. E. Clark, and M. D. Dunham, Eds.), pp. 131–134, University Presses of Florida, Gainesville, FL, 1979.

Cahill, T. A., "Proton Microprobes and Particle-Induced X-Ray Analytical Systems," *Annu. Rev. Nucl. Part. Sci., 30,* 211–252 (1980).

Cahill, T. A., "Innovative Aerosol Sampling Devices Based Upon PIXE Capabilities," *Nucl. Instrum. Methods, 181,* 473–480 (1981a).

Cahill, T. A., "Ion Beam Analysis of Environmental Samples," *Adv. Chem. Ser., 197,* 511–522 (1981b).

Calogirou, A., M. Duane, D. Kotzias, M. Lahaniati, and B. R. Larsen, "Polyphenylenesulfide, Noxon, an Ozone Scavenger for the Analysis of Oxygenated Terpenes in Air," *Atmos. Environ., 31,* 2741–2751 (1997).

Camel, V., and M. Caude, "Trace Enrichment Methods for the Determination of Organic Pollutants in Ambient Air," *J. Chromatogr. A, 710,* 3–19 (1995).

Campbell, M. J., J. C. Sheppard, and B. F. Au, "Measurement of Hydroxyl Concentration in Boundary Layer Air by Monitoring CO Oxidation," *Geophys. Res. Lett., 6,* 175–178 (1979).

Campbell, M. J., B. D. Hall, J. C. Sheppard, P. L. Utley, R. J. O'Brien, T. M. Hard, and L. A. George, "Intercomparison of Local Hydroxyl Measurements by Radiocarbon and FAGE Techniques," *J. Atmos. Sci., 52,* 3421–3427 (1995).

Campos, F. X., Y. Jiang, and E. R. Grant, "Triple-Resonance Spectroscopy of the Higher Excited States of $NO_2$: Rovibronic Interactions, Autoionization, and *J*-Uncoupling in the (100) Manifold," *J. Chem. Phys., 93,* 2308–2327 (1990).

Cantrell, C. A., and D. H. Stedman, "A Possible Technique for the Measurement of Atmospheric Peroxy Radicals," *Geophys. Res. Lett., 9,* 846–849 (1982).

Cantrell, C. A., D. H. Stedman, and G. J. Wendel, "Measurement of Atmospheric Peroxy Radicals by Chemical Amplification," *Anal. Chem., 56,* 1496–1502 (1984).

Cantrell, C. A., R. E. Shetter, J. A. Lind, A. H. McDaniel, and J. G. Calvert, "An Improved Chemical Amplifier Technique for Peroxy Radical Measurements," *J. Geophys. Res., 98,* 2897–2909 (1993).

Cantrell, C. A., R. E. Shetter, and J. Calvert, "Peroxy Radical Chemistry during FIELDVOC 1993 in Brittany, France," *Atmos. Environ., 30,* 3947–3957 (1996).

Cantrell, C. A., R. E. Shetter, J. G. Calvert, F. L. Eisele, and D. J. Tanner, "Some Considerations of the Origin of Nighttime Peroxy Radicals Observed in MLOPEX 2c," *J. Geophys. Res., 102,* 15899–15913 (1997a).

Cantrell, C. A., R. E. Shetter, J. G. Calvert, F. L. Eisele, E. Williams, K. Baumann, W. H. Brune, P. S. Stevens, and J. H. Mather, "Peroxy Radicals from Photostationary State Deviations and Steady State Calculations during the Tropospheric OH Photochemistry Experiment at Idaho Hill, Colorado, 1993," *J. Geophys. Res., 102,* 6369–6378 (1997b).

Cao, X.-L., and C. N. Hewitt, "Build-up of Artifacts on Adsorbents during Storage and Its Effect on Passive Sampling and Gas Chromatography-Flame Ionization Detection of Low Concentrations of Volatile Organic Compounds in Air," *J. Chromatogr. A, 688,* 368–374 (1994).

Carpenter, L. J., P. S. Monks, B. J. Bandy, S. A. Penkett, I. E. Galbally, and C. P. Meyer, "A Study of Peroxy Radicals and Ozone Photochemistry at Coastal Sites in the Northern and Southern Hemispheres," *J. Geophys. Res., 102,* 25417–25427 (1997).

Carroll, M. A., and L. Emmons, "Access $NO_x$ and $NO_y$ Measurements On-Line," *EOS, 77,* 34 (1996).

Carslaw, N., L. J. Carpenter, J. M. C. Plane, B. J. Allan, R. A. Burgess, K. C. Clemitshaw, H. Coe, and S. A. Penkett, "Simultaneous Observations of Nitrate and Peroxy Radicals in the Marine Boundary Layer," *J. Geophys. Res., 102,* 18917–18933 (1997a).

Carslaw, N., J. M. C. Plane, H. Coe, and E. Cuevas, "Observations of the Nitrate Radical in the Free Troposphere at Izana de Tenerife," *J. Geophys. Res., 102,* 10613–10622 (1997b).

Carson, P. G., K. R. Neubauer, M. V. Johnston, and A. S. Wexler, "On-Line Chemical Analysis of Aerosols by Rapid Single-Particle Mass Spectrometry," *J. Aerosol Sci., 26,* 535–545 (1995).

Carson, P. G., M. V. Johnston, and A. S. Wexler, "Real-Time Monitoring of the Surface and Total Composition of Aerosol Particles," *Aerosol Sci. Technol., 26,* 291–300 (1997a).

Carson, P. G., M. V. Johnston, and A. S. Wexler, "Laser Desorption/Ionization of Ultrafine Aerosol Particles," *Rapid Commun. Mass Spectrosc., 11,* 993–996 (1997b).

Cass, G. R., M. H. Conklin, J. J. Shah, J. J. Huntzicker, and E. S. Macias, "Elemental Carbon Concentrations: Estimation of and Historical Data Base," *Atmos. Environ., 18,* 153–162 (1983).

Castaldi, M. J., and S. M. Senkan, "Real-Time, Ultrasensitive Monitoring of Air Toxics by Laser Photoionization Time-of-Flight Mass Spectrometry," *J. Air Waste Manage. Assoc., 48,* 77–81 (1998).

Chan, C. Y., T. M. Hard, A. A. Mehrabzadeh, L. A. George, and R. J. O'Brien, "Third-Generation FAGE Instrument for Tropospheric Hydroxyl Radical Measurement," *J. Geophys. Res., 95,* 18569–18576 (1990).

Chan, W. H., D. B. Orr, and D. H. S. Chung, "An Evaluation of Artifact $SO_4^{2-}$ Formation on Nylon Filters under Field Conditions," *Atmos. Environ., 20,* 2397–2401 (1986).

Chan, Y. C., R. W. Simpson, G. H. McTainsh, and P. D. Vowles, "Characterisation of Chemical Species in $PM_{2.5}$ and $PM_{10}$ Aerosols in Brisbane, Australia," *Atmos. Environ., 31,* 3773–3785 (1997).

Chapman, E., K. Busness, J. Thorp, D. V. Kenny, and C. W. Spicer, "Continuous Airborne Measurements of Gaseous Formic and Acetic Acids over the Western North Atlantic," *Geophys. Res. Lett., 22,* 405–408 (1995).

Chien, C.-J., M. J. Charles, K. G. Sexton, and H. E. Jeffries, "Analysis of Airborne Carboxylic Acids and Phenols as Their Pentafluorobenzyl Derivatives: Gas Chromatography/Ion Trap Mass Spectrometry with a Novel Chemical Ionization Reagent, PFBOH," *Environ. Sci. Technol., 32,* 299–309 (1998).

Chow, J. C., "Measurement of Methods to Determine Compliance with Ambient Air Quality Standards for Suspended Particles," *J. Air Waste Manage. Assoc., 45,* 320–382 (1995).

Cicerone, R. J., and R. Zellner, "The Atmospheric Chemistry of Hydrogen Cyanide (HCN)," *J. Geophys. Res., 88,* 10689–10696 (1983).

Claiborn, C. S., and V. P. Aneja, "Measurements of Atmospheric Hydrogen Peroxide in the Gas Phase and in Cloud Water at Mt. Mitchell, North Carolina," *J. Geophys. Res., 96,* 18771–18787 (1991).

Clarkson, T. S., R. J. Martin, and J. Rudolph, "Ethane and Propane in the Southern Marine Troposphere," *Atmos. Environ., 31,* 3763–3771 (1997).

Clausen, P. A., and P. Wolkoff, "Degradation Products of Tenax TA Formed during Sampling and Thermal Desorption Analysis: Indicators of Reactive Species Indoors," *Atmos. Environ., 31,* 715–725 (1997).

Clemitshaw, K. C., L. J. Carpenter, S. A. Penkett, and M. E. Jenkin, "A Calibrated Peroxy Radical Chemical Amplifier for Ground-Based Tropospheric Measurements," *J. Geophys. Res., 102,* 25405–25416 (1997).

Cofer, W. R., III, and R. A. Edahl, Jr., "A New Technique for Collection, Concentration, and Determination of Gaseous Tropospheric Formaldehyde," *Atmos. Environ., 20,* 979–984 (1986).

Coffey, M. T., W. G. Mankin, and R. J. Cicerone, "Spectroscopic Detection of Stratospheric Hydrogen Cyanide," *Science, 214,* 333–335 (1981).

Conner, W. D., "An Inertial-Type Particle Separator for Collecting Large Samples," *J. Air Pollut. Control Assoc., 16,* 35–38 (1966).

Cooke, D. D., and M. Kerker, "Response Calculations for Light Scattering Aerosol Particle Counters," *Appl. Opt., 14,* 734–739 (1975).

Copeland, R. A., M. J. Dyer, and D. R. Crosley, "Rotational-Level-Dependent Quenching of $A^2\Sigma^+$ OH and OD," *J. Chem. Phys., 82,* 4022–4032 (1985).

Copeland, R. A., and D. R. Crosley, "Temperature Dependent Electronic Quenching of OH($A^2\Sigma^+$, $v' = 0$) between 230 and 310 K," *J. Chem. Phys., 84,* 3099–3105 (1986).

Corkum, R., W. W. Biesbrecht, T. Bardsley, and E. A. Cherniak, "Peroxyacetyl Nitrate (PAN) in the Atmosphere at Simcoe, Canada," *Atmos. Environ., 20,* 1241–1248 (1986).

Cox, X. B., and R. W. Linton, "Particle Analysis by X-Ray Photoelectron Spectroscopy," in *Physical and Chemical Characterization of Individual Airborne Particles* (K. R. Spurny, Ed.), Chap. 18, pp. 341–357, Ellis Horwood, Chichester, 1986.

Crosley, D. R., "Rotational and Translational Effects in Collisions of Electronically Excited Diatomic Hydrides," *J. Phys. Chem., 93,* 6273–6282 (1989).

Crosley, D. R., "Local Measurement of Tropospheric $HO_x$," in *NASA Conference Publication 3245*, Summary of Workshop Held at SRI International, Menlo Park, California, 1994.

Crosley, D. R., "The Measurement of OH and $HO_2$ in the Atmosphere," *J. Atmos. Sci., 52,* 3299–3314 (1995a).

Crosley, D. R., "Laser Fluorescence Detection of Atmospheric Hydroxyl Radicals," in *Problems and Progress in Atmospheric Chemistry* (J. R. Barker, Ed.), *Advanced Series in Physical Chemistry* (C.-Y. Ng, Ed.), Vol. 3, World Scientific, Singapore, 1995b.

Crosley, D. R., "$NO_y$ Blue Ribbon Panel," *J. Geophys. Res., 101,* 2049–2052 (1996).

Cunningham, P. T., B. D. Holt, S. A. Johnson, D. L. Drapcho, and R. Kumar, "Acidic Aerosols: Oxygen-18 Studies of Formation and Infrared Studies of Occurrence and Neutralization," in *Chemistry of Particles, Fogs, and Rain* (J. L. Durham, Ed.), Acid Precipitation Series (J. I. Teasley, Series Ed.), pp. 53–130, Butterworth, Stoneham, MA, 1984.

Dale, J. M., M. Yang, W. B. Whitten, and J. M. Ramsey, "Chemical Characterization of Single Particles by Laser Ablation/Desorption in a Quadrupole Ion Trap Mass Spectrometer," *Anal. Chem., 66,* 3431–3435 (1994).

Damrauer, L., "Luminol-Based Nitrogen Dioxide Detector," *Anal. Chem., 55,* 937–940 (1983).

Das, M., and V. P. Aneja, "Analysis of Gaseous Hydrogen Peroxide Concentrations in Raleigh, North Carolina," *J. Air Waste Manage. Assoc., 44,* 176–180 (1994).

Dasgupta, P. K., and V. K. Gupta, "Membrane-Based Flow Injection System for Determination of Sulfur(IV) in Atmospheric Water," *Environ. Sci. Technol., 20,* 524–526 (1986).

Dasgupta, P. K., S. Dong, H. Hwang, H.-C. Yang, and Z. Genfa, "Continuous Liquid-Phase Fluorometry Coupled to a Diffusion Scrubber for the Real-Time Determination of Atmospheric Formaldehyde, Hydrogen Peroxide, and Sulfur Dioxide," *Atmos. Environ., 22,* 949–964 (1988).

Dasgupta, P. K., S. Dong, and H. Hwang, "Diffusion Scrubber-Based Field Measurements of Atmospheric Formaldehyde and Hydrogen Peroxide," *Aerosol Sci. Technol., 12,* 98–104 (1990).

Daum, P. H., L. I. Kleinman, A. J. Hills, A. L. Lazrus, A. C. D. Leslie, K. Busness, and J. Boatman, "Measurement and Interpretation of Concentrations of $H_2O_2$ and Related Species in the Upper Midwest during Summer," *J. Geophys. Res., 95,* 9857–9871 (1990).

Davenport, J. E., and H. B. Singh, "Systematic Development of Reactive Tracer Technology to Determine Hydroxyl Radical Concentrations in the Troposphere," *Atmos. Environ., 21,* 1969–1981 (1987).

Davis, E. J., "A History of Single Aerosol Particle Levitation," *Aerosol Sci. Technol., 26,* 212–254 (1997).

Davis, W. D., "Continuous Mass Spectrometric Analysis of Particulates by Use of Surface Ionization," *Environ. Sci. Technol., 11,* 587–592 (1977a).

Davis, W. D., "Continuous Mass Spectrometric Determination of Concentration of Particulate Impurities in Air by Use of Surface Ionization," *Environ. Sci. Technol., 11,* 593–596 (1977b).

Dawson, G. A., and J. C. Farmer, "Soluble Atmospheric Trace Gases in the Southwestern United States. 2. Organic Species HCHO, HCOOH, $CH_3COOH$," *J. Geophys. Res., 93,* 5200–5206 (1988).

Delumyea, R. G., L.-C. Chu, and E. S. Macias, "Determination of Elemental Carbon Component of Soot in Ambient Aerosol Samples," *Atmos. Environ., 14,* 647–652 (1980).

De Haan, D., T. Brauers, K. Oum, J. Stutz, T. Nordmeyer, and B. J. Finlayson-Pitts, "Heterogeneous Chemistry in the Troposphere: Experimental Approaches and Applications to the Chemistry of Sea Salt Particles," *Int. Rev. Phys. Chem., 18,* (1999).

DeMore, W. B., S. P. Sander, D. M. Golden, R. F. Hampson, M. J. Kurylo, C. J. Howard, A. R. Ravishankara, C. E. Kolb, and M. J. Molina, "Chemical Kinetics and Photochemical Data for Use in

Stratospheric Modeling," in JPL Publication 97-4, Jet Propulsion Laboratory, Pasadena, CA, January 15, 1997.

Derwent, R. G., P. G. Simmonds, S. Seuring, and C. Dimmer, "Observation and Interpretation of the Seasonal Cycles in the Surface Concentrations of Ozone and Carbon Monoxide at Mace Head, Ireland from 1990 to 1994," *Atmos. Environ., 32,* 145–157 (1998).

de Serves, C., and H. B. Ross, "Comparison of Collection Devices for Atmospheric Peroxides," *Environ. Sci. Technol., 27,* 2712–2718 (1993).

De Vries, H. S. M., F. J. M. Harren, G. P. Wyers, R. P. Otjes, J. Slanina, and J. Reuss, "Non-intrusive, Fast, and Sensitive Ammonia Detection by Laser Photothermal Deflection," *Atmos. Environ., 29,* 1069–1074 (1995).

Dewulf, J., and H. Van Langenhove, "Analytical Techniques for the Determination and Measurement Data of 7 Chlorinated $C_1$- and $C_2$-Hydrocarbons and 6 Monocyclic Aromatic Hydrocarbons in Remote Air Masses: An Overview," *Atmos. Environ., 31,* 3291–3307 (1997).

Dierck, I., D. Michaud, L. Wouters, and R. Van Grieken, "Laser Microprobe Mass Analysis of Individual North Sea Aerosol Particles," *Environ. Sci. Technol., 26,* 802–808 (1992).

Dollard, G. J., T. J. Davies, B. M. R. Jones, P. D. Nason, J. Chandler, P. Dumitrean, M. Delaney, D. Watkins, and R. A. Field, "The UK Hydrocarbon Monitoring Network," in *Volatile Organic Compounds in the Atmosphere, Issues in Environmental Science and Technology* (R. E. Hester and R. M. Harrison, Eds.), pp. 37–50, The Royal Society of Chemistry, Cambridge, U.K., 1995.

Dorn, H.-P., U. Brandenburger, T. Brauers, and M. Hausmann, "A New *In-Situ* Laser Long-Path Absorption Instrument for the Measurement of Tropospheric OH Radicals," *J. Atmos. Sci., 52,* 3373–3380 (1995a).

Dorn, H.-P., R. Neuroth, and A. Hofzumahaus, "Investigation of OH Absorption Cross Sections of Rotational Transitions in the $A^2\Sigma^+$, $v' = 0 \leftarrow X^2\Pi$, $v'' = 0$ Band under Atmospheric Conditions: Implications for Tropospheric Long-Path Absorption Measurements," *J. Geophys. Res., 100,* 7397–7409 (1995b).

Dorn, H.-P., U. Brandenburger, T. Brauers, M. Hausmann, and D. H. Ehhalt, "*In-Situ* Detection of Tropospheric OH Radicals by Folded Long-Path Laser Absorption. Results from the POPCORN Field Campaign in August 1994," *Geophys. Res. Lett., 23,* 2537–2540 (1996).

Dubey, M. K., T. F. Hanisco, P. O. Wennberg, and J. G. Anderson, "Monitoring Potential Photochemical Interference in Laser-Induced Fluorescence Measurements of Atmospheric OH," *Geophys. Res. Lett., 23,* 3215–3218 (1996).

Durham, J. L., T. G. Ellestad, L. Stockburger, K. T. Knapp, and L. L. Spiller, "A Transition-Flow Reactor Tube for Measuring Trace Gas Concentrations," *JAPCA, 36,* 1228–1232 (1986).

Durham, J. L., L. L. Spiller, and T. G. Ellestad, "Nitric Acid–Nitrate Aerosol Measurements by a Diffusion Denuder: A Performance Evaluation," *Atmos. Environ., 21,* 589–598 (1987).

Eatough, D. J., A. Wadsworth, D. A. Eatough, J. W. Crawford, L. D. Hansen, and E. A. Lewis, "A Multiple-System, Multi-Channel Diffusion Denuder Sampler for the Determination of Fine-Particulate Organic Material in the Atmosphere," *Atmos. Environ., 27A,* 1213–1219 (1993).

Eatough, D. J., L. J. Kewis, M. Eatough, and E. A. Lewis, "Sampling Artifacts in the Determination of Particulate Sulfate and $SO_2$(g) in the Desert Southwest Using Filter Pack Samplers," *Environ. Sci. Technol., 29,* 787–791 (1995).

Edgerton, S. A., M. W. Holdren, D. L. Smith, and J. J. Shah, "Inter-urban Comparison of Ambient Volatile Organic Compound Concentrations in U.S. Cities," *JAPCA, 39,* 729–732 (1989).

Ehhalt, D. H., F. Rohrer, A. Wahner, M. J. Prather, and D. R. Blake, "On the Use of Hydrocarbons for the Determination of Tropospheric OH Concentrations," *J. Geophys. Res., 103,* 18981–18997 (1998).

Eisele, F. L., "Direct Tropospheric Ion Sampling and Mass Identification," *Int. J. Mass Spectrom. Ion Processes, 54,* 119–126 (1983).

Eisele, F. L., and D. J. Tanner, "Ion-Assisted Tropospheric OH Measurements," *J. Geophys. Res., 96,* 9295–9308 (1991).

Eisele, F. L., and J. D. Bradshaw, "The Elusive Hydroxyl Radical. Measuring OH in the Atmosphere," *Anal. Chem., 65,* 927A–939A (1993).

Eisele, F. L., G. H. Mount, F. C. Fehsenfeld, J. Hardner, E. Marovich, D. D. Parrish, J. Roberts, M. Trainer, and D. Tanner, "Intercomparison of Tropospheric OH and Ancillary Trace Gas Measurements at Fritz Peak Observatory, Colorado," *J. Geophys. Res., 99,* 18605–18626 (1994).

Eisele, F. L., D. J. Tanner, C. A. Cantrell, and J. G. Calvert, "Measurements and Steady State Calculations of OH Concentrations at Mauna Loa Observatory," *J. Geophys. Res., 101,* 14665–14679 (1996).

Eisele, F. L., R. L. Mauldin III, D. J. Tanner, J. R. Fox, T. Mouch, and T. Scully, "An Inlet/Sampling Duct for Airborne OH and Sulfuric Acid Measurements," *J. Geophys. Res., 102,* 27993–28001 (1997).

Eisele, F. L., and P. H. McMurry, "Recent Progress in Understanding Particle Nucleation and Growth," *Philos. Trans. R. Soc. London B, 352,* 191–201 (1997).

Eldering, A., and R. M. Glasgow, "Short-Term Particulate Matter Mass and Aerosol-Size Distribution Measurements: Transient Pollution Episodes and Bimodal Aerosol-Mass Distributions," *Atmos. Environ., 32,* 2017–2024 (1998).

Emmons, L. K., M. A. Carroll, D. A. Hauglustaine, G. P. Brasseur, C. Atherton, J. Penner, S. Sillman, H. Levy II, F. Rohrer, W. M. F. Wauben, P. F. J. Van Velthoven, Y. Wang, D. Jacob, P. Bakwin, R. Dickerson, B. Doddridge, C. Gerbig, R. Honrath, G. Hübler, D. Jafe, Y. Kondo, J. W. Munger, A. Torres, and A. Volz-Thomas, "Climatologies of $NO_x$ and $NO_y$: A Comparison of Data and Models," *Atmos. Environ., 31,* 1851–1904 (1997).

Environmental Science & Technology/News, "European News," *Environ. Sci. Technol., 31,* 557A (1997).

Erle, F., K. Pfeilsticker, and U. Platt, "On the Influence of Tropospheric Clouds on Zenith-Scattered-Light Measurements of Stratospheric Species," *Geophys. Res. Lett., 22,* 2725–2728 (1995).

Evans, G. F., T. A. Lumpkin, D. L. Smith, and M. C. Somerville, "Measurements of VOCs from the TAMS Network," *J. Air Waste Manage. Assoc., 42,* 1319–1323 (1992).

Fahey, D. W., G. Hübler, D. D. Parrish, E. J. Williams, R. B. Norton, B. A. Ridley, H. B. Singh, S. C. Liu, and F. C. Fehsenfeld, "Reactive Nitrogen Species in the Troposphere: Measurements of NO, $NO_2$, $HNO_3$, Particulate Nitrate, Peroxyacetyl Nitrate (PAN), $O_3$, and Total Reactive Odd Nitrogen ($NO_y$) at Niwot Ridge, Colorado," *J. Geophys. Res., 91,* 9781–9793 (1986).

Fan, Q., and P. K. Dasgupta, "Continuous Automated Determination of Atmospheric Formaldehyde at the Parts per Trillion Level," *Anal. Chem., 66,* 551–556 (1994).

Faude, F., and J. Goschnick, "XPS, SIMS, and SNMS Applied to a Combined Analysis of Aerosol Particles from a Region of Considerable Air Pollution in the Upper Rhine Valley," *Fresenius' J. Anal. Chem., 358,* 67–72 (1997).

Febo, R., C. Perrino, and M. Cortiello, "A Denuder Technique for the Measurement of Nitrous Acid in Urban Atmospheres," *Atmos. Environ., 27A,* 1721–1728 (1993).

Febo, A., C. Perrino, M. Gherardi, and R. Sparapani, "Evaluation of a High-Purity and High-Stability Continuous Generation System for Nitrous Acid," *Environ. Sci. Technol., 29,* 2390–2395 (1995).

Febo, R., and C. Perrino, "Measurement of High Concentrations of Nitrous Acid inside Automobiles," *Atmos. Environ., 29,* 345–351 (1995).

Febo, A., C. Perrino, and I. Allegrini, "Measurement of Nitrous Acid in Milan, Italy, by DOAS and Diffusion Denuders," *Atmos. Environ., 30,* 3599–3609 (1996).

Fehsenfeld, F. C., R. R. Dickerson, G. Hübler, W. T. Luke, L. J. Nunnermacker, E. J. Williams, J. M. Roberts, J. G. Calvert, C. M. Curran, A. C. Delany, C. S. Eubank, D. W. Fahey, A. Fried, B. W. Gandrud, A. O. Langford, P. C. Murphy, R. B. Norton, K. E. Pickering, and B. A. Ridley, "A Ground-Based Intercomparison of NO, $NO_x$, and $NO_y$ Measurement Techniques," *J. Geophys. Res., 92,* 14710–14722 (1987).

Fehsenfeld, F. C., J. W. Drummond, U. K. Roychowdhury, P. J. Galvin, E. J. Williams, M. P. Buhr, D. D. Parrish, G. Hübler, A. O. Langford, J. G. Calvert, B. A. Ridley, F. Grahek, B. G. Heikes, G. L. Kok, J. D. Shetter, J. G. Walega, C. M. Elsworth, R. B. Norton, D. W. Fahey, P. C. Murphy, C. Hovermale, V. A. Mohnen, K. L. Demerjian, G. I. Mackay, and H. I. Schiff, "Intercomparison of $NO_2$ Measurement Techniques," *J. Geophys. Res., 95,* 3579–3597 (1990).

Fehsenfeld, F. C., L. G. Huey, D. T. Sueper, R. B. Norton, E. J. Williams, F. L. Eisele, R. L. Mauldin III, and D. J. Tanner, "Ground-Based Intercomparison of Nitric Acid Measurement Techniques," *J. Geophys. Res., 103,* 3343–3353 (1998).

Fels, M., and W. Junkermann, "The Occurrence of Organic Peroxides in Air at a Mountain Site," *Geophys. Res. Lett., 21,* 341–344 (1994).

Felton, C. C., J. C. Sheppard, and M. J. Campbell, "The Radiochemical Hydroxyl Radical Measurement Method," *Environ. Sci. Technol., 24,* 1841–1847 (1990).

Felton, C. C., J. C. Sheppard, and M. J. Campbell, "Precision of the Radiochemical OH Measurement Method," *Atmos. Environ., 26,* 2105–2109 (1992).

Ferek, R. J., and D. A. Hegg, "Measurements of Dimethyl Sulfide and $SO_2$ during GTE/CITE 3," *J. Geophys. Res., 98,* 23435–23442 (1993).

Ferm, M., "Method for Determination of Atmospheric Ammonia," *Atmos. Environ., 13,* 1385–1393 (1979).

Ferm, M., and A. Sjödin, "A Sodium Carbonate Denuder for Determination of Nitrous Acid in the Atmosphere," *Atmos. Environ., 19,* 979–983 (1985).

Ferm, M., "A $Na_2CO_3$-Coated Denuder and Filter for Determination of Gaseous $HNO_3$ and Particulate $NO_3^-$ in the Atmosphere," *Atmos. Environ., 20,* 1193–1201 (1986).

Finlayson-Pitts, B. J., and J. N. Pitts, Jr., *Atmospheric Chemistry: Fundamentals and Experimental Techniques,* Wiley, New York, 1986.

Fischer, H., C. Nikitas, U. Parchatka, T. Zenker, G. W. Harris, P. Matuska, R. Schmitt, D. Mihelcic, P. Muesgen, H.-W. Paetz, M. Schultz, and A. Volz-Thomas, "Trace Gas Measurements during the Oxidizing Capacity of the Tropospheric Atmosphere Campaign 1993 at Izana," *J. Geophys. Res., 103,* 13505–13518 (1998).

Fishman, J., C. E. Watson, J. C. Larsen, and J. A. Logan, "Distribution of Tropospheric Ozone Determined from Satellite Data," *J. Geophys. Res., 95,* 3599–3617 (1990).

Fitz, D. R., G. J. Doyle, and J. N. Pitts, Jr., "An Ultrahigh Volume Sampler for the Multiple Filter Collection of Respirable Particulate Matter," *J. Air Pollut. Control Assoc., 33,* 877–879 (1983).

Flagan, R. C., "History of Electrical Aerosol Measurements," *Aerosol Sci. Technol., 28,* 301–380 (1998).

Flocke, F., A. Volz-Thomas, H.-J. Buers, W. Pätz, H.-J. Garthe, and D. Kley, "Long-Term Measurements of Alkyl Nitrates in Southern Germany. 1. General Behavior and Seasonal and Diurnal Variation," *J. Geophys. Res., 103,* 5729–5746 (1998).

Fox, D. L., L. Stockburger, W. Weathers, C. W. Spicer, G. I. Mackay, H. I. Schiff, D. J. Eatough, F. Mortensen, L. D. Hansen, P. B. Shepson, T. E. Kleindienst, and E. O. Edney, "Intercomparison of Nitric Acid Diffusion Denuder Methods with Tunable Diode Laser Absorption Spectroscopy," *Atmos. Environ., 22,* 575–585 (1988).

Francois, F., W. Maenhaut, J.-L. Colin, R. Losno, M. Schulz, T. Stahlschmidt, L. Spokes, and T. Jickells, "Intercomparison of Elemental Concentrations in Total and Size-Fractionated Aerosol Samples Collected during the Mace Head Experiment, April 1991," *Atmos. Environ., 29,* 837–849 (1995).

Fraser, M. P., G. R. Cass, B. R. T. Simoneit, and R. A. Rasmussen, "Air Quality Model Evaluation Data for Organics. 5. $C_6$–$C_{22}$ Nonpolar and Semipolar Aromatic Compounds," *Environ. Sci. Technol., 32,* 1760–1770 (1998).

Fried, A., S. Sewell, B. Henry, B. P. Wert, T. Gilpin, and J. R. Drummond, "Tunable Diode Laser Absorption Spectrometer for Ground-Based Measurements of Formaldehyde," *J. Geophys. Res., 102,* 6253–6266 (1997).

Friedbacher, G., M. Grasserbauer, Y. Meslmani, N. Klaus, and M. J. Higatsberger, "Investigation of Environmental Aerosol by Atomic Force Microscopy," *Anal. Chem., 67,* 1749–1754 (1995).

Fuchs, N. A., and A. G. Sutugin, *Highly Dispersed Aerosols,* Ann Arbor Science Publishers, Ann Arbor, MI, 1970.

Fung, K., "Particulate Carbon Speciation by $MnO_2$ Oxidation," *Aerosol Sci. Technol., 12,* 122–127 (1990).

Fung, K. H., and I. N. Tang, "Relative Raman Scattering Cross-Section Measurements with Suspended Particles," *Appl. Spectrosc., 45,* 734–737 (1991).

Fung, K. H., and I. N. Tang, "Analysis of Aerosol Particles by Resonance Raman Scattering Technique," *Appl. Spectrosc., 46,* 159–162 (1992a).

Fung, K. H., and I. N. Tang, "Aerosol Particle Analysis by Resonance Raman Spectroscopy," *J. Aerosol Sci., 23,* 301–307 (1992b).

Fung, K. H., D. G. Imre, and I. N. Tang, "Detection Limits for Sulfates and Nitrates in Aerosol Particles by Raman Spectroscopy," *J. Aerosol Sci., 25,* 479–485 (1994).

Gaffney, J. S., N. A. Marley, and E. W. Prestbo, "Peroxyacyl Nitrates (PANs): Their Physical and Chemical Properties," in *The Handbook of Environmental Chemistry* (O. Hutzinger, Ed.), Vol. 4, Part B, pp. 4–38, Springer-Verlag, Berlin, 1989.

Gaffney, J. S., N. A. Marley, and E. W. Prestbo, "Measurements of Peroxyacetyl Nitrate at a Remote Site in the Southwestern United States: Tropospheric Implications," *Environ. Sci. Technol., 27,* 1905–1910 (1993).

Gaffney, J. S., N. A. Marley, R. S. Martin, R. W. Dixon, L. G. Reyes, and C. J. Popp, "Potential Air Quality Effects of Using Ethanol-Gasoline Fuel Blends: A Field Study in Albuquerque, New Mexico," *Environ. Sci. Technol., 31,* 3053–3061 (1997).

Gaffney, J. S., R. M. Bornick, Y.-H. Chen, and N. A. Marley, "Capillary Gas Chromatographic Analysis of Nitrogen Dioxide and PANs with Luminol Chemiluminescent Detection," *Atmos. Environ., 32,* 1445–1454 (1998).

Gaffney, J. S., N. A. Marley, and P. V. Doskey, "Peroxyacetyl Nitrate and Hydrocarbon Measurements in Mexico City," Invited Paper, Special Session on Mexico City Air Quality, Spring Meeting of the American Geophysical Union (AGU), Boston, Massachusetts, May 25–28, 1998, *Atmos. Environ.,* in press (1999).

Ganor, E., Z. Levin, and R. Van Griekens, "Composition of Individual Aerosol Particles above the Israelian Mediterranean Coast during the Summer Time," *Atmos. Environ., 32,* 1631–1642 (1998).

Gao, R. S., E. R. Keim, E. L. Woodbridge, S. J. Ciciora, M. H. Proffitt, T. L. Thompson, R. J. Mclaughlin, and D. W. Fahey, "New Photolysis System for $NO_2$ Measurements in the Lower Stratosphere," *J. Geophys. Res., 99,* 20673–20681 (1994).

Gard, E., M. J. Kleeman, D. S. Gross, L. S. Hughes, J. O. Allen, B. D. Morrical, D. P. Fergenson, T. Dienes, M. E. Gälli, R. J. Johnson, G. R. Cass, and K. A. Prather, "Direct Observation of Heterogeneous Chemistry in the Atmosphere," *Science, 279,* 1184–1187 (1998).

Gard, E., J. E. Mayer, B. D. Morrical, T. Dienes, D. P. Fergenson, and K. A. Prather, "Real-Time Analysis of Individual Atmospheric Aerosol Particles: Design and Performance of a Portable ATOFMS," *Anal. Chem., 69,* 4083–4091 (1997).

Ge, Z., A. S. Wexler, and M. V. Johnston, "Multicomponent Aerosol Crystallization," *J. Colloid Interface Sci., 183,* 68–77 (1996).

Ge, Z., A. S. Wexler, and M. V. Johnston, "Deliquescence Behavior of Multicomponent Aerosols," *J. Phys. Chem. A, 102,* 173–180 (1998a).

Ge, Z., A. S. Wexler, and M. V. Johnston, "Laser Desorption/Ionization of Single Ultrafine Multicomponent Aerosols," *Environ. Sci. Technol., 32,* 3218–3223 (1998b).

Genfa, Z., P. K. Dasgupta, and S. Dong, "Measurement of Atmospheric Ammonia," *Environ. Sci. Technol., 23,* 1467–1474 (1989).

Gholson, A. R., R. K. M. Jayanty, and J. F. Storm, "Evaluation of Aluminum Canisters for the Collection and Storage of Air Toxics," *Anal. Chem., 62,* 1899–1902 (1990).

Gilpin, T., E. Apel, A. Fried, B. Wert, J. Calvert, Z. Genfa, P. Dasgupta, J. W. Harder, B. Heikes, B. Hopkins, H. Westberg, T. Kleindienst, Y.-N. Lee, X. Zhou, W. Lonneman, and S. Sewell, "Intercomparison of Six Ambient [$CH_2O$] Measurement Techniques," *J. Geophys. Res., 102,* 21161–21188 (1997).

Goldan, P. D., W. C. Kuster, F. C. Fehsenfeld, and S. A. Montzka, "Hydrocarbon Measurements in the Southeastern United States: The Rural Oxidants in the Southern Environment (ROSE) Program 1990," *J. Geophys. Res., 100,* 25945–25963 (1995).

Gong, Q., and K. L. Demerjian, "Hydrocarbon Losses on a Regenerated Nafion Dryer," *J. Air Waste Manage. Assoc., 45,* 490–493 (1995).

Gong, Q., and K. L. Demerjian, "Measurement and Analysis of $C_2$–$C_{10}$ Hydrocarbons at Whiteface Mountain, New York," *J. Geophys. Res., 102,* 28059–28069 (1997).

Goschnick, J., J. Schuricht, and H. J. Ache, "Calibration of Depth Profiles of Microparticles Measured with Plasma-Based Secondary Neutral Mass Spectrometry," *Fresenius' J. Anal. Chem., 349,* 203–205 (1994a).

Goschnick, J., J. Schuricht, and H. J. Ache, "Depth-Structure of Airborne Microparticles Sampled Downwind from the City of Karlsruhe in the River Rhine Valley," *Fresenius' J. Anal. Chem., 350,* 426–430 (1994b).

Granby, K., C. S. Christensen, and C. Lohse, "Urban and Semi-Rural Observations of Carboxylic Acids and Carbonyls," *Atmos. Environ., 31,* 1403–1415 (1997a).

Granby, K., A. H. Egelov, T. Nielsen, and C. Lohse, "Carboxylic Acids: Seasonal Variation and Relation to Chemical and Meteorological Parameters," *J. Atmos. Chem., 28,* 195–207 (1997b).

Greenberg, J. P., D. Helmig, and P. R. Zimmerman, "Seasonal Measurements of Nonmethane Hydrocarbons and Carbon Monoxide at the Mauna Loa Observatory during the Mauna Loa Observatory Photochemistry Experiment 2," *J. Geophys. Res., 101,* 14581–14598 (1996).

Gregory, G. L., J. M. Hoell, Jr., M. A. Carroll, B. A. Ridley, D. D. Davis, J. Bradshaw, M. O. Rodgers, S. T. Sandholm, H. I. Schiff, D. R. Hastie, D. R. Karecki, G. I. Mackay, G. W. Harris, A. L. Torres, and A. Fried, "An Intercomparison of Airborne Nitrogen Dioxide Instruments," *J. Geophys. Res., 95,* 10103–10127 (1990a).

Gregory, G. L., J. M. Hoell, Jr., B. J. Huebert, S. E. Van Bramer, P. J. LeBel, S. A. Vay, R. M. Marinaro, H. I. Schiff, D. R. Hastie, G. I. Mackay, and D. R. Karecki, "An Intercomparison of Airborne Nitric Acid Measurements," *J. Geophys. Res., 95,* 10089–10102 (1990b).

Gregory, G. L., J. M. Hoell, Jr., A. L. Torres, M. A. Carroll, B. A. Ridley, M. O. Rodgers, J. Bradshaw, S. Sandholm, and D. D. Davis, "An Intercomparison of Airborne Nitric Oxide Measurements: A Second Opportunity," *J. Geophys. Res., 95,* 10129–10138 (1990c).

Gregory, G. L., D. D. Davis, N. Beltz, A. R. Bandy, R. J. Ferek, and D. C. Thornton, "An Intercomparison of Aircraft Instrumentation for Tropospheric Measurements of Sulfur Dioxide," *J. Geophys. Res., 98,* 23325–23352 (1993).

Griffith, D. W. T., and G. Schuster, "Atmospheric Trace Gas Analysis Using Matrix Isolation-Fourier Transform Infrared Spectroscopy," *J. Atmos. Chem., 5,* 59–81 (1987).

Griffith, D. W. T., "Matrix Isolation Spectroscopy in Atmospheric Chemistry," in *Air Monitoring by Spectroscopic Techniques* (M. W. Sigrist, Ed.), *Chemical Analysis Series,* Vol. 127, Chap. 7, pp. 471–514, Wiley, New York, 1994.

Griffiths, P. R., and J. A. de Haseth, *Fourier Transform Infrared Spectrometry,* Wiley, New York, 1986.

Grisar, R., H. Bottner, M. Tacke, and G. Restelli, Eds., *Monitoring of Gaseous Pollutants by Tunable Diode Lasers, Proceedings of the* International Symposium, Freiburg, Germany, October 17–18, 1991, Kluwer Academic, Dordrecht/Norwell, MA, 1992.

Grosjean, D., and K. Fung, "Collection Efficiencies of Cartridges and Microimpingers for Sampling of Aldehydes in Air as 2,4- Dinitrophenylhydrazones," *Anal. Chem., 54,* 1221–1224 (1982).

Grosjean, D., "Liquid Chromatography Analysis of Chloride and Nitrate with 'Negative' Ultraviolet Detection: Ambient Levels and Relative Abundance of Gas-Phase Inorganic and Organic Acids in Southern California," *Environ. Sci. Technol., 24,* 77–81 (1990).

Grosjean, D., and S. S. Parmar, "Interferences from Aldehydes and Peroxyacetyl Nitrate When Sampling Urban Air Organic Acids on Alkaline Traps," *Environ. Sci. Technol., 24,* 1021–1026 (1990).

Grosjean, D., E. C. Tuazon, and E. Fujita, "Ambient Formic Acid in Southern California Air: A Comparison of Two Methods, Fourier Transform Infrared Spectroscopy and Alkaline Trap-Liquid Chromatography with UV Detection," *Environ. Sci. Technol., 24,* 144–146 (1990).

Grosjean, D., and E. L. Williams, II, "A Passive Sampler for Airborne Formaldehyde," *Atmos. Environ., 26A,* 2923–2928 (1992).

Grosjean, D., E. L. Williams, II, and E. Grosjean, "Peroxyacyl Nitrates at Southern California Mountain Forest Locations," *Environ. Sci. Technol., 27,* 110–121 (1993a).

Grosjean, D., E. L. Williams, II, and E. Grosjean, "Ambient Levels of Peroxy-*n*-butyryl Nitrate at a Southern California Mountain Forest Smog Receptor Location," *Environ. Sci. Technol., 27,* 326–331 (1993b).

Grosjean, E., D. Grosjean, M. P. Fraser, and G. R. Cass, "Air Quality Model Evaluation Data for Organics. 2. $C_1$–$C_{14}$ Carbonyls in Los Angeles Air," *Environ. Sci. Technol., 30,* 2687–2703 (1996a).

Grosjean, E., D. Grosjean, M. P. Fraser, and G. R. Cass, "Air Quality Model Evaluation Data for Organics. 3. Peroxyacetyl Nitrate and Peroxypropionyl Nitrate in Los Angeles Air," *Environ. Sci. Technol., 30,* 2704–2714 (1996b).

Grosjean, E., D. Grosjean, R. Gunawardena, and R. A. Rasmussen, "Ambient Concentrations of Ethanol and Methyl *tert*-Butyl Ether in Porto Alegre, Brazil, March 1996–April 1997," *Environ. Sci. Technol., 32,* 736–742 (1998a).

Grosjean, E., D. Grosjean, and R. A. Rasmussen, "Ambient Concentrations, Sources, Emission Rates, and Photochemical Reactivity of $C_2$–$C_{10}$ Hydrocarbons in Porto Alegre, Brazil," *Environ. Sci. Technol., 32,* 2061–2069 (1998b).

Grosjean, E., R. A. Rasmussen, and D. Grosjean, "Ambient Levels of Gas Phase Pollutants in Porto Alegre, Brazil," *Atmos. Environ., 32,* 3371–3379 (1998c).

Guizard, S., D. Chapoulard, M. Horani, and D. Gauyacq, "Detection of NO Traces Using Resonantly Enhanced Multiphoton Ionization: A Method for Monitoring Atmospheric Pollutants," *Appl Phys. B, 48,* 471–477 (1989).

Gunz, D. W., and M. R. Hoffmann, "Atmospheric Chemistry of Peroxides: A Review," *Atmos. Environ., 24A,* 1601–1633 (1990).

Haan, D., P. Martinerie, and D. Raynaud, "Ice Core Data of Atmospheric Carbon Monoxide over Antarctica and Greenland during the Last 200 Years," *Geophys. Res. Lett., 23,* 2235–2238 (1996).

Hamm, S., G. Helas, and P. Warneck, "Acetonitrile in the Air over Europe," *Geophys. Res. Lett., 16,* 483–486 (1989).

Hansen, A. B., H. Skov, and T. Nielsen, "Comparison of Volatile Non-Methane Hydrocarbon Concentrations and Profiles at Different Locations: Open Land, Urban Background, and Street," personal communication (1998).

Hansen, K. J., B. N. Hansen, E. Cravens, and R. E. Sievers, "Supercritical Fluid Extraction—Gas Chromatographic Analysis of Organic Compounds in Atmospheric Aerosols," *Anal. Chem., 67,* 3541–3549 (1995).

Hanst, P. L., "Spectroscopic Methods for Air Pollution Measurement," *Adv. Environ. Sci. Technol., 2,* 91–213 (1971).

Hanst, P. L., and S. T. Hanst, "Gas Measurement in the Fundamental Infrared Region," in *Air Monitoring by Spectroscopic Techniques* (M. W. Sigrist, Ed.), *Chemical Analysis Series,* Vol. 127, Chap. 6, pp. 335–470, Wiley, New York, 1994.

Hara, K., T. Kikuchi, K. Furuya, M. Hayashi, and Y. Fujii, "Characterization of Antarctic Aerosol Particles Using Laser Microprobe Mass Spectrometry," *Environ. Sci. Technol., 30,* 385–391 (1996).

Hard, T. M., R. J. O'Brien, C. Y. Chan, and A. A. Mehrabzadeh, "Tropospheric Free Radical Determination by FAGE," *Environ. Sci. Technol., 18,* 768–777 (1984).

Hard, T. M., C. Y. Chan, A. A. Mehrabzadeh, and R. J. O'Brien, "Diurnal $HO_2$ Cycles at Clean Air and Urban Sites in the Troposphere," *J. Geophys. Res., 97,* 9785–9794 (1992a).

Hard, T. M., A. A. Mehrabzadeh, C. Y. Chan, and R. J. O'Brien, "FAGE Measurements of Tropospheric HO with Measurements and Model of Interferences," *J. Geophys. Res., 97,* 9795–9817 (1992b).

Hard, T. M., L. A. George, and R. J. O'Brien, "FAGE Determination of Tropospheric HO and $HO_2$," *J. Atmos. Sci., 52,* 3354–3372 (1995).

Harder, J. W., R. O. Jakoubek, and G. H. Mount, "Measurement of Tropospheric Trace Gases by Long-Path Differential Absorption Spectroscopy during the 1993 OH Photochemistry Experiment," *J. Geophys. Res., 102,* 6215–6226 (1997a).

Harder, J. W., A. Fried, S. Sewell, and B. Henry, "Comparison of Tunable Diode Laser and Long-Path Ultraviolet–Visible Spectroscopic Measurements of Ambient Formaldehyde Concentrations during the 1993 OH Photochemistry Experiment," *J. Geophys. Res., 102,* 6267–6282 (1997b).

Harris, G. W., W. P. L. Carter, A. M. Winer, J. N. Pitts, Jr., U. Platt, and D. Perner, "Observations of Nitrous Acid in the Los Angeles Atmosphere and Implications for Predictions of Ozone-Precursor Relationships," *Environ. Sci. Technol., 16,* 414–419 (1982).

Harrison, R. M., J. D. Peak, and G. M. Collins, "Tropospheric Cycle of Nitrous Acid," *J. Geophys. Res., 101,* 14429–14439 (1996).

Harrison, R. M., M. Jones, and G. Collins, "Measurements of the Physical Properties of Particles in the Urban Atmosphere," *Atmos. Environ., 33,* 309–321 (1999).

Hartsell, B. E., V. P. Aneja, and W. A. Lonneman, "Relationships between Peroxyacetyl Nitrate, $O_3$, and $NO_y$ at the Rural Southern Oxidants Study Site in Central Piedmont, North Carolina, Site SONIA," *J. Geophys. Res., 99,* 21033–21041 (1994).

Hastie, D. R., G. I. Mackay, T. Iguchi, B. A. Ridley, and H. I. Schiff, "Tunable Diode Laser Systems for Measuring Trace Gases in Tropospheric Air," *Environ. Sci. Technol., 17,* 352A–364A (1983).

Hastie, D. R., P. B. Shepson, N. Reid, P. B. Roussel, and O. T. Melo, "Summertime $NO_x$, $NO_y$, and Ozone at a Site in Rural Ontario," *Atmos. Environ., 30,* 2157–2165 (1996).

Hebestreit, K., J. Stutz, D. Rosen, V. Matveiv, M. Peleg, M. Luria, and U. Platt, "DOAS Measurements of Tropospheric Bromine Oxide in Mid-Latitudes," *Science, 283,* 55–57 (1999).

Heikes, B. G., "Aqueous $H_2O_2$ Production from $O_3$ in Glass Impingers," *Atmos. Environ., 18,* 1433–1445 (1984).

Heikes, B., M. Lee, D. Jacob, R. Talbot, J. Bradshaw, H. Singh, D. Blake, B. Anderson, H. Fuelberg, and A. M. Thompson, "Ozone, Hydroperoxides, Oxides of Nitrogen, and Hydrocarbon Budgets in the Marine Boundary Layer over the South Atlantic," *J. Geophys. Res., 101,* 24221–24234 (1996).

Heintz, F., U. Platt, H. Flentje, and R. Dubois, "Long-Term Observation of Nitrate Radicals at the Tor Station, Kap Arkona (Rügen)," *J. Geophys. Res., 101,* 22891–22910 (1996).

Heitmann, H., and F. Arnold, "Composition Measurements of Tropospheric Ions," *Nature, 306,* 747–751 (1983).

Helmig, D., and J. P. Greenberg, "Automated *in situ* Gas Chromatographic–Mass Spectrometric Analysis of ppt Level Volatile Organic Trace Gases Using Multistage Solid-Adsorbent Trapping," *J. Chromatogr. A, 677,* 123–132 (1994).

Helmig, D., and L. Vierling, "Water Adsorption Capacity of the Solid Adsorbents Tenax TA, Tenax GR, Carbotrap, Carbotrap C, Carbosieve SIII, and Carboxen 569 and Water Management Techniques for the Atmospheric Sampling of Volatile Organic Trace Gases," *Anal. Chem., 67,* 4380–4386 (1995).

Helmig, D., "Artifact-Free Preparation, Storage, and Analysis of Solid Adsorbent Sampling Cartridges Used in the Analysis of Volatile Organic Compounds in Air," *J. Chromatogr. A, 732,* 414–417 (1996).

Helmig, D., "Ozone Removal Techniques in the Sampling of Atmospheric Volatile Organic Trace Gases," *Atmos. Environ., 31,* 3635–3651 (1997).

Hering, S. V., R. C. Flagan, and S. K. Friedlander, "Design and Evaluation of New Low-Pressure Impactor. I.," *Environ. Sci. Technol., 12,* 667–673 (1978).

Hering, S. V., S. K. Friedlander, J. J. Collins, and L. W. Richards, "Design and Evaluation of a New Low-Pressure Impactor. 2.," *Environ. Sci. Technol., 13,* 184–188 (1979).

Hering, S. V., D. R. Lawson, I. Allegrini, A. Febo, C. Perrino, M. Possanzini, J. E. Sickles, II, K. G. Anlauf, A. Wiebe, B. R. Appel, W. John, J. Ondo, S. Wall, R. S. Braman, R. Sutton, G. R. Cass, P. A. Solomon, D. J. Eatough, N. L. Eatough, E. C. Ellis, D. Grosjean, B. B. Hicks, J. D. Womack, J. Horrocks, K. T. Knapp, T. G. Ellestad, R. J. Paur, W. J. Mitchell, M. Pleasant, E. Peake, A. MacLean, W. R. Pierson, W. Brachaczek, H. I. Schiff, G. I. Mackay, C. W. Spicer, D. H. Stedman, A. M. Winer, H. W. Biermann, and E. C. Tuazon, "The Nitric Acid Shootout: Field Comparison of Measurement Methods," *Atmos. Environ., 22,* 1519–1539 (1988).

Herriott, D., H. Kogelnik, and R. Kompfner, "Off-Axis Paths in Spherical Mirror Interferometers," *Appl. Opt., 3,* 523–526 (1964).

Herriott, D. R., and H. J. Schulte, "Folded Optical Delay Lines," *Appl. Opt, 4,* 883–889 (1965).

Herzberg, G., *Molecular Spectra and Molecular Structure*, 2nd ed., Van Nostrand–Reinhold, New York, 1950.

Hewitt, C. N., and G. L. Kok, "Formation and Occurrence of Organic Hydroperoxides in the Troposphere: Laboratory and Field Observations," *J. Atmos. Chem., 12,* 181–194 (1991).

Hewitt, C. N., X.-L. Cao, C. Boissard, and S. C. Duckham, "Atmospheric VOCs from Natural Sources," in *Volatile Organic Compounds in the Atmosphere, Issues in Environmental Science and Technology* (R. E. Hester and R. M. Harrison, Eds.), pp. 17–36, The Royal Society of Chemistry, Cambridge, UK, 1995.

Hinds, W. C., *Aerosol Technology*, Wiley, New York, 1982.

Hinz, K.-P., R. Kaufmann, and B. Spengler, "Laser-Induced Mass Analysis of Single Particles in the Airborne State," *Anal. Chem., 66,* 2071–2076 (1994).

Hinz, K.-P., R. Kaufmann, and B. Spengler, "Simultaneous Detection of Positive and Negative Ions from Single Airborne Particles by Real-Time Laser Mass Spectrometry," *Aerosol Sci. Technol., 24,* 233–242 (1996).

Hippler, M., and J. Pfab, "Detection and Probing of Nitric Oxide (NO) by Two-Colour Laser Photoionisation (REMPI) Spectroscopy on the A ← X Transition," *Chem. Phys. Lett., 243,* 500–505 (1995).

Hisham, M. W. M., and D. Grosjean, "Sampling of Atmospheric Nitrogen Dioxide Using Triethanolamine: Interference from Peroxyacetyl Nitrate," *Atmos. Environ., 24,* 2523–2525 (1990).

Ho, M. H., and R. A. Richards, "Enzymatic Method for the Determination of Formaldehyde," *Environ. Sci. Technol., 24,* 201–204 (1990).

Hoek, G., B. Forsberg, M. Borowska, S. Hlawiczka, E. Vaskövi, H. Welinder, M. Branis, I. Benes, F. Kotesovec, L. O. Hagen, J. Cyrys, M. Jantunen, W. Roemer, and B. Brunekreef, "Wintertime PM10 and Black Smoke Concentrations across Europe: Results from the Peace Study," *Atmos. Environ., 31,* 3609–3622 (1997).

Hoell, J. M., Jr., G. L. Gregory, D. S. McDougal, G. W. Sachse, and G. F. Hill, "An Intercomparison of Carbon Monoxide Measurement Techniques," *J. Geophys. Res., 90,* 12881–12889 (1985).

Hoell, J. M., Jr., G. L. Gregory, D. S. McDougal, A. L. Torres, D. D. Davis, J. Bradshaw, M. O. Rodgers, B. A. Ridley, and M. A. Carroll, "Airborne Intercomparison of Nitric Oxide Measurement Techniques," *J. Geophys. Res., 92,* 1995–2008 (1987a).

Hoell, J. M., Jr., G. L. Gregory, D. S. McDougal, G. W. Sachse, G. F. Hill, E. P. Condon, and R. A. Rasmussen, "Airborne Intercomparison of Carbon Monoxide Measurement Techniques," *J. Geophys. Res., 92,* 2009–2019 (1987b).

Hoff, R. M., L. Guise-Bagley, R. M. Staebler, H. A. Wiebe, J. Brook, B. Georgi, and T. Düsterdiek, "Lidar, Nephelometer, and *in Situ* Aerosol Experiments in Southern Ontario," *J. Geophys. Res., 101,* 19199–19209 (1996).

Hoffer, E. M., E. L. Kothny, and B. R. Appel, "Simple Method for Microgram Amounts of Sulfate in Atmospheric Particulates," *Atmos. Environ., 13,* 303–306 (1979).

Hofzumahaus, A., U. Aschmutat, M. Heßling, F. Holland, and D. H. Ehhalt, "The Measurement of Tropospheric OH Radicals by Laser-Induced Fluorescence Spectroscopy during the POPCORN Field Campaign," *Geophys. Res. Lett., 23,* 2541–2544 (1996).

Hofzumahaus, A., T. Brauers, U. Aschmutat, U. Brandenburger, H.-P. Dorn, M. Hausmann, M. Heßling, F. Holland, C. Plass-Dülmer, M. Sedlacek, M. Weber, and D. H. Ehhalt, "Reply" to paper by Brauers *et al.*, 1996, *Geophys. Res. Lett., 24,* 3039–3040 (1997).

Hofzumahaus, A., U. Aschmutat, U. Brandenburger, T. Brauers, H.-P. Dorn, M. Hausmann, M. Heßling, F. Holland, C. Plass-Dülmer, and D. H. Ehhalt, "Intercomparison of Tropospheric OH Measurements by Different Laser Techniques during the POPCORN Campaign 1994," *J. Atmos. Chem., 31,* 227–246 (1998).

Holland, F., M. Hessling, and A. Hofzumahaus, "*In-Situ* Measurement of Tropospheric OH Radicals by Laser-Induced Fluorescence—A Description of the KFA Instrument," *J. Atmos. Sci., 52,* 3393–3401 (1995).

Holland, F., U. Aschmutat, M. Heßling, A. Hofzumahaus, and D. H. Ehhalt, "Highly Time Resolved Measurements of OH during POPCORN Using Laser-Induced Fluorescence Spectroscopy," in *Atmospheric Measurements during POPCORN—Characterization of the Photochemistry over a Rural Area*, pp. 205–225, Kluwer Academic, Dordrecht/Norwell, MA, 1998.

Horn, D., and G. C. Pimentel, "2.5-km Low-Temperature Multiple-Reflection Cell," *Appl. Opt., 10,* 1892–1898 (1971).

Horvath, H., "Experimental Calibration for Aerosol Light Absorption Measurements Using the Integrating Plate Method—Summary of the Data," *Aerosol Sci., 28,* 1149–1161 (1997).

Hu, J., and D. H. Stedman, "Atmospheric $RO_x$ Radicals at an Urban Site: Comparison to a Simple Theoretical Model," *Environ. Sci. Technol., 29,* 1655–1659 (1995).

Hübler, G., D. Perner, U. Platt, A. Toennissen, and D. H. Ehhalt, "Ground-Level OH Radical Concentration: New Measurements by Optical Absorption," *J. Geophys. Res., 89,* 1309–1319 (1984).

Huebert, B. J., and A. L. Lazrus, "Tropospheric Gas-Phase and Particulate Nitrate Measurements," *J. Geophys. Res., 85,* 7322–7328 (1980).

Huebert, B. J., S. E. Vanbramer, P. J. Lebel, S. A. Vay, A. L. Torres, H. I. Schiff, D. Hastie, G. Hubler, J. D. Bradshaw, M. A. Carroll, D. D. Davis, B. A. Ridley, M. O. Rodgers, S. T. Sandholm, and S. Dorris, "Measurements of Nitric Acid to $NO_x$ Ratio in the Troposphere," *J. Geophys. Res., 95,* 10193–10198 (1990).

Huey, L. G., and E. R. Lovejoy, "Reactions of $SiF_5^-$ with Atmospheric Trace Gases: Ion Chemistry for Chemical Ionization Detection of $HNO_3$ in the Troposphere," *Int. J. Mass Spectrom. Ion Processes, 155,* 133–140 (1996).

Huey, L. G., E. J. Dunlea, E. R. Lovejoy, D. R. Hanson, R. B. Norton, F. C. Fehsenfeld, and C. J. Howard, "Fast Time Response Measurements of $HNO_3$ in Air with a Chemical Ionization Mass Spectrometer," *J. Geophys. Res., 103,* 3355–3360 (1998).

Huffman, H. D., "Comparison of the Light Absorption Coefficient and Carbon Measures for Remote Aerosols: An Independent Analysis of Data from the Improve Network—I," *Atmos. Environ., 30,* 73–83 (1996).

Huntzicker, J. J., R. L. Johnson, J. J. Shah, and R. A. Cary, "Analysis of Organic and Elemental Carbon in Ambient Aerosols by a Thermal-Optical Method," in *Particulate Carbon: Atmospheric Life Cycles* (G. T. Wolff and R. L. Klimisch, Eds.), pp. 79–88, Plenum, New York, 1982.

Igawa, M., J. W. Munger, and M. R. Hoffmann, "Analysis of Aldehydes in Cloud- and Fogwater Samples by HPLC with a Postcolumn Reaction Detector," *Environ. Sci. Technol., 23,* 556–561 (1989).

Iwaski, I., S. Utsumi, K. Hagino, and T. Ozawa, "A New Spectrophotometric Method for the Determination of Small Amounts of Chloride Using the Mercury Thiocyanate Method," *Bull. Chem. Soc. Jpn., 29,* 860–864 (1956).

Jach, T., and C. J. Powell, "X-Ray Photoemission Spectroscopy of Environmental Particles," *Environ. Sci. Technol., 18,* 58–61 (1984).

Jaffrezo, J. L., N. Calas, and M. Bouchet, "Carboxylic Acids Measurements with Ionic Chromatography," *Atmos. Environ., 32,* 2705–2708 (1998).

Japar, S. M., A. C. Szkariat, R. A. Gorse, Jr., E. K. Heyerdahl, R. I. Johnson, J. A. Rau, and J. J. Huntzicker, "Comparison of Solvent

Extraction and Thermal-Optical Carbon Analysis Methods: Application to Diesel Vehicle Exhaust Aerosol," *Environ. Sci. Technol., 18,* 231–234 (1984).

Jayne, J. T., D. C. Leard, X. Zhang, P. Davidovits, K. A. Smith, C. E. Kolb, and D. R. Worsnop, "Development of an Aerosol Mass Spectrometer for Size and Composition Analysis of Submicron Particles," *Aerosol Sci. Technol.,* in press (1999).

Johansson, T. B., R. E. Van Grieken, J. W. Nelson, and J. W. Winchester, "Elemental Trace Analysis of Small Samples by Proton Induced X-Ray Emission," *Anal. Chem., 47,* 855–860 (1975).

John, W., "Particle–Surface Interactions: Charge Transfer, Energy Loss, Resuspension, and Deagglomeration," *Aerosol Sci. Technol., 23,* 2–24 (1995).

Johnson, J., and R. Yost, "Tandem Mass Spectrometry for Trace Analysis," *Anal. Chem., 57,* 758–768 (1985).

Johnston, M. V., and A. S. Wexler, "MS of Individual Aerosol Particles," *Anal. Chem., 67,* 721A–726A (1995).

Kalabokas, P., P. Carlier, P. Fresnet, G. Mouvier, and G. Toupance, "Field Studies of Aldehyde Chemistry in the Paris Area," *Atmos. Environ., 22,* 147–155 (1988).

Kanda, Y., and M. Taira, "Chemiluminescent Method for Continuous Monitoring of Nitrous Acid in Ambient Air," *Anal. Chem., 62,* 2084–2087 (1990).

Kasparian, J., E. Frejafon, P. Rambaldi, J. Yu, B. Vezin, J. P. Wolf, P. Ritter, and P. Viscardi, "Characterization of Urban Aerosols Using SEM-Microscopy, X-Ray, and Lidar Measurements," *Atmos. Environ., 32,* 2957–2967 (1998).

Kaufmann, R. L., "Laser Microprobe Mass Spectroscopy (LAMMA) of Particulates," in *Physical and Chemical Characterization of Individual Airborne Particles* (K. R. Spurny, Ed.), Chap. 13, pp. 227–250, Ellis Horwood, Chichester, 1986.

Kaupp, H., and G. Umlauf, "Atmospheric Gas–Particle Partitioning of Organic Compounds: Comparison of Sampling Methods," *Atmos. Environ., 26A,* 2259–2267 (1992).

Keene, W. C., R. W. Talbot, M. O. Andreae, K. Beecher, H. Berresheim, M. Castro, J. C. Farmer, J. N. Galloway, M. R. Hoffmann, S.-M. Li, J. R. Maben, J. W. Munger, R. B. Norton, A. A. P. Pszenny, H. Puxbaum, H. Westberg, and W. Winiwarter, "An Intercomparison of Measurement Systems for Vapor and Particulate Phase Concentrations of Formic and Acetic Acids," *J. Geophys. Res., 94,* 6457–6471 (1989).

Keene, W. C., J. R. Maben, A. A. P. Pszenny, and J. N. Galloway, "Measurement Technique for Inorganic Chlorine Gases in the Marine Boundary Layer," *Environ. Sci. Technol., 27,* 866–874 (1993).

Kelly, T. J., C. W. Spicer, and G. F. Ward, "An Assessment of the Luminol Chemiluminescence Technique for Measurement of $NO_2$ in Ambient Air," *Atmos. Environ., 24A,* 2397–2403 (1990).

Kelly, T. J., and M. W. Holdren, "Applicability of Canisters for Sample Storage in the Determination of Hazardous Air Pollutants," *Atmos. Environ., 29,* 2595–2608 (1995).

Khare, P., G. S. Satsangi, N. Kimar, K. M. Kumari, and S. S. Srivastava, "Surface Measurements of Formaldehyde and Formic and Acetic Acids at a Subtropical Semiarid Site in India," *J. Geophys. Res., 102,* 18997–19005 (1997).

Klaus, N., "Aerosol Analysis by Secondary-Ion Mass-Spectrometry," in *Physical and Chemical Characterization of Individual Airborne Particles* (K. R. Spurny, Ed.), Chap. 17, pp. 331–340, Ellis Horwood, 1986.

Kleindienst, T. E., P. B. Shepson, D. N. Hodges, C. M. Nero, R. R. Arnts, P. K. Dasgupta, H. Hwang, G. L. Kok, J. A. Lind, A. L. Lazrus, G. I. Mackay, L. K. Mayne, and H. I. Schiff, "Comparison of Techniques for Measurement of Ambient Levels of Hydrogen Peroxide," *Environ. Sci. Technol., 22,* 53–61 (1988a).

Kleindienst, T. E., P. B. Shepson, C. M. Nero, R. R. Arnts, S. B. Tejada, G. I. Mackay, L. K. Mayne, H. I. Schiff, J. A. Lind, G. L. Kok, A. L. Lazrus, P. K. Dasgupta, and S. Dong, "An Intercomparison of Formaldehyde Measurement Techniques at Ambient Concentrations," *Atmos. Environ., 22,* 1931–1939 (1988b).

Kleindienst, T. E., E. E. Hudgens, D. F. Smith, F. F. McElroy, and J. J. Bufalini, "Comparison of Chemiluminescence and Ultraviolet Ozone Monitor Responses in the Presence of Humidity and Photochemical Pollutants," *J. Air Waste Manage. Assoc., 43,* 213–222 (1993).

Kleindienst, T. E., "Recent Developments in the Chemistry and Biology of Peroxyacetyl Nitrate," *Res. Chem. Intermed., 20,* 335–384 (1994).

Kleindienst, T. E., E. W. Corse, F. T. Blanchard, and W. A. Lonneman, "Evaluation of the Performance of DNPH-Coated Silica Gel and $C_{18}$ Cartridges in the Measurement of Formaldehyde in the Presence and Absence of Ozone," *Environ. Sci. Technol., 32,* 124–130 (1998).

Klemp, M., A. Peters, and R. Sacks, "High-Speed GC Analysis of VOCs: Sample Collection and Inlet Systems," *Environ. Sci. Technol., 28,* 369A–376A (1994).

Kley, D., and M. McFarland, "Chemiluminescence Detector for NO and $NO_2$," *Atmos. Technol., 12,* 63–69 (1980).

Kliner, D. A. V., B. C. Daube, J. D. Burley, and S. C. Wofsy, "Laboratory Investigation of the Catalytic Reduction Technique for Measurement of Atmospheric $NO_y$," *J. Geophys. Res., 102,* 10759–10776 (1997).

Knop, G., and F. Arnold, "Stratospheric Trace Gas Detection Using a New Balloon-Borne ACIMS Method: Acetonitrile, Acetone, and Nitric Acid," *Geophys. Res. Lett., 14,* 1262–1265 (1987a).

Knop, G., and F. Arnold, "Atmospheric Acetonitrile Measurements in the Tropopause Region Using Aircraft-Borne Active Chemical Ionization Mass Spectrometry," *Planet. Space Sci., 35,* 259–266 (1987b).

Kok, G. L., K. Thompson, and A. L. Lazrus, "Derivatization Technique for the Determination of Peroxides in Precipitation," *Anal. Chem., 58,* 1192–1194 (1986).

Kok, G. L., A. J. Schanot, P. F. Lindgren, P. K. Dasgupta, D. A. Hegg, P. V. Hobbs, and J. F. Boatman, "An Airborne Test of Three Sulfur Dioxide Measurement Techniques," *Atmos. Environ., 24A,* 1903–1908 (1990).

Kok, G. L., S. E. McLaren, and T. A. Staffelbach, "HPLC Determination of Atmospheric Organic Hydroperoxides," *J. Atmos. Oceanic Technol., 12,* 282–289 (1995).

Koppmann, R., F. J. Johnen, A. Khedim, J. Rudolph, A. Wedel, and B. Wiards, "The Influence of Ozone on Light Nonmethane Hydrocarbons during Cryogenic Preconcentration," *J. Geophys. Res., 100,* 11383–11391 (1995).

Koutrakis, P., J. M. Wolfson, J. L. Slater, M. Brauer, J. D. Spengler, R. K. Stevens, and C. L. Stone, "Evaluation of an Annular Denuder/Filter Pack System to Collect Acidic Aerosols and Gases," *Environ. Sci. Technol., 22,* 1463–1468 (1988).

Koutrakis, P., C. Sioutas, S. T. Ferguson, J. M. Wolfson, J. D. Mulik, and R. M. Burton, "Development and Evaluation of a Glass Honeycomb Denuder/Filter Pack System to Collect Atmospheric Gases and Particles," *Environ. Sci. Technol., 27,* 2497–2501 (1993).

Krieger, M. S., and R. A. Hites, "Diffusion Denuder for the Collection of Semivolatile Organic Compounds," *Environ. Sci. Technol., 26,* 1551–1555 (1992).

Krochmal, D., and L. Górski, "Determination of Nitrogen Dioxide in Ambient Air by Use of a Passive Sampling Technique and Triethanolamine as Absorbent," *Environ. Sci. Technol., 25,* 531–535 (1991).

Krol, M., P. J. van Leeuwen, and J. Lelieveld, "Global OH Trend Inferred from Methylchloroform Measurements," *J. Geophys. Res., 103,* 10697–10711 (1998).

Kuntz, R., W. Lonneman, G. Namie, and L. A. Hull, "Rapid Determination of Aldehydes in Air Analyses," *Anal. Lett., 13,* 1409–1415 (1980).

Kuwata, K., M. Uebori, H. Yamasaki, Y. Kuge, and Y. Kiso, "Determination of Aliphatic Aldehydes in Air by Liquid Chromatography," *Anal. Chem., 55,* 2013–2016 (1983).

Lacheur, R. M., L. B. Sonnenberg, P. C. Singer, R. F. Christman, and M. J. Charles, "Identification of Carbonyl Compounds in Environmental Samples," *Environ. Sci. Technol., 27,* 2745–2753 (1993).

Lam, G. C. K., D. Y. C. Leung, M. Niewiadomski, S. W. Pang, A. W. F. Lee, and P. K. K. Louie, "Street-Level Concentrations of Nitrogen Dioxide and Suspended Particulate Matter in Hong Kong," *Atmos. Environ., 33,* 1–11 (1999).

Lammel, G., and J. N. Cape, "Nitrous Acid and Nitrite in the Atmosphere," *Chem. Soc. Rev., 25,* 361–369 (1996).

Langford, A. O., P. D. Goldan, and F. C. Fehsenfeld, "A Molybdenum Oxide Annular Denuder System for Gas Phase Ambient Ammonia Measurements," *J. Atmos. Chem., 8,* 359–376 (1989).

Langford, A. O., and F. C. Fehsenfeld, "Natural Vegetation as a Source or Sink for Atmospheric Ammonia: A Case Study," *Science, 255,* 581–583 (1992).

Larsen, B., T. Bomboi-Mingarro, E. Brancaleoni, A. Calogirou, A. Cecinato, C. Coeur, I. Chatzianestis, M. Duane, M. Frattoni, J.-L. Fugit, U. Hansen, V. Jacob, N. Mimikos, T. Hoffmann, S. Owen, R. Perez-Pastor, A. Reichmann, G. Seufert, M. Staudt, and R. Steinbrecher, "Sampling and Analysis of Terpenes in Air. An Interlaboratory Comparison," *Atmos. Environ., 31,* 35–49 (1997).

Lawrence Berkeley Laboratory (LBL), *Instrumentation for Environmental Monitoring, Air*, Vol. 1, Part 2, September 1979, pp. 301–378.

Lawson, D. R., H. W. Biermann, E. C. Tuazon, A. M. Winer, G. I. Mackay, H. I. Schiff, G. L. Kok, P. K. Dasgupta, and K. Fung, "Formaldehyde Measurement Methods Evaluation and Ambient Concentrations during the Carbonaceous Species Methods Comparison Study," *Aerosol Sci. Technol., 12,* 64–76 (1990).

Lazendorf, E. J., T. F. Hanisco, N. M. Donahue, and P. O. Wennberg, "Comment on: 'The Measurement of Tropospheric OH Radicals by Laser-Induced Fluorescence Spectroscopy during the POPCORN Field Campaign,' by Hofzumahaus *et al.* and 'Intercomparison of Tropospheric OH Radical Measurements by Multiple Folded Long-Path Laser Absorption and Laser Induced Fluorescence,' by Brauers *et al.*," *Geophys. Res. Lett., 24,* 3037–3038 (1997).

Lazrus, A. L., G. L. Kok, S. N. Gitlin, and J. A. Lind, "Automated Fluorometric Method for Hydrogen Peroxide in Atmospheric Precipitation," *Anal. Chem., 57,* 917–922 (1985).

Lazrus, A. L., G. L. Kok, J. A. Lind, S. N. Gitlin, B. G. Heikes, and R. E. Shetter, "Automated Fluorometric Method for Hydrogen Peroxide in Air," *Anal. Chem., 58,* 594–597 (1986).

Lazrus, A. L., K. L. Fong, and J. A. Lind, "Automated Fluorometric Determination of Formaldehyde in Air," *Anal. Chem., 60,* 1074–1078 (1988).

Le Lacheur, R. M., L. B. Sonnenberg, P. C. Singer, R. F. Christman, and M. J. Charles, "Identification of Carbonyl Compounds in Environmental Samples," *Environ. Sci. Technol., 27,* 2745–2753 (1993).

Lee, J. H., Y. Chen, and I. N. Tang, "Heterogeneous Loss of Gaseous $H_2O_2$ in an Atmospheric Air Sampling System," *Environ. Sci. Technol., 25,* 339–342 (1991).

Lee, J. H., D. F. Leahy, I. N. Tang, and L. Newman, "Measurement and Speciation of Gas Phase Peroxides in the Atmosphere," *J. Geophys. Res., 98,* 2911–2915 (1993).

Lee, S.-H., J. Hirokawa, Y. Kajii, and H. Akimoto, "New Method for Measuring Low NO Concentrations Using Laser Induced Two Photon Ionization," *Rev. Sci. Instrum., 68,* 2891–2897 (1997).

Lee, Y.-N., and X. Zhou, "Method for the Determination of Some Soluble Atmospheric Carbonyl Compounds," *Environ. Sci. Technol., 27,* 749–756 (1993).

Lee, Y.-N., X. Zhou, and K. Hallock, "Atmospheric Carbonyl Compounds at a Rural Southeastern United States Site," *J. Geophys. Res., 100,* 25933–25944 (1995).

Leibrock, E., and J. Slemr, "Method for Measurement of Volatile Oxygenated Hydrocarbons in Ambient Air," *Atmos. Environ., 31,* 3329–3339 (1997).

Lemire, G. W., J. B. Simeonsson, and R. C. Sausa, "Monitoring of Vapor-Phase Nitro Compounds Using 226-nm Radiation: Fragmentation with Subsequent No Resonance-Enhanced Multiphoton Ionization Detection," *Anal. Chem., 65,* 529–533 (1993).

Letokhov, V. S., *Laser Photoionization Spectroscopy*, Academic Press, San Diego, 1987.

Levin, J.-O., R. Lindahl, and K. Andersson, "Monitoring of Parts-Per-Billion Levels of Formaldehyde Using a Diffusive Sampler," *JAPCA, 39,* 44–47 (1989).

Lewin, E. E., R. G. de Pena, and J. P. Shimshock, "Atmospheric Gas and Particle Measurements at a Rural Northeastern U.S. Site," *Atmos. Environ., 20,* 59–70 (1986).

Lin, C.-I., M. Baker, and R. J. Charlson, "Absorption Coefficient of Atmospheric Aerosol: A Method for Measurement," *Appl. Opt., 12,* 1356–1363 (1973).

Lindgren, P. F., and P. K. Dasgupta, "Measurement of Atmospheric Sulfur Dioxide by Diffusion Scrubber Coupled Ion Chromatography," *Anal. Chem., 61,* 19–24 (1989).

Lindskog, A., Y. Andersson-Sköld, P. Grennfelt, and J. Mowrer, "Concentration Profiles of Hydrocarbons during Episodes in Relation to Emission Pattern, Model Calculations, and Oxidants," *J. Atmos. Chem., 14,* 425–438 (1992).

Lindskog, A., and J. Moldanova, "The Influence of the Origin, Season, and Time of the Day on the Distribution of Individual NMHC Measured at Rörvik, Sweden," *Atmos. Environ., 18,* 2383–2398 (1994).

Lipari, F., and S. J. Swarin, "Determination of Formaldehyde and Other Aldehydes in Automobile Exhaust with an Improved 2,4-Dinitrophenylhydrazine Method," *J. Chromatogr., 247,* 297–306 (1982).

Lipari, F., and S. J. Swarin, "2,4-Dinitrophenylhydrazine-Coated Florisil Sampling Cartridges for the Determination of Formaldehyde in Air," *Environ. Sci. Technol., 19,* 70–74 (1985).

Liu, B. Y. H., D. Y. H. Pui, and H. J. Fissan, *Aerosols, Science, Technology, and Industrial Applications of Airborne Particles*, Elsevier, New York, 1984.

Liu, D.-Y., D. Rutherford, M. Kinsey, and K. A. Prather, "Real-Time Monitoring of Pyrotechnically Derived Aerosol Particles in the Troposphere," *Anal. Chem., 69,* 1808–1814 (1997).

Liu, P., P. J. Ziemann, D. B. Kittelson, and P. H. McMurry, "Generating Particle Beams of Controlled Dimensions and Divergence: I. Theory of Particle Motion in Aerodynamic Lenses and Nozzle Expansions," *Aerosol Sci. Technol., 22,* 293–313 (1995a).

Liu, P., P. J. Ziemann, D. B. Kittelson, and P. H. McMurry, "Generating Particle Beams of Controlled Dimensions and Divergence: II. Experimental Evaluation of Particle Motion in Aerodynamic Lenses and Nozzle Expansions," *Aerosol Sci. Technol., 22,* 314–324 (1995b).

Lundgren, D. A., F. S. Harris, Jr., W. H. Marlow, M. Lippmann, W. E. Clark, and M. D. Durham, Eds., *Aerosol Measurement*, University Press of Florida, Gainesville, FL, 1979.

Luria, M., C. C. Van Valin, J. F. Boatman, D. L. Wellman, and R. F. Pueschel, "Sulfur Dioxide Flux Measurements over the Western Atlantic Ocean," *Atmos. Environ., 21,* 1631–1636 (1987).

Macdonald, A. M., K. G. Anlauf, C. M. Banic, W. R. Leaitch, and H. A. Wiebe, "Airborne Measurements of Aqueous and Gaseous Hydrogen Peroxide during Spring and Summer in Ontario, Canada," *J. Geophys. Res., 100,* 7253–7262 (1995).

Mackay, G. I., H. I. Schiff, A. Wiebe, and K. Anlauf, "Measurements of $NO_2$, $H_2CO$, and $HNO_3$ by Tunable Diode Laser Absorption Spectroscopy during the 1985 Claremont Intercomparison Study," *Atmos. Environ., 22,* 1555–1564 (1988).

Maeda, Y., K. Aoki, and M. Munemori, "Chemiluminescence Method for the Determination of Nitrogen Dioxide," *Anal. Chem., 52,* 307–311 (1980).

Maeda, Y., and N. Takenaka, "Chemiluminescence Determination of Trace Amounts of Ammonia and Halogen Species in the Environment," in *Optical Methods in Atmospheric Chemistry,* SPIE, Vol. 1715, pp. 185–193, Bellingham, WA, 1992.

Mansoori, B. A., M. V. Johnston, and A. S. Wexler, "Quantitation of Ionic Species in Single Microdroplets by On-Line Laser Desorption/Ionization," *Anal. Chem., 66,* 3681–3687 (1994).

March, R. E., "Ion Trap Mass Spectrometry," *Int. J. Mass Spectrom. Ion Processes, 118 / 119,* 71–135 (1992).

Marijnissen, J., B. Scarlett, and P. Verheijen, "Proposed On-Line Aerosol Analysis Combining Size Determination, Laser-Induced Fragmentation, and Time-of-Flight Mass Spectroscopy," *J. Aerosol Sci., 19,* 1307–1310 (1988).

Marple, V. A., and K. Willeke, "Inertial Impactors," in *Aerosol Measurement* (D. A. Lundgren, F. S. Harris, Jr., W. H. Marlow, M. Lippmann, W. E. Clark, and M. D. Durham, Eds.), pp. 90–107, University Press of Florida, Gainesville, FL, 1979.

Marple, V. A., K. L. Rubow, and S. M. Behm, "A Microorifice Uniform Deposit Impactor (MOUDI): Description, Calibration, and Use," *Aerosol Sci. Technol., 14,* 434–446 (1991).

Marshall, T. L., C. T. Chaffin, R. M. Hammaker, and W. G. Fateley, "An Introduction to Open-Path FT-IR Atmospheric Monitoring," *Environ. Sci. Technol., 28,* 224–232 (1994).

Martens, A. E., and J. D. Keller, "An Instrument for Sizing and Counting Airborne Particles," *Am. Ind. Hyg. Assoc. J., 29,* 257–267 (1968).

Marti, J. J., R. J. Weber, M. T. Saros, J. G. Vasiliou, and P. H. McMurry, "Modification of the TSI 3025 Condensation Particle Counter for Pulse Height Analysis," *Aerosol Sci. Technol., 25,* 214–218 (1996).

Martin, D., M. Tsivou, B. Bonsang, C. Abonnel, T. Carsey, M. Springer-Young, A. Pszenny, and K. Suhre, "Hydrogen Peroxide in the Marine Atmospheric Boundary Layer during the Atlantic Stratocumulus Transition Experiment/Marine Aerosol and Gas Exchange Experiment in the Eastern Subtropical North Atlantic," *J. Geophys. Res., 10,* 6003–6015 (1997).

Mather, J. H., P. S. Stevens, and W. H. Brune, "OH and $HO_2$ Measurements Using Laser-Induced Fluorescence," *J. Geophys. Res., 102,* 6427–6436 (1997).

Matisová, E., and S. Škrabáková, "Carbon Sorbents and Their Utilization for the Preconcentration of Organic Pollutants in Environmental Samples," *J. Chromatogr. A, 707,* 145–179 (1995).

Mauldin, R. L., III, D. J. Tanner, and F. L. Eisele, "A New Chemical Ionization Mass Spectrometer Technique for the Fast Measurement of Gas Phase Nitric Acid in the Atmosphere," *J. Geophys. Res., 103,* 3361–3367 (1998).

McCaffrey, C. A., J. MacLachlan, and B. I. Brookes, "Adsorbent Tube Evaluation for the Preconcentration of Volatile Organic Compounds in Air for Analysis by Gas Chromatography–Mass Spectrometry," *Analyst, 119,* 897–902 (1994).

McClenny, W. A., K. D. Oliver, and E. H. Daughtrey, Jr., "Analysis of VOCs in Ambient Air Using Multisorbent Packings for VOC Accumulation and Sample Drying," *J. Air Waste Manage. Assoc., 45,* 792–800 (1995).

McDermott, W. T., R. C. Ockovic, and M. R. Stolzenburg, "Counting Efficiency of an Improved 30-A Condensation Nucleus Counter," *Aerosol Sci. Technol, 14,* 278–287 (1991).

McDiarmid, R., and A. SabljiX, "Experimental Assignments of the 3*p* Rydberg States of Acetone," *J. Chem. Phys., 89,* 6086–6095 (1988).

McDow, S. R., and J. J. Huntzicker, "Vapor Adsorption Artifact in the Sampling of Organic Aerosol: Face Velocity Effects," *Atmos. Environ., 24A,* 2563–2571 (1990).

McElroy, F. F., V. L. Thompson, D. M. Holland, W. A. Lonneman, and R. L. Sella, "Cryogenic Preconcentration-Direct FID Method for Measurement of Ambient NMOC: Refinement and Comparison with GC Speciation," *JAPCA, 36,* 710–714 (1986).

McKeen, S. A., M. Trainer, E. Y. Hsie, R. K. Tallamraju, and S. C. Liu, "On the Indirect Determination of Atmospheric OH Radical Concentrations from Reactive Hydrocarbon Measurements," *J. Geophys. Res., 95,* 7493–7500 (1990).

McKeown, P. J., M. V. Johnston, and D. M. Murphy, "On-Line Single-Particle Analysis by Laser Desorption Mass Spectrometry," *Anal. Chem., 63,* 2069–2073 (1991).

McManus, J. B., P. L. Kebabian, and M. S. Zahniser, "Astigmatic Mirror Multiple Pass Absorption Cells for Long Pathlength Spectroscopy," *Appl. Opt., 34,* 3336–3348 (1995).

McMurry, P. H., M. Litchy, P.-F. Huang, X. Cai, B. J. Turpin, W. D. Dick, and A. Hanson, "Elemental Composition and Morphology of Individual Particles Separated by Size and Hygroscopicity with the TDMA," *Atmos. Environ., 30,* 101–108 (1996).

Meyer, C. P., C. M. Elsworth, and I. E. Galbally, "Water Vapor Interference in the Measurement of Ozone in Ambient Air by Ultraviolet Absorption," *Rev. Sci. Instrum., 62,* 223–228 (1991).

Middlebrook, A. M., D. S. Thomson, and D. M. Murphy, "On the Purity of Laboratory-Generated Sulfuric Acid Droplets and Ambient Particles Studied by Laser Mass Spectrometry," *Aerosol Sci. Technol., 27,* 293–307 (1997).

Mihelcic, D., P. Müsgen, and D. H. Ehhalt, "An Improved Method of Measuring Tropospheric $NO_2$ and $RO_2$ by Matrix Isolation and Electron Spin Resonance," *J. Atmos. Chem., 3,* 341–361 (1985).

Mihelcic, D., A. Volz-Thomas, H. W. Pätz, D. Kley, and M. Mihelcic, "Numerical Analysis of ESR Spectra from Atmospheric Samples," *J. Atmos. Chem., 11,* 271–297 (1990).

Mihelcic, D., D. Klemp, P. Müsgen, H. W. Pätz, and A. Volz-Thomas, "Simultaneous Measurements of Peroxy and Nitrate Radicals at Schauinsland," *J. Atmos. Chem., 16,* 313–335 (1993).

Mihele, C. M., and D. R. Hastie, "The Sensitivity of the Radical Amplifier to Ambient Water Vapour," *Geophys. Res. Lett., 25,* 1911–1913, 3167 (1998).

Miller, D. P., "Low-Level Determination of Nitrogen Dioxide in Ambient Air Using the Palmes Tube," *Atmos. Environ., 22,* 945–947 (1988).

Monks, P. S., L. J. Carpenter, S. A. Penkett, and G. P. Ayers, "Nighttime Peroxy Radical Chemistry in the Remote Marine Boundary Layer over the Southern Ocean," *Geophys. Res. Lett., 23,* 535–538 (1996).

Moosmüller, H., W. P. Arnott, and C. F. Rogers, "Methods for Real-Time, *In Situ* Measurement of Aerosol Light Absorption," *J. Air Waste Manage. Assoc., 47,* 157–166 (1997).

Morawaska, L., S. Thomas, N. Bofinger, D. Wainwright, and D. Neale, "Comprehensive Characterization of Aerosols in a Subtropical Urban Atmosphere: Particle Size Distribution and Correlation with Gaseous Pollutants," *Atmos. Environ., 32,* 2467–2478 (1998).

Morikawa, T., S. Wakamatsu, M. Tanaka, I. Uno, T. Kamiura, and T. Maeda, "$C_2$–$C_5$ Hydrocarbon Concentrations in Central Osaka," *Atmos. Environ., 32,* 2007–2016 (1998).

Moschonas, N., and S. Glavas, "$C_3$–$C_{10}$ Hydrocarbons in the Atmosphere of Athens, Greece," *Atmos. Environ., 30,* 2769–2772 (1996).

Mount, G. H., "The Measurement of Tropospheric OH by Long Path Absorption. 1. Instrumentation," *J. Geophys. Res., 97,* 2427–2444 (1992).

Mount, G. H., and F. L. Eisele, "An Intercomparison of Tropospheric OH Measurements at Fritz Peak Observatory, Colorado," *Science, 256,* 1187–1190 (1992).

Mount, G. H., and J. W. Harder, "The Measurement of Tropospheric Trace Gases at Fritz Peak Observatory, Colorado, by Long-Path Absorption: OH and Ancillary Gases," *J. Atmos. Sci., 52,* 3342–3353 (1995).

Mount, G. H., F. L. Eisele, D. J. Tanner, J. W. Brault, P. V. Johnston, J. W. Harder, E. J. Williams, A. Fried, and R. Shetter, "An Intercomparison of Spectroscopic Laser Long-Path and Ion-Assisted *in-Situ* Measurements of Hydroxyl Concentrations during the Tropospheric OH Photochemistry Experiment, Fall 1993," *J. Geophys. Res., 102,* 6437–6455 (1997a).

Mount, G. H., J. W. Brault, P. V. Johnston, E. Marovich, R. O. Jakoubek, C. J. Volpe, J. Harder, and J. Olson, "Measurement of Tropospheric OH by Long-Path Laser Absorption at Fritz Peak Observatory, Colorado, during the OH Photochemistry Experiment, Fall 1993," *J. Geophys. Res., 102,* 6393–6413 (1997b).

Mowrer, J., and A. Lindskog, "Automatic Unattended Sampling and Analysis of Background Levels of $C_2$–$C_5$ Hydrocarbons," *Atmos. Environ., 25A,* 1971–1979 (1991).

Mulik, J., R. Puckett, D. Williams, and E. Sawicki, "Ion Chromatographic Analysis of Sulfate and Nitrate in Ambient Aerosols," *Anal. Lett., 9,* 653–663 (1976).

Mullin, J. B., and J. P. Riley, "The Spectrophotometric Determination of Nitrate in Natural Waters with Particulate Reference to Sea Water," *Anal. Chim. Acta, 12,* 464–480 (1955).

Munger, J. W., D. J. Jacob, B. C. Daube, L. W. Horowitz, W. C. Keene, and B. G. Heikes, "Formaldehyde, Glyoxal, and Methylglyoxal in Air and Cloudwater at a Rural Mountain Site in Central Virginia," *J. Geophys. Res., 100,* 9325–9333 (1995).

Munro, R., R. Siddans, W. J. Reburn, and B. J. Kerridge, "Direct Measurement of Tropospheric Ozone Distributions from Space," *Nature, 392,* 168–171 (1998).

Murphy, D. M., and D. S. Thomson, "Laser Ionization Mass Spectroscopy of Single Aerosol Particles," *Aerosol Sci. Technol., 22,* 237–249 (1995).

Murphy, D. M., and D. S. Thomson, "Chemical Composition of Single Aerosol Particles at Idaho Hill: Positive Ion Measurements," *J. Geophys. Res., 102,* 6341–6352 (1997a).

Murphy, D. M., and D. S. Thomson, "Chemical Composition of Single Aerosol Particles at Idaho Hill: Negative Ion Measurements," *J. Geophys. Res., 102,* 6353–6368 (1997b).

Myers, R. L., and W. L. Fite, "Electrical Detection of Airborne Particulates Using Surface Ionization Techniques," *Environ. Sci. Technol., 9,* 334–336 (1975).

Narcisi, R. S., and A. D. Bailey, "Mass Spectrometric Measurements of Positive Ions at Altitudes from 64 to 112 Kilometers," *J. Geophys. Res., 70,* 3687–3700 (1965).

Navas, M. J., A. M. Jiménez, and G. Galán, "Air Analysis: Determination of Nitrogen Compounds by Chemiluminescence," *Atmos. Environ., 31,* 3603–3608 (1997).

Nejedly, Z., J. L. Campbell, W. J. Teesdale, J. F. Dlouhy, T. F. Dann, R. M. Hoff, J. R. Brook, and H. A. Wiebe, "Inter-Laboratory Comparison of Air Particulate Monitoring Data," *J. Air Waste Manage. Assoc., 48,* 386–397 (1998).

Neubauer, K. R., M. V. Johnston, and A. S. Wexler, "Chromium Speciation in Aerosols by Rapid Single-Particle Mass Spectrometry," *Int. J. Mass Spectrom. Ion Processes, 151,* 77–87 (1995).

Neubauer, K. R., S. T. Sum, M. V. Johnston, and A. S. Wexler, "Sulfur Speciation in Individual Aerosol Particles," *J. Geophys. Res., 101,* 18701–18707 (1996).

Neubauer, K. R., M. V. Johnston, and A. S. Wexler, "On-Line Analysis of Aqueous Aerosols by Laser Desorption Ionization," *Int. J. Mass Spectrom. Ion Processes, 163,* 29–37 (1997).

Neubauer, K. R., M. V. Johnston, and A. S. Wexler, "Humidity Effects on the Mass Spectra of Single Aerosol Particles," *Atmos. Environ., 32,* 2521–2529 (1998).

Nielsen, T., A. H. Egeløv, K. Granby, and H. Skov, "Observations on Particulate Organic Nitrates and Unidentified Components of $NO_y$," *Atmos. Environ., 29,* 1757–1769 (1995).

Nielsen, T., J. Platz, K. Granby, A. B. Hansen, H. Skov, and A. H. Egeløv, "Particulate Organic Nitrates: Sampling and Night/Day Variation," *Atmos. Environ., 32,* 2601–2608 (1998).

Noble, C. A., T. Nordmeyer, K. Salt, B. Morrical, and K. A. Prather, "Aerosol Characterization Using Mass Spectrometry," *Trends Anal. Chem., 13,* 218–222 (1994).

Noble, C. A., and K. A. Prather, "Real-Time Measurement of Correlated Size and Composition Profiles of Individual Atmospheric Aerosol Particles," *Environ. Sci. Technol., 30,* 2667–2680 (1996).

Nolte, C. G., P. A. Solomon, T. Fall, L. G. Salmon, and G. R. Cass, "Seasonal and Spatial Characteristics of Formic and Acetic Acids Concentrations in the Southern California Atmosphere," *Environ. Sci. Technol., 31,* 2547–2553 (1997).

Nondek, L., D. R. Rodler, and J. W. Birks, "Measurement of Sub-ppbv Concentrations of Aldehydes in a Forest Atmosphere Using a New HPLC Technique," *Environ. Sci. Technol., 26,* 1174–1178 (1992).

Nordmeyer, T., and K. A. Prather, "Real-Time Measurement Capabilities Using Aerosol Time-of-Flight Mass Spectrometry," *Anal. Chem., 66,* 3540–3542 (1994).

Nouaime, G., S. B. Bertman, C. Seaver, D. Elyea, H. Huang, P. B. Shepson, T. K. Starn, D. D. Riemer, R. G. Zika, and K. Olszyna, "Sequential Oxidation Products from Tropospheric Isoprene Chemistry: MACR and MPAN at a $NO_x$-Rich Forest Environment in the Southeastern United States," *J. Geophys. Res., 103,* 22463–22471 (1998).

Novakov, T., P. K. Mueller, A. E. Alcocer, and J. W. Otvos, "Chemical Composition of Pasadena Aerosol by Particle Size and Time of Day. III. Chemical States of Nitrogen and Sulfur by Photoelectron Spectroscopy," *J. Colloid. Interface Sci., 39,* 225–234 (1972).

Novelli, P. C., L. P. Steele, and P. P. Tans, "Mixing Ratios of Carbon Monoxide in the Troposphere," *J. Geophys. Res., 97,* 20731–20750 (1992).

Novelli, P. C., V. S. Connors, H. G. Reichle, Jr., B. E. Anderson, C. A. M. Brenninkmeijer, E. G. Brunke, B. G. Doddridge, V. W. J. H. Kirchhoff, K. S. Lam, K. A. Masarie, T. Matsuo, D. D. Parrish, H. E. Scheel, and L. P. Steele, "An Internally Consistent Set of Globally Distributed Atmospheric Carbon Monoxide Mixing Ratios Developed Using Results from an Intercomparison of Measurements," *J. Geophys. Res., 103,* 19285–19293 (1998a).

Novelli, P. C., K. A. Masarie, and P. M. Lang, "Distributions and Recent Changes of Carbon Monoxide in the Lower Troposphere," *J. Geophys. Res., 103,* 19015–19033 (1998b).

Noxon, J. F., "Nitrogen Dioxide in the Stratosphere and Troposphere Measured by Ground-Based Absorption Spectroscopy," *Science, 189,* 547–549 (1975).

Noxon, J. F., R. B. Norton, and W. R. Henderson, "Observation of Atmospheric $NO_3$," *Geophys. Res. Lett., 5,* 675–678 (1978).

Morikawa, T., S. Wakamatsu, M. Tanaka, I. Uno, T. Kamiura, and T. Maeda, "$C_2$–$C_5$ Hydrocarbon Concentrations in Central Osaka," *Atmos. Environ., 32,* 2007–2016 (1998).

Moschonas, N., and S. Glavas, "$C_3$–$C_{10}$ Hydrocarbons in the Atmosphere of Athens, Greece," *Atmos. Environ., 30,* 2769–2772 (1996).

Mount, G. H., "The Measurement of Tropospheric OH by Long Path Absorption. 1. Instrumentation," *J. Geophys. Res., 97,* 2427–2444 (1992).

Mount, G. H., and F. L. Eisele, "An Intercomparison of Tropospheric OH Measurements at Fritz Peak Observatory, Colorado," *Science, 256,* 1187–1190 (1992).

Mount, G. H., and J. W. Harder, "The Measurement of Tropospheric Trace Gases at Fritz Peak Observatory, Colorado, by Long-Path Absorption: OH and Ancillary Gases," *J. Atmos. Sci., 52,* 3342–3353 (1995).

Mount, G. H., F. L. Eisele, D. J. Tanner, J. W. Brault, P. V. Johnston, J. W. Harder, E. J. Williams, A. Fried, and R. Shetter, "An Intercomparison of Spectroscopic Laser Long-Path and Ion-Assisted *in-Situ* Measurements of Hydroxyl Concentrations during the Tropospheric OH Photochemistry Experiment, Fall 1993," *J. Geophys. Res., 102,* 6437–6455 (1997a).

Mount, G. H., J. W. Brault, P. V. Johnston, E. Marovich, R. O. Jakoubek, C. J. Volpe, J. Harder, and J. Olson, "Measurement of Tropospheric OH by Long-Path Laser Absorption at Fritz Peak Observatory, Colorado, during the OH Photochemistry Experiment, Fall 1993," *J. Geophys. Res., 102,* 6393–6413 (1997b).

Mowrer, J., and A. Lindskog, "Automatic Unattended Sampling and Analysis of Background Levels of $C_2$–$C_5$ Hydrocarbons," *Atmos. Environ., 25A,* 1971–1979 (1991).

Mulik, J., R. Puckett, D. Williams, and E. Sawicki, "Ion Chromatographic Analysis of Sulfate and Nitrate in Ambient Aerosols," *Anal. Lett., 9,* 653–663 (1976).

Mullin, J. B., and J. P. Riley, "The Spectrophotometric Determination of Nitrate in Natural Waters with Particulate Reference to Sea Water," *Anal. Chim. Acta, 12,* 464–480 (1955).

Munger, J. W., D. J. Jacob, B. C. Daube, L. W. Horowitz, W. C. Keene, and B. G. Heikes, "Formaldehyde, Glyoxal, and Methylglyoxal in Air and Cloudwater at a Rural Mountain Site in Central Virginia," *J. Geophys. Res., 100,* 9325–9333 (1995).

Munro, R., R. Siddans, W. J. Reburn, and B. J. Kerridge, "Direct Measurement of Tropospheric Ozone Distributions from Space," *Nature, 392,* 168–171 (1998).

Murphy, D. M., and D. S. Thomson, "Laser Ionization Mass Spectroscopy of Single Aerosol Particles," *Aerosol Sci. Technol., 22,* 237–249 (1995).

Murphy, D. M., and D. S. Thomson, "Chemical Composition of Single Aerosol Particles at Idaho Hill: Positive Ion Measurements," *J. Geophys. Res., 102,* 6341–6352 (1997a).

Murphy, D. M., and D. S. Thomson, "Chemical Composition of Single Aerosol Particles at Idaho Hill: Negative Ion Measurements," *J. Geophys. Res., 102,* 6353–6368 (1997b).

Myers, R. L., and W. L. Fite, "Electrical Detection of Airborne Particulates Using Surface Ionization Techniques," *Environ. Sci. Technol., 9,* 334–336 (1975).

Narcisi, R. S., and A. D. Bailey, "Mass Spectrometric Measurements of Positive Ions at Altitudes from 64 to 112 Kilometers," *J. Geophys. Res., 70,* 3687–3700 (1965).

Navas, M. J., A. M. Jiménez, and G. Galán, "Air Analysis: Determination of Nitrogen Compounds by Chemiluminescence," *Atmos. Environ., 31,* 3603–3608 (1997).

Nejedly, Z., J. L. Campbell, W. J. Teesdale, J. F. Dlouhy, T. F. Dann, R. M. Hoff, J. R. Brook, and H. A. Wiebe, "Inter-Laboratory Comparison of Air Particulate Monitoring Data," *J. Air Waste Manage. Assoc., 48,* 386–397 (1998).

Neubauer, K. R., M. V. Johnston, and A. S. Wexler, "Chromium Speciation in Aerosols by Rapid Single-Particle Mass Spectrometry," *Int. J. Mass Spectrom. Ion Processes, 151,* 77–87 (1995).

Neubauer, K. R., S. T. Sum, M. V. Johnston, and A. S. Wexler, "Sulfur Speciation in Individual Aerosol Particles," *J. Geophys. Res., 101,* 18701–18707 (1996).

Neubauer, K. R., M. V. Johnston, and A. S. Wexler, "On-Line Analysis of Aqueous Aerosols by Laser Desorption Ionization," *Int. J. Mass Spectrom. Ion Processes, 163,* 29–37 (1997).

Neubauer, K. R., M. V. Johnston, and A. S. Wexler, "Humidity Effects on the Mass Spectra of Single Aerosol Particles," *Atmos. Environ., 32,* 2521–2529 (1998).

Nielsen, T., A. H. Egeløv, K. Granby, and H. Skov, "Observations on Particulate Organic Nitrates and Unidentified Components of $NO_y$," *Atmos. Environ., 29,* 1757–1769 (1995).

Nielsen, T., J. Platz, K. Granby, A. B. Hansen, H. Skov, and A. H. Egeløv, "Particulate Organic Nitrates: Sampling and Night/Day Variation," *Atmos. Environ., 32,* 2601–2608 (1998).

Noble, C. A., T. Nordmeyer, K. Salt, B. Morrical, and K. A. Prather, "Aerosol Characterization Using Mass Spectrometry," *Trends Anal. Chem., 13,* 218–222 (1994).

Noble, C. A., and K. A. Prather, "Real-Time Measurement of Correlated Size and Composition Profiles of Individual Atmospheric Aerosol Particles," *Environ. Sci. Technol., 30,* 2667–2680 (1996).

Nolte, C. G., P. A. Solomon, T. Fall, L. G. Salmon, and G. R. Cass, "Seasonal and Spatial Characteristics of Formic and Acetic Acids Concentrations in the Southern California Atmosphere," *Environ. Sci. Technol., 31,* 2547–2553 (1997).

Nondek, L., D. R. Rodler, and J. W. Birks, "Measurement of Sub-ppbv Concentrations of Aldehydes in a Forest Atmosphere Using a New HPLC Technique," *Environ. Sci. Technol., 26,* 1174–1178 (1992).

Nordmeyer, T., and K. A. Prather, "Real-Time Measurement Capabilities Using Aerosol Time-of-Flight Mass Spectrometry," *Anal. Chem., 66,* 3540–3542 (1994).

Nouaime, G., S. B. Bertman, C. Seaver, D. Elyea, H. Huang, P. B. Shepson, T. K. Starn, D. D. Riemer, R. G. Zika, and K. Olszyna, "Sequential Oxidation Products from Tropospheric Isoprene Chemistry: MACR and MPAN at a $NO_x$-Rich Forest Environment in the Southeastern United States," *J. Geophys. Res., 103,* 22463–22471 (1998).

Novakov, T., P. K. Mueller, A. E. Alcocer, and J. W. Otvos, "Chemical Composition of Pasadena Aerosol by Particle Size and Time of Day. III. Chemical States of Nitrogen and Sulfur by Photoelectron Spectroscopy," *J. Colloid. Interface Sci., 39,* 225–234 (1972).

Novelli, P. C., L. P. Steele, and P. P. Tans, "Mixing Ratios of Carbon Monoxide in the Troposphere," *J. Geophys. Res., 97,* 20731–20750 (1992).

Novelli, P. C., V. S. Connors, H. G. Reichle, Jr., B. E. Anderson, C. A. M. Brenninkmeijer, E. G. Brunke, B. G. Doddridge, V. W. J. H. Kirchhoff, K. S. Lam, K. A. Masarie, T. Matsuo, D. D. Parrish, H. E. Scheel, and L. P. Steele, "An Internally Consistent Set of Globally Distributed Atmospheric Carbon Monoxide Mixing Ratios Developed Using Results from an Intercomparison of Measurements," *J. Geophys. Res., 103,* 19285–19293 (1998a).

Novelli, P. C., K. A. Masarie, and P. M. Lang, "Distributions and Recent Changes of Carbon Monoxide in the Lower Troposphere," *J. Geophys. Res., 103,* 19015–19033 (1998b).

Noxon, J. F., "Nitrogen Dioxide in the Stratosphere and Troposphere Measured by Ground-Based Absorption Spectroscopy," *Science, 189,* 547–549 (1975).

Noxon, J. F., R. B. Norton, and W. R. Henderson, "Observation of Atmospheric $NO_3$," *Geophys. Res. Lett., 5,* 675–678 (1978).

Noxon, J. F., R. B. Norton, and E. Marovich, "$NO_3$ in the Troposphere," *Geophys. Res. Lett., 7,* 125–128 (1980).

O'Brien, J. M., P. B. Shepson, K. Muthuramu, C. Hao, H. Niki, D. R. Hastie, R. Taylor, and P. B. Roussel, "Measurements of Alkyl and Multifunctional Organic Nitrates at a Rural Site in Ontario," *J. Geophys. Res., 100,* 22795–22804 (1995).

Okabe, H., P. L. Splitstone, and J. J. Ball, "Ambient and Source $SO_2$ Detector Based on a Fluorescence Method," *J. Air Pollut. Control Assoc., 23,* 514–516 (1973).

Parrish, D. D., M. Trainer, M. P. Buhr, B. A. Watkins, and F. C. Fehsenfeld, "Carbon Monoxide Concentrations and Their Relation to Concentrations of Total Reactive Oxidized Nitrogen at Two Rural U.S. Sites," *J. Geophys. Res., 96,* 9309–9320 (1991).

Parrish, D. D., M. P. Buhr, M. Trainer, R. B. Norton, J. P. Shimshock, F. C. Fehsenfeld, K. G. Anlauf, J. W. Bottenheim, Y. Z. Tang, H. A. Wiebe, J. M. Roberts, R. L. Tanner, L. Newman, V. C. Bowersox, K. J. Olszyna, E. M. Bailey, M. O. Rodgers, T. Wang, H. Berresheim, U. K. Roychowdhury, and K. L. Demerjian, "The Total Reactive Oxidized Nitrogen Levels and the Partitioning between the Individual Species at Six Rural Sites in Eastern North America," *J. Geophys. Res., 98,* 2927–2939 (1993).

Parrish, D. D., J. S. Holloway, and F. C. Fehsenfeld, "Routine, Continuous Measurement of Carbon Monoxide with Parts per Billion Precision," *Environ. Sci. Technol., 28,* 1615–1618 (1994).

Patashnick, H., and E. G. Rupprecht, "Continuous $PM_{10}$ Measurements Using the Tapered Element Oscillating Microbalance," *J. Air Waste Manage. Assoc., 41,* 1079–1083 (1991).

Pate, B., R. K. M. Jayanty, M. R. Peterson, and G. F. Evans, "Temporal Stability of Polar Organic Compounds in Stainless Steel Canisters," *J. Air Waste Manage. Assoc., 42,* 460–462 (1992).

Penkett, S. A., N. J. Blake, P. Lightman, A. R. W. Marsh, P. Anwyl, and G. Butcher, "The Seasonal Variation of Nonmethane Hydrocarbons in the Free Troposphere over the North Atlantic Ocean: Possible Evidence for Extensive Reaction of Hydrocarbons with the Nitrate Radical," *J. Geophys. Res., 98,* 2865–2885 (1993).

Perkins, M. D., and F. L. Eisele, "First Mass Spectrometric Measurements of Atmospheric Ions at Ground Level," *J. Geophys. Res., 89,* 9649–9657 (1984).

Perner, D., D. H. Ehhalt, H. W. Pätz, U. Platt, E. P. Röth, and A. Volz, "OH-Radicals in the Lower Troposphere," *Geophys. Res. Lett., 3,* 466–468 (1976).

Perner, D., and U. Platt, "Detection of Nitrous Acid in the Atmosphere by Differential Optical Absorption," *Geophys. Res. Lett., 6,* 917–920 (1979).

Perrino, C., F. De Santis, and A. Febo, "Criteria for the Choice of a Denuder Sampling Technique Devoted to the Measurement of Atmospheric Nitrous and Nitric Acids," *Atmos. Environ., 24A,* 617–626 (1990).

Perros, P. E., "Large-Scale Distribution of Peroxyacetylnitrate from Aircraft Measurements during the TROPOZ II Experiment," *J. Geophys. Res., 99,* 8269–8279 (1994).

Pfab, J., "Laser-Induced Fluorescence and Ionization Spectroscopy of Gas Phase Species," in *Spectroscopy in Environmental Science* (R. J. H. Clark and R. E. Hester, Eds.), Chap. 4, pp. 149–222, Wiley, New York, 1995.

Phalen, R. F., "Evaluation of an Exploded-Wire Aerosol Generator for Use in Inhalation Studies," *Aerosol Sci., 3,* 395–409 (1972).

Piringer, M., E. Ober, H. Puxbaum, and H. Kromp-Kolb, "Occurrence of Nitric Acid and Related Compounds in the Northern Vienna Basin during Summertime Anticyclonic Conditions," *Atmos. Environ., 31,* 1049–1057 (1997).

Plane, J. M. C., and N. Smith, "Atmospheric Monitoring by Differential Optical Absorption Spectroscopy," in *Spectroscopy in Environmental Science* (R. J. H. Clark and R. E Hester, Eds.), pp. 223–262, Wiley, New York, 1995.

Platt, U., D. Perner, G. W. Harris, A. M. Winer, and J. N. Pitts, Jr., "Observations of Nitrous Acid in an Urban Atmosphere by Differential Optical Absorption," *Nature, 285,* 312–314 (1980a).

Platt, U., D. Perner, A. M. Winer, G. W. Harris, and J. N. Pitts, Jr., "Detection of $NO_3$ in the Polluted Troposphere by Differential Optical Absorption," *Geophys. Res. Lett., 7,* 89–92 (1980b).

Platt, U., D. Perner, J. Schröder, C. Kessler, and A. Toennissen, "The Diurnal Variation of $NO_3$," *J. Geophys. Res., 86,* 11965–11970 (1981).

Platt, U., "Differential Optical Absorption Spectroscopy (DOAS)," in *Air Monitoring by Spectroscopic Techniques* (M. W. Sigrist, Ed.), *Chemical Analysis Series,* Vol. 127, pp. 27–84, Wiley, New York, 1994.

Platt, U., and M. Hausmann, "Spectroscopic Measurement of the Free Radicals $NO_3$, BrO, IO, and OH in the Troposphere," *Res. Chem. Intermed., 20,* 557–578 (1994).

Platt, U., and C. Janssen, "Observation and Role of the Free Radicals $NO_3$, ClO, BrO, and IO in the Troposphere," *Faraday Discuss., 100,* 175–198 (1995).

Pleil, J. D., and A. B. Lindstrom, "Collection of a Single Alveolar Exhaled Breath for Volatile Organic Compounds Analysis," *Am. J. Indust. Med., 28,* 109–121 (1995).

Porter, K., and D. H. Volman, "Flame Ionization Detection of Carbon Monoxide for Gas Chromatographic Analysis," *Anal. Chem., 34,* 748–749 (1962).

Pósfai, M., J. R. Anderson, P. R. Buseck, and H. Sievering, "Compositional Variations of Sea-Salt-Mode Aerosol Particles from the North Atlantic," *J. Geophys. Res., 100,* 23063–23074 (1995).

Pósfai, M., H. Xu, J. R. Anderson, and P. R. Buseck, "Wet and Dry Sizes of Atmospheric Aerosol Particles: An AFM–TEM Study," *Geophys. Res. Lett., 25,* 1907–1910 (1998).

Possanzini, M., V. Di Palo, M. Petricca, R. Fratarcangeli, and D. Brocco, "Measurements of Lower Carbonyls in Rome Ambient Air," *Atmos. Environ., 30,* 3757–3764 (1996).

Prather, K. A., T. Nordmeyer, and K. Salt, "Real-Time Characterization of Individual Aerosol Particles Using Time-of-Flight Mass Spectrometry," *Anal. Chem., 66,* 1403–1407 (1994).

Prinn, R., D. Cunnold, P. Simmonds, F. Alyea, R. Boldi, A. Crawford, P. Fraser, D. Gutzler, D. Hartley, R. Rosen, and R. Rasmussen, "Global Average Concentration and Trend for Hydroxyl Radicals Deduced from ALE/GAGE Trichloroethane (Methyl Chloroform) Data for 1978–1990," *J. Geophys. Res., 97,* 2445–2461 (1992).

Prinn, R. G., R. F. Weiss, B. R. Miller, J. Huang, F. N. Alyea, D. M. Cunnold, P. J. Fraser, D. E. Hartley, and P. G. Simmonds, "Atmospheric Trends and Lifetime of $CH_3CCl_3$ and Global OH Concentrations," *Science, 269,* 187–192 (1995).

Pszenny, A. A., W. C. Keene, D. J. Jacob, S. Fan, J. R. Maben, M. P. Zetwo, M. Springer-Young, and J. N. Galloway, "Evidence of Inorganic Chlorine Gases Other Than Hydrogen Chloride in Marine Surface Air," *Geophys. Res. Lett., 20,* 699–702 (1993).

Pui, D. Y. H., C. W. Lewis, C.-J. Tsai, and B. Y. H. Liu, "A Compact Coiled Denuder for Atmospheric Sampling," *Environ. Sci. Technol., 24,* 307–312 (1990).

Raabe, O. G., "The Generation of Aerosols of Fine Particles," in *Fine Particles: Aerosol Generation, Measurement, Sampling, and Analysis* (B. Y. L. Liu, Ed.), pp. 57–110, Academic Press, New York, 1976.

Raes, F., and A. Reineking, "A New Diffusion Battery Design for the Measurement of Sub-20 nm Aerosol Particles: The Diffusion Carrousel," *Atmos. Environ., 19,* 385–388 (1985).

Ramamurthi, M., and K. H. Leong, "Generation of Monodisperse Metallic, Metal Oxide, and Carbon Aerosols," *J. Aerosol Sci., 18,* 175–191 (1987).

Rao, A. M. M., G. G. Pandit, P. Sain, S. Sharma, T. M. Krishnamoorthy, and K. S. V. Nambi, "Non-Methane Hydrocarbons in Industrial Locations of Bombay," *Atmos. Environ., 31,* 1077–1085 (1997).

Rappenglück, P. Fabian, P. Kalabokas, L. G. Viras, and I. C. Ziomas, "Quasi-Continuous Measurements of Non-Methane Hydrocarbons (NMHC) in the Greater Athens Area during Medcaphot-Trace," *Atmos. Environ., 32,* 2103–2121 (1998).

Rapsomanikis, S., M. Wake, A.-M. N. Kitto, and R. M. Harrison, "Analysis of Atmospheric Ammonia and Particulate Ammonium by a Sensitive Fluorescence Method," *Environ. Sci. Technol., 22,* 948–952 (1988).

Reents, W. D., Jr., S. W. Downey, A. B. Emerson, A. M. Mujsce, A. J. Muller, D. J. Siconolfi, J. D. Sinclair, and A. G. Swanson, "Single Particle Characterization by Time-of-Flight Mass Spectrometry," *Aerosol Sci. Technol., 23,* 263–270 (1995).

Reichle, H. G., Jr., V. S. Connors, J. A. Holland, R. T. Sherrill, H. A. Wallio, J. C. Casas, E. P. Condon, B. B. Gormsen, and W. Seiler, "The Distribution of Middle Tropospheric Carbon Monoxide during Early October 1984," *J. Geophys. Res., 95,* 9845–9856 (1990).

Reid, J., J. Shewchun, B. K. Garside, and E. A. Ballik, "High Sensitivity Pollution Detection Employing Tunable Diode Lasers," *Appl. Opt., 17,* 300–307 (1978).

Reilly, P. T. A., R. A. Gieray, W. B. Whitten, and J. M. Ramsey, "Real-Time Characterization of the Organic Composition and Size of Individual Diesel Engine Smoke Particles," *Environ. Sci. Technol., 32,* 2672–2679 (1998).

Reiner, T., M. Hanke, and F. Arnold, "Atmospheric Peroxy Radical Measurements by Ion Molecule Reaction-Mass Spectrometry: A Novel Analytical Method Using Amplifying Chemical Conversion to Sulfuric Acid," *J. Geophys. Res., 102,* 1311–1326 (1997).

Reiner, T., M. Hanke, and F. Arnold, "Aircraft-Borne Measurements of Peroxy Radicals in the Middle Troposphere," *Geophys. Res. Lett., 25,* 47–50 (1998).

Reponen, A., J. Ruuskanen, A. Mirme, E. Pärjälä, G. Hoek, W. Roemer, J. Hosiokangas, J. Pekkanen, and M. Jantunen, "Comparison of Five Methods for Measuring Particulate Matter Concentrations in Cold Winter Climate," *Atmos. Environ., 30,* 3873–3879 (1996).

Ridley, B. A., M. A. Carroll, G. L. Gregory, and G. W. Sachse, "NO and $NO_2$ in the Troposphere: Technique and Measurements in Regions of a Folded Tropopause," *J. Geophys. Res., 93,* 15813–15830 (1988).

Ridley, B. A., and F. E. Grahek, "A Small, Low Flow, High Sensitivity Reaction Vessel for NO Chemiluminescence Detectors," *J. Atmos. Oceanic Technol., 1,* 307–311 (1990).

Ridley, B. A., J. D. Shetter, J. G. Walega, S. Madronich, C. M. Elsworth, F. E. Grahek, F. C. Fehsenfeld, R. B. Norton, D. D. Parrish, G. Hübler, M. Buhr, E. J. Williams, E. J. Allwine, and H. H. Westberg, "The Behavior of Some Organic Nitrates at Boulder and Niwot Ridge, Colorado," *J. Geophys. Res., 95,* 13949–13961 (1990a).

Ridley, B. A., J. D. Shetter, B. W. Gandrud, L. J. Salas, H. B. Singh, M. A. Carroll, G. Hübler, D. L. Albritton, D. R. Hastie, H. I. Schiff, G. I. Mackay, D. R. Karechi, D. D. Davis, J. D. Bradshaw, M. O. Rodgers, S. T. Sandholm, A. L. Torres, E. P. Condon, G. L. Gregory, and S. M. Beck, "Ratios of Peroxyacetyl Nitrate to Active Nitrogen Observed during Aircraft Flights over the Eastern Pacific Ocean and Continental United States," *J. Geophys. Res., 95,* 10179–10192 (1990b).

Ridley, B. A., E. L. Atlas, J. G. Walega, G. L. Kok, T. A. Staffelbach, J. P. Greenberg, F. E. Grahek, P. G. Hess, and D. D. Montzka, "Aircraft Measurements Made during the Spring Maximum of Ozone over Hawaii: Peroxides, CO, $O_3$, $NO_y$, Condensation Nuclei, Selected Hydrocarbons, Halocarbons, and Alkyl Nitrates between 0.5 and 9 km Altitude," *J. Geophys. Res., 102,* 18935–18961 (1997).

Ridley, B., J. Walega, G. Hübler, D. Montzka, E. Atlas, D. Hauglustaine, F. Grahek, J. Lind, T. Campos, R. Norton, J. Greenberg, S. Schauffler, S. Oltmans, and S. Whittlestone, "Measurements of $NO_x$ and PAN and Estimates of $O_3$ Production over the Seasons during Mauna Loa Observatory Photochemistry Experiment 2," *J. Geophys. Res., 103,* 8323–8339 (1998).

Riemer, D., W. Pos, P. Milne, C. Farmer, R. Zika, E. Apel, K. Olszyna, T. Kleindienst, W. Lonneman, S. Bertman, P. Shepson, and T. Starn, "Observations of Nonmethane Hydrocarbons and Oxygenated Volatile Organic Compounds at a Rural Site in the Southeastern United States," *J. Geophys. Res., 103,* 28111–28128 (1998).

Rinsland, C. P., M. R. Gunson, P.-H. Wang, R. F. Arduini, B. A. Baum, P. Minnis, A. Goldman, M. C. Abrams, R. Zander, E. Mahieu, R. J. Salawitch, H. A. Michelsen, F. W. Irion, and M. J. Newchurch, "ATMOS/ATLAS 3 Infrared Profile Measurements of Trace Gases in the November, 1994 Tropical and Subtropical Upper Troposphere," *J. Quant. Spectrosc. Radiat. Transfer, 60,* 891–901 (1998).

Riveros, H. G., A. Alba, P. Ovalle, B. Silva, and E. Sandoval, "Carbon Monoxide Trend, Meteorology, and Three-Way Catalysts in Mexico City," *J. Air Waste Manage. Assoc., 48,* 459–462 (1998).

Roberts, J. M., J. Williams, K. Baumann, M. P. Buhr, P. D. Goldan, J. Holloway, G. Hübler, W. C. Kuster, S. A. McKeen, T. B. Ryerson, M. Trainer, E. J. Williams, F. C. Fehsenfeld, S. B. Bertman, G. Nouaime, C. Seaver, G. Grodzinsky, M. Rodgers, and V. L. Young, "Measurements of PAN, PPN, and MPAN Made during the 1994 and 1995 Nashville Intensives of the Southern Oxidant Study: Implications for Regional Ozone Production from Biogenic Hydrocarbons," *J. Geophys. Res., 103,* 22473–22490 (1998).

Rodgers, M. O., and D. D. Davis, "A UV-Photofragmentation/Laser-Induced Fluorescence Sensor for the Atmospheric Detection of HONO," *Environ. Sci. Technol., 23,* 1106–1112 (1989).

Rodler, D. R., L. Nondek, and J. W. Birks, "Evaluation of Ozone and Water Vapor Interferences in the Derivatization of Atmospheric Aldehydes with Dansylhydrazine," *Environ. Sci. Technol., 27,* 2814–2820 (1993).

Roscoe, H. K., and K. C. Clemitshaw, "Measurement Techniques in Gas-Phase Tropospheric Chemistry: A Selective View of the Past, Present, and Future," *Science, 276,* 1065–1072 (1997).

Rosell-Llompart, J., I. G. Loscertales, D. Bingham, and J. F. de la Mora, "Sizing Nanoparticles and Ions with a Short Differential Mobility Analyzer," *J. Aerosol Sci., 27,* 695–719 (1996).

Rudolph, J., B. Vierkorn-Rudolph, and F. X. Meixner, "Large-Scale Distribution of Peroxyacetylnitrate Results from the STRATOZ III Flights," *J. Geophys. Res., 92,* 6653–6661 (1987).

Rudolph, J., A. Khedim, and D. Wagenbach, "The Seasonal Variation of Light Nonmethane Hydrocarbons in the Antarctic Troposphere," *J. Geophys. Res., 94,* 13039–13044 (1989).

Sachse, G. W., G. F. Hill, L. O. Wade, and M. G. Perry, "Fast-Response, High-Precision Carbon Monoxide Sensor Using a Tunable Diode Laser Absorption Technique," *J. Geophys. Res., 92,* 2071–2081 (1987).

Sacks, R., and M. Akard, "High-Speed GC Analysis of VOCs: Tunable Selectivity and Column Selection," *Environ. Sci. Technol., 28,* 428A–433A (1994).

Sakugawa, H., and I. R. Kaplan, "Atmospheric $H_2O_2$ Measurement: Comparison of Cold Trap Method with Impinger Bubbling Method," *Atmos. Environ., 21,* 1791–1798 (1987).

Sakugawa, H., I. R. Kaplan, W. Tsai, and Y. Cohen, "Atmospheric Hydrogen Peroxide," *Environ. Sci. Technol., 24,* 1452–1461 (1990).

Salas, L. J., and H. B. Singh, "Measurements of Formaldehyde and Acetaldehyde in the Urban Ambient Air," *Atmos. Environ., 20,* 1301–1304 (1986).

Sandholm, S. T., J. D. Bradshaw, K. S. Dorris, M. O. Rodgers, and D. D. Davis, "An Airborne Compatible Photofragmentation Two-Photon Laser-Induced Fluorescence Instrument for Measuring Background Tropospheric Levels of NO, $NO_x$, and $NO_2$," *J. Geophys. Res., 95,* 10155–10161 (1990).

Sandholm, S., J. Olson, J. Bradshaw, R. Talbot, H. Singh, G. Gregory, D. Blake, B. Anderson, G. Sachse, J. Barrick, J. Collins, K. Klemm, B. Lefer, O. Klemm, K. Gorzelska, D. Herlth, and D. O'Hara, "Summertime Partitioning and Budget of $NO_y$ Compounds in the Troposphere over Alaska and Canada: ABLE 3B," *J. Geophys. Res., 99,* 1837–1861 (1994).

Sandholm, S., S. Smyth, R. Bai, and J. Bradshaw, "Recent and Future Improvements in Two-Photon Laser-Induced Fluorescence NO Measurement Capabilities," *J. Geophys. Res., 102,* 28651–28661 (1997).

Sanhueza, E., M. Santana, D. Trapp, C. de Serves, L. Figueroa, R. Romero, A. Rondón, and L. Donoso, "Field Measurement Evidence for an Atmospheric Chemical Source of Formic and Acetic Acids in the Tropic," *Geophys. Res. Lett., 23,* 1045–1048 (1996).

Saros, M. T., R. J. Weber, J. J. Marti, and P. H. McMurry, "Ultrafine Aerosol Measurement Using a Condensation Nucleus Counter with Pulse Height Analysis," *Aerosol Sci. Technol, 25,* 200–213 (1996).

Sauer, F., G. Schuster, C. Schäfer, and G. K. Moortgat, "Determination of $H_2O_2$ and Organic Peroxides in Cloud- and Rain-Water on the Kleiner Feldberg during FELDEX," *Geophys. Res. Lett., 23,* 2605–2608 (1996).

Sauer, F., S. Limbach, and G. K. Moortgat, "Measurements of Hydrogen Peroxide and Individual Organic Peroxides in the Marine Troposphere," *Atmos. Environ., 31,* 1173–1184 (1997).

Scheibel, H. G., and J. Porstendörfer, "Generation of Monodisperse Ag- and NaCl-Aerosols with Particle Diameters between 2 and 300 nm," *J. Aerosol Sci., 14,* 113–126 (1983).

Schendel, J. S., R. E. Stickel, C. A. van Dijk, S. T. Sandholm, D. D. Davis, and J. D. Bradshaw, "Atmospheric Ammonia Measurement Using a VUV/Photofragmentation Laser-Induced Fluorescence Technique," *Appl. Opt., 29,* 4924–4937 (1990).

Schiff, H. I., D. R. Hastie, G. I. Mackay, T. Iguchi, and B. A. Ridley, "Tunable Diode Laser Systems for Measuring Trace Gases in Tropospheric Air," *Environ. Sci. Technol., 17,* 352A–364A (1983).

Schiff, H. I., G. I. Mackay, C. Castledine, G. W. Harris, and Q. Tran, "Atmospheric Measurements of Nitrogen Dioxide with a Sensitive Luminol Instrument," *Water, Air Soil Pollution, 30,* 105–114 (1986).

Schiff, H. I., D. R. Karecki, G. W. Harris, D. R. Hastie, and G. I. Mackay, "A Tunable Diode Laser System for Aircraft Measurements of Trace Gases," *J. Geophys. Res., 95,* 10147–10153 (1990).

Schiff, H. I., G. I. Mackay, and J. Bechara, "The Use of Tunable Diode Laser Absorption Spectroscopy for Atmospheric Measurements," *Res. Chem. Intermed., 20,* 525–556 (1994a).

Schiff, H. I., G. I. Mackay, and J. Bechara, "The Use of Tunable Diode Laser Absorption Spectroscopy for Atmospheric Measurements," in *Air Monitoring by Spectroscopic Techniques* (M. W. Sigrist, Ed.), *Chemical Analysis Series,* Vol. 127, pp. 239–333, Wiley, New York, 1994b.

Schmidt, S., M. F. Appel, R. M. Garnica, R. N. Schindler, and Th. Benter, "Atmospheric Pressure Laser Ionization (APLI). A New Analytical Technique for Highly Selective Detection of Ultra-Low Concentrations in the Gas Phase," *Anal Chem.,* in press (1999).

Schneider, J., V. Bürger, and F. Arnold, "Methyl Cyanide and Hydrogen Cyanide Measurements in the Lower Stratosphere: Implications for Methyl Cyanide Sources and Sinks," *J. Geophys. Res., 102,* 25501–25506 (1997).

Schrader, B., "Micro Raman, Fluorescence, and Scattering Spectroscopy of Single Particles," in *Physical and Chemical Characterization of Individual Airborne Particles (K. R. Spurny, Ed.), Chap.* 19, pp. 358–379, Ellis Horwood, Chichester, 1986.

Schreiner, J., C. Voigt, K. Mauersberger, P. McMurry, and P. Ziemann, "Aerodynamic Lens System for Producing Particle Beams at Stratospheric Pressures," *Aerosol Sci. Technol., 29,* 50–56 (1998).

Schuetzle, D., A. L. Crittenden, and R. J. Charlson, "Application of Computer Controlled High Resolution Mass Spectrometry to the Analysis of Air Pollutants," *J. Air Pollut. Control Assoc., 23,* 704–709 (1973).

Schultz, M., M. Heitlinger, D. Mihelcic, and A. Volz-Thomas, "Calibration Source for Peroxy Radicals with Built-In Actinometry Using $H_2O$ and $O_2$ Photolysis at 185 nm," *J. Geophys. Res., 100,* 18811–18816 (1995).

Schwarz, F. P., H. Okabe, and J. K. Whittaker, "Fluorescence Detection of Sulfur Dioxide in Air at the Parts Per Billion Level," *Anal. Chem., 46,* 1024–1028 (1974).

Scott, W. E., E. R. Stephens, P. L. Hanst, and R. C. Doerr, "Further Developments in the Chemistry of the Atmosphere," Paper presented at the 22nd Midyear Meeting of the American Petroleum Institute's Division of Refining, Philadelphia, PA, May 14, 1957.

Shaw, W. J., C. W. Spicer, and D. V. Kenny, "Eddy Correlation Fluxes of Trace Gases Using a Tandem Mass Spectrometer," *Atmos. Environ., 32,* 2887–2898 (1998).

Shepson, P. B., T. E. Kleindienst, and H. B. McElhoe, "A Cryogenic Trap/Porous Polymer Sampling Technique for the Quantitative Determination of Ambient Volatile Organic Compound Concentrations," *Atmos. Environ., 21,* 579–587 (1987).

Shepson, P. B., D. R. Hastie, H. I. Schiff, M. Polizzi, J. W. Bottenheim, K. Anlauf, G. I. Mackay, and D. R. Karecki, "Atmospheric Concentrations and Temporal Variations of $C_1$–$C_3$ Carbonyl Compounds at Two Rural Sites in Central Ontario," *Atmos. Environ., 25A,* 2001–2015 (1991).

Shields, H. C., and C. J. Weschler, "Analysis of Ambient Concentrations of Organic Vapors with a Passive Sampler," *JAPCA, 37,* 1039–1045 (1987).

Sickles, J. E., II, L. L. Hodson, E. F. Rickman, Jr., M. L. Saeger, D. L. Hardison, A. R. Turner, C. K. Sokol, E. D. Estes, and R. J. Paur, "Comparison of the Annular Denuder System and the Transition Flow Reactor for Measurements of Selected Dry Deposition Species," *JAPCA, 39,* 1218–1224 (1989).

Simeonsson, J. B., G. W. Lemire, and R. C. Sausa, "Laser-Induced Photofragmentation/Photoionization Spectrometry: A Method for Detecting Ambient Oxides of Nitrogen," *Anal. Chem., 66,* 2272–2278 (1994).

Simon, P. K., and P. K. Dasgupta, "Continuous Automated Measurement of Gaseous Nitrous and Nitric Acids and Particulate Nitrite and Nitrate," *Environ. Sci. Technol., 29,* 1534–1541 (1995).

Singh, H. B., W. Viezee, and L. J. Salas, "Measurements of Selected $C_2$–$C_5$ Hydrocarbons in the Troposphere: Latitudinal, Vertical, and Temporal Variations," *J. Geophys. Res., 93,* 15861–15878 (1988).

Singh, H. B., E. Condon, J. Vedeer, D. O'Hara, B. A. Ridley, B. W. Gandrud, J. D. Shetter, L. J. Salas, B. Huebert, G. Hübler, M. A.

Carroll, D. L. Albritton, D. D. Davis, J. D. Bradshaw, S. T. Sandholm, M. O. Rodgers, S. M. Beck, G. L. Gregory, and P. J. LeBel, "Peroxyacetyl Nitrate Measurements during CITE 2: Atmospheric Distribution and Precursor Relationships," *J. Geophys. Res., 95,* 10163–10178 (1990).

Singh, H. B., W. Viezee, Y. Chen, A. N. Thakur, Y. Kondo, R. W. Talbot, G. L. Gregory, G. W. Sachse, D. R. Blake, J. D. Bradshaw, Y. Wang, and D. J. Jacob, "Latitudinal Distribution of Reactive Nitrogen in the Free Troposphere over the Pacific Ocean in Late Winter/Early Spring," *J. Geophys. Res., 103,* 28237–28246 (1998).

Sinha, M. P., C. E. Giffin, D. D. Norris, T. J. Estes, V. L. Vilker, and S. K. Friedlander, "Particle Analysis by Mass Spectrometry," *J. Colloid Interface Sci., 87,* 140–153 (1982).

Sinha, M. P., "Laser-Induced Volatilization and Ionization of Microparticles," *Rev. Sci. Instrum., 55,* 886–891 (1984).

Sinha, M. P., and S. K. Friedlander, "Real-Time Measurement of Sodium Chloride in Individual Aerosol Particles by Mass Spectrometry," *Anal. Chem., 57,* 1880–1883 (1985).

Sinha, M. P., and S. K. Friedlander, "Mass Distribution of Chemical Species in a Polydisperse Aerosol: Measurement of Sodium Chloride in Particles by Mass Spectrometry," *J. Colloid Inteface Sci., 112,* 573–582 (1986).

Sirju, A.-P., and P. B. Shepson, "Laboratory and Field Investigation of the DNPH Cartridge Technique for the Measurement of Atmospheric Carbonyl Compounds," *Environ. Sci. Technol., 29,* 384–392 (1995).

Sjödin, A., "Studies of the Diurnal Variation of Nitrous Acid in Urban Air," *Environ. Sci. Technol., 22,* 1086–1089 (1988).

Skoog, D. A., F. J. Holler, and T. A. Nieman, *Principles of Instrumental Analysis,* 5th ed., Harcourt Brace & Company, Philadelphia, PA, 1998.

Slemr, F., G. W. Harris, D. R. Hastie, G. I. Mackay, and H. I. Schiff, "Measurement of Gas Phase Hydrogen Peroxide in Air by Tunable Diode Laser Absorption Spectroscopy," *J. Geophys. Res., 91,* 5371–5378 (1986).

Slemr, J., W. Junkermann, and A. Volz-Thomas, "Temporal Variations in Formaldehyde, Acetaldehyde, and Acetone and Budget of Formaldehyde at a Rural Site in Southern Germany," *Atmos. Environ., 30,* 3667–3676 (1996).

Smith, G. P., and D. R. Crosley, "A Photochemical Model of Ozone Interference Effects in Laser Detection of Tropospheric OH," *J. Geophys. Res., 95,* 16427–16442 (1990).

Smith, J. P., and S. Solomon, "Atmospheric $NO_3$. 3. Sunrise Disappearance and the Stratospheric Profile," *J. Geophys. Res., 95,* 13819–13827 (1990).

Smith, J. P., S. Solomon, R. W. Sanders, H. L. Miller, L. M. Perliski, J. G. Keys, and A. L. Schmeltekopf, "Atmospheric $NO_3$. 4. Vertical Profiles at Middle and Polar Latitudes at Sunrise," *J. Geophys. Res., 98,* 8983–8989 (1993).

Smith, N., J. M. C. Plane, C.-F. Nien, and P. A. Solomon, "Nighttime Radical Chemistry in the San Joaquin Valley," *Atmos. Environ., 29,* 2887–2897 (1995).

Solberg, S., T. Krognes, F. Stordal, Ø. Hov, H. J. Beine, D. A. Jaffe, K. C. Clemitshaw, and S. A. Penkett, "Reactive Nitrogen Compounds at Spitsbergen in the Norwegian Arctic," *J. Atmos. Chem., 28,* 209–225 (1997).

Solomon, P. A., S. M. Larson, T. Fall, and G. R. Cass, "Basinwide Nitric Acid and Related Species Concentrations Observed during the Claremont Nitrogen Species Comparison Study," *Atmos. Environ., 22,* 1587–1594 (1988).

Solomon, P. A., L. G. Salmon, T. Fall, and G. R. Cass, "Spatial and Temporal Distribution of Atmospheric Nitric Acid and Particulate Nitrate Concentrations in the Los Angeles Area," *Environ. Sci. Technol., 26,* 1594–1601 (1992).

Spagnolo, G. S., and D. Paoletti, "Automatic System for Three Fractions Sampling of Aerosol Particles in Outdoor Environments," *J. Air Waste Manage. Assoc., 44,* 702–706 (1994).

Spicer, C. W., "Photochemical Atmospheric Pollutants Derived from Nitrogen Oxides," *Atmos. Environ., 11,* 1089–1095 (1977).

Spicer, C. W., D. V. Kenny, G. F. Ward, and I. H. Billick, "Transformations, Lifetimes, and Sources of $NO_2$, HONO, and $HNO_3$ in Indoor Environments," *J. Air Waste Manage. Assoc., 43,* 1479–1485 (1993a).

Spicer, C. W., Y. Yanagisawa, J. D. Mulik, and I. H. Billick, "The Prevalence of Nitrous Acid in Indoor Air and Its Impact on $NO_2$ Measurement Made by Passive Samplers," *Indoor Air '93, 3,* 277–282 (1993b).

Spicer, C. W., D. V. Kenny, W. J. Shaw, K. M. Busness, and E. G. Chapman, "A Laboratory in the Sky—New Frontiers in Measurements Aloft," *Environ. Sci. Technol., 28,* 412A–420A (1994a).

Spicer, C. W., D. V. Kenny, G. F. Ward, I. H. Billick, and N. P. Leslie, "Evaluation of $NO_2$ Measurement Methods for Indoor Air Quality Applications," *J. Air Waste Manage Assoc., 44,* 163–168 (1994b).

Spicer, C. W., E. G. Chapman, B. J. Finlayson-Pitts, R. A. Plastridge, J. M. Hubbe, J. M. Fast, and C. M. Berkowitz, "Unexpectedly High Concentrations of Molecular Chlorine in Coastal Air," *Nature, 394,* 353–356 (1998).

Spivakovsky, C. M., R. Yevich, J. A. Logan, S. C. Wofsy, M. B. McElroy, and M. J. Prather, "Tropospheric OH in a Three-Dimensional Chemical Tracer Model: An Assessment Based on Observations of $CH_3CCl_3$," *J. Geophys. Res., 95,* 18441–18471 (1990).

Spurny, K. R., "Sampling Methods and Sampling Preparation," in *Physical and Chemical Characterization of Individual Airborne Particles* (K. R. Spurny, Ed.), Chap. 3, pp. 40–71, Ellis Horwood, Chichester, 1986.

Staffelbach, T., A. Neftel, and P. K. Dasgupta, "Artifact Peroxides Produced during Cryogenic Sampling of Ambient Air," *Geophys. Res. Lett., 22,* 2605–2608 (1995).

Staffelbach, T. A., G. L. Kok, B. G. Heikes, B. McCully, G. I. Mackay, D. R. Karecki, and H. I. Schiff, "Comparison of Hydroperoxide Measurements Made during the Mauna Loa Observatory Photochemistry Experiment 2," *J. Geophys. Res., 101,* 14729–14739 (1996).

Stephens, E. R., P. L. Hanst, R. C. Doerr, and W. E. Scott, "Reactions of Nitrogen Dioxide and Organic Compounds in Air," *Ind. Eng. Chem., 48,* 1498–1504 (1956a).

Stephens, E. R., W. E. Scott, P. L. Hanst, and R. C. Doerr, "Recent Developments in the Study of the Organic Chemistry of the Atmosphere," *J. Air Pollut. Control Assoc., 6,* 159–165 (1956b).

Stephens, E. R., "Long-Path Infrared Spectroscopy for Air Pollution Research," *Soc. Appl. Spectrosc., 12,* 80–84 (1958).

Stephens, E. R., and M. A. Price, "Smog Aerosol: Infrared Spectra," *Science, 168,* 1584–1586 (1970).

Stephens, E. R., and M. A. Price, "Comparison of Synthetic and Smog Aerosols," *J. Colloid Interface Sci., 39,* 272–286 (1972).

Stephens, E. R., "Valveless Sampling of Ambient Air for Analysis by Capillary Gas Chromatography," *JAPCA, 39,* 1202–1205 (1989).

Stevens, P. S., J. H. Mather, and W. H. Brune, "Measurement of Tropospheric OH and $HO_2$ by Laser-Induced Fluorescence at Low Pressure," *J. Geophys. Res., 99,* 3543–3557 (1994).

Stevens, P. S., J. H. Mather, W. H. Brune, F. Eisele, D. Tanner, A. Jefferson, C. Cantrell, R. Shetter, S. Sewall, A. Fried, B. Henry, E. Williams, K. Baumann, P. Goldan, and W. Kuster, "$HO_2$/OH and $RO_2$/$HO_2$ Ratios during the Tropospheric OH

Photochemistry Experiment: Measurement and Theory," *J. Geophys. Res., 102,* 6379–6391 (1997).

Stoffels, J. J., "A Direct-Inlet Mass Spectrometer for Real-Time Analysis of Airborne Particles," *Int. J. Mass Spectrom. Ion Phys., 40,* 217–222 (1981a).

Stoffels, J. J., "A Direct Inlet for Surface-Ionization Mass Spectrometry of Airborne Particles," *Int. J. Mass Spectrom. Ion Phys., 40,* 223–234 (1981b).

Stoffels, J. J., and C. R. Lagergren, "On the Real-Time Measurement of Particles in Air by Direct-Inlet Surface-Ionization Mass Spectrometry," *Int. J. Mass Spectrom. Ion Phys., 40,* 243–254 (1981).

Stoffels, J. J., and J. Allen, "Mass Spectrometry of Single Particles *In Situ*," in *Physical and Chemical Characterization of Individual Airborne Particles* (K. R. Spurny, Ed.), Chap. 20, pp. 380–399, Ellis Horwood, Chichester, 1986.

Stolzenburg, M. R., and P. H. McMurry, "An Ultrafine Aerosol Condensation Nucleus Counter," *Aerosol Sci. Technol., 14,* 48–65 (1991).

Stutz, J., and U. Platt, "Numerical Analysis and Estimation of the Statistical Error of Differential Optical Absorption Spectroscopy Measurements with Least-Squares Methods," *Appl. Opt., 35,* 6041–6053 (1996).

Stutz, J., and U. Platt, "Improving Long-Path Differential Optical Absorption Spectroscopy with a Quartz-Fiber Mode Mixer," *Appl. Opt., 36,* 1105–1115 (1997).

Suppan, P., P. Fabian, L. Vyras, and S. E. Gryning, "The Behaviour of Ozone and Peroxyacetyl Nitrate Concentrations for Different Wind Regimes during the MEDCAPHOT-TRACE Campaign in the Greater Area of Athens, Greece," *Atmos. Environ., 32,* 2089–2102 (1998).

Sweet, C. W., and D. F. Gatz, "Summary and Analysis of Available $PM_{2.5}$ Measurements in Illinois," *Atmos. Environ., 32,* 1129–1133 (1998).

Talbot, R. W., K. M. Beecher, R. C. Harriss, and W. R. Cofer III, "Atmospheric Geochemistry of Formic and Acetic Acids at a Mid-Latitude Temperate Site," *J. Geophys. Res., 93,* 1638–1652 (1988).

Talbot, R. W., A. S. Vijgen, and R. C. Harriss, "Measuring Tropospheric $HNO_3$: Problems and Prospects for Nylon Filter and Mist Chamber Techniques," *J. Geophys. Res., 95,* 7553–7561 (1990).

Talbot, R. W., J. D. Bradshaw, S. T. Sandholm, H. B. Singh, G. W. Sachse, J. Collins, G. L. Gregory, B. Anderson, D. Blake, J. Barrick, E. V. Browell, K. I. Klemm, B. L. Lefer, O. Klemm, K. Gorzelska, J. Olson, D. Herlth, and D. O'Hara, "Summertime Distribution and Relations of Reactive Odd Nitrogen Species and $NO_y$ in the Troposphere over Canada," *J. Geophys. Res., 99,* 1863–1885 (1994).

Tanner, D. J., and F. L. Eisele, "Ions in Oceanic and Continental Air Masses," *J. Geophys. Res., 96,* 1023–1031 (1991).

Tanner, D. J., and F. L. Eisele, "Present OH Measurement Limits and Associated Uncertainties," *J. Geophys. Res., 100,* 2883–2892 (1995).

Tanner, D. J., A. Jefferson, and F. L. Eisele, "Selected Ion Chemical Ionization Mass Spectrometric Measurement of OH," *J. Geophys. Res., 102,* 6415–6425 (1997).

Tanner, R. L., A. H. Miguel, J. B. de Andrade, J. S. Gaffney, and G. E. Streit, "Atmospheric Chemistry of Aldehydes: Enhanced Peroxyacetyl Nitrate Formation from Ethanol-Fueled Vehicular Emissions," *Environ. Sci. Technol., 22,* 1026–1034 (1988).

Tanner, R. L., and D. E. Schorran, "Measurements of Gaseous Peroxides near the Grand Canyon—Implication for Summertime Visibility Impairment from Aqueous-Phase Secondary Sulfate Formation," *Atmos. Environ., 29,* 1113–1122 (1995).

Tanner, R. L., B. Zielinska, E. Uberna, G. Harshfield, and A. P. McNichol, "Concentrations of Carbonyl Compounds and the Carbon Isotopy of Formaldehyde at a Coastal Site in Nova Scotia during the NARE Summer Intensive," *J. Geophys. Res., 101,* 28961–28970 (1996).

Thakur, A. N., H. B. Singh, P. Mariani, Y. Chen, Y. Wang, D. J. Jacob, G. Brasseur, J.-F. Müller, and M. Lawrence, "Distribution of Reactive Nitrogen Species in the Remote Free Troposphere: Data and Model Comparisons," *Atmos. Environ., 33,* 1403–1422 (1999).

Thomson, D. S., A. M. Middlebrook, and D. M. Murphy, "Thresholds for Laser-Induced Ion Formation from Aerosols in a Vacuum Using Ultraviolet and Vacuum-Ultraviolet Laser Wavelengths," *Aerosol Sci. Technol., 26,* 544–559 (1997).

Tobias, H. J., P. M. Kooiman, K. S. Docherty, and P. J. Ziemann, "Real-Time Chemical Analysis of Organic Aerosols Using a Thermal Desorption Particle Beam Mass Spectrometer," *Aerosol Sci. Technol.,* in press (1999).

Trapp, D., and C. De Serves, "Intercomparison of Formaldehyde Measurements in the Tropical Atmosphere," *Atmos. Environ., 29,* 3239–3243 (1995).

Traxel, K., and U. Wätjen, "Particle-Induced X-Ray Emission Analysis (PIXE) of Aerosols," in *Physical and Chemical Characterization of Individual Airborne Particles* (K. R. Spurny, Ed.), Chap. 16, pp. 298–330, Ellis Horwood, Chichester, 1986.

Tremmel, H. G., W. Junkermann, and F. Slemr, "On the Distribution of Hydrogen Peroxide in the Lower Troposphere over the Northeastern United States during Late Summer 1988," *J. Geophys. Res., 98,* 1083–1099 (1993).

Tremmel, H. G., W. Junkermann, and F. Slemr, "Distribution of Organic Hydroperoxides during Aircraft Measurements over the Northeastern United States," *J. Geophys. Res., 99,* 5295–5307 (1994).

Tsai, C.-J., and S.-N. Perng, "Artifacts of Ionic Species for Hi-Vol $PM_{10}$ and $PM_{10}$ Dichotomous Samplers," *Atmos. Environ., 32,* 1605–1613 (1998).

Tuazon, E. C., R. A. Graham, A. M. Winer, R. R. Easton, J. N. Pitts, Jr., and P. L. Hanst, "A Kilometer Pathlength Fourier-Transform Infrared System for the Study of Trace Pollutants in Ambient and Synthetic Atmospheres," *Atmos. Environ., 12,* 865–875 (1978).

Tuazon, E. C., A. M. Winer, R. A. Graham, and J. N. Pitts, Jr., "Atmospheric Measurements of Trace Pollutants by Kilometer-Pathlength FT-IR Spectroscopy," *Adv. Environ. Sci. Technol., 10,* 259–300 (1980).

Tuazon, E. C., A. M. Winer, and J. N. Pitts, Jr., "Trace Pollutant Concentrations in a Multiday Smog Episode in the California South Coast Air Basin by Long Path Length Fourier Transform Infrared Spectroscopy," *Environ. Sci. Technol., 15,* 1232–1237 (1981).

Tuckermann, M., R. Ackermann, C. Gölz, H. Lorenzen-Schmidt, T. Senne, J. Stutz, B. Trost, W. Unold, and U. Platt, "DOAS-Observation of Halogen Radical-Catalysed Arctic Boundary Layer Ozone Destruction during the ARCTOC-Campaigns 1995 and 1996 in Ny-Ålesund, Spitsbergen," *Tellus, 49B,* 533–555 (1997).

Turner, J. R., and S. V. Hering, "Greased and Oiled Substrates as Bounce-Free Impaction Surfaces," *J. Aerosol Sci., 18,* 215–224 (1987).

Turpin, B. J., S.-P. Liu, K. S. Podolske, M. S. P. Gomes, S. J. Eisenreich, and P. H. McMurry, "Design and Evaluation of a Novel Diffusion Separator for Measuring Gas/Particle Distributions of Semivolatile Organic Compounds," *Environ. Sci. Technol., 27,* 2441–2449 (1993).

Turpin, B. J., J. J. Huntzicker, and S. V. Hering, "Investigation of Organic Aerosol Sampling Artifacts in the Los Angeles Basin," *Atmos. Environ., 28,* 3061–3071 (1994).

Van Valin, C. C., M. Luria, J. D. Ray, and J. F. Boatman, "Hydrogen Peroxide and Ozone over the Northeastern United States in June 1987," *J. Geophys. Res., 95,* 5689–5695 (1990).

Večeřa, Z., and P. K. Dasgupta, "Measurement of Ambient Nitrous Acid and a Reliable Calibration Source for Gaseous Nitrous Acid," *Environ. Sci. Technol., 25,* 255–260 (1991).

Vega, E., I. García, D. Apam, M. E. Ruíz, and M. Barbiaux, "Application of a Chemical Mass Balance Receptor Model to Respirable Particulate Matter in Mexico City," *J. Air Waste Manage. Assoc., 47,* 524–529 (1997).

Viggiano, A. A., "*In situ* Mass Spectrometry and Ion Chemistry in the Stratosphere and Troposphere," *Mass Spectrom. Rev., 12,* 115–137 (1993).

Vogt, R., and B. J. Finlayson-Pitts, "A Diffuse Reflectance Infrared Fourier Transform Spectroscopic (DRIFTS) Study of the Surface Reaction of NaCl with Gaseous $NO_2$ and $HNO_3$," *J. Phys. Chem., 98,* 3747–3755 (1994); correction, *ibid, 95,* 13052 (1995).

Volz-Thomas, A., *et al.*, "The PRICE (Peroxy Radical Intercomparison Exercise): An Introduction," *Proc. XXI IUGG,* 13263 (1995).

Wang, Y., T. S. Raihala, A. P. Jackman, and R. St. John, "Use of Tedlar Bags in VOC Testing and Storage: Evidence of Significant VOC Losses," *Environ. Sci. Technol., 30,* 3115–3117 (1996).

Wayne, R. P., "Fourier Transformed," *Chem. Br., 23,* 440–445 (1987).

Weatherburn, M. W., "Phenol–Hypochlorite Reaction for Determination of Ammonia," *Anal. Chem., 39,* 971–974 (1967).

Weaver, A., S. Solomon, R. W. Sanders, K. Arpag, and H. L. Miller, Jr., "Atmospheric $NO_3$. 5. Off-Axis Measurements at Sunrise: Estimates of Tropospheric $NO_3$ at 40°N," *J. Geophys. Res., 101,* 18605–18612 (1996).

Weber, R. J., M. R. Stolzenburg, S. N. Pandis, and P. H. McMurry, "Inversion of Ultrafine Condensation Nucleus Counter Pulse Height Distributions to Obtain Nanoparticle (~3–10 nm) Size Distributions," *J. Aerosol Sci., 29,* 601–615 (1998).

Wedding, J. B., Y. J. Kim, and J. P. Lodge, Jr., "Interpretation of Selected EPA Field Data on Particulate Matter Samplers: Rubidoux and Phoenix II," *JAPCA, 36,* 164–170 (1986).

Weinheimer, A. J., T. L. Campos, and B. A. Ridley, "The In-Flight Sensitivity of Gold-Tube $NO_y$ Converters to HCN," *Geophys. Res. Lett., 25,* 3943–3946 (1998).

Weinstein-Lloyd, J. B., J. H. Lee, P. H. Daum, L. I. Kleinman, L. J. Nunnermacker, S. R. Springston, and L. Newman, "Measurements of Peroxides and Related Species during the 1995 Summer Intensive of the Southern Oxidants Study in Nashville, Tennessee," *J. Geophys. Res., 103,* 22361–22373 (1998).

Weiss, R. E., and A. P. Waggoner, "Optical Measurements of Airborne Soot in Urban, Rural and Remote Locations," in *Particulate Carbon: Atmospheric Life Cycle* (G. T. Wolff and R. L. Klimisch, Eds.), pp. 317–325, Plenum, New York, 1982.

Wendel, G. J., D. H. Stedman, C. A. Cantrell, and L. Damrauer, "Luminol-Based Nitrogen Dioxide Detector," *Anal. Chem., 55,* 937–940 (1983).

Werle, P., R. Muecke, and F. Slemr, "Development of a Prototype IR-FM Absorption Spectrometer: Design Criteria and System Performance," in *Monitoring of Gaseous Pollutants by Tunable Diode Lasers* (R. Grisar, H. Boettner, M. Tacke and G. Restelli, Eds.), pp. 169–182, Kluwer Academic, Dordrecht, The Netherlands, 1992.

West, P. W., and G. C. Gaeke, "Fixation of Sulfur Dioxide as Disulfitomercurate(II) and Subsequent Colorimetric Estimation," *Anal. Chem., 28,* 1816–1819 (1956).

Westberg, H., and P. Zimmerman, "Analytical Methods Used to Identify Nonmethane Organic Compounds in Ambient Atmospheres," *Adv. Chem. Ser., 232,* 275–290 (1993).

Whitby, K. T., and W. E. Clark, "Electric Aerosol Particle Counting and Size Distribution for the 0.015 to 1 $\mu$m Size Range," *Tellus, 18,* 573–586 (1966).

Whitby, K. T., and K. Willeke, "Single Particle Optical Counters: Principles and Field Use," in *Aerosol Measurement* (D. A. Lundgren, F. S. Harris, Jr., W. H. Marlow, M. Lippman, W. E. Clark, and M. D. Durham, Eds.), pp. 145–182, University Press of Florida, Gainesville, FL, 1979.

White, J. U., "Long Optical Paths of Large Aperture," *J. Opt. Soc. Am., 32,* 285–288 (1942).

White, J. U., "Very Long Optical Paths in Air," *J. Opt. Soc. Am., 66,* 411–416 (1976).

Whittle, E., D. A. Dows, and G. C. Pimentel, "Matrix Isolation Method for the Experimental Study of Unstable Species," *J. Chem. Phys., 22,* 1943 (1954).

Wiedensohler, A., P. Aalto, D. Covert, J. Heintzenberg, and P. McMurry, "Intercomparison of Three Methods to Determine Size Distributions of Ultrafine Aerosols with Low Number Concentrations," *J. Aerosol Sci., 24,* 551–554 (1993).

Wiedensohler, A., P. Aalto, D. Covert, J. Heintzenberg, and P. H. McMurry, "Intercomparison of Four Methods to Determine Size Distributions of Low-Concentration (~100 $cm^{-3}$), Ultrafine Aerosols ($3 < D_p < 10$ nm) with Illustrative Data from the Arctic," *Aerosol Sci. Technol., 21,* 95–109 (1994).

Wiener, R. W., K. Okazaki, and K. Willeke, "Influence of Turbulence on Aerosol Sampling Efficiency," *Atmos. Environ., 22,* 917–928 (1988).

Wieser, P., and R. Wurster, "Application of Laser-Microprobe Mass Analysis to Particle Collections," in *Physical and Chemical Characterization of Individual Airborne Particles* (K. R. Spurny, Ed.), Chap. 14, pp. 251–270, Ellis Horwood, 1986.

Willeke, K., Ed., *Generation of Aerosols,* Ann Arbor Science Publishers, Ann Arbor, MI, 1980.

Williams, E. J., S. T. Sandholm, J. D. Bradshaw, J. S. Schendel, A. O. Langford, P. K. Quinn, P. J. LeBel, S. A. Vay, P. D. Roberts, R. B. Norton, B. A. Watkins, M. P. Buhr, D. D. Parrish, J. G. Calvert, and F. C. Fehsenfeld, "An Intercomparison of Five Ammonia Measurement Techniques," *J. Geophys. Res., 97,* 11591–11611 (1992).

Williams, E. J., J. M. Roberts, K. Baumann, S. B. Bertman, S. Buhr, R. B. Norton, and F. C. Fehsenfeld, "Variations in $NO_y$ Composition at Idaho Hill, Colorado," *J. Geophys. Res., 102,* 6297–6314 (1997).

Williams, E. J., K. Baumann, J. M. Roberts, S. B. Bertman, R. B. Norton, F. C. Fehsenfeld, S. R. Springston, L. J. Nunnermacker, L. Newman, K. Olszyna, J. Meagher, B. Hartsell, E. Edgerton, J. R. Pearson, and M. O. Rodgers, "Intercomparison of Ground-Based $NO_y$ Measurement Techniques," *J. Geophys. Res., 103,* 22261–22280 (1998).

Williams, E. L., II, and D. Grosjean, "Removal of Atmospheric Oxidants with Annular Denuders," *Environ. Sci. Technol., 24,* 811–814 (1990).

Williams, E. L., II, E. Grosjean, and D. Grosjean, "Ambient Levels of the Peroxyacyl Nitrates PAN, PPN, and MPAN in Atlanta, Georgia," *J. Air Waste Manage. Assoc., 43,* 873–879 (1993).

Wilson, J. C., and B. Y. H. Liu, "Aerodynamic Particle Size Measurement by Laser-Doppler Velocimetry," *J. Aerosol Sci., 11,* 139–150 (1980).

Winer, A. M., and H. W. Biermann, "Long Pathlength Differential Optical Absorption Spectroscopy (DOAS) Measurements of Gaseous HONO, $NO_2$, and HCHO in the California South Coast Air Basin," *Res. Chem. Intermed., 20,* 423–445 (1994).

Wingen, L. M., J. C. Low, and B. J. Finlayson-Pitts, "Chromatography, Absorption, and Fluorescence: A New Instrumental Analysis

Experiment on the Measurement of Polycyclic Aromatic Hydrocarbons in Cigarette Smoke," *J. Chem. Educ., 75,* 1599–1603 (1998).

Winklmayr, W., G. P. Reischl, A. O. Lindner, and A. Berner, "A New Electromobility Spectrometer for the Measurement of Aerosol Size Distributions in the Size Range from 1 to 100 nm," *J. Aerosol Sci., 22,* 289–296 (1991).

Witkowski, R. E., W. A. Cassidy, and G. W. Penney, "The Design and Deployment of an ESP Atmospheric Particle Collector at the South Pole Clean Air Facility," *JAPCA, 38,* 1168–1171 (1988).

Wolff, G. T., and R. L. Klimisch, Eds., *Particulate Carbon: Atmospheric Life Cycle*, Plenum, New York, 1982.

Wood, S. H., and K. A. Prather, "Time-of-Flight Mass Spectrometry Methods for Real Time Analysis of Individual Aerosol Particles," *Trends Anal. Chem., 17,* 346–356 (1998).

Wright, B. M., "A New Dust-Feed Mechanism," *J. Sci. Instrum., 27,* 12–15 (1950).

Yang, M., J. M. Dale, W. B. Whitten, and J. M. Ramsey, "Laser Desorption Mass Spectrometry of a Levitated Single Microparticle in a Quadrupole Ion Trap," *Anal. Chem., 67,* 1021–1025 (1995a).

Yang, M., J. M. Dale, W. B. Whitten, and J. M. Ramsey, "Laser Desorption Tandem Mass Spectrometry of Individual Microparticles in an Ion Trap Mass Spectrometer," *Anal. Chem., 67,* 4330–4334 (1995b).

Yang, M., P. T. A. Reilly, K. B. Boraas, W. B. Whitten, and J. M. Ramsey, "Real-Time Chemical Analysis of Aerosol Particles Using an Ion Trap Mass Spectrometer," *Rapid Commun. Mass Spectrom., 10,* 347–351 (1996).

Yeh, H.-C., "Electrical Techniques," in *Aerosol Measurement: Principles, Techniques, and Applications* (K. Willeke and P. A. Baron, Eds.), pp. 410–426, Van Nostrand–Reinhold, New York, 1993.

Yokelson, R. J., D. W. T. Griffith, and D. E. Ward, "Open-Path Fourier Transform Infrared Studies of Large-Scale Laboratory Biomass Fires," *J. Geophys. Res., 101,* 21067–21080 (1996).

Yokelson, R. J., D. E. Ward, R. A. Susott, J. Reardon, and D. W. T. Griffith, "Emissions from Smoldering Combustion of Biomass Measured by Open-Path Fourier Transform Infrared Spectroscopy," *J. Geophys. Res., 102,* 18865–18877 (1997a).

Yokelson, R. J., J. G. Goode, R. A. Susott, R. E. Babbitt, D. E. Ward, S. P. Baker, W. M. Hao, and D. W. T. Griffith, "Smoke Chemistry Measurements by Airborne Fourier Transform Infrared Spectroscopy (AFTIR)," IGAC International Symposium on Atmospheric Chemistry and Future Global Environment, Nagoya, Japan, November 11–13, 1997b.

Yu, J., H. E. Jeffries, and R. M. Le Lacheur, "Identifying Airborne Carbonyl Compounds in Isoprene Atmospheric Photooxidation Products by Their PFBHA Oximes Using Gas Chromatography/Ion Trap Mass Spectrometry," *Environ. Sci. Technol., 29,* 1923–1932 (1995).

Yu, J., R. C. Flagan, and J. H. Seinfeld, "Identification of Products Containing –COOH, –OH, and –C=O in Atmospheric Oxidation of Hydrocarbons," *Environ. Sci. Technol., 32,* 2357–2370 (1998).

Zahniser, M. S., D. D. Nelson, J. B. McManus, J. H. Shorter, J. Wormhoudt, and C. E. Kolb, "Tunable Infrared Laser Spectroscopy for Atmospheric Trace Gas Detection," Presented at the National Meeting of the American Chemical Society, Division of Environmental Chemistry, Preprints of Extended Abstracts, *37,* 273–276 (1997).

Zander, R., C. P. Rinsland, C. B. Farmer, J. Namkung, R. H. Norton, and J. M. Russell III, "Concentrations of Carbonyl Sulfide and Hydrogen Cyanide in the Free Upper Troposphere and Lower Stratosphere Deduced from ATMOS/Spacelab 3 Infrared Solar Occultation Spectra," *J. Geophys. Res., 93,* 1669–1678 (1988).

Zenker, T., H. Fischer, C. Nikitas, U. Parchatka, G. W. Harris, D. Mihelcic, P. Müsgen, H. W. Pätz, M. Schultz, A. Volz-Thomas, R. Schmitt, T. Behmann, M. Weißenmayer, and J. P. Burrows, "Intercomparison of NO, $NO_2$, $NO_y$, $O_3$, and $RO_x$ Measurements during the Oxidizing Capacity of the Tropospheric Atmosphere (OCTA) Campaign 1993 at Izana," *J. Geophys. Res., 103,* 13615–13634 (1998).

Zhang, D., Y. Maeda, and M. Munemori, "Chemiluminescence Method for Direct Determination of Sulfur Dioxide in Ambient Air," *Anal. Chem., 57,* 2552–2555 (1985).

Zhang, J.-X., and P. M. Aker, "Spectroscopic Probing of Aerosol Particle Interfaces," *J. Chem. Phys., 99,* 9366–9375 (1993).

Zhang, X., and P. H. McMurry, "Theoretical Analysis of Evaporative Losses of Adsorbed or Absorbed Species during Atmospheric Aerosol Sampling," *Environ. Sci. Technol., 25,* 456–459 (1991).

Zhang, X. Q., and P. H. McMurry, "Theoretical Analysis of Evaporative Losses from Impactor and Filter Deposits," *Atmos. Environ., 21,* 1779–1789 (1987).

Zhou, X., and K. Mopper, "Measurement of Sub-Parts-per-Billion Levels of Carbonyl Compounds in Marine Air by a Simple Cartridge Trapping Procedure Followed by Liquid Chromatography," *Environ. Sci. Technol., 24,* 1482–1485 (1990).

Zhou, X., and K. Mopper, "Carbonyl Compounds in the Lower Marine Troposphere over the Caribbean Sea and Bahamas," *J. Geophys. Res., 98,* 2385–2392 (1993).

Zielinska, B., and E. Fujita, "The Composition and Concentration of Hydrocarbons in the Range of C2 to C18 in Downtown Los Angeles, CA," *Res. Chem. Intermed., 20,* 321–334 (1994).

Zielinska, B., J. C. Sagebiel, G. Harshfield, A. W. Gertler, and W. R. Pierson, "Volatile Organic Compounds up to $C_{20}$ Emitted from Motor Vehicles: Measurement Methods," *Atmos. Environ., 30,* 2269–2286 (1996).

Ziemann, P. J., P. Liu, D. B. Kittelson, and P. H. McMurry, "Electron Impact Charging Properties of Size-Selected, Submicrometer Organic Particles," *J. Phys. Chem., 99,* 5126–5138 (1995).

Ziemann, P. J., and P. H. McMurry, "Spatial Distribution of Chemical Components in Aerosol Particles As Determined from Secondary Electron Yield Measurements: Implications for Mechanisms of Multicomponent Aerosol Crystallization," *J. Colloid Interface Sci., 193,* 250–258 (1997).

Ziemann, P. J., and P. H. McMurry, "Secondary Electron Yield Measurements as a Means for Probing Organic Films on Aerosol Particles," *Aerosol Sci. Technol., 28,* 77–90 (1998).

Zika, R. G., and E. S. Saltzman, "Interaction of Ozone and Hydrogen Peroxide in Water: Implications for Analysis of $H_2O_2$ in Air," *Geophys. Res. Lett., 9,* 231–234 (1982).